

Do Diradicals Behave Like Radicals?

Thijs Stuyver,^{†,*} Bo Chen,^{‡,†,*} Tao Zeng,^{§,||,*} Paul Geerlings,[†] Frank De Proft,[†] and Roald Hoffmann^{*,‡}

[†]Algemene Chemie, Vrije Universiteit Brussel, Pleinlaan 2, 1050 Brussels, Belgium

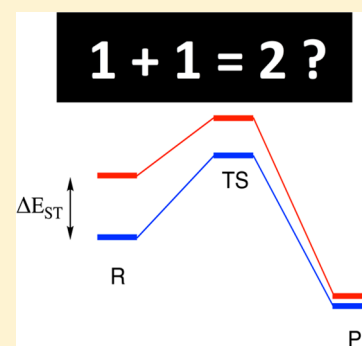
[‡]Department of Chemistry and Chemical Biology, Cornell University, Ithaca New York 14853, United States

[§]Department of Chemistry, York University, Toronto, Ontario M3J1P3, Canada

^{||}Department of Chemistry, Carleton University, Ottawa, Ontario K1S5B6, Canada

S Supporting Information

ABSTRACT: This review sets out to understand the reactivity of diradicals and how that may differ from monoradicals. In the first part of the review, we delineate the electronic structure of a diradical with its two degenerate or nearly degenerate molecular orbitals, occupied by two electrons. A classification of diradicals based on whether or not the two SOMOs can be located on different sites of the molecule is useful in determining the ground state spin. Important is a delocalized to localized orbital transformation that interchanges “closed-shell” to “open-shell” descriptions. The resulting duality is useful in understanding the dual reactivity of singlet diradicals. In the second part of the review, we examine, with a consistent level of theory, activation energies of prototypical radical reactions (dimerization, hydrogen abstraction, and addition to ethylene) for representative organic diradicals and diradicaloids in their two lowest spin states. Differences and similarities in reactivity of diradicals vs monoradicals, based on either a localized or delocalized view, whichever is suitable, are then discussed. The last part of this review begins with an extensive, comparative, and critical survey of available measures of diradical character and ends with an analysis of the consequences of diradical character for selected diradicaloids.



CONTENTS

1. Introduction	11292	10.3. Diradicals and Diradical(oid)s of Classes 1 and 2: Cyclobutadiene and Trimethylenemethane	11306
2. How to Read This Paper	11293	10.3.1. Cyclobutadiene, a Diradical(oid)	11306
3. Diradical Wave-Functions and Energies	11294	10.3.2. Trimethylenemethane, a Diradical	11307
3.1. The Four Electronic States of Two Electrons Occupying Two Degenerate Orbitals	11294	10.4. Symmetry May Determine the Class of a Diradical	11308
3.2. The Relative Energies of the Diradical States	11295	10.5. The Reactivity of CBD and TMM States	11309
4. On the Way to Diradicaloids	11296	10.5.1. The Reactivity of ³ A _{2g} CBD and ³ A ₂ TMM	11309
4.1. Closed-Shell Molecules	11296	10.5.2. The Reactivity of Singlet vs Triplet States of CBD and TMM	11310
4.2. Diradicaloids	11296	10.6. Reactivity of <i>para</i> -Quinodimethane and its Analogues	11313
5. Two Classes of Diradicals	11297	10.6.1. The Molecules and Their States	11313
5.1. Class 1: Diradicals Whose Singly Occupied Orbitals Can Be Localized on Different Sites	11297	10.6.2. The Reactivity of ³ B _{1u} PQDM and ³ B ₂ MQDM	11314
5.1.1. Diradical and Zwitterionic States	11298	10.6.3. The Reactivity of Singlet vs Triplet in PQDM and MQDM	11315
5.2. Class 2: Diradicals Whose Orbitals Are Inherently Delocalized	11299	10.7. Oxygen, a Most Unreactive Diradical	11317
5.3. Alternative Terminologies	11300	10.7.1. The Electronic States of O ₂	11318
6. Another View of Diradicals	11300	10.7.2. A VB Description of O ₂	11318
7. The Closed-Shell/Open-Shell Ambiguity for Diradicaloids	11300	10.7.3. The MO Description of O ₂	11318
8. Does the Ambiguity Really Matter?	11301	10.7.4. The Reactivity of ³ Σ _g ⁻ O ₂	11319
9. Radical Reactivity	11302	10.7.5. Dimerization and Oligomerization	11319
10. Diradical and Diradicaloid Reactivity	11302		
10.1. Introduction and Expectations	11302		
10.2. Alkyl Chain Diradicals	11303		

Received: April 27, 2019

Published: October 8, 2019



10.7.6. Abstraction	11320
10.7.7. Addition to Ethylene	11320
10.7.8. Reactivity of $^1\Delta_g$ O ₂	11320
11. Ways to Think about Diradicaloid Reactivity	11322
11.1. Radical Reactions and Preparation	11322
11.2. Preparation as a Way to Think about Diradical(oid) Reactivity	11324
12. Preliminary Summary of Diradical Reactivity	11324
13. Measures of Diradical Character	11327
13.1. For Molecular Orbital Wave Functions	11327
13.1.1. Diradical Character Indices Based on Configuration Interaction (CI) Coefficients	11327
13.1.2. An Indicator for Polar Bonds	11328
13.1.3. The Essential Link Between Diradical Measures and Correlation	11329
13.1.4. Polyradical Character Indices Based on Natural Occupancies	11329
13.1.5. Caution	11329
13.1.6. Distribution of Unpaired Electrons	11329
13.1.7. Overestimation of Polyradical Character Due to Dynamic Correlation	11330
13.1.8. Measures Based on Collectivity Number and Hole–Particle Density	11331
13.1.9. Overestimation from Spin Contamination	11331
13.1.10. Comparison of the Occupancy-Based Diradical Indicators Using H ₂ and PQDM as Test Examples	11332
13.1.11. A Polyradical Index Based on “Thermal” Occupation	11332
13.2. Diradical Measures from Valence Bond Theory	11333
13.2.1. Wave Functions in Valence Bond Theory	11333
13.2.2. Ozone and Its Sulfur Analogues	11333
13.2.3. Polyenes	11333
13.3. Measures Based on Spin Properties	11334
13.3.1. A Peep at the Wave Function Through Spin	11334
13.3.2. Measures Based on Local Spin Properties	11334
13.4. Closing Comments on Di(poly)radical Indices	11335
14. Some Typical Diradicals and Diradicaloids	11336
14.1. Polyacenes	11336
14.2. Extended π -Diradicaloids	11337
14.3. Arynes	11337
14.4. Main Group Diradical(oid)s	11339
14.5. Transition Metal Diradicaloids	11339
15. Conclusions	11340
Associated Content	11341
Supporting Information	11341
Author Information	11341
Corresponding Authors	11341
ORCID	11341
Present Address	11341
Notes	11341
Biographies	11341
Acknowledgments	11342
Dedication	11342
Abbreviations Used	11342
References	11342

1. INTRODUCTION

It is hard to imagine complex chemistry without diradicals. For any cyclic molecule, a diradical is in a way the obverse of a bond. If in an organic ring you break the latter, you have a diradical, or its relative, a zwitterion.

The senior author of this paper, senior only in age, may have been responsible in his youth for a momentary shift in focus away from diradicals by providing the organic community with a framework of thinking about too many reactions as likely concerted. Organic intermediates that are or may be diradicals, have, however, been on his mind for >50 years. They have not lost their interest to him and the other authors.

Why? Why are diradicals intrinsically interesting and remain important in chemistry? One reason has been mentioned: diradicals are, so to speak, the other side of bonding. Second, diradicals often have short lifetimes and yet must be there. That creates an experimental challenge to their detection and identification. Or their stabilization. People like challenges. Third, given a diradical, there is an inherent choice for its electronic structure, one we will delineate in exquisite detail in this paper: a choice of spin state, of reactivity, and choices are always intriguing, for people or molecules.

Perhaps a word is in order here on what a simple radical means to a chemist. Be it an H atom, or a methyl radical \bullet CH₃, a radical contains an unpaired electron. That electron might be detected by its electron spin resonance signal or its magnetism, but to a chemist, at the heart of radical character is reactivity, unless the radical site is sterically protected. Let us use methyl radical as an example: it dimerizes without activation energy to ethane; it adds, with small activation energy, to ethylene (initiating polymerization); it abstracts hydrogen or chlorine atoms from other molecules with low (\sim 10 kcal/mol) activation energies. These reactivities are widely utilized chemically and biologically.¹

The basic electronic characteristic of diradicals has been clear for more than 50 years. Diradicals can be molecules whose Lewis structure have two unpaired electrons, for example, non-Kekulé hydrocarbons² such as trimethylenemethane **1**, bisaminoxyls **2**, molecules like Dimroth’s hydrocarbon **3**, or antiaromatic annulenes, such as cyclobutadiene **4**, where even though a Lewis structure shows no unpaired electrons, there are two degenerate or nearly degenerate orbitals that are occupied by two electrons (see Figure 1). Dioxygen **5** is a diradical, and so is the copper(II) acetate dimer **6**.

There is yet another large group of molecules, with slightly bigger HOMO–LUMO gaps (sometimes tunable) than diradicals, which, for the purpose of this paper, we will call diradicaloids. Some diradicaloids are given in Figure 2 and will be discussed later.

At least two states, a singlet and a triplet, compete to be the ground state of a diradical.^{3–5} In a way, this competition may be seen as the defining feature of a diradical. Even if the basic facts about the resultant electronic structures are known (and we will describe them, as clearly as we can), essential questions of chemical importance remain: What is the chemical reactivity of a diradical? What are typical activation barriers for different reactions of a diradical? Do the reactivities differ by spin state? How does the chemical reactivity of a diradical compare to that of a monoradical?

A second motivating reason for this review is that the literature on diradicals has grown remarkably, and in it attributions of open-shell or closed-shell character to the

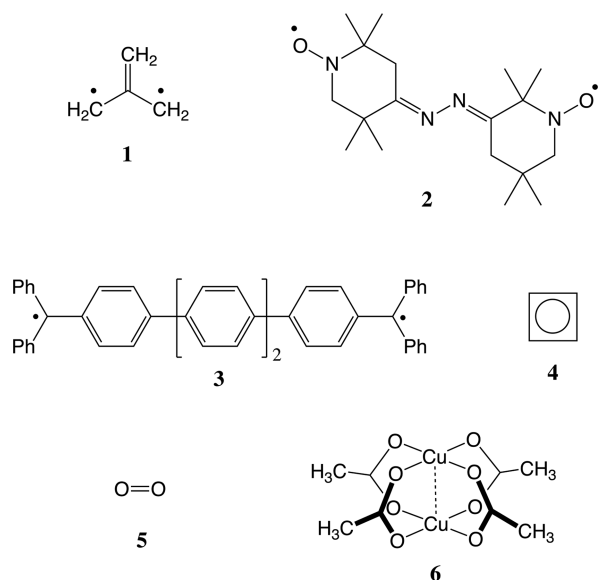


Figure 1. Some examples of diradicals. Trimethylenemethane **1**, a bis-aminoxyl **2**, Dimroth's hydrocarbon **3**, square cyclobutadiene **4**, molecular oxygen **5**, and copper(II) acetate dimer **6**.

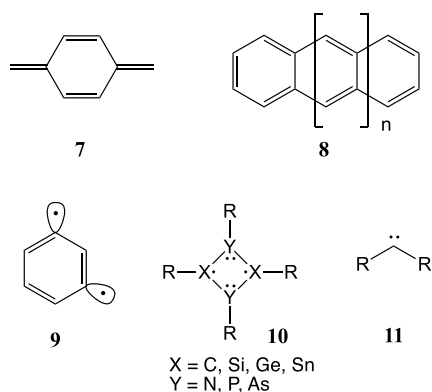


Figure 2. Examples of diradicaloids.

fascinating species observed ... run wild. The attributions, and attendant measures of diradical character, are, to put it charitably, diverse. We think it is worthwhile to compare the various measures of diradical character and to relate them to radical reactivity.

A further, quite specific factor stimulated this work, and that is a seeming disjunction between some theoretical calculations and chemical intuition. Many calculations suggest (by measures we will discuss) significant diradical and polyradical character for molecules that do not show any typical radical reactivity in the way chemists expect. To be specific, high level calculations (DMRG, RDM-CASSCF, and others) on oligoacenes show substantial, growing diradical, tetradical, etc., character as the size of the molecule increases.^{6–13} For the popular pentacene **12** (Figure 3), the number of effective unpaired electrons is estimated to be around 2 using the HG-I index (eq 53).⁶ This molecule is indeed reactive.¹⁴ Unrestricted Hartree–Fock calculations on buckminsterfullerene **13** show as many as 10 unpaired electrons.^{15–17} Despite its five times larger number of “unpaired electrons”, fullerene is way more stable than pentacene, being an almost rock-stable molecule.¹⁸ If one focuses on the number of unpaired electrons per carbon, the chemistry does not check out either, so to speak. What is going

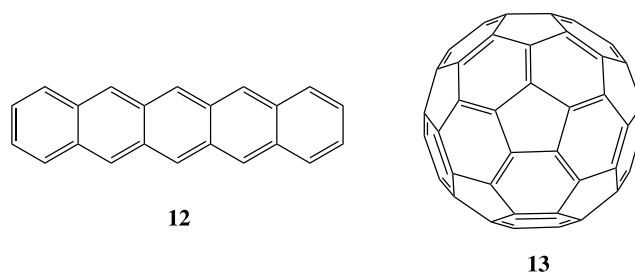


Figure 3. Pentacene **12** and buckminsterfullerene **13**.

on? Admittedly, other calculations for C_{60} show no diradical character,¹⁹ and indeed one of the things we would like to take apart in this paper is the thorny subject of different measures of diradical character and how they should be interpreted.

2. HOW TO READ THIS PAPER

Diradicals or diradicaloids (defined in section 3) are molecules with two orbitals degenerate or near each other in energy, in which two electrons find themselves. The literature is replete with stories of the competition between a high spin (triplet) and a low spin (singlet) state for being the ground state of the molecule. The magnitude of the singlet–triplet splitting, and strategies for tuning that splitting, have productively occupied the community.

This paper moves in another direction: one implication of the descriptor diradical (or diradicaloid) is that these molecules are radicals twice over, and, aside from the magnetic consequences of being singlets and triplets, there are for diradicals obvious reactivity implications. We know very well what radicals do: briefly, in the absence of steric encumbrance (or protection, depending on your point of view), at ambient temperatures radicals dimerize in a shot and with low activation barriers (ca. 10 kcal/mol), add to olefins and abstract H atoms or chlorines. Our concern in this work is with the reactivity of diradicals in the various spin states available to them.

As we approached the question, we came across another problem, which is the estimation of diradical character. Not an observable, for sure, yet given human predilection for quantification, the diradical field has been creative in (some might say afflicted by) devising a variety of estimates of diradical character. Especially for diradicaloids, which have intermediate diradical character. We were pushed to a careful examination of what is out there.

How shall one read this paper? The review begins with what the community knows very well: the definition and zeroth-order energetics of the six microstates, a triplet and three singlets, arising from placing two electrons in two orbitals. We follow in this the work of Borden and Davidson and that of Salem and Rowland. The knowledgeable reader can pass over this lightly, as well as over the obvious fuzzy definition of diradicaloids, the middle ground between diradicals and nice closed-shell molecules in section 4.

The next section, although equally obvious, we feel deserves careful reading as it delineates two classes of radicals. They are harder to describe than to recognize, and because of the varied interests of the workers in the field (who have studied one class or the other, but usually not both), the two classes are not, in our opinion, sufficiently distinguished. The first are diradicals in which the two singly occupied orbitals can be localized in different areas (like the 1s orbitals of two H atoms far apart), and a second class where this is never true. At this point, we delineate

an ambiguity in describing the two lower singlet states of diradicals as open-shell and closed-shell and face up to a transformation of the wave function that interchanges this character for one class of diradicals.

Up to this point, we will have been in a review mode. With the definitions carefully made, we proceed to the computational sandwich filling of the review, the foundation for a set of conclusions about diradical reactivity. We limit ourselves here to several classes of organic, mainly π -diradicals, while being very much aware of excellent work, especially by the Malrieu group, on diradicaloids based on electrons on transition metal centers as well as main group (but not C-based) diradicaloids. We pick three characteristic reactions: dimerization, abstraction of H from SiH_4 , and addition to ethylene. Using a consistent methodology, we establish a simple radical reactivity standard by computing activation energies for these three reactions of simple alkyl radicals.

In a series of carefully worked-through computational studies, we examine (laboriously) the activation energies for the same reactions of the following diradicals: alkyl diradicals of varying chain length, cyclobutadiene, trimethylenemethane, *para*- and *meta*-quinodimethane, and O_2 . And we do so for the triplet state and the lowest singlet state of each. Many of these reactions have been studied in the literature before, so this part of the work also has a review nature. But our labors here represent original work as well because of the consistent methodology and the systematic exploration of the substrates and the spin states of the reagents. Typical radical reactivity is thereby distinguished from typical closed-shell/concerted reactivity. A special section is devoted to bridge the two types of reactivity by introducing the concept of a preparation step.

The reader may skip ahead to the conclusions of this section, in section 12, although the careful reading on the way of at least one chemically specific section and section 11 is recommended.

We turn next to an extensive section, or set of subsections, on measures of diradical character. We believe that such a comprehensive (and critical!) survey and description of various methodologies, which number in the dozens, has not appeared before in the literature.

At this point, we will have returned to the review mode. Before a final set of conclusions, we sketch, certainly incompletely, but with many leading references, extensive literature studies of other diradicals and diradicaloids, including polyacenes, extended π -system diradicaloids (of much interests in the recent synthetic literature), arynes, and ones centered on main group atoms (such as Si or P) and on transition metals. Throughout this review, we pay careful attention to previous experimental and theoretical work, while at the same time introducing a consistent and coherent analysis of a variety of diradicals, diradicaloids, and polyradicals, and their chemical reactivity.

3. DIRADICAL WAVE-FUNCTIONS AND ENERGIES

3.1. The Four Electronic States of Two Electrons Occupying Two Degenerate Orbitals

We need to define as clearly as possible the various electronic states available to a diradical. Fortunately, this has been laid out in a pedagogically effective fashion by Salem, Michl, Borden, and their co-workers, so we will start by economically rehearsing (some would say rehashing) their argument. This section simply tries to set out as clear a statement of the problem as possible. The start of our exposition follows explicitly that of Borden and Davidson.^{3,20,21}

The characteristic feature that gives rise to a diradical occurs when, in a molecule (or atom), two electrons occupy two orbitals, labeled as ψ_x and ψ_y , of the same (degenerate) or nearly the same (pseudodegenerate) energy.^{3,4,22–25} Let us first examine the case of truly degenerate orbitals. Two electrons can be distributed between two orbitals in six different ways (Figure 4).

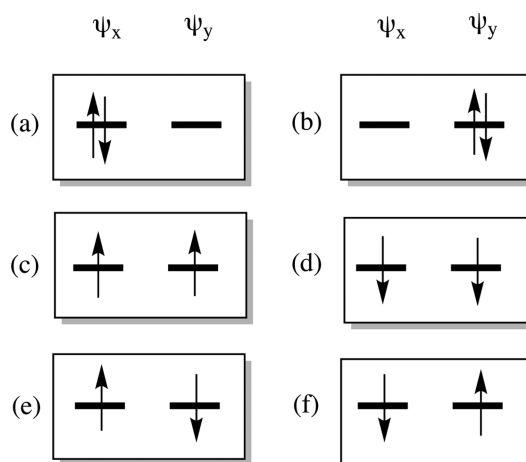


Figure 4. Six possible electronic configurations that can be obtained by distributing two electrons among two degenerate orbitals ψ_x and ψ_y .

Configurations (a) and (b) are singlets. They correspond to the so-called closed-shell configurations and can be combined (\pm) to form the symmetry-adapted two-configuration (TC) singlet states:

$$\Psi_{S_{TC\pm}} = \frac{|\psi_x^\alpha(1)\psi_x^\beta(2)\rangle \pm |\psi_y^\alpha(1)\psi_y^\beta(2)\rangle}{\sqrt{2}} = \frac{|\psi_x^2\rangle \pm |\psi_y^2\rangle}{\sqrt{2}} \quad (1)$$

Here the Dirac ket signifies a single Slater determinant. Configurations (c) and (d) on the other hand correspond to the $M_S = \pm 1$ components of a triplet (T):

$$\Psi_{T_{+1}} = |\psi_x^\alpha(1)\psi_y^\alpha(2)\rangle \quad (2)$$

$$\Psi_{T_{-1}} = |\psi_x^\beta(1)\psi_y^\beta(2)\rangle \quad (3)$$

The final two configurations, (e) and (f), do not represent pure spin states; their linear combinations give the $M_S = 0$ triplet component and the open-shell (OS) singlet:

$$\begin{aligned} \Psi_{T_0} &= \frac{|\psi_x^\alpha(1)\psi_y^\beta(2)\rangle + |\psi_x^\beta(1)\psi_y^\alpha(2)\rangle}{\sqrt{2}} \\ &= \frac{[\psi_x(1)\psi_y(2) - \psi_y(1)\psi_x(2)][\alpha(1)\beta(2) + \beta(1)\alpha(2)]}{2} \end{aligned} \quad (4)$$

$$\begin{aligned} \Psi_{S_{OS}} &= \frac{|\psi_x^\alpha(1)\psi_y^\beta(2)\rangle - |\psi_x^\beta(1)\psi_y^\alpha(2)\rangle}{\sqrt{2}} \\ &= \frac{[\psi_x(1)\psi_y(2) + \psi_y(1)\psi_x(2)][\alpha(1)\beta(2) - \beta(1)\alpha(2)]}{2} \end{aligned} \quad (5)$$

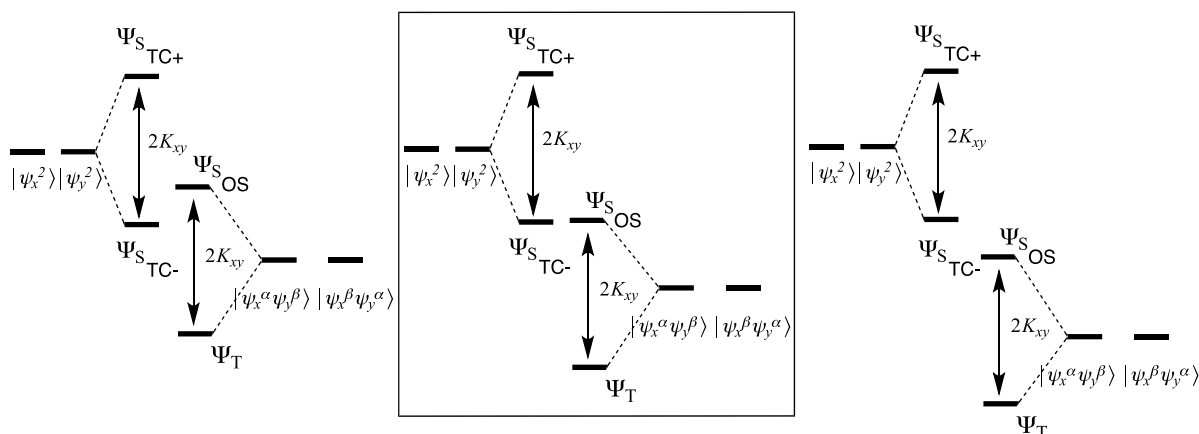


Figure 5. Relative energy levels of the four states arising from distributing two electrons in two orbitals. The positioning of these two couples of states is governed by eq 11. The three cases from left to right correspond to, respectively, the right-hand side of the equation being positive, 0, and negative.

3.2. The Relative Energies of the Diradical States

We turn to the energies of these states. Under the condition that no magnetic field is applied and ignoring the small spin-dipole coupling between the unpaired electrons and spin-orbit coupling, the three components of the triplet state are degenerate. The energy of this state is

$$E_T = h_x + h_y + J_{xy} - K_{xy} \quad (6)$$

where h_x and h_y are, respectively, the one-electron energies of the ψ_x and ψ_y orbitals, while J_{xy} and K_{xy} are the relevant Coulomb and exchange integrals:

$$J_{xy} = \iint \psi_x^2(1) \frac{e^2}{r_{12}} \psi_y^2(2) d\mathbf{r}_1 d\mathbf{r}_2 \quad (7)$$

$$K_{xy} = \iint \psi_x(1)\psi_y(1) \frac{e^2}{r_{12}} \psi_x(2)\psi_y(2) d\mathbf{r}_1 d\mathbf{r}_2 \quad (8)$$

For degenerate ψ_x and ψ_y , $h_x = h_y$. The antisymmetric spatial function in the triplet state nullifies the probability of having the two electrons simultaneously appearing at the same place and makes it small for positions nearby. This reduces the interelectron interaction by K_{xy} in eq 8, which is always a positive number.²⁶

The energy of the singlet wave function $\Psi_{S_{os}}$ reads

$$E_{S_{os}} = h_x + h_y + J_{xy} + K_{xy} \quad (9)$$

In contrast to the triplet state, the symmetric spatial function in the singlet state increases the probability of having the two electrons in the same region of space, and hence raises the singlet energy by K_{xy} .

Equations 6 and 9 together predict that, if the optimal MOs ψ_x and ψ_y for the triplet and the open-shell singlet are the same, the energy of the triplet is $2K_{xy}$ lower than that of the open-shell singlet. This $2K_{xy}$ difference in energy reflects that the Pauli repulsion prevents the proximity of electrons with parallel spin and hence lowers their electrostatic repulsion energy. This energy lowering underlies Hund's rule. The reason for the italics is that we wish to anticipate a future discussion of "violations" of Hund's rule. These may arise when the optimal MOs differ in the singlet and triplet states and also when configuration interaction introduces dynamic spin polarization and dynamic electron correlation.^{27,28} The reader is referred on this point to the beautifully worked-through analysis of Malrieu et al.²⁹

The energies of the pair of closed-shell singlet wave functions are given by

$$E_{S_{TC\pm}} = h_x + h_y + \frac{J_{xx} + J_{yy}}{2} \pm K_{xy} \quad (10)$$

According to eq 10, the energy of the $\Psi_{S_{TC-}}$ wave function is $2K_{xy}$ lower than that of the $\Psi_{S_{TC+}}$ wave function.

The energy difference between the lower closed-shell singlet and the open shell singlet then is

$$E_{S_{os}} - E_{S_{TC-}} = J_{xy} - \frac{J_{xx} + J_{yy}}{2} + 2K_{xy} \quad (11)$$

The above energetic considerations have been made under the approximation that all the states can be described with a single set of frozen orbitals. Also, we have limited our treatment here to the two electrons in the two degenerate orbitals and ignored the presence of other electrons in lower orbitals; see section S1 in the Supporting Information for a derivation of these expressions in the more general case where the interactions with core electrons are taken into account. Also, note that the interaction between the states has not yet been considered.

The argument laid out up to this point leads to the conclusion that the four states resulting from the distribution of two electrons in two degenerate orbitals, ψ_x and ψ_y , can be grouped into two pairs, each of them with a fixed spacing of $2K_{xy}$, and the positioning of these two pairs relative to one another, as governed by eq 11, will determine the final ordering of the states. A general overview of the different possibilities can be found in Figure 5. Note the further complexity of the state ordering, causing a different appearance from the three panels in Figure 5. For example, when the gap between $E_{S_{os}}$ and $E_{S_{TC-}}$ is equal to $2K_{xy}$ for the first panel in Figure 5, $\Psi_{S_{TC-}}$ and Ψ_T will be degenerate, so will $\Psi_{S_{TC+}}$ and $\Psi_{S_{os}}$.

The potential variability in the ordering of the states of diradicals, as exemplified by Figure 5, is also retrieved experimentally, even as we run ahead of ourselves in specifying examples. For instance, bis-nitroxide **2** has a clear triplet ground state, meaning that $\Psi_{S_{TC-}}$ is discernably higher in energy than Ψ_T .⁴ For Dimroth's hydrocarbon, **3**, on the other hand, these two states are almost degenerate.⁴ Square cyclobutadiene (CBD, **6**) even has a singlet ground state. This is the outcome of what

has been called dynamic spin polarization involving the pair of electrons in the lowest bonding π orbital (which is a configuration interaction effect that lowers the energy of the singlet but not the triplet), which is not considered in the energy expressions above.³

Please note a difference in terminology in the literature on this point. Borden and Davidson called this interaction, which involves orbitals and electrons beyond the minimum 2o2e space, dynamic spin polarization.³⁰ This interaction was simply called spin polarization by Salem earlier,^{31–34} but it only involves determinants with spin-conserved 1-hole–1-particle (1h–1p) excitations from occupied orbitals lower than the degenerate set to unoccupied orbitals higher than the set. Therefore, it is of dynamic charge polarization nature in the language of Malrieu et al.²⁷ The spin polarization of Malrieu et al. involves spin-flipped 1h–1p excitations, which are required to maintain eigenfunctions of the total spin squared operator (\hat{S}^2).

For molecular oxygen, O_2 , S , as well as D_{3h} trimethylenemethane (TMM, **1**), only three spectroscopic states (one triplet and two singlet) can be found; here the lower closed-shell singlet and the open-shell singlet are degenerate and give one singlet state, corresponding to the middle panel of Figure 5.^{3,22} Note from eq 11 that degeneracy between $\Psi_{S_{os}}$ and $\Psi_{S_{TC-}}$ is obtained if $\frac{J_{xx} + J_{yy}}{2} = J_{xy} + 2K_{xy}$. As we will explicitly see later on for the O_2 example, this equality is usually induced by symmetry.

Further insight into the spacing of the energy levels can only be obtained once the detailed nature of the (pseudo)degenerate orbitals of the diradical studied is considered. This will be the subject of one of the following sections, but let us first take a look at what happens when the restriction of degenerate orbitals (the starting point of any diradical discussion) is lifted as we enter the realm of the diradicaloids.

4. ON THE WAY TO DIRADICALOIDS

4.1. Closed-Shell Molecules

In the previous sections, we focused on a system of two perfectly degenerate orbitals, ψ_x and ψ_y . Symmetry-wise, the probability of both electrons being located in one orbital is equal to the probability of having both in the other. This is reflected in eq 1 by the two configurations contributing equally to $\Psi_{S_{TC-}}$ and $\Psi_{S_{TC+}}$. The ground state for such systems can either be a singlet (to be called singlet diradicals) or a triplet (triplet diradicals), as has been laid out in the previous section.

We now consider another extreme, the one in which there is no chance that the ground state of the system is a triplet state. This would be a closed-shell molecule and is the obvious consequence of a substantial energy gap between the two orbitals. As a result, the configuration with both electrons in the lower-lying molecular orbital (which corresponds to the highest occupied molecular orbital (HOMO); ψ_H) will be far more favorable than the configuration in which one or both electrons are in the higher-lying orbital (which corresponds to the lowest unoccupied molecular orbital (LUMO); ψ_L).^{4,35} In the extreme case, it may be possible to neglect this second configuration completely in $\Psi_{S_{TC-}}$ (and the first configuration in $\Psi_{S_{TC+}}$), so that single configuration states $\Psi_H = |\psi_H^2\rangle$ and $\Psi_L = |\psi_L^2\rangle$ are obtained, with energies:

$$E_H = 2h_H + J_{HH} \quad (12)$$

$$E_L = 2h_L + J_{LL} \quad (13)$$

The subscripts H and L stand for HOMO and LUMO. The three components of Ψ_T and $\Psi_{S_{os}}$ retain their wave function and energy formulas, and hence

$$E_T = h_H + h_L + J_{HL} - K_{HL} \quad (14)$$

$$E_{S_{os}} = h_H + h_L + J_{HL} + K_{HL} \quad (15)$$

Because of the energy difference between the two orbitals considered (h_L significantly $> h_H$), Ψ_T will also be considerably higher in energy than Ψ_H . The lowest-lying orbital now dominates in the ground state of the molecule (usually labeled S_0), with basically no admixture of Ψ_L ; the triplet (T_1) is the first excited state of the molecule.

4.2. Diradicaloids

A diradicaloid can be defined as a system that is in between a diradical and a closed-shell molecule. For diradicaloids, the two orbitals are not degenerate, but the energy gap between them is not large enough either to neglect the Ψ_L configuration in the singlet ground state (more precisely, the extent to which the Ψ_L configuration mixes in the ground state is determined by the “ t/U ” ratio, familiar to the physics community, cf. ref 29).³⁶ The energy levels and the contributing wave functions of the two closed-shell configurations in the wave functions are displayed schematically in Figure 6.

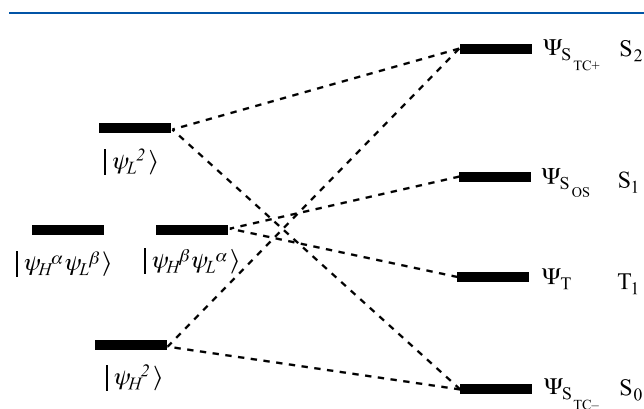


Figure 6. Electron configurations and their energies (schematic), in the case of a moderate gap between the two orbitals. Notations of the corresponding spectroscopic states are shown.

For diradicaloids, similar expressions for the different states can be constructed as for diradicals. The main difference is that h_x and h_y are now nontrivially different (thus turning them into h_H and h_L) and are the main determinants of the energies of the closed and open shell states as shown. The ground state of a diradicaloid is usually a singlet, described by a configuration interaction (CI) wave function,

$$\begin{aligned} \Psi_{S_{TC-}} &= C_1 |\psi_H^\alpha(1)\psi_H^\beta(2)\rangle - C_2 |\psi_L^\alpha(1)\psi_L^\beta(2)\rangle \\ &= C_1 |\psi_H^2\rangle - C_2 |\psi_L^2\rangle \end{aligned} \quad (16)$$

where both C_1 and C_2 are of the same sign and C_1/C_2 will be quite large if the system resembles more a closed-shell system, but will decrease as the molecule becomes more diradical-like. When C_1/C_2 approaches 1, a diradical is attained (vide infra). The triplet state will be, in general, the lowest excited state of the system. Aside from diradical(oid)s, systems with more than two

orbitals close to each other in energy also exist. In such cases, the two-configuration wave function may not be sufficient to describe the ground state, and more configurations will be needed. These systems may be said to have triradical, tetraradical, or polyradical character.

Diradicaloids have been attracting increasing interest across chemistry due to their potential applications in several fields of modern chemical physics, e.g., in singlet fission,^{37–50} molecular electronics,^{51–59} nonlinear optics,^{60–62} and H₂ activation.⁶³ The physical reason why diradical character is important for these properties is not always easy to express, even as we (and others) have tried. In some cases, the connection is clear; in singlet fission it is important to position T_1 relatively low with respect to S_1 . In other cases, this connection is more indirect/obscure. For example, the large third-order nonlinear optical susceptibilities exhibited by diradicaloids have been attributed in its simplest formulation to large fluctuations of the electrons in systems with intermediate diradical character when electric fields are applied.^{64,65}

A selection of diradicaloids is given in Figure 2. Some might look like diradicals at first sight, such as *meta*-benzynes and the four-membered ring 6π -electron system,^{66,67} as their Lewis structures each have two unpaired electrons. Some are readily recognized as diradicaloids, even if they have seemingly normal Lewis structures, for instance, *para*-quinodimethane and oligoacenes. Some, such as carbenes, are rarely considered diradicaloids. Yet the molecules in this important class of organic intermediates (or their group 14 ER₂ analogues) feature two nearby energy levels, two electrons, and exist as singlet (e.g., SiH₂) or triplet (CH₂) ground states. The singlet–triplet energy difference in them can be tuned by substitution over tens of kcal/mol in now well-understood ways.^{68,69} Carbenes fit very well into the diradicaloid category. The various systems we sketch in Figure 2 all have small to moderate energy gaps between the considered orbitals, and the ground states are most often singlets with low-lying triplet states. We consider them all as diradicaloids.

Note that our classification is prejudiced toward main group chemistry, organic and inorganic. Spin balances between low and high spin transition metal complexes form another fertile universe of diradical and polyradical chemistry. Which we, regretfully, do not broach here. For a carefully reasoned account of these, please see the reviews of Malrieu, Caballol, Calzado, de Graaf, and Guihéry.²⁷

To end this section, we show schematically in Figure 7 the evolution of the lower energy levels as one moves from diradicals over diradicaloids to closed-shell molecules. The diradicaloid zone is denoted in gray; it would be hard to define the boundaries of this zone. However, it is clear that many molecules fall into this range. Note that we implicitly classified all molecules with a triplet ground state as being in the class of diradicals in Figure 7 (vide infra).

A general feature of a gray zone (see Figure 7) is that people will argue vehemently as to which case a given system belongs. Our intent here is not to add to the discord by defining seemingly precise criteria for membership in a group. Rather, we wish to build bridges, the least of which is the one in the title of this paper, when will a diradical display radical reactivity? When the time is right, we will explore the different ways to express diradical character as we try to obtain some understanding of just what this diradical character means for the reactivity.

However, first and foremost, a closer look at the ordering of the states and their “nature” for diradicals and diradicaloids is

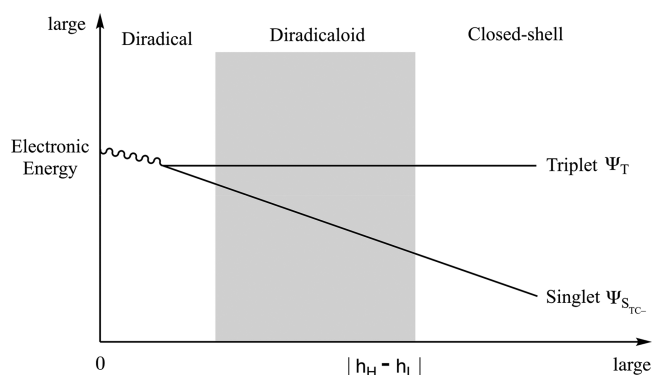


Figure 7. Schematic evolution of the energies of the (singlet, triplet) pair as the degeneracy of the two frontier orbitals is lifted.⁴ Note that h_H and h_L , i.e., the one-electron energies associated with the HOMO and LUMO, respectively, are not the full orbital energies, but their difference does reflect the energy gap between the two orbitals. The triplet energy is used here as the baseline, without implication that its absolute energy is constant. In the diradical region, whether there is a crossing of the two spin states depends on the magnitudes of the Coulomb and exchange integrals (and potential spin polarization effects);^{27–29} in any case, the singlet–triplet energy difference is usually small. The wavy line tries to symbolize this ambiguity.

required before moving on to one of the main goals of this paper, understanding of the reactivity of diradicals and diradicaloids.

5. TWO CLASSES OF DIRADICALS

Broadly speaking, two classes of diradicals can be distinguished. The first class contains those with a pair of orbitals that can be localized on different atoms (these have been called “disjoint”⁷⁰ diradicals, vide infra). The second class contains those for which this is not the case (“joint” or “non-disjoint” diradicals). Even though the distinction between these two classes and their terminology originates from the work of Borden and Davidson, we will borrow heavily from the original ideas of Salem and Rowland in introducing them below.^{4,23} Note that the “disjoint/joint” terminology used here differs from the terminology used by Malrieu and co-workers. In their work, the description of a diradical as “disjoint” indicates that the considered system is not described by a Lewis or Kekulé pairing.⁷¹

5.1. Class 1: Diradicals Whose Singly Occupied Orbitals Can Be Localized on Different Sites

Let us first focus on class 1 diradicals by considering a simple two-site model. Two localized, nonbonding orbitals (χ_a, χ_b) are located on two sites a and b that are symmetry-related to each other and can form a pair of in-phase (potentially bonding) and out-of-phase (antibonding) delocalized orbitals (ψ_H and ψ_L ; subscripts H again stands for HOMO, L for LUMO; see Figure 8),

$$\psi_H = \sqrt{\frac{1}{2}} (\chi_a + \chi_b) \quad (17)$$

$$\psi_L = \sqrt{\frac{1}{2}} (\chi_a - \chi_b) \quad (18)$$

Usually, ψ_H and ψ_L are not degenerate, but under some special circumstances, they can be turned into degenerate nonbonding but delocalized orbitals, ψ_x and ψ_y (the notation we used earlier in the case of real degeneracy), by minimizing the overlap between χ_a and χ_b .³⁵ Focusing on H₂, for which the localized orbitals are the 1s atomic orbitals on the two atoms, and ψ_H and

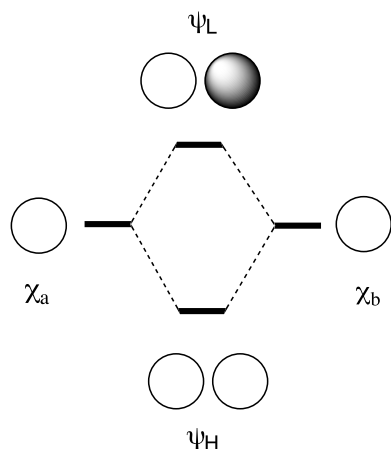


Figure 8. Combination of the two localized, nonbonding orbitals (χ_a , χ_b) into the delocalized bonding (ψ_H) and antibonding (ψ_L) orbitals in the two-site model.

ψ_L correspond to σ_g and σ_w this situation will be reached upon separating the hydrogen atoms to the dissociation limit. The original ψ_H and ψ_L have evolved into the still delocalized, yet degenerate, ψ_x and ψ_y . Another example is ethylene, whose π and π^* orbitals become the degenerate e orbitals when the two methylene units are twisted to the perpendicular D_{2d} structure. Without any bonding/antibonding character, the delocalized e orbitals can be localized to $2p_\pi$ orbitals, one on each of the two C atoms without energy cost (vide infra).

Expanding beyond the two-site model explored above, one can generally classify the perfect diradicals, for which the degenerate orbitals can be localized to different atoms or sites, as class 1 diradicals. For example, as we will discuss below, the two degenerate frontier orbitals of square CBD can adopt both unequivocally delocalized (Figure 9, top) and localized forms (Figure 9, bottom).

5.1.1. Diradical and Zwitterionic States. For all diradicals of class 1, a straightforward transformation from the delocalized orbitals, ψ_x and ψ_y (called ψ_H and ψ_L in the beginning of this section) to localized orbitals on different sites of the molecule, χ_a and χ_b , can be performed, e.g., for the rectangular CBD:

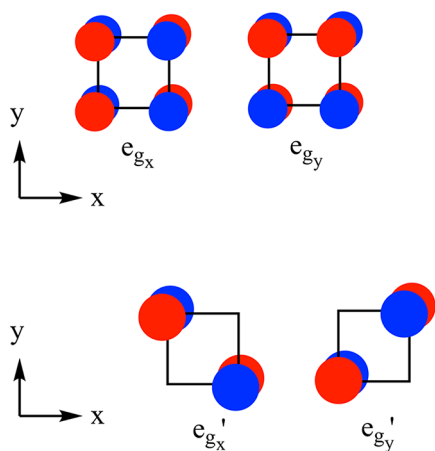


Figure 9. (top) Delocalized pair of degenerate frontier orbitals for CBD (e_{gx} and e_{gy}). e_{gx} has bonding character along the y direction and antibonding character in the x direction. e_{gy} reverses these characteristics. (bottom) Transformed frontier orbitals of square CBD, e_{gx}' and e_{gy}' localized on different, nonadjacent sites of the molecule.

$$\chi_a = e'_{gx} = \sqrt{\frac{1}{2}}(e_{gx} + e_{gy}) = \sqrt{\frac{1}{2}}(\psi_x + \psi_y) \quad (19)$$

$$\chi_b = e'_{gy} = \sqrt{\frac{1}{2}}(e_{gx} - e_{gy}) = \sqrt{\frac{1}{2}}(\psi_x - \psi_y) \quad (20)$$

Please note that the prime of e'_{gx} and e'_{gy} is to differentiate them from the delocalized e_{gx} and e_{gy} , not to denote that they are symmetric with respect to the horizontal symmetry plane. Throughout the paper, we drop the prime and double-prime symbols that label the σ_h -parity of the CBD e_g orbitals because the parity does not play any role in our discussion. Within the previously discussed two-site model, χ_a and χ_b are orbitals perfectly localized on a single site (cf. Figure 8). Beyond the two-site model, these orbitals are localized in the sense that they no longer share a considerable region of space, unlike the original delocalized orbitals (Figure 9). For conceptual simplicity, let us focus our thoughts in the discussion below once more on the two-site situation, although the analysis is completely equivalent expanding beyond this model.

If we substitute ψ_x and ψ_y in eqs 19 and 20 into eqs 1 and 5, then the following is obtained,

$$\begin{aligned} \Psi_{S_{os}} &= \frac{1}{2}[\psi_x(1)\psi_y(2) + \psi_y(1)\psi_x(2)][\alpha(1)\beta(2) \\ &\quad - \beta(1)\alpha(2)] \\ &= \frac{1}{2}[\chi_a(1)\chi_a(2) - \chi_b(1)\chi_b(2)][\alpha(1)\beta(2) - \beta(1)\alpha(2)] \end{aligned} \quad (21)$$

$$\begin{aligned} \Psi_{S_{TC-}} &= \sqrt{\frac{1}{2}}(|\psi_x^2\rangle - |\psi_y^2\rangle) \\ &= \frac{1}{2}[\psi_x(1)\psi_x(2) - \psi_y(1)\psi_y(2)][\alpha(1)\beta(2) - \beta(1)\alpha(2)] \\ &= \frac{1}{2}[\chi_a(1)\chi_b(2) + \chi_b(1)\chi_a(2)][\alpha(1)\beta(2) - \beta(1)\alpha(2)] \end{aligned} \quad (22)$$

Something remarkable has happened here. By transforming from delocalized to localized orbitals, these two states have, in a way, swapped their character. $\Psi_{S_{os}}$, the formal open-shell singlet, which had one electron in each delocalized orbital, turns out to actually be a *zwitterionic* or ionic closed-shell state. For in it the two electrons are on the same site, a or b , and occupy the same localized orbital. $\Psi_{S_{TC-}}$ on the other hand, the formal closed-shell singlet, which had two electrons in a single delocalized orbital, can be viewed as a “diradical state” when it is transformed to localized orbitals; the two electrons in it will always be on different sites, i.e., they avoid each other. The two remaining states, Ψ_T and $\Psi_{S_{TC+}}$, do not undergo a similar character swapping when going from the delocalized to a localized representation, i.e., they are indifferent to the orbital transformation, so that Ψ_T corresponds to a diradical state and $\Psi_{S_{TC+}}$ to a zwitterionic state.

The interchangeability between $\Psi_{S_{os}}$ and $\Psi_{S_{TC-}}$ through orbital transformation was first noted in the very important and pedagogically effective paper by Salem and Rowland mentioned before.⁴

Because we are now working in terms of localized orbitals χ_a and χ_b , it becomes possible to make more definite statements about the relative energy of the different states discussed in the first section. Because the exchange integral will not be large

unless the orbitals involved are in the same region of space, we know that the exchange between two localized orbitals on two different sites, K_{ab} , will be small in general.^{72,73} Furthermore, it should be clear that the Coulomb repulsion between two electrons on the same site (J_{aa} , J_{bb}) will be much higher than the repulsion between two electrons on different sites (J_{ab}). As a result, the two diradical states in the localized representation will be lower in energy than the zwitterionic states (cf. eq 11 and the two boxes in Figure 10), and the spacing between the two states

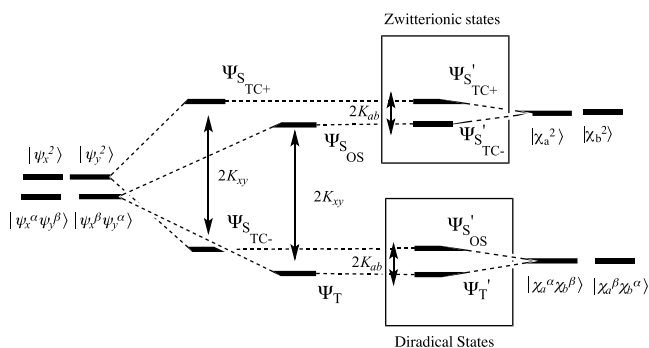


Figure 10. Four states starting from delocalized orbitals on the left and from localized orbitals on the right for diradicals of class 1. K_{ab} is usually small.

(as well as the spacing between the two zwitterionic states) will be small (other effects such as dynamic spin polarization of the core electrons might also prevent the paired states from becoming degenerate).³ Note that the energy of the different states is not affected when transforming from delocalized to localized orbitals (see Figure 10).

As a final comment on the equivalence of the delocalized and localized representations and the resulting duality of both descriptions (see also section 8), we would like to point out some remarkable properties of the integrals appearing in Figure 10 and governing the spacing between the individual states. The exchange integral in the delocalized basis, K_{xy} can straightforwardly be related to the difference between the sum of the two one-site Coulomb integrals J_{aa} and J_{bb} and twice the two site Coulomb integral J_{ab} , i.e., $K_{xy} = 1/4 (J_{aa} + J_{bb} - 2J_{ab})$. In this way, by an orthogonal transformation between localized and delocalized orbitals, an exchange integral, inherently quantum mechanical in nature, is transformed into a combination of Coulomb integrals with a classical, electrostatic interpretation. The resulting combination of Coulomb integrals is proportional to the energy difference between the single determinants associated with covalent and ionic contributions in a VB context.

5.2. Class 2: Diradicals Whose Orbitals Are Inherently Delocalized

For the second class of diradicals, a localization of orbitals in separate atoms is not possible. Two examples of this class of diradicals are O_2 and trimethylenemethane. Although the orbitals can still be transformed as in eqs 19 and 20,

$$\psi_{x'} = \frac{\psi_x + \psi_y}{\sqrt{2}} \quad (23)$$

and

$$\psi_{y'} = \frac{\psi_x - \psi_y}{\sqrt{2}} \quad (24)$$

the resulting orbitals will never be nicely localized on different sites, so that $K_{x'y'}$ will not be small in general. Yet, just like before, the orbital transformation in eqs 23 and 24 leads to a swap in character of $\Psi_{S_{OS}}$ and $\Psi_{S_{TC-}}$.

$$\begin{aligned} \Psi_{S_{OS}} &= \frac{1}{2}[\psi_x(1)\psi_y(2) + \psi_y(1)\psi_x(2)][\alpha(1)\beta(2) - \beta(1)\alpha(2)] \\ &= \frac{1}{2}[\psi_{x'}(1)\psi_{y'}(2) - \psi_{y'}(1)\psi_{x'}(2)][\alpha(1)\beta(2) - \beta(1)\alpha(2)] \end{aligned} \quad (25)$$

$$\begin{aligned} \Psi_{S_{TC-}} &= \sqrt{\frac{1}{2}}(|\psi_x^2\rangle - |\psi_y^2\rangle) \\ &= \frac{1}{2}[\psi_x(1)\psi_x(2) - \psi_y(1)\psi_y(2)][\alpha(1)\beta(2) - \beta(1)\alpha(2)] \\ &= \frac{1}{2}[\psi_{x'}(1)\psi_{y'}(2) + \psi_{y'}(1)\psi_{x'}(2)][\alpha(1)\beta(2) - \beta(1)\alpha(2)] \end{aligned} \quad (26)$$

A consequence of the new orbitals not being fully localized on different sites is that it is less obvious to assign a diradical or zwitterionic nature to the singlet states. Rather, one can say that for diradicals of class 2, a closed-shell/open-shell ambiguity is present and that the use of either of these two terms is only meaningful if the set of degenerate MOs considered is specified.

Even though the orbital transformation does not lead to perfectly localized orbitals for diradicals of class 2, we tend to transform the orbitals (say $\psi_{x'}$ and $\psi_{y'}$) to minimize the exchange integral to express the four states. As a result, the “open-shell” states in terms of the transformed orbitals $\psi_{x'}$ and $\psi_{y'}$ will generally be lower in energy than the “closed-shell” states (the third column in Figure 11). This is consistent with the

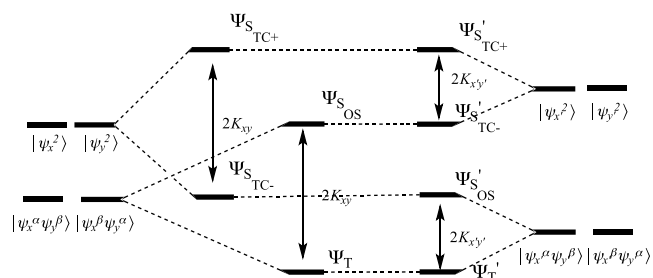


Figure 11. Four states starting from fully delocalized orbitals on the left and from transformed, less delocalized orbitals on the right for diradicals of the second class. Notice the big gap $2K_{x'y'}$ for class 2 diradicals, compared with the small gap $2K_{ab}$ for class 1 diradicals in Figure 10.

electrostatic argument that within the two states related by the transformation, the one that involves more charge-transfer character has higher energy and shall be assigned as a zwitterionic state, while the other will be labeled as a diradical state. The ambiguity is thus reduced. We should note that O_2 is a special case; for this molecule, the exchange integral is invariant with respect to the rotation due to symmetry so that $K_{xy} = K_{x'y'}$, leading to $\Psi_{S_{TC-}}$ and $\Psi_{S_{OS}}$ being degenerate. A similar situation arises for D_{3h} TMM as well. For these molecules, the true closed-shell/open-shell ambiguity occurs.

Transformed orbitals like the ones we have used throughout this section (eqs 19 and 20 and eqs 23 and 24) are often called generalized valence bond (GVB) orbitals. For the first class of diradicals, the two GVB orbitals are localized on different sites

(ergo they are also called localized orbitals; they may still overlap, however, depending on the intersite distance), and for the second class of diradicals, this is not the case.

5.3. Alternative Terminologies

In the previous subsections, we explained that the key difference between the two classes of diradicals above is the ability to localize their singly occupied orbitals on different sites so that they do not share a considerable region of space. This feature is important because it governs the magnitude of the exchange interaction $K_{ab}/K_{x'y'}$. It is exactly this realization which inspired Borden and Davidson to name the two classes of diradicals “disjoint” and “joint” (or “non-disjoint”), respectively.³ “Disjoint” diradicals are those whose singly occupied orbitals can be localized on different sites, i.e., on disjoint sets of atoms (leading to a small exchange interaction K_{ab} , i.e., class 1 diradicals); “joint” diradicals are those whose orbitals cannot be localized in such a way (leading to a non-negligible exchange interaction $K_{x'y'}$, i.e., class 2 diradicals). As a side note, similar ideas as the joint/disjoint concept, borrowed from graph theory, were used by Ovchinnikov to prove a remarkable theorem concerning the ground state spin multiplicity of large alternant organic hydrocarbons and the existence of organic ferromagnets.⁷⁴

Additionally, we note here that in their landmark paper, Salem and Rowland used a different classification system. Instead of distinguishing between localizable (disjoint) and nonlocalizable (nondisjoint) diradicals, they focused on the symmetry of the orbitals and distinguished between homosymmetric, heterosymmetric, and nonsymmetric diradicals. The identification of zwitterionic and diradical states ensues naturally.⁴

In the description of the different types of diradicals in this section, we have tried to combine the two points of view and classification methods. We adopted the dichotomy of Borden and Davidson,³ which enables the straightforward assignment of the spin multiplicity of the ground state of diradicals while holding on to the detailed consideration of the nature of the different states (diradical/zwitterionic) found in the work by Salem and Rowland.⁴

6. ANOTHER VIEW OF DIRADICALS

In the first section, we started by stating that the characteristic feature of diradicals is that they have a pair of degenerate orbitals in which two electrons reside. However, some electron paramagnetic resonance (EPR)/electron spin resonance (ESR) spectroscopists take a slightly different definition. They consider species as diradicals only when an ESR spectrum characteristic of two doublet states instead of a triplet state is obtained for them. This corresponds to the two diradical states being degenerate. The upside of this reasoning is that an objective and experimentally measurable criterion for diradicals is used. However, as we noted in the preceding section, only true diradicals of the first class ($K_{xy} \approx 0$) comply to this definition. The second class of diradicals never will. Therefore, we consider such a spectroscopic definition as too strict.

Organic chemists generally take a different view. They will consider all molecules with a triplet ground state as diradicals, even though this does not always mean that two frontier orbitals will be degenerate (cf. carbenes). This line of thinking originates from the distinct reactivity of triplet species compared to traditional closed-shell molecules; for instance, their stereoselectivity, or lack of it, becomes essential. Because the main focus of this work is reactivity, we broaden our definition of

diradicals slightly in the remainder of this work. From now on, the term “diradical” will refer to all molecules that have (pseudo)degenerate HOMO and LUMO as well as all molecules that have a triplet ground state.

7. THE CLOSED-SHELL/OPEN-SHELL AMBIGUITY FOR DIRADICALOIDS

In section 5, a closed-shell/open-shell transformation for diradicals, with an attendant ambiguity, was discussed. That is, from a mathematical perspective, the set of MOs must be specified before referring to a state as open-shell or closed-shell. A similar ambiguity exists for the ground state of diradicaloids ($\Psi_{\text{src-}}$). As discussed before, diradicaloids have singlet ground states, represented by two-configuration wave functions. These two configurations are closed-shell configurations based on the often-delocalized MOs (HOMO and LUMO). Note that it is possible to define GVB orbitals for diradicaloids, in the same way as it was done for diradicals in the previous section (although the transformation is now no longer orthogonal),

$$\Psi_{x'} = \sqrt{c_1} \psi_H + \sqrt{c_2} \psi_L \quad (27)$$

and

$$\Psi_{y'} = \sqrt{c_1} \psi_H - \sqrt{c_2} \psi_L \quad (28)$$

This way, $\Psi_{\text{src-}}$ will become an open-shell state when expressed in terms of GVB orbitals,

$$\begin{aligned} \Psi_{\text{src-}} &= c_1 |\psi_H^2\rangle - c_2 |\psi_L^2\rangle \\ &= \frac{1}{\sqrt{2}} [c_1 \psi_H(1) \psi_H(2) - c_2 \psi_L(1) \psi_L(2)] [\alpha(1) \beta(2) \\ &\quad - \beta(1) \alpha(2)] \\ &= \frac{1}{2\sqrt{2}} [\psi_{x'}(1) \psi_{y'}(2) + \psi_{y'}(1) \psi_{x'}(2)] [\alpha(1) \beta(2) \\ &\quad - \beta(1) \alpha(2)] = \Psi'_{\text{SOS}} \end{aligned} \quad (29)$$

Note that in the limit of an infinitely big HOMO–LUMO gap ($c_1 = 1$; $c_2 = 0$), eq 29 will collapse to a single closed-shell configuration. This is also manifested by the overlap between $\psi_{x'}$ and $\psi_{y'}$:

$$\langle \psi_{x'} | \psi_{y'} \rangle = c_1 - c_2 \quad (30)$$

Under the normalization constraint $c_1^2 + c_2^2 = 1$, when $\langle \psi_{x'} | \psi_{y'} \rangle = 1$, $c_1 = 1$, and $c_2 = 0$; when $\langle \psi_{x'} | \psi_{y'} \rangle = 0$, $c_1 = \sqrt{\frac{1}{2}}$ and $c_2 = \sqrt{\frac{1}{2}}$. Therefore, perfect overlap between $\psi_{x'}$ and $\psi_{y'}$ gives a closed-shell and perfect orthogonality gives a diradical. This orthogonality reflects the tendency of two electrons to avoid each other, a strong correlation (i.e., nondynamical correlation). The configurational coefficients (i.e., the orbitals' overlap) point to a measure of diradical character, hardly the only such measure, as we will see later on in section 13.

A final note we would like to make in this paragraph is that the classification of diradicals in 2 classes can also be extended to diradicaloids. In perfect analogy to the diradical situation, if the HOMO and LUMO orbitals in the diradicaloid can be transformed to (almost) disjoint, localized orbitals, we are dealing with a diradicaloid of class 1, when this is not the case, we end up in class 2. Note that according to eq 30, the (perfect) localization of the GVB orbitals observed in class 1 diradicals is

gradually reduced as the degeneracy of the frontier orbitals is broken and one moves toward a diradicaloid of class 1.

A well-known example of this breakdown of the localization picture is H_2 in its bonding limit. At this limit, we can still transform the HOMO and LUMO so that the resultant localized orbitals resemble the 1s atomic orbitals. However, the 1s-like orbital on one H atom must have an orthogonalization tail extended to the other atom. These orbitals are not disjoint as in the dissociation limit. In this sense, the classification becomes less meaningful as the HOMO–LUMO gap increases. This is reasonable because the larger gap brings us closer to the closed-shell zone in Figure 7.

8. DOES THE AMBIGUITY REALLY MATTER?

In the previous sections, we have considered the orbital transformations between a localized and delocalized perspective at length and we have stressed the existence of an inherent closed-shell/open-shell ambiguity. In mathematical terms, this ambiguity is absolute; neither of the two perspectives is more “right” or “wrong” than the other. In practice, however, one can argue that in many situations it is “natural” to discuss the diradical character of species using a specific set of orbitals (the localized ones). The justification for such a preferential set of orbitals is then inherently rooted in purely physical (rather than mathematical) arguments.

For example, for class 1 diradicals and diradicaloids, whose HOMO and LUMO can be unambiguously localized on different atoms or sites, the localized orbitals are the most appropriate to use for the expression of the open-shell singlet and two-configuration states. This is consistent with the traditional perspective of bonding between two unpaired electrons in the originally localized, nonbonding orbitals; when the bonding is weak, one ends up with a diradicaloid/diradical. This localized perspective for class 1 diradicals perhaps aligns better with the term “diradical”, i.e., two radicals, two unpaired electrons in two (localized) orbitals in the lowest singlet or triplet states. In contrast, in a delocalized perspective, the two electrons are formally paired in the lowest singlet wave function.

For class 2 diradicals and diradicaloids, the preferred set of orbitals is less obvious. One logical choice is to use the orbitals that minimize the Ψ_{SOS} energy, and correspondingly maximize the $\Psi_{\text{STC-}}$ energy. As mentioned above, this choice is based on the electrostatic argument that it takes energy to transfer an electron from one site to another, and therefore, $\Psi_{\text{STC-}}$ with higher energy is more naturally considered as a charge-transfer or a zwitterionic state. The corresponding lower-lying Ψ_{SOS} is hence an open-shell configuration with the two unpaired electrons on the two sites, which may nevertheless be highly delocalized.

True ambiguity occurs for species whose Ψ_{SOS} and $\Psi_{\text{STC-}}$ are degenerate, irrespective of any orbital transformation. Most often this is a consequence of symmetry; typical examples are O_2 and TMM in D_{3h} structure. In reality, when such a molecule is embedded in a chemical environment, for instance, when it is interacting with another approaching molecule, the symmetry is broken and such a degeneracy will be lifted; we may hence unambiguously assign open-shell and zwitterionic singlet states. The definition of open-shell and zwitterionic singlet states in a chemical environment is case-specific. Elaborations on this subject will be seen in sections 10–12 below.

We stress that the delocalized point of view is by no means mathematically incorrect, so that it is perfectly fine to switch back and forth between the two perspectives in specific circumstances. We will see for example that for the study of the reactivity of diradical(oid) compounds, which is the subject of the next few sections, the localized view is most convenient for understanding radical-type reactivity such as H atom abstractions and radical additions, whereas the delocalized point of view is more suitable for understanding closed-shell type reactivity such as Lewis acid/base reactions or concerted pericyclic reactions.

When in succeeding sections, we turn to the reactivity of singlet diradical(oid), the ambiguity becomes more than an arbitrary orbital transformation, and turns into a duality. It allows the molecule to react like a closed-shell species, e.g., in concerted pericyclic reactions, **and** as an open-shell species, e.g., in stepwise reactions. We call this dual reactivity of singlet diradical(oid)s the closed-shell/open-shell duality. On the contrary, triplet diradicals that are described unambiguously by an open-shell wave functions only react in stepwise manner.

The closed-shell/open-shell ambiguity does not play any role in judging whether a molecule is a diradical or how diradical-like it is. One may freely choose to write the singlet ground state wave function of H_2 in its dissociation limit in the Ψ_{SOS} or the $\Psi_{\text{STC-}}$ form. But the $\Psi_{\text{STC-}}$ form does not disguise the system as a closed-shell system. As a matter of fact, none of the measures of diradical character that we discuss in section 13 is obscured or led astray by the ambiguity. In short, while this ambiguity of mathematical nature offers alternative perspectives in studying reactivities of diradical(oid)s, it does not manifest itself in chemical or physical observables.

The duality we have explored in this section is one of a number of seemingly contradictory situations science encounters, in which two (or more) views of a physical or chemical phenomenon seem to have different consequences. The complementarity principle, perhaps first voiced in its generality by Niels Bohr,^{75,76} allows us to come to peace with this situation. The classic locus of discussion is the wave-particle duality; to this Bohr added the observables linked by Heisenberg’s uncertainty principle—position/momentum, energy/time, as well as others. Here is what Niels Bohr writes:⁷⁷

“Within the scope of classical physics, all characteristic properties of a given object can in principle be ascertained by a single experimental arrangement, although in practice various arrangements are often convenient for the study of different aspects of the phenomena. In fact, data obtained in such a way simply supplement each other and can be combined into a consistent picture of the behaviour of the object under investigation. In quantum mechanics, however, evidence about atomic objects obtained by different experimental arrangements exhibits a novel kind of complementary relationship. Indeed, it must be recognized that such evidence which appears contradictory when combination into a single picture is attempted, exhaust all conceivable knowledge about the object. Far from restricting our efforts to put questions to nature in the form of experiments, the notion of complementarity simply characterizes the answers we can receive by such inquiry, whenever the interaction between the measuring instruments and the objects form an integral part of the phenomena.”

Focusing on chemistry, one could add the well-known and long-standing discussions of localized vs delocalized orbitals or

the controversy around the use of valence bond vs molecular orbital descriptions.^{78,79} Even within the MO description, it has been known for decades that the solutions of the molecular Hartree–Fock equations, the canonical molecular orbitals, which are delocalized in nature, can be subject to a unitary transformation, without altering (up to a phase factor) the total molecular (monodeterminantal) wave function.²⁶ Within this context, several localization procedures have been put forward already many years ago, yielding a transformation matrix retrieving inner shells, lone pairs, and two-center bonds.^{80,81} The duality of these two descriptions has been exploited to discuss different types of molecular properties, e.g., ionization phenomena and electronic transitions (invoking Koopmans theorem) for canonical orbitals,²⁶ and, e.g., hybridization characteristics of lone pairs and two center bonds with localized orbitals.⁸² We also note the duality of interpretation of a critical energy gap in section 5.1.1 as being determined by either an exchange integral between delocalized orbitals or a sum of Coulomb integrals between localized functions.

In further sections of this paper, we will show that the open-shell/closed-shell duality in fact allows us to discuss intelligently the full complexity of diradical and diradicaloid reactions.

9. RADICAL REACTIVITY

In the Introduction, we already mentioned the typical reactivity of simple radicals, quite distinct from that of ordinary closed-shell molecules. Three types of reactions, all facile (unless retarded in ways we will mention), are generally regarded as characteristic for radicals:^{1,83,84} dimerization, addition to olefins, and hydrogen (or halogen) atom abstraction. The goal of this section is to provide numerical values for the barriers of such reactions for some prototype radicals ($\text{H}\bullet$ and $\bullet\text{CH}_3$, both simple doublet species) to serve as a comparison standard for the ensuing investigation of the reactivity of diradicals.

Prototype examples of the characteristic types of reactions mentioned above have been selected, namely dimerization, addition to ethylene, and hydrogen abstraction from SiH_4 . The activation energies, as well as reaction energies/enthalpies, for these three reactions can be found in Table 1 for $\text{H}\bullet$ and $\bullet\text{CH}_3$.

Table 1. Activation Energies, ΔE^\ddagger , and Reaction Energies, ΔE , in kcal/mol, for Typical Reactions of $\text{H}\bullet$ and $\bullet\text{CH}_3$, Calculated at the (U)CCSD(T)/cc-pVTZ//((U)B3LYP/cc-pVTZ Levels of Theory

reaction label	reaction	ΔE^\ddagger	ΔE
A	$\text{H}\bullet + \text{H}_2\text{C}=\text{CH}_2 \rightarrow \text{H}_3\text{C}-\text{CH}_2\bullet$	2	-40
B	$\text{H}_3\text{C}\bullet + \text{H}_2\text{C}=\text{CH}_2 \rightarrow \text{CH}_3-\text{H}_2\text{C}-\text{CH}_2\bullet$	7	-27
C	$\text{H}\bullet + \bullet\text{H} \rightarrow \text{H}_2$	0	-108
D	$\text{H}_3\text{C}\bullet + \bullet\text{CH}_3 \rightarrow \text{H}_3\text{C}-\text{CH}_3$	0	-96
E	$\text{H}\bullet + \text{SiH}_4 \rightarrow \text{H}_2 + \text{H}_3\text{Si}$	5	-14
F	$\text{H}_3\text{C}\bullet + \text{SiH}_4 \rightarrow \text{CH}_4 + \text{H}_3\text{Si}\bullet$	9	-16

Throughout this paper, reactivity is gauged through activation energies. In the absence of dynamic simulations, we are unable to estimate preexponential factors in the expressions for rate constants.

The calculated values presented in Table 1 are in line with the activation energies, BDEs, and reaction energies/enthalpies found in the literature. For example, for the addition of hydrogen to ethylene (reaction A), theoretical values of 1.8 kcal/mol⁸⁵ and experimental values of 2.04 kcal/mol⁸⁶ have been reported for the activation energy. For the addition of a methyl radical to

ethylene (reaction B), a range of experimental values between 6.5 and 8.9 kcal/mol⁸⁷⁻⁹¹ and computational values ranging from 6.9 to 9.2 kcal/mol^{92,93} have been reported. For reactions C and D, experimental BDE values of 104 kcal/mol (for H_2) and 85 kcal/mol (for ethane C–C bond) can be found.⁹⁴ The activation energy for the abstraction of hydrogen from SiH_4 by a hydrogen radical has been experimentally determined at 4.1 kcal/mol,⁹⁵ whereas the abstraction by a methyl radical was reported to require an activation energy of 6.9–7 kcal/mol.⁹⁵⁻⁹⁷

All this data unequivocally supports the initial description of the chemistry of radicals—radicals are reactive.

The two examples that formed our focus up to this point feature completely (in the case of $\text{H}\bullet$) or greatly (in the case of $\bullet\text{CH}_3$) “unhindered” radical sites; the radical electrons are accessible and capable of wreaking havoc on any compound that happens to approach them, with very small barriers to reaction, easily overcome under ambient conditions. All the barriers mentioned above can be raised, dramatically so, either by adding steric encumbrance,⁹⁸⁻¹⁰¹ or by stabilizing the radicals electronically, or a combination of these two strategies. The electronic strategy often consists of the introduction of delocalization, leading to what in VB language would be termed resonance stabilization.¹⁰² Next to the simple incorporation of the radical center in a conjugated system, other approaches have also been proposed to this end. A notable and dramatic example is merostabilization (i.e., the stabilization due to the simultaneous interaction of both electron-donating and electron-accepting substituents with the same radical center, also known as the captodative effect).^{103,104} Furthermore, the partial delocalization of radical electrons to heteroatoms, down Mendeleev’s table, also tends to stabilize monoradicals. Sulfur, for example, has been used extensively in the design of persistent radicals.¹⁰⁵⁻¹⁰⁸ The reactivity of radicals (and the ways of decreasing it, mentioned above) is widely utilized chemically as well as biologically.^{83,109,110}

Still another way to stabilize radicals is to provide destabilization features in their reaction products: the kinetic persistence of aminoxyls, hydrazyls, and verdazyls with respect to dimerization stems from such causes.¹¹¹

As a side note, we should mention that our discussion of radical reactivity is mainly limited to compounds containing main-group elements. Transition metals are known to lead to relatively stable radicals due to their lower electronegativity compared to main-group elements and the availability of low-energy orbitals to accept electrons.¹¹² As signaled before, diradical transition metal complexes, as interesting as they are, fall beyond the scope of this work. Transition metal centers also provide ways to efficiently couple radical sites; the work of the Brown group is a clear introduction to this field.¹¹³

In the next few sections, the activation energies for the three characteristic radical reactions introduced in this section for $\text{H}\bullet$ and $\bullet\text{CH}_3$ will be determined for selected diradicals and compared to a corresponding monoradical analogue. The diradical/monoradical pairs compared will be structurally diverse, with examples of both the first and the second class of diradicals studied.

10. DIRADICAL AND DIRADICALOID REACTIVITY

10.1. Introduction and Expectations

The nature of the isolated diradical or diradicaloid itself, whether it is a singlet or a triplet ground state, is a question that has intrigued the chemical community for over 50 years and how

that ground state may be tuned. Our interest in the following sections is directed elsewhere, to reactivity. In the next few sections, we will address computationally, with ample references to experiment, two interesting questions regarding the reactivity of diradicals:

1. Is a diradical more or less reactive than a closely related monoradical? and
2. What is the difference, if any, in reactivity between the triplet and singlet states of a diradical?

If we have a molecule with two unpaired electrons, and if the two unpaired electrons are far away from each other, i.e., little Coulomb interaction J_{xy} , and even less exchange interaction K_{xy} between the two unpaired electrons, we would expect that each unpaired electron reacts independently as a monoradical (Figure 12). When the two unpaired electrons are close to each other,

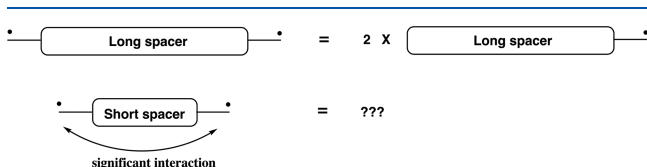


Figure 12. Would the interaction between the two radical centers in a diradical influence the reactivity of each center?

would one electron affect the reactivity of the other electron? How do the modified Coulomb and exchange interactions impact reactivity?

To approach these questions, we examine the potential energy surfaces (PESs) of four sets of reactions (Figure 13). For each

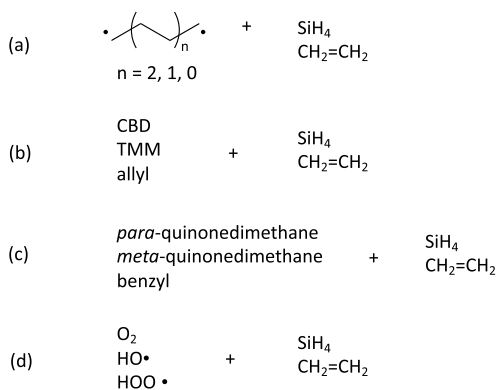


Figure 13. Reactions examined. CBD, cyclobutadiene; TMM, trimethylenemethane, $C(CH_2)_3$.

set, we compare the calculated barriers and reaction energies of two or three model reactions (addition to ethylene and H-abstraction from SiH_4 and sometimes dimerization) of diradicals with those of monoradicals. Both the lowest singlet and triplet states of a diradical are considered. Calculations on reactions in set (a) for reactions of alkyl chain linked diradicals with spacers of different length are expected to answer the question of how the interaction between the two radical centers affects the reactivity of each individual radical center. With set (b), we study reactions of diradicals of class 1 and class 2, respectively, and with set (c), a diradical of class 2 and a closely related diradicaloid. Finally in set (d), we will look at dioxygen, a very special and important diradical (belonging to class 2 as well).

Before diving into the calculations, a word on the expectations. Diradicals in their triplet states, with two singly occupied MOs, are expected to engage in similar reactions as monoradicals that usually involve the unpaired electron in the singly occupied orbitals. It seems rare, from what we see in the literature, that the two unpaired electrons in a triplet diradical participate simultaneously in a reaction.

Singlet diradicals can, in principle, behave much as triplet diradicals or monoradicals do, undergoing ethylene addition and H-abstraction, with, perhaps, different barriers. Singlet diradicals do have other, quite distinct, reaction modes available to them as well. We expect that they can engage in concerted reactions, in which the two formally unpaired electrons react simultaneously, forming two new bonds at once. This is because the two electrons with opposite spins are prone to couple and react like a pair. Further diversity in singlet reactivity arises from the fact that there are three singlet electronic configurations (derived, as we saw, from the two orbitals and two electrons space of a diradical) that can participate in reactions. On the contrary, there is only one triplet configuration (see Figure 5). Singlet diradicals can also fragment, driven by the formation of more stable, closed-shell molecules. For example, singlet butane-1,4-diyl ($\bullet CH_2CH_2CH_2CH_2\bullet$) can form two ethylenes in its ground state.¹¹⁴ Such a fragmentation is spin-allowed in the singlet manifold but disallowed in the triplet manifold.

These distinct reaction modes for singlet diradicals arise from the special interaction of the two radical centers in a singlet diradical. The feasibility of such interaction, a kind of quantum mechanical coherence, is subject to the constraints of geometry, orbital symmetry factors, and the relative stability of the diradical and closed-shell forms, which we will discuss in detail later on.

10.2. Alkyl Chain Diradicals

To bridge diradicals to monoradicals, we start by considering a class of compounds in their triplet states consisting of two radical centers connected through an *all-trans*-methylene linker of varying length, ${}^3\bullet CH_2-(CH_2-CH_2-)_nCH_2\bullet$ (Figure 14). The singlet states of these compounds may undergo barrierless fragmentation into ethylenes and/or cyclization to cyclic alkanes in certain conformations. We will return to these escape routes.

The optimal structures for the triplet states of these compounds have C_i or C_2 symmetry with all the carbon atoms coplanar; the hydrogen atoms of the terminal methylenes are neither in the plane containing all carbon atoms nor in the perpendicular plane. The angle (Φ) between the carbon plane and the plane containing a terminal methylene is calculated to fall in the range of 27° – 35° for all molecules, except for twisted ethylene where there is no carbon plane, and Φ denotes the angle between the two ethylene planes ($\Phi = 90^\circ$). The local p_z orbitals at the termini, containing the unpaired electrons, are therefore at angles of 55° – 63° to the plane of the saturated carbon chain. However, the preference is not great; the energy involved in rotating the terminal methylenes so that $\Phi = 0^\circ$ is <1 kcal/mol for $n = 1, 2, 3$. Clearly, the noncoplanarity of terminal ethylenes has no chemical significance.

For the longest alkyl chain diradical considered, ${}^3\bullet CH_2-(CH_2-CH_2-)_3CH_2\bullet$, the two radical centers do not interact/communicate in the optimized geometry. Consistent with this is the observation that the lowest singlet and triplet states are calculated to be (almost) exactly degenerate and that the energies of the degenerate delocalized MO orbitals are equal in the triplet state. The triplet state is appropriate for judging the orbital splitting, for in it the two orbitals occupied each by a

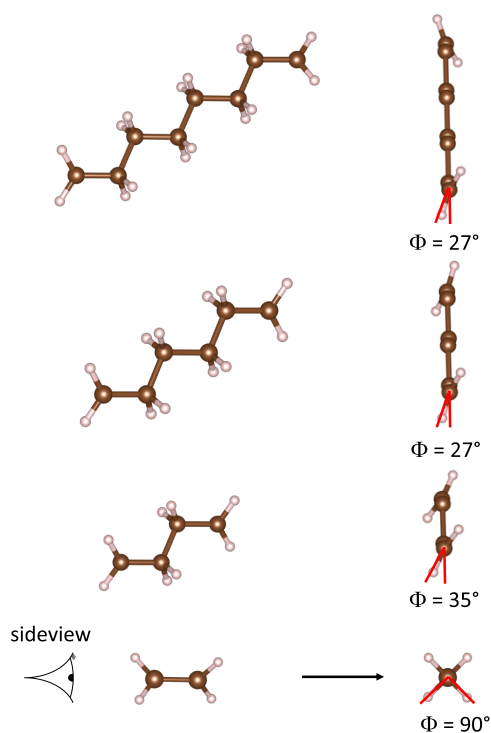


Figure 14. Optimized geometries for the triplet state of the alkyl chain diradicals with varying linker length, ${}^3\bullet\text{CH}_2-(\text{CH}_2-\text{CH}_2)_n\text{CH}_2\bullet$ ($n = 3, 2, 1, 0$). The angle between one terminal methylene plane and the carbon plane (Φ) is presented below each structure, which is given in two views (only the hydrogens on terminal CH_2 are shown on the right panel).

single electron are treated equally by the theory. As the linker becomes shorter, the two radical centers approach and the amount of communication between the centers increases (Table 2).

Consider, for example, triplet tetramethylene ${}^3\bullet\text{CH}_2-\text{CH}_2-\text{CH}_2-\text{CH}_2\bullet$; the energy splitting between the singly occupied orbitals for this compound amounts to 3 kcal/mol in its optimal geometry. This is not much, but this value can be increased considerably, to 17 kcal/mol, by twisting the radical centers to the point where the terminal p_z -orbitals are coplanar with the alkyl carbon σ -system ($\Phi = 90^\circ$). In this way, through-bond coupling can set in as a complement to any through-space interaction.^{115–117} In this orientation, the antisymmetric (A) combination of the p_z -orbitals mixes with the σ^* orbital of the middle C2–C3 bond, whereas the symmetric (S) combination

of the terminal p_z -orbitals mixes with the C2–C3 σ orbital, resulting in a stabilization of the A combination of orbitals and a destabilization of the S combination (Figure 15). The data in

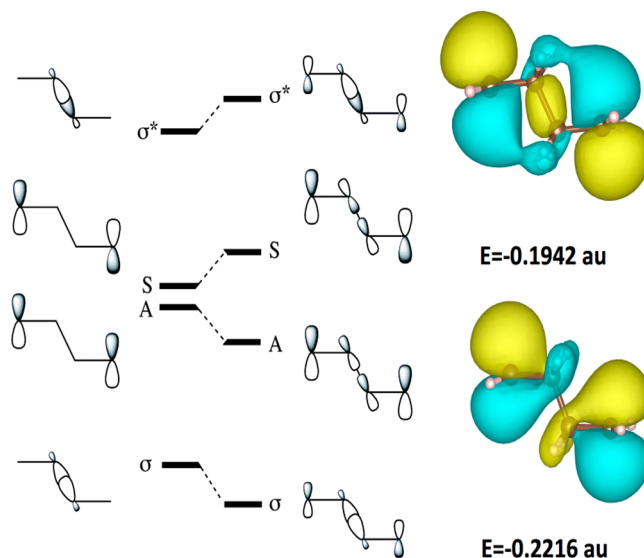


Figure 15. Through-bond coupling of the two radical orbitals via the middle C–C σ -bonds in ${}^3\bullet\text{CH}_2-\text{CH}_2-\text{CH}_2-\text{CH}_2\bullet$.¹¹⁶ The symmetric (S) and antisymmetric (A) combinations of the radical orbitals, with respect to the 2-fold rotation axis or the inversion center, have the right symmetry to interact with the σ and σ^* C–C MOs, respectively. The interaction diagram shows orbital energy changes when the through-bond interaction is turned on. The isosurfaces at 0.04 au of the singly occupied MOs calculated at UB3LYP/cc-pVTZ level of theory are presented on the right-hand side.

Table 2 clearly indicate that a similar phenomenon is present for all the other diradicals connected by a dimethylene ($-(\text{CH}_2\text{CH}_2)_n$) linker considered here, though for none of them is the effect of the through-bond coupling as pronounced as it is for ${}^3\bullet\text{CH}_2-\text{CH}_2-\text{CH}_2-\text{CH}_2\bullet$. The through-bond coupling phenomenon, with its exquisite and understood conformational dependence, has many ramifications; we (reluctantly) avoid discussing these here.

In the same geometry where the through-bond interaction is maximal, the electronic structure of the “closed-shell” singlet state of tetramethylene is described by a major configuration with two electrons in the A orbital (Figure 15) and a minor configuration with the electrons in the S orbital. The antibonding C2–C3 σ^* interaction in the (doubly occupied)

Table 2. Energy Splitting between the Two Singly Occupied Orbitals in the Triplet State of the Diradicals with a Varying CH_2 -Linker Length, (Calculated at UB3LYP/cc-pVTZ Level of Theory) and the Adiabatic Singlet-Triplet Gap ΔE_{ST} (Calculated at CASPT2(2,2)/cc-pVTZ Level of Theory; for ${}^1\bullet\text{CH}_2-\text{CH}_2\bullet$ and $\bullet\text{CH}_2-\text{CH}_2-\text{CH}_2\bullet$, the geometries were restricted to D_{2d} and C_{2v} Symmetry, Respectively, Instead of Allowing a Complete Relaxation^a

	orbital splitting in optimal geometry (kcal/mol)	orbital splitting in geometry with optimal coupling (kcal/mol)	ΔE_{ST} (kcal/mol)
${}^3\bullet\text{CH}_2-(\text{CH}_2-\text{CH}_2)_3\text{CH}_2\bullet$	0	3	0
${}^3\bullet\text{CH}_2-(\text{CH}_2-\text{CH}_2)_2\text{CH}_2\bullet$	0	6	0
${}^3\bullet\text{CH}_2-\text{CH}_2-\text{CH}_2-\text{CH}_2\bullet$	3	17	1
${}^3\bullet\text{CH}_2-\text{CH}_2-\text{CH}_2\bullet$	13	20	0.9 (C_{2v} geometry)
${}^3\bullet\text{CH}_2-\text{CH}_2\bullet$	0 (D_{2d} geometry)	139 (D_{2d} geometry)	-0.1 (D_{2d} geometry)

^aBoth the optimal geometry (almost no through-bond coupling) and the geometry with optimal through-bond coupling ($\Phi = 0^\circ$) were considered. Negative numbers for ΔE_{ST} indicate that the singlet state is lower in energy than the triplet.

A orbital leads to barrierless fragmentation of this molecule into two ethylenes in their ground states, releasing 41–42 kcal/mol energy. This fragmentation is a common pathway, an “escape channel” shared by all even-carbon-chain diradicals considered here, realizable through C–C single bond rotations into a conformation favoring the through-bond interaction.^{117–119}

To study the reaction of singlet tetramethylene (and other alkyl chain diradicals) with SiH₄ and ethylene, we chose an *all-trans* conformation that is a minimum on the PES ($\Phi = 35^\circ$ for tetramethylene) and at the same time disfavors the through-bond interaction in order to avoid the spontaneous fragmentation into ethylenes. However, we should note that the resulting diradical geometries are not the global minima of the corresponding $\bullet\text{CH}_2(\text{CH}_2)_n\text{CH}_2\bullet$ species, closed-shell rings are. For instance, Sirjean and his co-workers determined the *trans* geometry of the $\bullet\text{C}_4\text{H}_8\bullet$ diradical to be a local minimum on the PES of this system, separated from a lower energy *gauche* geometry by a barrier of a few kcal/mol,¹²⁰ and that geometry is much higher in energy than cyclobutane. See also the ancient discussion of the tetramethylene diradical by Hoffmann et al.¹¹⁷ The *trans* geometries of the diradical species considered here nevertheless serve us as model systems for the interaction of radical sites.

Trimethylene, $\bullet\text{CH}_2\text{—CH}_2\text{—CH}_2\bullet$, is a special case that has kept the organic community intrigued for years.^{121–124} The collapse product of the diradical is, of course, cyclopropane. The $\Phi = 0^\circ$ geometry is a local minimum. In it, the S and A combinations, with respect to the mirror plane exchanging C1 and C3 (Figure 16), are split in energy by some 13 kcal/mol

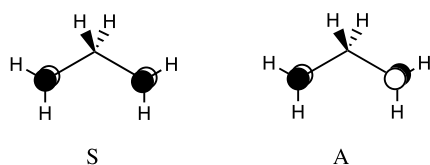


Figure 16. Symmetric (S) and antisymmetric (A) combinations of the radical orbitals, with respect to the mirror plane, of trimethylene.

(Table 2), with the S combination higher as a result of interaction with the central CH₂ π -type σ orbitals.^{116,125} Substitution at C2 can be used to tune this splitting dramatically;¹²⁶ once again, we struggle to avoid digression on this fascinating story.

In a final step, one can remove the alkyl linker altogether and connect the methyl radicals directly, resulting in the formation of an ethylene molecule. In a planar ethylene, the p_z -orbitals of course overlap significantly, leading to π bond formation. However, as mentioned before, the diradical situation can be recovered for this molecule by twisting the two p_z -orbitals out of plane; in the resulting D_{2d} geometry, the overlap integral between them is zero,¹²⁷ leading to exact degeneracy between the formally bonding and antibonding but essentially non-bonding combinations (cf. bottom entry of Table 2).

In their pioneering work on diradicals, Salem and Rowland reasoned that K_{xy} , the exchange interaction between the localized p_z -orbitals on the two sites of the 90° -twisted ethylene, should be substantial, based on the reported ΔE_{ST} of 8 kcal/mol, favoring the triplet state. The calculations which led to this value were performed in the 1960s.¹²⁸ More recent calculations, carried out within the framework of this study, as well as by others,¹²⁹ cast doubt on the accuracy of this result. Instead of 8 kcal/mol, values for ΔE_{ST} close to 0 kcal/mol were obtained at

the (2,2)CASPT2 level of theory. Thus, K_{xy} is actually small for D_{2d} twisted ethylene, in keeping with the predictions for diradicals of class 1. Incorporation of the electron correlation between the $2p-\pi$ MOs and the σ bond causes the singlet state to drop only slightly below the triplet state (± 1 kcal/mol).^{129,20}

Let us now turn to the reactivity of the set of alkyl chain diradical compounds discussed above. In a first step, the reaction barriers and energies of the model abstraction and addition reaction were computed for the triplet states and compared to the monoradical analogues (Table 3). In a next step, the

Table 3. Comparison of the Activation Energies (ΔE^\ddagger) and Reaction Energies (ΔE) in kcal/mol of H Abstraction from SiH₄ and Addition to Ethylene for $^3\bullet\text{CH}_2\text{—CH}_2\bullet$, $^3\bullet\text{CH}_2\text{—CH}_2\text{—CH}_2\bullet$, $^3\bullet\text{CH}_2\text{—(CH}_2\text{—CH}_2\text{—)}_2\text{CH}_2\bullet$, $^3\bullet\text{CH}_2\text{—(CH}_2\text{—CH}_2\text{—)}_3\text{CH}_2\bullet$, and Their Monoradical Analogues^a

	H abstraction from SiH ₄		addition to ethylene	
	ΔE^\ddagger	ΔE	ΔE^\ddagger	ΔE
$^3\bullet\text{CH}_2\text{—(CH}_2\text{—CH}_2\text{—)}_3\text{CH}_2\bullet$	9	−13	6	−26
$\text{CH}_3\text{—(CH}_2\text{—CH}_2\text{—)}_3\text{CH}_2\bullet$	9	−13	6	−26
$^3\bullet\text{CH}_2\text{—(CH}_2\text{—CH}_2\text{—)}_2\text{CH}_2\bullet$	9	−13	6	−26
$\text{CH}_3\text{—(CH}_2\text{—CH}_2\text{—)}_2\text{CH}_2\bullet$	9	−13	6	−26
$^3\bullet\text{CH}_2\text{—CH}_2\text{—CH}_2\text{—CH}_2\bullet$	9	−13	6	−26
$\text{CH}_3\text{—CH}_2\text{—CH}_2\text{—CH}_2\bullet$	9	−13	6	−26
$^3\bullet\text{CH}_2\text{—CH}_2\bullet$	10	−13	6	−25
$\text{CH}_3\text{—CH}_2\bullet$	9	−13	6	−25

^aCalculations were done at the (U)CCSD(T)/cc-pVTZ/(U)-B3LYP/cc-pVTZ level of theory.

reactivity of the singlet and triplet states for D_{2d} twisted ethylene and $^3\bullet\text{CH}_2\text{—CH}_2\text{—CH}_2\text{—CH}_2\bullet$ were determined for both reactions; these values can be found in Table 4. We did not

Table 4. Comparison of the Activation Energies (ΔE^\ddagger) and Reaction Energies (ΔE) in kcal/mol of H Abstraction from SiH₄ and Addition to Ethylene for the Singlet and Triplet States of $\bullet\text{CH}_2\text{—CH}_2\bullet$ and $\bullet\text{CH}_2\text{—CH}_2\text{—CH}_2\text{—CH}_2\bullet$ ^a

	H abstraction from SiH ₄		addition to ethylene	
	ΔE^\ddagger	ΔE	ΔE^\ddagger	ΔE
$^3\bullet\text{CH}_2\text{—CH}_2\text{—CH}_2\text{—CH}_2\bullet$	9	−13	8	−26
$^1\bullet\text{CH}_2\text{—CH}_2\text{—CH}_2\text{—CH}_2\bullet$	8	−13	6	−25
$^3\bullet\text{CH}_2\text{—CH}_2\bullet$	9	−13	7	−27
$^1\bullet\text{CH}_2\text{—CH}_2\bullet$	9	−13	7	−26

^aCalculations were done at CASPT2(4,4)/cc-pVTZ level of theory.

study diradical dimerization in detail here; in general, it is barrierless. This is in a special approaching geometry; in a Gibbs energy calculation, entropy factors would be influential.

From Table 3 and Table 4, it is clear that the presence of a second radical center does not influence much the reactivity of the compounds considered, irrespective of the extent of separation between these centers. The barriers and reaction energies calculated for the triplet species and their monoradical analogues differ at most by a few tenths of a kcal/mol, values below chemical accuracy. Similar conclusions can be drawn for the barriers and reaction energies beginning with the different spin states of the diradicals; the barriers and reaction energies are (almost) unaffected by a change from the lowest singlet state to the lowest triplet state. For $\bullet\text{CH}_2\text{—CH}_2\text{—CH}_2\text{—CH}_2\bullet$, the

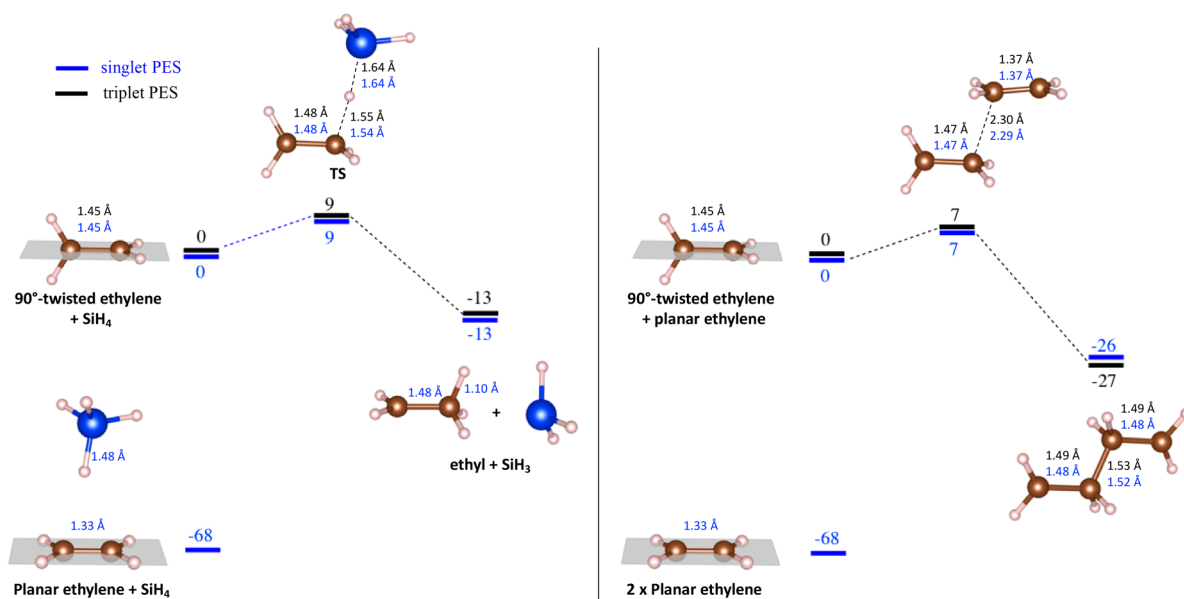


Figure 17. Singlet and triplet PESs for hydrogen abstraction from SiH_4 by twisted ethylene (left) and twisted ethylene addition to ethylene (right), calculated at CASPT2(4,4)/cc-pVTZ//CASPT2(4,4)/cc-pVDZ level of theory. Energies without ZPE in kcal/mol, bond distance in Å.

reaction barriers and energies for the two states differ by approximately 1 kcal/mol, corresponding to the calculated energy difference between these two states (Table 2). For $\bullet\text{CH}_2\text{—CH}_2\bullet$, ΔE_{ST} was estimated to be approximately 0 kcal/mol at CASPT2(2,2) level, and this is reflected in the values obtained for the barriers and reaction energies for both states being equal, with the exception of the reaction energy for addition to ethylene, which is 1 kcal/mol higher for the singlet than for the triplet state. This is a logical consequence of the determined ΔE_{ST} for the product of this reaction, $\bullet\text{CH}_2\text{—CH}_2\text{—CH}_2\text{—CH}_2\bullet$ (1 kcal/mol), and can be connected to the slight increase in (through-space) interaction between the radical centers for this molecule compared to D_{2d} twisted ethylene.

The potential energy surfaces of the above two reactions of twisted ethylene are shown in Figure 17. Consistent with the similar energetics for the singlet and triplet PESs, the calculated structures of the TS and product are similar for both spin states. Note that twisted ethylene is 68 kcal/mol higher in energy than the planar ethylene.

10.3. Diradicals and Diradical(oid)s of Classes 1 and 2: Cyclobutadiene and Trimethylenemethane

Cyclobutadiene (CBD) and trimethylenemethane (TMM) are two much-studied diradicals belonging to different classes; linear combinations of the degenerate (when square) frontier orbitals of CBD can be localized exclusively on a subset of carbon atoms, whereas those of TMM cannot. As such, CBD in its square geometry belongs to class 1 and TMM to class 2, in the typology defined above. Even though these two compounds are structurally very different, they both have a 4π -electron system. In this section, the reactivity of the lowest singlet and triplet states of these two diradicals are investigated and compared to those of cyclobutenyl, 2-methylallyl, and allyl radicals closely related to both.

10.3.1. Cyclobutadiene, a Diradical(oid). It is well-known that square CBD, in its “closed-shell” (from the delocalized perspective) singlet state, presents us with a classical Jahn–Teller situation, and it also happens to be a typical diradical of class 1. The degenerate e_g orbitals split in distinct

ways on excursions along the b_{1g} vibration of the molecule, taking it to two rectangular D_{2h} geometries (Figure 18).³⁰

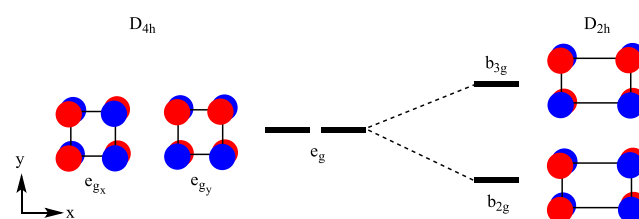


Figure 18. Splitting of degenerate e_g MOs upon a square-to-rectangular distortion in cyclobutadiene.

We now have a geometrical complication on top of the typical diradical one, and that is that the four states we usually consider may or may not be at their respective equilibrium geometries in the square D_{4h} symmetry. The ground state of CBD is known experimentally to be a rectangular 1A_g state; calculations indicate a square triplet, ${}^3A_{2g}$, about 11–12 kcal/mol higher than the 1A_g .^{130,131} Even at the square geometry, the singlet (${}^1B_{1g}$, correlating with D_{2h} 1A_g) is still lower in energy by about 3–6 kcal/mol than the triplet ${}^3A_{2g}$, due to the aforementioned dynamic spin polarization, violating Hund’s rule.^{131,132} The energy order of the lowest singlet and triplet, and two higher singlets is shown in Figure 19. Electron paramagnetic resonance (EPR) spectroscopy studies on a substituted CBD at elevated temperatures in the solid state suggest that the triplet excited state is accessible thermally.¹³³

As mentioned before, expressed using the delocalized e_g MOs in Figure 18, the lowest singlet state of the square CBD has a “closed-shell” two-configuration wave function,

$$|\Psi_{S_{\text{TS}}}\rangle = \sqrt{\frac{1}{2}} | \dots e_{gx}^2 \rangle - \sqrt{\frac{1}{2}} | \dots e_{gy}^2 \rangle \quad (31)$$

Although, as shown in eqs 21 and 22, this ground state of the typical class 1 diradical is correctly represented by an open-shell

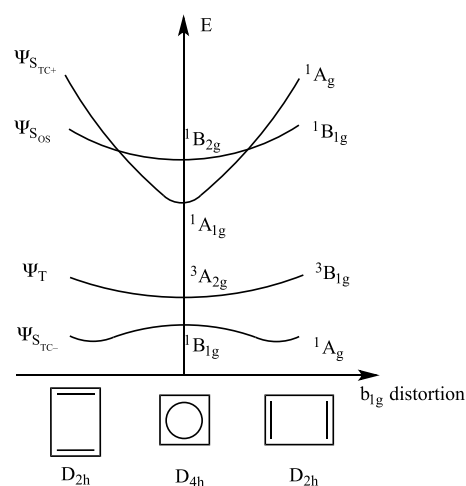


Figure 19. Schematic energy evolution of the four low-lying states in cyclobutadiene upon a square-to-rectangular distortion.¹³¹

wave function when the localized orbitals in Figure 9 are used instead.

Upon distortion to rectangular CBD, the wave function of the lowest singlet becomes

$$|\Psi_{S_{TC-}}\rangle = c_x | \dots b_{2g}^2 \rangle - c_y | \dots b_{3g}^2 \rangle \quad (32)$$

where now c_x and c_y are of the same sign and $|c_x| > |c_y|$ for distortion along the x -axis in Figure 18. The “open-shell” singlet ($\Psi_{S_{OS}}$) and the other “closed-shell” ($\Psi_{S_{TS}}$) singlet of rectangular CBD, based on the b_{2g} and b_{3g} MOs in Figure 18, are higher in energy. They correspond to the ${}^1B_{2g}$ and ${}^1A_{1g}$ states of square CBD, respectively. However, in terms of the localized orbitals ψ_x and ψ_y (cf. Figure 9, but then in the rectangular structure), the lowest singlet state’s wave function regains its genuine open-shell form,

$$|\Psi_{S_{OS}}\rangle = -\frac{c_x + c_y}{2} (|\dots \psi_x^\alpha \psi_y^\beta\rangle + |\dots \psi_y^\alpha \psi_x^\beta\rangle) + \frac{c_x - c_y}{2} (|\dots \psi_x^2\rangle + |\dots \psi_y^2\rangle) \quad (33)$$

We emphasize here once more the transformation between localized and delocalized orbitals to stress that CBD should not be considered as a closed-shell molecule because of the closed-shell configurations that make up its ground state wave function. As pointed out in the end of section 8, the closed-shell/open-shell duality does not matter in measuring diradical character of a molecule. Actually, only when the ground state wave function is dominated by one closed-shell configuration should we view the system as a closed-shell species.

As a final note, we want to point out that the analysis for CBD can in principle be expanded to any antiaromatic molecule, even charged ones such as $C_3H_3^-$ or $C_5H_5^+$. In each of these compounds, a degenerate orbital pair is present in the highly symmetric geometry (D_{3h} and D_{5h} , respectively), which will split under the influence of a Jahn–Teller distortion. As such, a similar plot to the one in Figure 19 can be constructed for these systems, with one big difference: because the degenerate orbital pair cannot be transformed to disjointly localized orbitals (cf. Figure S3.1 in the Supporting Information), these compounds correspond to diradical(ooid)s of class 2, so that the lowest triplet state curve can now be expected to be the lowest one. Indeed,

both $C_3H_3^-$ and $C_5H_5^+$ have been determined to possess a triplet ground state.^{134–136} In a way, these compounds can be viewed as a conceptual bridge connecting CBD to the trimethylenemethane molecule, the prototypical diradical of class 2 which will be discussed in detail.

10.3.2. Trimethylenemethane, a Diradical. In its D_{3h} geometry, trimethylenemethane (TMM) is a clear diradical of class 2. In this symmetry, the two e'' orbitals of the π -system are degenerate, but they cannot be transformed to disjointly localized orbitals (Figure 20).³ As a result, $K_{x'y'}$ is significant (cf. Figure 10).

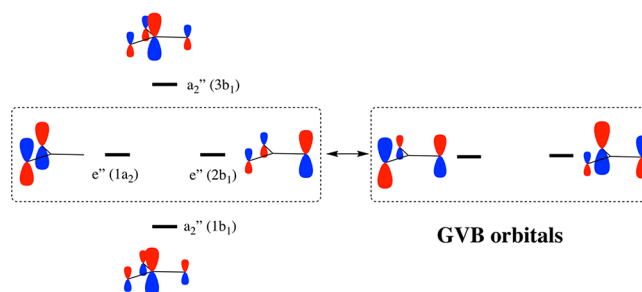


Figure 20. π -System of TMM at the D_{3h} geometry with the transformed GVB orbitals of the degenerate e'' pair on the right. Next to the D_{3h} symmetry labels, the corresponding C_{2v} labels have also been given in parentheses.

The lowest triplet state (${}^3A_2'$) is indisputably the ground state of TMM with a considerable (vertical) singlet–triplet gap, approximately 27 kcal/mol according to calculations by Krylov and co-workers.¹³⁷ As long as the D_{3h} symmetry is enforced, the two lowest lying singlet states are degenerate, and a similar state ordering is obtained as for O_2 (vide infra). The D_{3h} geometry represents the conical intersection of the PESs of two singlet states. There are three symmetry-related C_{2v} 1A_1 states (with one short and two long C–C bonds) as well as three 1B_2 states (with one long and two short C–C bonds) on the lowest singlet PES of the cone while maintaining the planar structure. Previous CASPT2/6-31G* calculations with a (4,4) active space suggest that the 1B_2 states might be minima, and 1A_1 TSs on the pseudorotation pathway around the D_{3h} structure.¹³⁸ However, neither the planar 1A_1 nor the 1B_2 state is the lowest singlet state for this diradical. The lowest singlet has one of the methylene groups twisted 90° (Figure 21). The resultant 1B_1 ground state correlates with the 1B_2 state at the planar C_{2v} structure.

The third singlet state (${}^1A_1'$) adheres again to D_{3h} symmetry (Figure 21).¹³⁹ Krylov and co-workers calculated the vertical excitation energy of this state to be approximately 89 kcal/mol.¹³⁷

Experimentally, TMM was first observed in 1966, when Dowd reported the EPR spectrum for the ground state of the molecule, isolated in a glassy matrix at 88K.¹⁴⁰ Subsequently, Dowd and his co-workers verified the triplet nature and the 3-fold symmetry of this state.^{141–143} Later on, low-temperature matrix infrared (IR) spectra were also recorded by Maier et al.¹⁴⁴ Lineberger and co-workers determined the 1A_1 state to lie 16 kcal/mol above the triplet ground state by photoelectron spectroscopy.¹⁴⁵ The values predicted through ab initio molecular orbital and valence bond calculations range between 14 and 20 kcal/mol (our own calculations lead to a value in the higher end of this range; cf. Figure 21).^{145–150} Because most reliable calculations predict the splitting between the two lowest

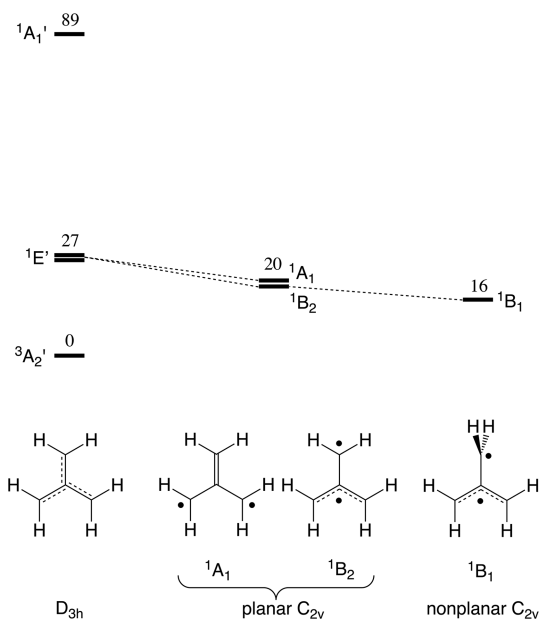


Figure 21. Ordering of the states when D_{3h} symmetry is enforced (left) and when this constraint is lifted (middle and right). The calculated excitation energies (in kcal/mol) for the D_{3h} geometries have been added on the left,¹³⁷ the singlet–triplet gap in the middle, and the energy of the nonplanar 1B_1 state on the right. The schematic geometries of the different states are presented at the bottom of the figure.

singlet states at their optimal geometries to amount to a value between 0 and 3 kcal/mol, Lineberger and co-workers estimated the actual singlet–triplet gap, i.e., the spacing between the ${}^3A_2'$

and 1B_1 , at 13–16 kcal/mol, which is in agreement with our own value of 16 kcal/mol.¹⁴⁵

As we will see later, the D_{3h} TMM and the O_2 molecule share similar electronic structure, with the ${}^3A_2'$, ${}^1E'$, and ${}^1A_1'$ states of the former correspond to the ${}^3\Sigma_g^-$, ${}^1\Delta_g$, and ${}^1\Sigma_g^+$ states of the latter. The correspondence is clearly seen by comparing the energy levels at the left side of Figure 21 and those in Figure 42. The extra e' vibrational degrees of freedom of the TMM allows the Jahn–Teller distortion that splits the degeneracy of the ${}^1E'$ state, while with the O–O stretching as the only totally symmetric vibrational degree of freedom, the degeneracy of the ${}^1\Delta_g$ state remains.

10.4. Symmetry May Determine the Class of a Diradical

The orbital degeneracies of CBD in D_{4h} symmetry and D_{3h} TMM both arise from the E -type irreducible representations of the two respective point groups. CBD is a class 1 diradical(oid) for which the open-shell/closed-shell ambiguity does not occur, while TMM is a class 2 diradical for which the ambiguity occurs. Interestingly, there is a symmetry reason for the two species belonging to the two different classes.

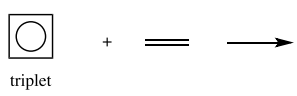
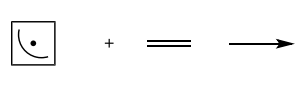
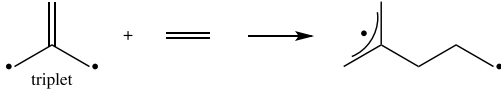
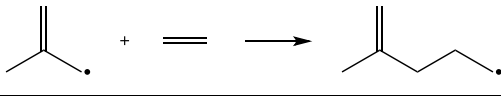
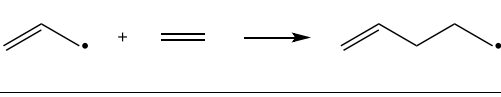
Regardless of the transformation within the degenerate e -type orbitals, the symmetries of the formally $\Psi_{S_{OS}}$ and $\Psi_{S_{TC-}}$ states are given by symmetrized direct products of the e spatial orbitals, $(e_x(1)e_y(2) + e_x(2)e_y(1))$ and $(e_x(1)e_x(2) - e_y(2)e_y(1))$. The symmetrized direct products of the E -type irreducible representations in tetragonal point groups (C_{4v} , D_{2d} , D_{4v} , D_{4h} , etc.) lead to an A -type and two B -type irreducible representations. The A -type state is the $\Psi_{S_{TC+}}$ state. The two B -type states are in general nondegenerate; the low-lying one can be unambiguously assigned as the $\Psi_{S_{OS}}$ and the higher one as $\Psi_{S_{TC-}}$, according to the electrostatic argument in section 5.

Table 5. Comparison of the Activation Energies (ΔE^\ddagger) and Reaction Energies (ΔE) of H-Atom Abstraction from SiH_4 , for ${}^3A_2'$ TMM, ${}^3A_{2g}$ CBD, with the Allyl Radical ($H_2C=CH-CH_2\bullet$), and a Selection of Substituted Allyls, Calculated at (U)CCSD(T)/cc-pVTZ//((U)B3LYP/cc-pVTZ Level of Theory^a

Reaction Label	Reaction	ΔE^\ddagger	ΔE
G		17	0
H		15	-2
I		15	0
J		16	-1
K		18	1

^aThe energies (kcal/mol) are obtained from electronic energies without ZPE correction.

Table 6. Comparison of the Activation Energies (ΔE^\ddagger) and Reaction Energies (ΔE) of Addition to Ethylene for $^3A_2'$ TMM, $^3A_{2g}$ CBD, the Allyl Radical ($H_2C=CH-CH_2\bullet$), and a Selection of Substituted Allyls, Calculated at (U)CCSD(T)/cc-pVTZ// (U)B3LYP/cc-pVTZ Level of Theory^a

Reaction Label	Reaction	ΔE^\ddagger	ΔE
L		12	-15
M		11	-17
N		10	-13
O		12	-6
P		13	-11

^aThe energies (kcal/mol) are obtained from electronic energies without ZPE correction.

On the contrary, the symmetrized direct products of the E -type irreducible representations in trigonal point groups (C_{3v} , D_3 , D_{3h} , etc.) result in an A -type and an E -type irreducible representation. $\Psi_{S_{os}}$ and $\Psi_{S_{TC-}}$ form the E -type state and remain degenerate regardless of the transformation of the e -type orbitals. This prevents us from assigning one of the E component state as $\Psi_{S_{os}}$ uniquely. The true open-shell/closed-shell ambiguity occurs.

The group theory of symmetrized direct products of E -type irreducible representations is well-known and summarized, e.g., in Table 2.3 of Bersuker's classic text, ref 151. From this table, we see that the symmetry-induced class 1 diradical(oid), such as CBD, only occurs for systems with a $4k$ -fold principal symmetry axis, and when the degenerate orbitals belong to the E_k irreducible representation. All the other symmetry-induced diradical(oid)s belong to class 2. CBD (with D_{4h} symmetry) and the perpendicularly twisted ethylene (with D_{2d} symmetry) are special cases of the symmetry-induced class 1 diradical(oid)s with $k = 1$.

10.5. The Reactivity of CBD and TMM States

10.5.1. The Reactivity of $^3A_{2g}$ CBD and $^3A_2'$ TMM. The computed reaction and activation energies for $^3A_2'$ TMM and $^3A_{2g}$ CBD abstracting a hydrogen from SiH_4 and adding to ethylene are shown in Table 5 and Table 6, respectively. For comparison, the energetics of structurally closely related radicals (cyclobutenyl vs CBD, 2-methylallyl vs TMM, and allyl) were also computed and provided in Table 5 and Table 6. The reason for enlarging the reference set is to allow a fairer comparison in degree of strain and substitution patterns.

Table 5 and Table 6 demonstrate that the lowest triplet states for CBD and TMM have similar reactivity with respect to their monoradical analogues. For $^3A_{2g}$ CBD, the barriers for both reactions are 1–2 kcal/mol larger than those for cyclobutenyl,

but for $^3A_2'$ TMM the barriers are 1–2 kcal/mol smaller than those for 2-methylallyl.

The reactivity difference among the three species can be explained by comparing the spin density at respective reacting sites. Allyl radical has two equivalent resonance structures (Figure 22), so the spin density is, to a first approximation, 1/2

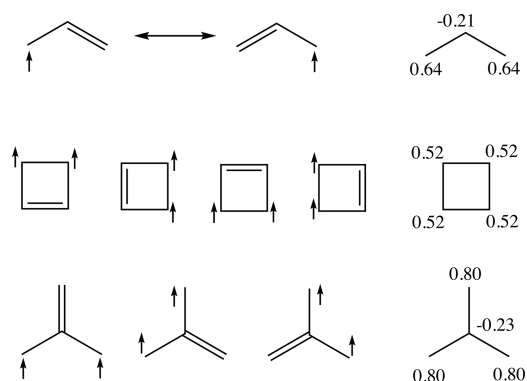


Figure 22. Resonance structures of allyl, CBD, and TMM (triplet states for the latter two) and calculated spin densities on the carbons (spin densities on hydrogens not shown) at UB3LYP/cc-pVTZ level.

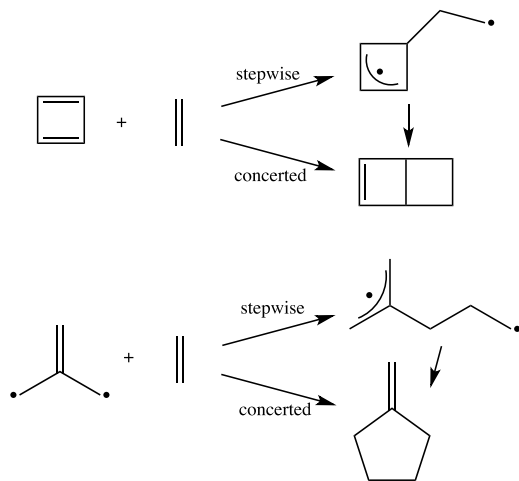
on each of the terminal carbons. In a proper calculation of the radical spin densities, one would (and does) find a negative spin density at the central carbon, and spin densities at the radical termini that are slightly higher than 0.5 (top right in Figure 22).^{152,153} Triplet CBD has two unpaired electrons distributed over four equivalent carbons (see resonance structures in Figure 22), giving an approximate spin density of 1/2 for each carbon. Triplet TMM is different in that the two unpaired electrons can only be localized on the three peripheral carbons (i.e., no coefficients on the central carbon in the two SOMOs), leading to approximate 2/3 spin density on each peripheral carbon. The

calculated spin density confirms this reasoning (cf. Figure 22). Note the further intrusion of negative spin densities.

The higher the spin density on the reacting site, the more reactive the radical should be. Here the assumption is that steric effects do not play an important role. For the three molecules considered here, their respective reacting sites are relatively sterically unhindered. Triplet CBD has a similar spin density to allyl and is slightly more reactive than allyl. The greater reduction of angle strain in CBD upon reactions that change the carbon hybridization from sp^2 to sp^3 , compared with allyl, is likely the reason for this increased reactivity of triplet CBD compared to allyl. Triplet TMM has a much larger spin density on the reacting carbon and therefore is more reactive than allyl and triplet CBD. It seems that spin density is a good measure of the reactivity of a radical or diradical for those reactions where only one radical center is involved. We already mentioned in a previous section that one can stabilize a radical through delocalization, which essentially reduces the spin density of the radical center, leading to reduced reactivity. We also note here that atom-condensed spin densities (especially of triplet states) have already previously been connected to reactivity within the context of (spin-polarized) conceptual density functional theory of radicals in earlier work by the General Chemistry Research Group (ALGC) at the Vrije Universiteit Brussel, as well as by others.^{154–157}

10.5.2. The Reactivity of Singlet vs Triplet States of CBD and TMM. The reactivities of the singlet vs the triplet states for both diradicals were compared for H-abstractions from SiH_4 and additions to ethylene. For the additions, we looked at both the stepwise and concerted pathways (Scheme 1). For the

Scheme 1. Two-Step and Concerted Pathways for the Addition of the Lowest Singlet States of CBD and TMM to Ethylene



stepwise pathways, only the first transition states were considered. For singlet TMM, pathways starting from the nonplanar 1B_1 state, which is the lowest singlet state of TMM, are considered. Instead of a single-reference CCSD(T) method, CASPT2/cc-pVTZ calculations were employed for proper accounting of the multireference character of the singlet states of TMM and CBD.

The computed potential energy surfaces for these pathways are shown in Figures 23–26. Also included in these figures are some higher energy states of CBD or TMM at nonoptimal geometries or in excited electronic states (for example, the

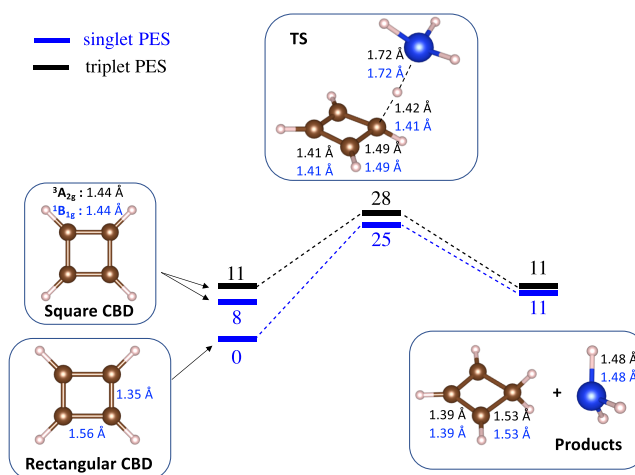


Figure 23. Potential energy surfaces (energies in kcal/mol) for H atom abstraction from SiH_4 by CBD. Key bond distances are shown. Numbers in black and blue correspond to triplet and singlet PES, respectively. The two product molecules were optimized as separate molecules, as were the reactants (CBD and SiH_4). The structures of the TS were optimized in C_s symmetry. Calculations were done at the CASPT2/cc-pVTZ level of theory. A (6/6) active space was used for the TS. See Supporting Information for active orbitals.

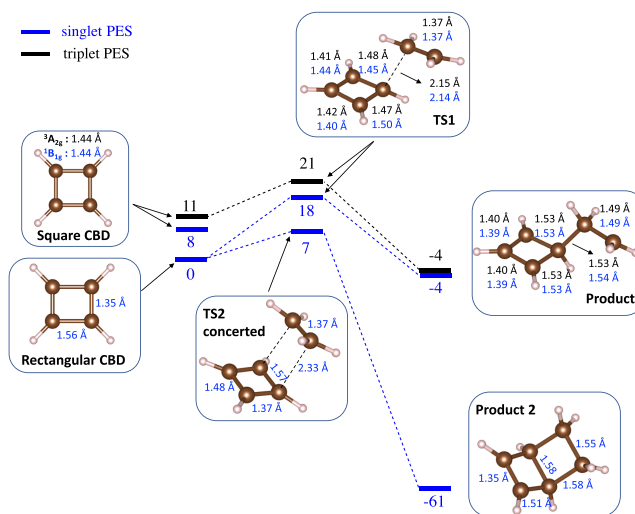


Figure 24. Potential energy surfaces (energies in kcal/mol) for reaction of ethylene with CBD. Key bond distances are shown. Numbers in black and blue correspond to triplet and singlet PES, respectively. Reactants (CBD and ethylene) were optimized as separate molecules. Calculations were done at the CASPT2/cc-pVTZ level of theory. A (6/6) active space was used for the TS. See Supporting Information for active orbitals.

square singlet state of CBD and the planar singlet states of TMM). Focusing on the stepwise pathways, one common feature emerges from the PESs in Figures 23–26. The singlet–triplet separation is the largest in the reactant molecule (CBD or TMM); it decreases in the transition state and finally reaches zero in the diradical intermediate. For example, whereas the energy difference between the rectangular 1A_g state of CBD and the excited $^3A_{2g}$ state amounts to approximately 11 kcal/mol, the energy difference at the transition state for the H atom abstraction reaction has already decreased to 3 kcal/mol and drops to 0 kcal/mol for the reaction product (Figure 23). For TMM, the energy difference between the $^3A_2'$ and the 1B_2 is

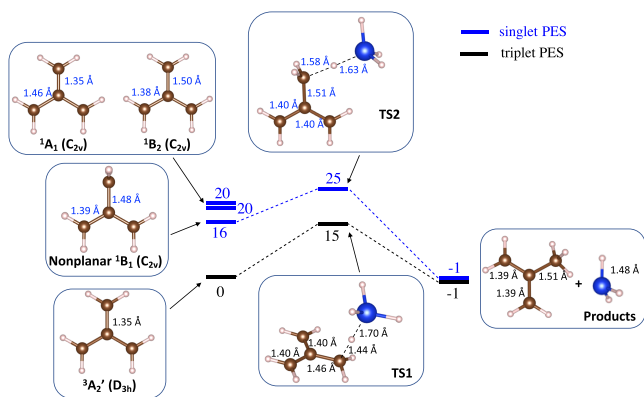


Figure 25. Potential energy surfaces (energies in kcal/mol) for H atom abstraction from SiH_4 by TMM. Key bond distances are shown. Numbers in black and blue correspond to triplet and singlet PES respectively. Reactants (TMM and SiH_4) and products were optimized as separate molecules. The structures of the transition states were optimized in C_s symmetry. Calculations were done at the CASPT2/cc-pVTZ level of theory. A (6/6) active space was used for the TSs. See Supporting Information for active orbitals.

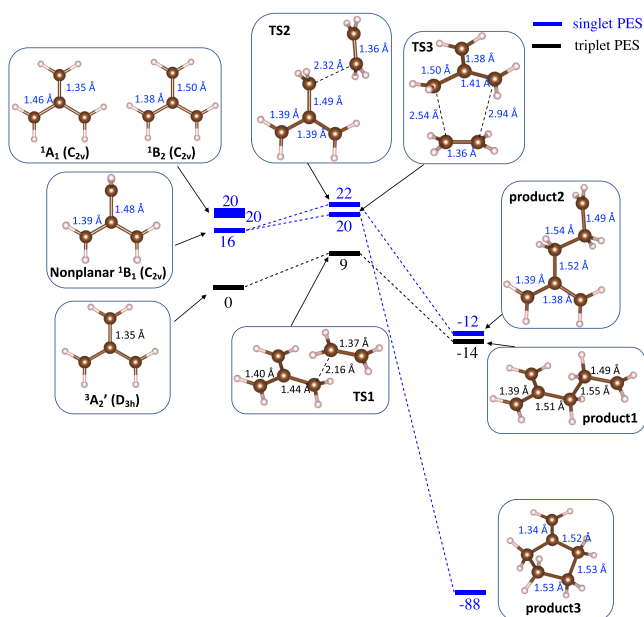


Figure 26. Potential energy surfaces (energies in kcal/mol) for reaction of ethylene with TMM. Key bond distances are shown. Numbers in black and blue correspond to triplet and singlet PES, respectively. Reactants (TMM and ethylene) were optimized as separate molecules. Calculations were done at the CASPT2/cc-pVTZ level of theory. A (6/6) active space was used for the TSs. See Supporting Information for active orbitals.

calculated as 16 kcal/mol for the reactants, 10 kcal/mol for the transition state, and 0 kcal/mol for the reaction products (Figure 25).

The underlying reason for the decreasing singlet–triplet gap as the reaction proceeds is the further spatial separation of the two unpaired electrons as the reaction proceeds to form the diradical intermediate of the stepwise pathway compared with in the reactant molecules. It is clear from Scheme 1 that the two unpaired electrons become more localized in the intermediate, each at different parts of the diradical intermediate. The decrease in communication between the two radical centers (cf. Figure 8

and Figure 9) means reduced exchange interactions K_{xy} between the two unpaired electrons. Henceforth, we use the generic K_{xy} to represent exchange integrals between singly occupied orbitals and no longer make a distinction between K_{ab} in class 1 diradical(oid)s and $K_{x'y'}$ in class 2 diradical(oid)s (cf. Figure 10 and Figure 11). As discussed in section 3.2, the exchange integral determines the singlet–triplet gap of a diradical system. Thus, the singlet–triplet separation decreases as the stepwise reaction proceeds toward the diradical intermediate. Note that this phenomenon is independent of the ground state spin of the diradical reactant. The PESs in Figures 23–26 for reactions of both CBD, with a singlet ground state, and TMM, with a triplet ground state, are similar.

The reaction barrier and reaction energy data are extracted from Figures 23–26 and shown in Table 7, and there compared

Table 7. Activation Energies (ΔE^\ddagger) and Reaction Energies (ΔE) of H Abstraction from SiH_4 and Addition to Ethylene for the Lowest Singlet and Triplet States of CBD (Rectangular 1A_g and Square $^3A_{2g}$) and TMM (Nonplanar 1B_1 and D_{3h} $^3A_2'$), Calculated at CASPT2(6,6)/cc-pVTZ Level of Theory^a

	H abstraction from SiH_4		addition to ethylene	
	ΔE^\ddagger	ΔE	ΔE^\ddagger	ΔE
CBD (rectangular 1A_g)	25	11	18	-4
CBD (square $^3A_{2g}$)	17	0	11	-15
TMM (nonplanar 1B_1)	9	-17	6	-28
TMM ($^3A_2'$)	15	0	9	-14
allyl	18	1	12	-12

^aData for only the first steps of stepwise pathways are shown. See Supporting Information for active space specification. The energies (kcal/mol) are relative electronic energies without ZPE correction.

with the computed data for allyl. It is clear that the barrier is generally larger for the ground spin state and smaller for the excited spin state. For CBD, the (rectangular) 1A_g state is the ground state, and its barriers and reaction energies are much higher compared to the corresponding reactions for the triplet state. For TMM, the situation is the reverse; the $^3A_2'$ state is the ground state, so the singlet state (nonplanar 1B_1) exhibits the lower barrier and reaction energy. This behavior is, of course, consistent with, and a result of, the decreasing singlet–triplet gap as the reaction proceeds from reactants to diradical intermediates. One should take note that in the second step of diradical recombination (cf. Scheme 1), which we did not consider throughout this analysis, the singlet–triplet gap should increase again, as a result of the growing HOMO–LUMO gap.

Having discussed the singlet vs triplet reactivity in the stepwise reactions in Scheme 1, we now move to the concerted pathways. It should be obvious that the concerted pathways are unavailable for triplet states. We have not examined reaction paths which begin with a triplet and in which intersystem crossing to the ground state occurs. The reaction profiles for concerted additions to ethylene by CBD and TMM are presented in Figure 24 and Figure 26, respectively.

It is obvious that the [4 + 2] cycloaddition between CBD and ethylene affording a bicyclic molecule is allowed (Scheme 1); as expected, CASPT2 computations found a concerted TS for this cycloaddition. Whether a formal [3 + 2] cycloaddition between TMM and ethylene giving methylenecyclopentane (Scheme 1) is allowed or forbidden seems less obvious, but frontier MO

analysis shows that this reaction is allowed (Figure 27). CASPT2 calculations found a concerted but asynchronous TS for this cycloaddition (TS3 in Figure 26), very close in energy to the stepwise radical addition TS (TS2).

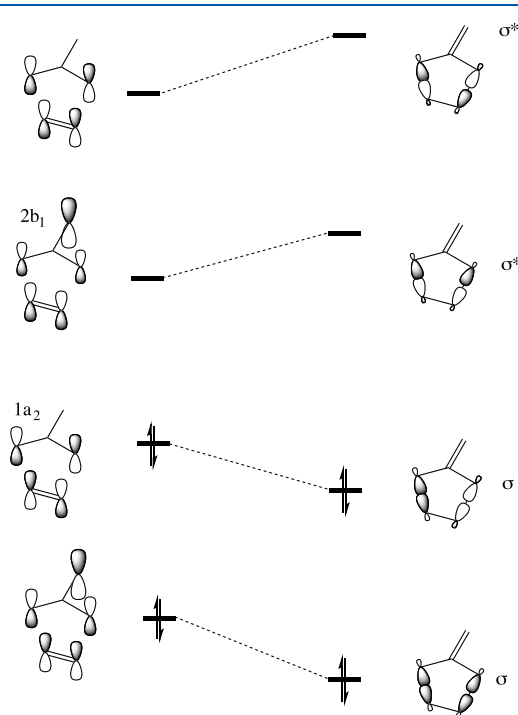


Figure 27. Frontier MO analysis shows that the [3 + 2] cycloaddition between singlet TMM and ethylene is allowed. The $1a_2$ and $2b_1$ MOs of TMM are originally very close in energy in a C_{2v} structure (degenerate in a D_{3h} structure) but split in energy as an ethylene molecule approaches so as to effect the concerted cycloaddition. The $1a_2$ MO is stabilized by interaction with π^* LUMO of ethylene; the $2b_1$ is destabilized by the π HOMO of ethylene.

For both CBD + ethylene and TMM + ethylene, the barriers of concerted pathways are, as expected, lower than those of stepwise pathways on the singlet surface, although only by 2 kcal/mol in the case of TMM. It should be noted that the TS of a concerted pathway on the singlet surface is not necessarily lower in energy than that of the stepwise pathway on the triplet surface. TMM provides an example (Figure 26); the stepwise TS1 is 11 kcal/mol lower than the concerted TS3. This is related to the fact that the triplet is much more stable (16 kcal/mol) than the singlet in TMM itself.

These data suggest that the concerted reactivity is at least as favorable as the stepwise, diradical reactivity explored so far; the barriers are lower and the reactions are much, much more exothermic. As such, we can expect that concerted mechanisms will be dominant for the singlet states of these diradicals. The difference in barriers and reaction energies between the concerted reactions for TMM and CBD can be attributed to a release of strain in the geometry induced by the formation of a ladderane product (vide infra).

Whether CBD reacts in a stepwise (diradical) or concerted ("closed-shell") manner has previously been studied both experimentally and theoretically.^{158–160} Limanto et al. carried out a wide variety of intramolecular cycloaddition reactions involving cyclobutadiene. The stereochemical outcomes, as well as the calculated reaction profiles, all pointed toward dominance of the concerted [4 + 2] or [2 + 2] cycloadditions (Figure

28).^{158,159} In one of their publications on this topic, the authors did identify one experimental observation that could not be

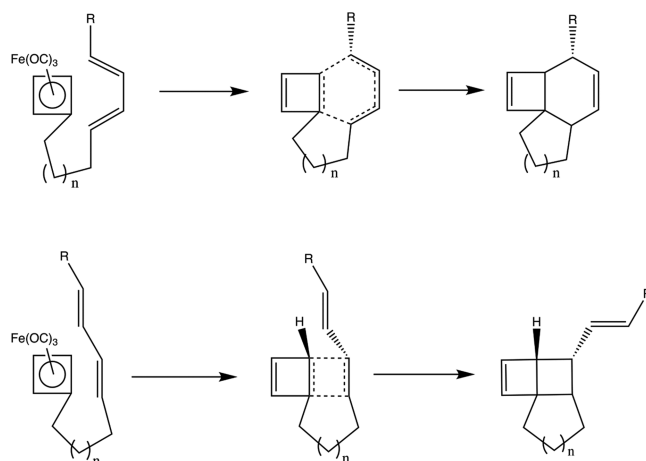


Figure 28. Intramolecular [4 + 2] (up) and [2 + 2] (down) Diels–Alder reactions involving cyclobutadiene, carried out by Limanto et al.^{158,159}

immediately explained by the proposed reaction mechanism. Several possible explanations were put forward, of which a potential bifurcation of the reaction profile was deemed the most likely, thus not invalidating the proposed dominance of the concerted reaction mechanism.¹⁵⁹

Li and Houk studied theoretically the dimerization reaction of CBD and concluded that two CBD molecules will react without a significant potential energy barrier. According to their CASSCF calculations, the concerted *syn* addition also leads to a greater energy lowering than the *syn* diradical/stepwise addition.¹⁶⁰ Di Valentin and co-workers on the other hand considered the reaction of CBD with nitrene and concluded that the stepwise and concerted mechanism are both viable and are in true competition with one another.¹⁶¹

As mentioned before, CBD has also attracted significant interest as a potential monomer for the synthesis of ladderanes. Because of the high reactivity of CBD, such an oligomerization usually starts from a precursor of CBD, or CBD as a ligand in an $Fe(CO)_3$ complex. Upon in situ generation of free CBD, a rapid reaction toward ladderanes of various lengths proceeds.¹⁶² Mehta and co-workers determined that the regio- and stereochemistry of such oligomerization reactions (with substituted CBD monomers as starting points) follows the frontier orbital rules and can thus be characterized as a concerted reaction involving closed-shell reagents.¹⁶³

For TMM and its derivatives, experimental data exists which confirm the distinct reactivity for the singlet and triplet species of these compounds. The singlet states of TMM have been noted as being much more labile kinetically than the triplet ground state, in agreement with our results.¹⁶⁴ This is supported by the lack of experimental observation of the singlet states except for the photoelectron spectroscopy experiment by Lineberger and co-workers mentioned earlier;¹⁴⁵ the singlet states undergo fast ring-closing reactions to methylenecyclopropane, making their detection almost impossible.¹⁶⁵ This irreversible intramolecular ring-closing reaction is much faster than, for example, addition to ethylene. The triplet ground state of TMM is more long-lived and thus well-characterized but generally does not react with an (unsubstituted) alkene either. Instead, it undergoes a homocoupling leading to a dimer.^{166,167} Berson and co-workers

reported that triplet diyls react readily with molecular oxygen.¹⁶⁷ It appears that the practical use of TMM in organic synthesis is rather limited (unless it is incorporated in an organometallic complex).¹⁶⁸

The barrier of 4 kcal/mol, calculated for the (asynchronous) concerted addition to ethylene in Figure 26, combined with the competing (and barrierless) ring-closing reaction of singlet TMM mentioned earlier, explains the absence of any experimental data on the reactivity of the singlet states of TMM. The compound is simply too reactive to be observed. As such, direct evidence for a preference for concerted reactivity for these spin states is not available.

However, derivatives of TMM (diyls), such as the thermally or photochemically prepared 2-isopropylidene-1,3-diyl, have been employed frequently in cycloaddition reactions with trapping agents (diylphiles), leading to the selective generation of fused and bridged adducts in good yields.^{169,170} As a consequence, these derivatives enable a more in-depth study of the regio- and stereoselectivity of TMM-like compounds. In general, the singlet states lead to stereoselective products, indicating a (quasi-)concerted reaction mechanism in accordance with the orbital symmetry rules, whereas the triplet ground state often leads to a loss of stereochemical integrity upon reaction, indicating a clear two-step diradical mechanism.^{164,166,167,171}

Berson and co-workers demonstrated that next to a different stereoselectivity, a distinct regioselectivity can also be assigned to the $^3A_2'$ and the 1B_2 , 1A_1 states, i.e., a preference for either bridged or fused reaction products (Figure 29). This

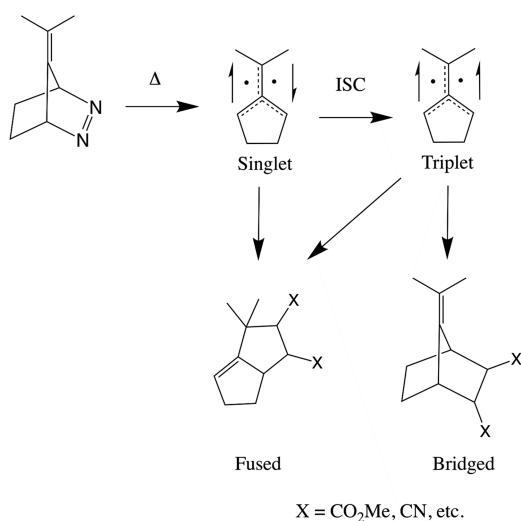


Figure 29. Formation of 2-isopropylidene-1,3-diyl and the subsequent reaction toward either a fused or bridged reaction product upon reaction with substituted ethylenes. The singlet states lead to regio- (and stereo)selective reaction products, whereas the triplet state generally leads to a mixture of reaction products.

regioselectivity was explained as either the result of an orbital overlap effect due to the twisted ethylene group of the 1B_2 state or an orbital symmetry effect upon reaction with the 1A_1 state.^{170,172,173}

For an overview of the chemistry of TMM derivatives (diyls), we refer to excellent reviews by R. D. Little,^{164,174} as well as to the recent perspective by Abe and co-workers.¹⁷⁵ A perspective on the transition metal mediated cycloaddition reactions

involving TMM can be found in the review of Lautens and co-workers.¹⁶⁸

10.6. Reactivity of *para*-Quinodimethane and its Analogues

10.6.1. The Molecules and Their States. 1,4-Dimethylene-2,5-cyclohexadiene, customarily called *para*-quinodimethane (PQDM; Figure 30) is a prototype example of a

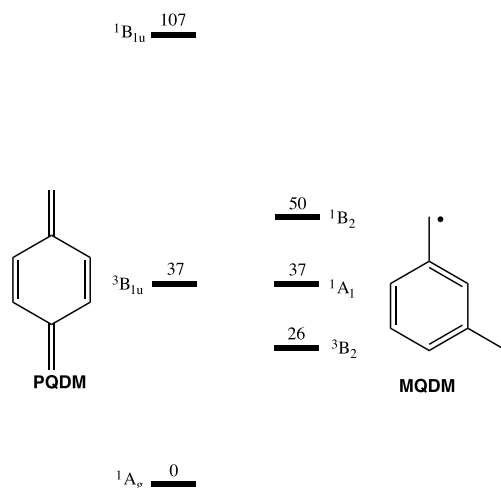


Figure 30. Ordering of low-lying electronic states of PQDM and MQDM (in kcal/mol), calculated at CASPT2(8,8)/cc-pVTZ level of theory.

diradicaloid, as already shown in Figure 2.^{176,177} Its HOMO and LUMO are not degenerate, but the energy gap between these delocalized molecular orbitals is not large enough to neglect the second configuration in the closed-shell 1A_g singlet ground state. The ordering of the states follows the scheme in Figure 5, with the lowest triplet state, the $^3B_{1u}$ state, 37 kcal/mol above the ground state singlet and the open-shell singlet, $^1B_{1u}$, 70 kcal/mol above $^3B_{1u}$ (the approximate value of $2K_{xy}$). Back in 1947, Coulson and co-workers estimated the singlet–triplet gap for this molecule to be around 8–9 kcal/mol.¹⁷⁸ However, calculations performed in the context of the current study at a CASPT2/cc-pVTZ level (as well as by others)^{71,179} lead to the much bigger gap cited. An experimental value is not available due to the extremely high reactivity of the lowest triplet state, which has inhibited its characterization up to today.¹⁸⁰

For *meta*-quinodimethane (MQDM; Figure 30), on the other hand, the frontier orbitals are degenerate in the Hückel approximation and close to each other in other theoretical approaches (note that their shape resembles those of the SOMOs of pentadienyl and heptadienyl, respectively). Because these molecular orbitals cannot be identified with disjointly localizable orbitals (Figure 31), this molecule is a class 2 diradical. Therefore, the triplet state Ψ_T is located significantly below the lowest singlet state $\Psi_{S_{rc}}$. Our calculations point to a singlet–triplet gap of 11 kcal/mol, in line with other values found in the literature.^{181–183} Experimentally, this gap has been determined by negative ion photoelectron spectroscopy as 9.6 ± 0.2 kcal/mol.¹⁸⁴

The geometries of the two triplet states are presented in Figure 32. The π -conjugation causes both systems to be entirely flat. Note in the structure of the reference benzyl the contribution of a quinoid structure (i.e., with short exocyclic double bond), evident from the bond alternation in the ring. The structure of triplet PQDM has a smaller contribution of the

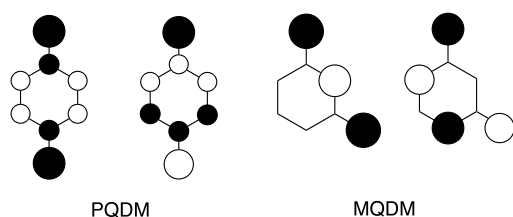


Figure 31. Sketch of the Hückel NBMOs of PQDM and MQDM.¹⁸⁵ Only the top lobes of these π orbitals are shown. The filled and empty circles represent, respectively, positive and negative coefficients in the wave function.

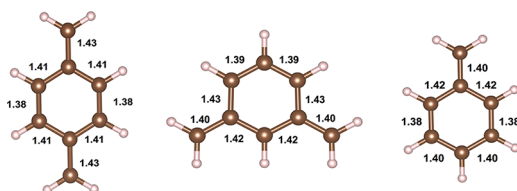


Figure 32. Geometries of $^3B_{1u}$ PQDM (left) and 3B_2 MQDM (middle) and benzyl radical (right). Only the C–C bond lengths (in Å) are displayed.

quinoid resonance (and thus larger contribution of the benzenoid resonance) compared with benzyl; the longer C–CH₂ bonds (1.43 Å) in triplet PQDM vs the shorter in benzyl (1.40 Å) attest to the above. This has a consequence in the reactivity of the methylene site in the two molecules, as discussed later. The exocyclic C–CH₂ bonds in triplet MQDM have almost the same distance as those in benzyl. The two much longer ring bonds (1.43 Å) indicate that triplet MQDM can be viewed as an allyl and a pentadienyl connected at the 2 and 4 positions of the latter.

We note that there is also an *ortho* isomer of quinodimethane, which we did not discuss here. The electronic structure of OQDM is anticipated to be similar to that of PQDM, with a closed-shell singlet ground state and a relatively low-lying triplet state.¹⁸⁵

10.6.2. The Reactivity of $^3B_{1u}$ PQDM and 3B_2 MQDM.

We will now compare the reactivity of these two diradical(oid)s with a monoradical analogue (benzyl) by considering the barriers and reaction energies for the set of characteristic radical reactions outlined in the section on monoradicals. The dimerization reaction was not treated explicitly at this point but will be discussed at the end of this section.

Table 8 gives the activation and reaction energies for the addition to ethylene and the abstraction of a hydrogen from

Table 8. Comparison of the Activation Energies (ΔE^\ddagger) and Reaction Energies (ΔE) of H Abstraction from SiH₄ and Addition to Ethylene for $^3B_{1u}$ PQDM, 3B_2 MQDM, and Benzyl^a

	H abstraction from SiH ₄		addition to ethylene	
	ΔE^\ddagger	ΔE	ΔE^\ddagger	ΔE
3 PQDM ($^3B_{1u}$)	10	–10	6	–23
3 MQDM (3B_2)	16	1	11	–12
benzyl	15	–2	10	–14

^aCalculations were performed at (U)CCSD(T)/cc-pVTZ//((U)-B3LYP/cc-pVTZ level of theory. The energies (kcal/mol) are obtained from electronic energies without ZPE correction.

SiH₄, for these compounds and compares these with the values obtained for the benzyl radical.

From Table 8, it is clear that the monoradical used as a reference (benzyl) has barriers intermediate between those calculated for the (localized) monoradicals (cf. Table 1 in section 9) and the delocalized ones, i.e., allyl and its analogues (cf. Table 5 and Table 6 in section 10.5). The reactions of benzyl are also intermediate in their exothermicity. These findings can be connected to the present, but hampered, delocalization in benzyl; delocalization of the radical electron toward the attached phenyl ring is not favorable because it requires the breaking aromatic stabilization. This is reflected in the relatively high spin density on the methylene group (0.73; Figure 33).

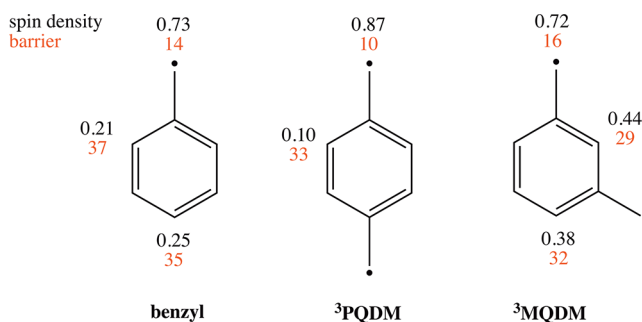


Figure 33. Spin densities and barrier heights (in kcal/mol, in red) for H atom abstraction from SiH₄, calculated at UB3LYP/cc-pVTZ level of theory.

Comparing the barriers and reaction energies of the triplet states of the diradical(oid)s with those for benzyl, one can see that for triplet MQDM they are quite similar; the barriers for both reactions are approximately 1 kcal/mol higher and the reaction energies 2 kcal/mol less exothermic than for benzyl. Triplet PQDM on the other hand has significantly lower barriers to reaction than benzyl (a difference of 4–5 kcal/mol), and its reactions are also 8–9 kcal/mol more exothermic. So, the effect of the presence of a second radical electron in triplet MQDM seems to be a slight, almost negligible, moderation of its reactivity relative to benzyl. Triplet PQDM, on the other hand, is calculated to be much more reactive than either triplet MQDM or benzyl. As before, the differences in the spin densities (0.72 for 3 MQDM and 0.87 for 3 PQDM compared to 0.73 for benzyl; Figure 33) are consistent with the evolution of the barriers and reaction energy.

From the results obtained, it can also be concluded that the two unpaired electrons in 3 PQDM (and to a minor extent also in 3 MQDM) are not entirely equivalent; the first radical reaction step occurs with different kinetics and thermochemistry compared to the second step (corresponding to a *para*-methyl-substituted benzyl radical). Or, from another perspective, the delocalized canonical orbitals of 3 PQDM (Figure 31) have more bonding and antibonding character than the counterparts of 3 MQDM. The electron that occupies the antibonding orbital is especially more reactive than the unpaired electrons of 3 MQDM.

We also calculated the barriers to hydrogen abstraction from SiH₄ for other positions in benzyl, 3 PQDM and 3 MQDM, other than the methylene group, at the UB3LYP/cc-pVTZ level of theory (Figure 33). For benzyl, the *ortho* and *para* attack have higher barriers of 37 and 35 kcal/mol, respectively, consistent with reduced spin densities on both of these sites. For 3 MQDM

and $^3\text{PQDM}$, a similar connection between the height of the barriers and the spin densities can be observed. It is notable, however, that the spin density on the *ortho*-position on $^3\text{PQDM}$ is much lower than the spin densities on sites on the other compounds with similar barriers.

A possible explanation of this somewhat anomalous result can be found in the interplay with the aromaticity in the phenyl ring. Recall that in $^3\text{PQDM}$ the phenyl ring retains almost its full aromaticity, as reflected in the very high spin densities on the methylene sites, pointing to very limited radical electron delocalization throughout the ring. So, there are two counteracting effects at work in this system: aromaticity (causing stabilization) and localization of the radical electrons (causing destabilization). A reaction at the *ortho*-position will inevitably cause a breakdown of the aromaticity within the ring, enabling the remaining radical electron to freely delocalize throughout the conjugated system. It is presumably this relief of “stress” that leads to the high, but lower than expected, reaction barrier of 33 kcal/mol.

Alternatively, one may take a more deductive approach and rationalize the reactivity trends observed through comparison of the transformed orbitals of PQDM and MQDM to the SOMO of benzyl at Hückel level of theory. Such an analysis, which can be done analytically, has been performed in great detail by Malrieu and co-workers.^{186–188} The results obtained this way are in line with the spin-density results discussed above, i.e., one retrieves significantly enhanced orbital amplitudes on the exocyclic methylene groups of PQDM etc.

10.6.3. The Reactivity of Singlet vs Triplet in PQDM and MQDM. In Table 9, the reactivity of the singlet vs the triplet

Table 9. Activation Energies (ΔE^\ddagger) and Reaction Energies (ΔE) of H Abstraction from SiH_4 and Addition to Ethylene for the $^1\text{A}_g$ and $^3\text{B}_{1u}$ States of PQDM, $^1\text{A}_1$ and $^3\text{B}_2$ states of MQDM, Calculated at CASPT2/cc-pVTZ Level of Theory^a

	H abstraction from SiH_4		addition to ethylene	
	ΔE^\ddagger	ΔE	ΔE^\ddagger	ΔE
PQDM ($^1\text{A}_g$)	31	26	23	14
PQDM ($^3\text{B}_{1u}$)	10	−10	7	−22
MQDM ($^1\text{A}_1$)	10	−11	7	−23
MQDM ($^3\text{B}_2$)	16	0	11	−12

^aOnly the first steps of stepwise pathways are considered. See Supporting Information for active space specification. The energies (kcal/mol) are relative electronic energies without ZPE correction.

states for both compounds were compared for the abstraction and addition reactions (see also Figure 34, Figure 35, Figure 37, and Figure 38).

Table 9 leads to the same conclusions as obtained in the previous section for CBD and TMM concerning the relative reactivity of the different states for QDM; the relative positioning of the singlet state compared to the triplet state determines whether this state will be more/less reactive. For the $^1\text{A}_1$ state of PQDM, we find relatively high barriers to both hydrogen abstraction and addition to ethylene (31 and 23 kcal/mol, respectively). This can be connected to the bigger-than-expected ΔE_{ST} for this molecule (37 kcal/mol). It seems clear to us that PQDM is further away from the true diradical situation than generally imagined.

It is interesting to note that the energy gap between the singlet and triplet PESs decreases as the reaction of PQDM with SiH_4 (Figure 34) or ethylene (Figure 35) proceeds from reactant to

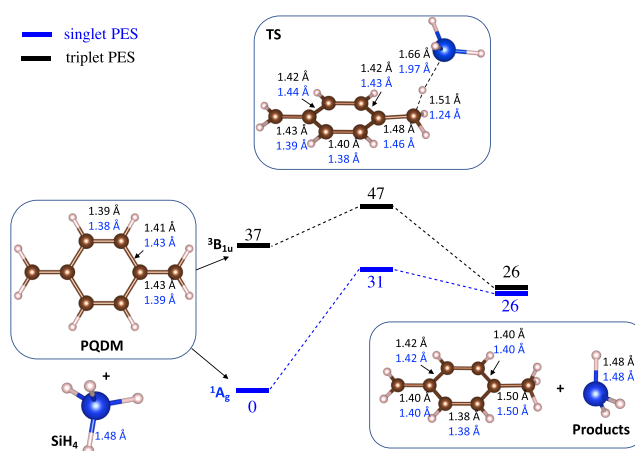


Figure 34. Potential energy surfaces (energies in kcal/mol) for H atom abstraction from SiH_4 by PQDM. Key bond distances are shown. Numbers in black and blue correspond to triplet and singlet PES, respectively. The two product molecules were optimized as separate molecules, as were the reactants (PQDM and SiH_4). The structures of the TS were optimized in C₂ symmetry. Calculations were done at the CASPT2/cc-pVTZ//CASPT2//cc-pVDZ level of theory. A (10/10) active space was used for the TS. See Supporting Information for active orbitals.

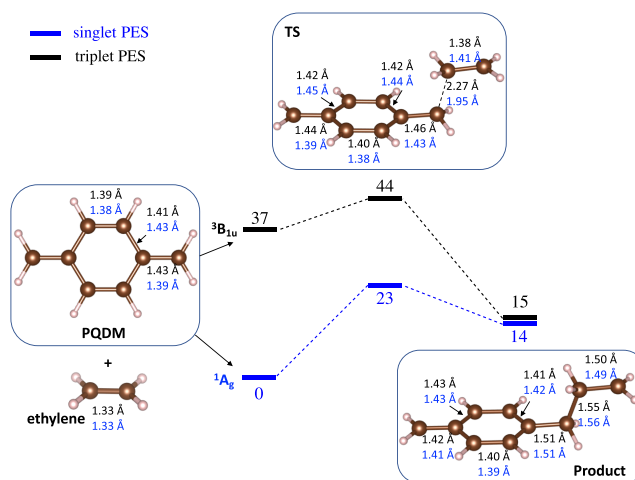


Figure 35. Potential energy surfaces (energies in kcal/mol) for reaction of ethylene with PQDM. Key bond distances are shown. Numbers in black and blue correspond to triplet and singlet PES, respectively. Reactants (PQDM and ethylene) were optimized as separate molecules. Calculations were done at the CASPT2/cc-pVTZ//CASPT2/cc-pVDZ level of theory. A (10/10) active space was used for the TS. See Supporting Information for active orbitals.

TS, and finally, to product. As discussed above, the appreciable gap between the HOMO and LUMO in PQDM gives rise to a closed-shell singlet ground state and a relatively big singlet–triplet gap. During the course of the reaction (take the H-abstraction example), the interaction between PQDM and SiH_4 is expected to reduce the gap between the two MOs. Figure 36 shows the comparison of the energies of relevant MOs in triplet PQDM and in the TS for H abstraction. The reason for using triplet PQDM in the analysis is that the two SOMOs, each being singly occupied, will be treated equally by the SCF process, so that one can compare their orbital energies. Both of the two calculated SOMOs show out-of-phase interactions with the Si–H σ MO in the TS. The energy of the higher SOMO remains

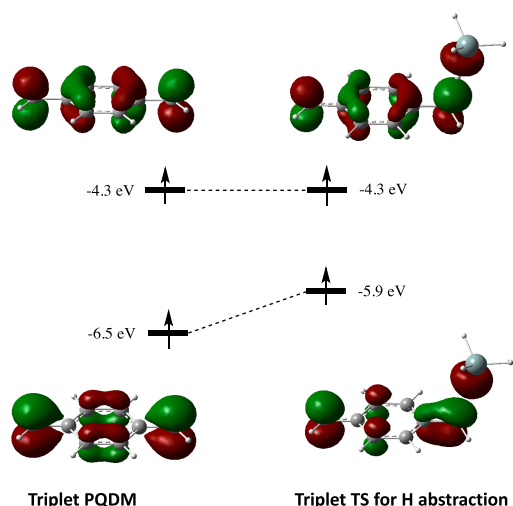


Figure 36. Two SOMOs in the reactant and the TS of the reaction of triplet PQDM + SiH₄. MO energies (α spins) in eV were calculated at UB3LYP/cc-pVTZ level of theory. MOs are plotted with isovalue = 0.05 atomic unit.

unchanged while the lower SOMO is pushed up in energy on going from the reactant to the TS. Consequently, the gap between the two SOMOs decreases, which explains the decreased singlet–triplet gap in the TS compared to the reactant.

Note that when the products, *para*-methylbenzyl and \bullet SiH₃, are formed, the two unpaired spins become spatially separated, analogous to the chain diradicals separated by methylene groups, discussed in section 10.2. This diradical can be considered as two radicals, and of course the singlet and triplet states will have a very similar energy.

The larger barrier on the singlet PES indicates a later TS, according to Hammond's postulate. Inspection of the optimized TS structures confirms this. The dissociating Si–H bond (Figure 34) needs to be elongated to 1.97 Å, and the shifting H atom needs come to a distance of 1.24 Å to one of the methylene carbon in PQDM, in order to reach the TS on the singlet PES. The corresponding distances are 1.66 and 1.51 Å for the triplet PES, which are much closer to those (1.70 and 1.44 Å) for the reference benzyl + SiH₄ reaction. Similarly, the forming C–C bond in the TS of PQDM + ethylene (Figure 35) is 0.3 Å shorter on the singlet PES than on the triplet PES, suggesting more difficulty in forming this C–C bond on the singlet PES.

PQDM represents the first diradicaloid whose reactivity is investigated here (next to a brief discussion of rectangular CBD). *The limited examples considered so far (H abstraction, addition to ethylene) suggest that in a reaction that forms two spatially separated radical centers, the HOMO–LUMO gap decreases naturally along the reaction course, leading to a reduced singlet–triplet gap along the reaction course.* Because the diradicaloid has a singlet ground state, the barrier on the singlet PES is always higher than that on the triplet PES. This diradicaloid-to-diradical transition, and the consequent change in the relative energy level of the spin states is summarized in Figure 7.

MQDM, as we noted, is a diradical with a triplet ground state, and as such quite different from the PQDM diradicaloid. Nevertheless, we also see the similar phenomenon of a decreasing singlet–triplet gap along the reaction courses of MQDM + SiH₄ (Figure 37) and MQDM + ethylene (Figure

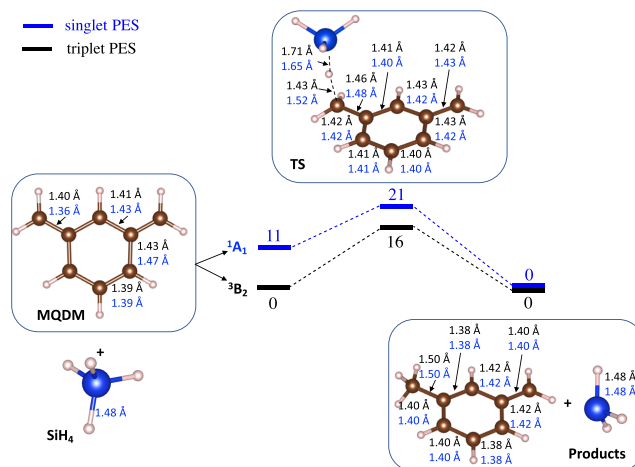


Figure 37. Potential energy surfaces (energies in kcal/mol) for H atom abstraction from SiH₄ by MQDM. Key bond distances are shown. Numbers in black and blue correspond to triplet and singlet PES, respectively. Reactants (MQDM and SiH₄) and products were optimized as separate molecules. The structures of the transition states were optimized in C_s symmetry. Calculations were done at the CASPT2/cc-pVTZ//CASPT2/cc-pVDZ level of theory. A (10/10) active space was used for the TSs. See Supporting Information for active orbitals.

38). However, the origin of this decreasing gap for MQDM is different from that for PQDM, as suggested by the MO analysis

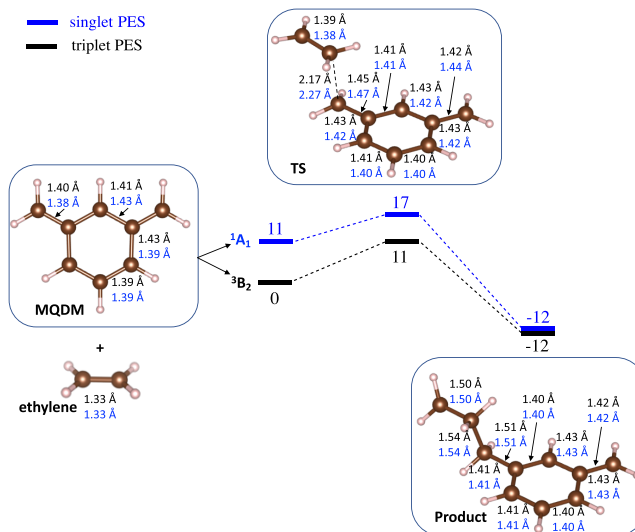


Figure 38. Potential energy surfaces (energies in kcal/mol) for reaction of ethylene with MQDM. Key bond distances are shown. Numbers in black and blue correspond to triplet and singlet PES, respectively. Reactants (MQDM and ethylene) were optimized as separate molecules. Calculations were done at the CASPT2/cc-pVTZ//CASPT2/cc-pVDZ level of theory. A (10/10) active space was used for the TSs. See Supporting Information for active orbitals.

in Figure 39. In both triplet MQDM and the TS, the energy differences between the two SOMOs are very small, rendering both systems diradicals. The extremely small gap between the two SOMOs is not likely to lead to a significantly decreased energy difference between the singlet and triplet along the respective reaction courses.

Comparing the two SOMOs in the TS for MQDM with those for PQDM, one important difference is that the two SOMOs for

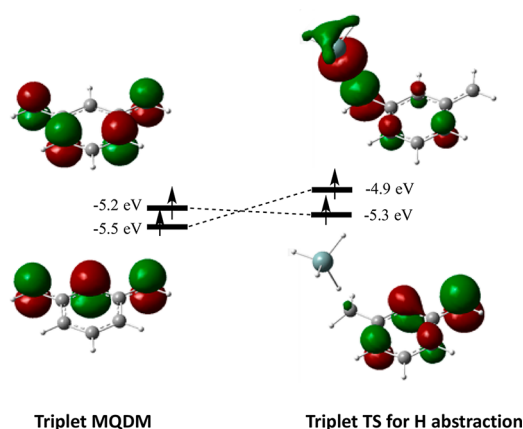


Figure 39. Two SOMOs in the reactant and the TS of the reaction of triplet MQDM + SiH₄. MO energies (α spins) in eV were calculated at UB3LYP/cc-pVTZ level of theory. MOs are plotted with isovalue = 0.05 atomic unit. Only one of the SOMOs interacts significantly with the Si–H bonding σ MO in the TS, in an out-of-phase manner, and this MO energy (–4.9 eV) is the highest.

the MQDM TS have a much greater spatial separation, i.e., the lower SOMO localizes more on the right side of the molecule and the higher SOMO more on the left side. In contrast, the two SOMOs in the TS for PQDM is similarly distributed across the whole molecule. The greater spatial separation of the two SOMOs of the TS for MQDM results in a smaller overlap and thus reduces the magnitude of the exchange integral K_{xy} (Figure 10) and eventually leads to reduced singlet–triplet gap.

Note that Hammond's postulate also applies to the comparison of singlet and triplet PESs for the reactions of MQDM with SiH₄ and ethylene in Figure 34, Figure 35, Figure 37, and Figure 38. The singlet PES has an earlier TS and a lower barrier than the triplet PES.

The structure and properties of PQDM have long attracted the interest of both experimentalists and theoreticians.^{64,178,189–192} In fact, one can trace this interest back all the way to at least 1937 (the year the senior author was born).¹⁹³ Initially, this compound mainly drew attention because of its role as an intermediate in the pyrolysis of *p*-xylylene, which leads to a polymer as a solid product.^{176,194–197} The intermediate PQDM only polymerized upon condensation (i.e., the molecules do not react with each other as long as they remain in the gas phase)^{196,198} and, beyond the initiation step, follows a radical polymerization mechanism.¹⁹⁸ For the initiation step, it has been proposed that PQDM in its “diradical” (excited triplet) state attacks ground state (singlet) PQDM, thus starting the polymerization.¹⁹⁹ These findings can be reconciled straightforwardly with the results in Table 9; in its ¹A_g ground state, PQDM is only moderately reactive, but upon excitation to its lowest triplet state (³B_{1u}), the barriers to reaction disappear almost entirely. More recently, it has been demonstrated that transition metal surfaces or metal oxides can prevent nucleation and propagation of the product polymer at room temperature, presumably by “locking” PQDM in its singlet state through the formation of a loose complex, destabilizing the triplet state.^{181,200,201}

An important side reaction of the polymerization process upon condensation of PQDM is a dimerization to 2,2-paracyclophane. Obviously, one way to reach this alternative product is by an intramolecular ring closing following the initiation step of the polymerization reaction (and an

intersystem crossing to transform the linear triplet dimer to a singlet one). However, one can wonder whether alternative mechanisms exist, for example, whether a concerted reaction between two singlet species is also possible. We keep in mind the entropic penalty that might be involved in such a mechanism. Analysis of the frontier orbitals for PQDM (Figure 40), or the

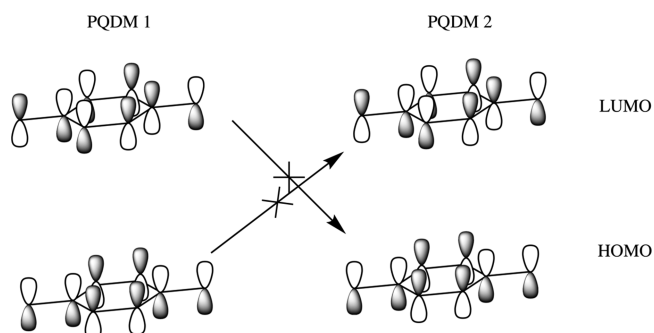


Figure 40. Frontier orbital analysis of PQDM. The frontier orbitals of the two molecules are **not** of corresponding symmetry, which would be required to favor dimerization to 2,2-paracyclophane.

construction of a full correlation diagram, leads to the conclusion that such a reaction pathway is symmetry-forbidden (it is formally a [6_s + 6_s] cycloaddition) and the convincing experimental arguments provided by Trahanovsky and co-workers confirm this.^{202,203}

Trahanovsky and Lorimor also demonstrated that zwitterionic intermediates play no role in this reaction either. So, dimerization (as well as polymerization) of PQDM follows a stepwise diradical mechanism. One could still argue that the diradical intermediate could be formed through a reaction between two singlet PQDMs as an alternative to a PQDM in the triplet state attacking a singlet one. But given that PQDM is unreactive in the gas phase at moderate temperatures, as already mentioned (so neither the dimer nor polymer is formed), and that condensation is required for any reaction to start,^{196,198} it should be clear that the mechanism involving a triplet compound is strongly favored. The analysis of the polymerization and dimerization reactions of PQDM further illustrates that the reactivity of the singlet and triplet state of a diradical(oid) can differ dramatically.

The reactivity of MQDM has received considerable attention as well. Goodman and Berson were able to trap MQDM by conjugated dienes to form indanes and *m*-cyclophenes.^{204–206} These trapping reactions occurred through a two-step cycloaddition mechanism involving a long-lived adduct diradical. Although direct evidence of the spin state of the intermediate could not be obtained, their data suggested that these reactions involved a triplet state.²⁰⁶

10.7. Oxygen, a Most Unreactive Diradical

What a remarkable molecule! All-important to life on earth, O₂ is the essential part of the greatest cycle of them all, that of respiration and photosynthesis. It is the only persistent paramagnetic molecule in our environment, and oxygen (which is how we will refer to the diatomic molecule, also called dioxygen) constitutes 21% of the atmosphere, while at the same time its reaction with all other elements (except gold) and with many molecules is exothermic, often highly so. The facts in the previous sentence are *prima facie* evidence of the thermodynamic instability (in reactions, not of the molecule

in and of itself) and, in spite of that, of the kinetic persistence of oxygen, and they are relevant to our diradical story.

10.7.1. The Electronic States of O₂. In O₂, we have six electrons distributed over a lower-lying degenerate π and a higher-lying, also degenerate, π^* orbital (see Figure 41). We clearly have a diradical before us.

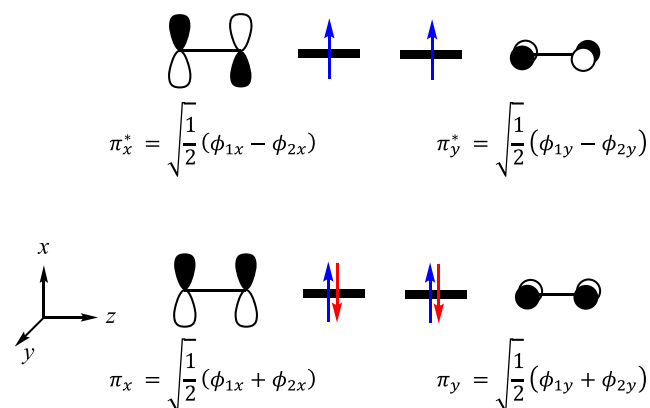


Figure 41. The π and π^* molecular orbitals of O₂, made from the $2p_x$ - π atomic orbitals (AOs), ϕ_{1x} and ϕ_{2x} , and $2p_y$ - π AOs, ϕ_{1y} and ϕ_{2y} , on oxygens 1 and 2. The molecule lies along the z axis. The α -spin electrons are colored blue and the β -spin electrons red. The normalization is a Hückel one, neglecting overlap.

In $D_{\infty h}$ symmetry, the three low-lying states of O₂ are ${}^3\Sigma_g^-$, ${}^1\Delta_g$, ${}^1\Sigma_g^+$ states; the ${}^1\Delta_g$ state is doubly degenerate. Figure 42 shows their order in energy.

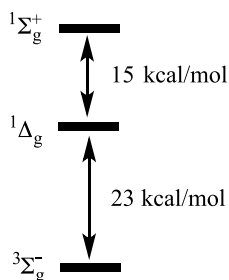


Figure 42. Low-lying states of O₂ and their energy ordering. The ${}^1\Delta_g$ state is a doubly degenerate state.

Considering Figure 42 in the context of our previous general diradical analysis, one can straightforwardly conclude that the ordering of the electronic states for the oxygen molecule corresponds to the middle case in Figure 5. The ${}^3\Sigma_g^-$ of O₂ lies approximately $2K_{xy} = 23$ kcal/mol lower in energy than the “open-shell”/“closed-shell” degenerate singlet state ${}^1\Delta_g$. We write out the detailed wave functions in section S3 of the Supporting Information; the open-shell/closed-shell ambiguity that we have alluded to is fully displayed in these functions. The still higher-lying second singlet ${}^1\Sigma_g^+$ is 38 kcal/mol above the ${}^3\Sigma_g^-$ ground state, almost twice of the difference between ${}^3\Sigma_g^-$ and ${}^1\Delta_g$ (Figure 42). This ${}^1\Sigma_g^+$ state is described by Ψ_{src} , and its energy is higher than Ψ_{src} by almost $2K_{xy}$ (see Figure 5).

The magnitude of $2K_{xy}$ makes for such large state splittings. Although the MOs π_x^* and π_y^* lie in orthogonal planes, they are not disjoint. In the ${}^3\Sigma_g^-$ state of O₂, the parallel spins of the

electrons keep the electrons from simultaneously appearing in these regions of space.

Although oxygen fits into the general description of diradicals given before, it is hard to understate how remarkable the properties of this molecule are. The origin of the extraordinary stability of O₂ can be traced back to the fine details of its electronic structure, as we have described in great detail elsewhere.²⁰⁷ We will summarize the complexity of the electronic structure of the ${}^3\Sigma_g^-$ state of O₂ below.

10.7.2. A VB Description of O₂. In a VB description of the molecule, we begin with the possible arrangements of four α and two β $2p_{x,y}$ electrons in O₂, as indicated in Figure 43. Note that at this stage there are no MOs as such; the electrons are placed in atomic orbitals.

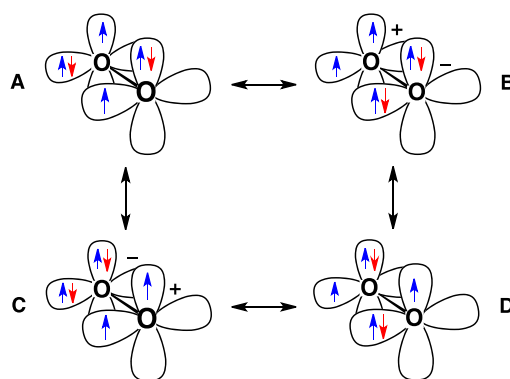


Figure 43. Possible distributions, A–D of four α and two β -spin electrons in the two orthogonal π systems of O₂. The α -spin electrons are colored blue and the β -spin electrons red. Reproduced with permission from ref 208. Copyright 2017 American Chemical Society.

Structures A and D in Figure 43 are expected to dominate the wave function, but there will be a contribution from the two zwitterionic structures, B and C. The resulting wave function, consisting of resonance structure A–D, is more than 100 kcal/mol lower in energy than simple valence structure A.^{208–210} That a VB approach gives a triplet ground state for O₂ has been known from the 1930s;^{211–213} that the triplet nature of the ground state of oxygen is difficult to explain is a myth.

10.7.3. The MO Description of O₂. In an MO approach, consider the restricted, open-shell, Hartree–Fock (ROHF) wave function for O₂. In the ROHF wave function,

$$\Psi(\text{ROHF}) = |\dots \pi_x^\alpha \pi_x^\beta \pi_y^\alpha \pi_y^\beta \pi_x^{*\alpha} \pi_y^{*\alpha}\rangle \quad (34)$$

where π and π^* are bonding and antibonding π MOs as defined in Figure 41, the two unpaired α -spins each occupy one of the two orthogonal, antibonding π_x^* and π_y^* MOs. This ROHF wave function represents maximum π bonding between the two oxygens; one can simply count the net bonding π electrons to come to a formal π bond order of 1.

However, this maximum bonding ROHF wave function is not the lowest energy one, as the interelectron correlation has not been considered. To improve the ROHF wave function, a second configuration is added to it. This configuration, $|\dots \pi_x^\alpha \pi_y^\alpha \pi_x^{*\alpha} \pi_x^{*\beta} \pi_y^{*\alpha} \pi_y^{*\beta}\rangle$, in which each β -spin electron is assigned to the antibonding π^* MO of one of the two orthogonal π systems, is schematically shown to the right of Figure 44. As discussed below, this second configuration introduces correlation between the motions of the two β -spin electrons so that the Coulomb repulsion between them is reduced. Other valence

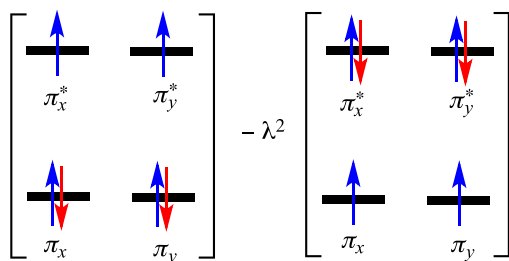


Figure 44. Schematic of the two-configuration (TC)SCF wave function for the triplet ground state of O₂. The α -spin electrons are colored blue and the β -spin electrons red. λ^2 is the mixing coefficient of the two configurations.

configurations, such as the one with only one β -spin being excited to the π^* MO, cannot (by symmetry) mix into the wave function.

The resulting two-configuration (TC)SCF wave function (unnormalized) for triplet O₂ is then

$$\Psi(\text{TCSCF}) = |\dots \pi_x^\alpha \pi_x^\beta \pi_y^\alpha \pi_y^\beta \pi_x^{\alpha*} \pi_y^{\alpha*} \pi_x^{\alpha*} \pi_y^{\alpha*}\rangle - \lambda^2 |\dots \pi_x^\alpha \pi_x^{\alpha*} \pi_y^\alpha \pi_y^{\alpha*} \pi_x^{\beta} \pi_y^{\beta} \pi_x^{\beta} \pi_y^{\beta}\rangle \quad (35)$$

where the mixing coefficient, λ^2 , can be determined variationally. Because the second configuration is much higher in energy than the first, λ^2 should be significantly less than 1.

One notes that the two configurations in eq 35 or Figure 44 both have α -spins in all four MOs and only differ by whether the β -spins are in the π or π^* MO. Because the MOs for two electrons of the same spin can be added or subtracted without changing a many-electron wave function (this corresponds to adding or subtracting rows and columns in a Slater determinant), the pair of α -spin electrons in the π and π^* MOs in each of the two orthogonal π systems can be taken to be localized, one in each AO (cf. the GVB orbitals). The MO description of the α spins in this way returns to the VB description; the resulting localized α spins are just represented by the same resonance structures we showed Figure 43.

The occupation schemes of the α -spin electrons are identical in the two configurations. In other words, addition of the second configuration to the ROHF wave function does not introduce any correlation between the α -spin electrons, nor does it introduce any correlation between the α -spin and β -spin.

However, the major effect of the addition of second configuration is to introduce correlation between the two β -spin electrons, so that they tend to be on different oxygen atoms, thus significantly reducing their Coulomb repulsion. In terms of the resonance structures in Figure 43, the ROHF wave function for the triplet ground state of O₂ gives equal weight to all four structures; after addition of the second configuration, resonance structures A and D have higher weights than ionic structures B and C.

To show the correlation between the β -spin electrons more conveniently, we abbreviate the TCSCF wave function in eq 35, leaving out the α -spins (even though there are four of them, and only two β spins), as

$$\Psi(\text{TCSCF}) = |\dots \pi_x^\beta \pi_y^\beta\rangle - \lambda^2 |\dots \pi_x^{\beta*} \pi_y^{\beta*}\rangle \quad (36)$$

In the limiting case where $\lambda^2 = 1$, the wave function can be rewritten and expanded in terms of the AOs in Figure 41 as

$$\Psi(\text{TCSCF}) = |\dots \phi_{1x}^\beta \phi_{2y}^\beta\rangle - |\dots \phi_{2x}^{\beta*} \phi_{1y}^{\beta*}\rangle \quad (37)$$

which always keeps the two β -spin electrons on different oxygens (the subscripts 1 and 2 indicate different oxygens); the Coulombic repulsion between them is thus minimized at the cost of bonding interaction.

In variationally optimizing λ , the energy of the TCSCF wave function is minimized by finding the best compromise between maximizing bonding in the two orthogonal π systems and minimizing the Coulombic repulsion between the β -spin electrons in them. A TCSCF/cc-pVTZ calculation on the triplet ground state of O₂, which is the same as a CASSCF/cc-pVTZ calculation (with an active space consisting of the two π and the two π^* MOs, and the six π electrons in them), gives $\lambda^2 = 0.24$.

Either way (VB or MO theory), one obtains a triplet ground state for O₂ and a very substantial resonance energy for that $^3\Sigma_g^-$ state. We refer the reader to our separate discussion of the stability and persistence of this remarkable triplet molecule.²⁰⁸

The set of oxygen states is completed by the high-lying $^1\Sigma_g^+$ state, which corresponds to Ψ_{SIC} in our general description of diradicals.

We turn to a comparison of the reactivity of $^3\Sigma_g^-$ and $^1\Delta_g$ O₂.

10.7.4. The Reactivity of $^3\Sigma_g^-$ O₂. Table 10 gives the computed heats and activation energies for $^3\Sigma_g^-$ O₂ dimerizing,

Table 10. Comparison of the Activation Energies (ΔE^\ddagger) and Reaction Energies (ΔE) of Dimerization, H-Atom Abstraction from SiH₄, and Addition to Ethylene for Triplet O₂, $\bullet\text{OOH}$, and $\bullet\text{OH}$ ^a

	di(oligo)merization		H abstraction from SiH ₄		addition to ethylene	
	ΔE^\ddagger	ΔE	ΔE^\ddagger	ΔE	ΔE^\ddagger	ΔE
O ₂ ($^3\Sigma_g^-$)	107 ^a	95 (cyclic O ₄) 83 (cyclic chair O ₆) 100 (cyclic crown O ₈)	44	40	37	33
$\bullet\text{OOH}$	0 ^b	-15	18	1	13	-4
$\bullet\text{OH}$	0 ^c	-49	0	-30	0	-29

^aSee Figure 46 below for the structure of this transition state. Calculations were done at (16/12)MS-CASPT2/cc-pVTZ level of theory. ^bObtained by scanning the middle O–O bond in HOO–OOH from 1.45 to 3.50 Å while maintaining a C₂ geometry. Calculations were done at (6/4)CASPT2/cc-pVTZ level of theory. ^cObtained by scanning the O–O bond in HO–OH from 1.47 to 3.00 Å while maintaining a C₂ geometry. Calculations were done at full-valence active space (14/10)CASPT2/cc-pVTZ level of theory. ^dCalculations were done at (U)CCSD(T)/cc-pVTZ//((U)B3LYP/cc-pVTZ level of theory, unless otherwise noted. The energies (kcal/mol) are electronic energies without ZPE correction.

abstracting a hydrogen from SiH₄ and adding to ethylene, and compares these with some O-centered simple radicals, $\bullet\text{OH}$ and $\bullet\text{OOH}$. Let us discuss these in turn.

10.7.5. Dimerization and Oligomerization. The oligomers of O₂ fall into two classes. The first are amply documented: weakly bound, yet quite detectable van der Waals complexes.^{214,215} The second group are listed in Table 10, and are so far only theoretically calculated O–O covalently bonded dimers, trimers, tetramers, each a local minimum, but very much unstable relative to the ground state of the diatomic.

The reader will know the very different story of the oligomers of S₂, whose dimers and trimers are bound by 71 and 103 kcal/

mol relative to the diatomic ground state. The attendant activation energies for oligomerization of triplet S_2 are low. The reason for this drastic difference between O_2 and S_2 is described in detail elsewhere;²⁰⁸ the substantial resonance stabilization of ${}^3\Sigma_g^- O_2$ is central to the argument.

10.7.6. Abstraction. The high activation energy for H abstraction by triplet O_2 from silane in Table 10 is there also for other abstractions. In the detailed study of the $2H_2 + O_2 \rightarrow 2H_2O$ reaction by Filatov, Reckien, Peyerimhoff, and Shaik,²¹⁶ the first reaction step is an abstraction one, leading to singlet or triplet coupled $\bullet OOH$ and $\bullet H$ radicals. This reaction encounters a very large barrier of 61 and 66 kcal/mol, respectively, for the triplet and the singlet states of the coupled radicals, because the very large resonance energy of O_2 makes this step highly endothermic.⁹¹ This highly endothermic first step is in fact the rate-determining step of the overall highly exothermic reaction, $2H_2 + O_2 \rightarrow 2H_2O$, which explains why those hydrogen balloons we explode for our students do not go off unless we supply a spark or a radical initiator.

In general, ${}^3\Sigma_g^- O_2$ reacts with difficulty with closed-shell compounds. So, for instance, the abstraction by triplet O_2 of a hydrogen from water would be endothermic by some 69 kcal/mol. Even from hydrogen peroxide, the abstraction of an H is endothermic by 37 kcal/mol. The origin of this endothermicity is the loss of resonance stabilization of the diatomic, to which we have already alluded. However, ${}^3\Sigma_g^- O_2$ does react readily with radicals, molecules that have one unpaired electron,²¹⁷ and with some very reactive closed-shell substrates, such as (for example) white phosphorus.²¹⁸

10.7.7. Addition to Ethylene. The calculated barrier of ${}^3\Sigma_g^- O_2$ addition to ethylene forming one C–O bond and yielding a diradical is similar to that of H abstraction, i.e., a high activation energy is needed for this reaction to occur.

In general, for the three types of reactions discussed above, ${}^3\Sigma_g^- O_2$ is the least reactive, showing largest barriers. For $\bullet OOH$, with a relatively small resonance stabilization, and for $\bullet OH$, where there is no resonance stabilization, the barriers to dimerization, H atom abstraction, and addition of ethylene are much lower than the corresponding reaction barriers for the highly resonance-stabilized, triplet O_2 .

10.7.8. Reactivity of ${}^1\Delta_g O_2$. Figure 45 shows the two Lewis structures for ${}^1\Delta_g O_2$. This ${}^1\Delta_g$ state is a doubly degenerate state, whose wave function can be expressed as either open-shell or

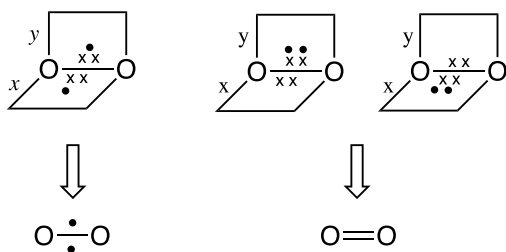


Figure 45. Two Lewis structures of ${}^1\Delta_g O_2$, one diradical-like, the other closed-shell-like. The top panel shows explicitly the 6 π electrons in both π_x and π_y planes. Crosses designate electrons in bonding π orbitals and dots antibonding π^* orbital. For the diradical-like structure, there are 3 π electrons in each of the x and y planes. For the closed-shell-like structure, the 2 + 4 uneven distribution of the 6 π electrons in either of the two equivalent configurations results in a full double bond in one of the two π planes. The structures in the bottom panel are shorthand for those in the top panel.

closed-shell singlet (see section S3 of the Supporting Information). Therefore, it is expected that the ${}^1\Delta_g$ state would both engage in typical radical reactions and react as a closed-shell molecule. It is important to note that the Lewis structure $O=O$ privileges one π system over the other, and in fact, it is the average of the two equivalent $O=O$ Lewis structures (one has the electron pair in π_x^* , and the other in π_y^*) that gives the proper representation of the closed-shell, singlet, wave function of ${}^1\Delta_g O_2$.

Table 11 summarizes the results. In general, the ${}^1\Delta_g$ state of O_2 is more reactive than the triplet one, featuring lower barriers

Table 11. Activation Energies (ΔE^\ddagger) and Reaction Energies (ΔE) of Dimerization to Cyclic O_4 , H Abstraction from SiH_4 , and Addition to Ethylene for the ${}^3\Sigma_g^-$ and ${}^1\Delta_g$ States of O_2 , Calculated at CASPT2/cc-pVTZ Level of Theory^a

	dimerization		H abstraction from SiH_4		addition to ethylene	
	Δ^\ddagger	ΔE	ΔE^\ddagger	ΔE	ΔE^\ddagger	ΔE
${}^3\Sigma_g^-$	107	101	49	46	40	37
${}^1\Delta_g$	62	56	33	22	24	15

^aSee section S2 of the Supporting Information for active space specification. The energies (kcal/mol) are relative electronic energies without ZPE correction.

in the three types of diagnostic reactions. We discuss them in detail below.

We start with dimerization. The calculated potential energy surfaces for singlet and triplet O_2 dimerization to singlet cyclic O_4 are shown in Figure 46. The ${}^1\Delta_g$ states of two molecules of O_2 are 45 kcal/mol higher in energy than the ${}^3\Sigma_g^-$ states, two times the experimental singlet–triplet energy gap (ΔE_{ST}). Both the triplet and singlet dimerize forming cyclic O_4 via the same singlet transition state, which was calculated to be 107 kcal/mol higher than two molecules of triplet O_2 separated by 5 Å. In the transition state (this is the lowest energy one), the two forming O–O bonds are of the same length, indicative of a concerted mechanism. Attempts to locate a stepwise transition state, with only one O–O bond forming in a C_2 geometry, failed; optimizations always led to the same D_2 transition state. Orbital correlation diagram analysis (cf. section S4 in the Supporting Information) shows that this dimerization is symmetry-forbidden. The reason that this symmetry-forbidden reaction is calculated to have a concerted TS might simply be that there is no other minimum on the singlet potential energy surface. Our CASPT2 calculations show that the two low-lying singlet states, 1A_g and 1B_u , of linear O_4 in C_{2h} symmetry are not minima. A stepwise pathway thus cannot lead to any stable products, only back to reactants. There appear to be no $\bullet O-O-O-O\bullet$ diradicals that are local minima in the system.

Given that the computed energy of the TS for dimerization of ${}^3\Sigma_g^-$ (or ${}^1\Delta_g$) O_2 is only 6 kcal/mol above the cyclic O_4 local minimum, O_4 will readily decompose to two molecules of ${}^3\Sigma_g^- O_2$.

For H abstraction from SiH_4 by O_2 , Figure 47 shows that the calculated barrier is lower on the singlet PES than on the triplet PES. The calculated Si–H bond being broken is extended less in the singlet TS than in the triplet TS, indicative of an early TS for the singlet relative to the triplet; this agrees with Hammond's postulate that the less endothermic reaction will have an earlier TS. The molecules we denote as product in Figure 47 are actually two weakly coupled monoradicals, which can react

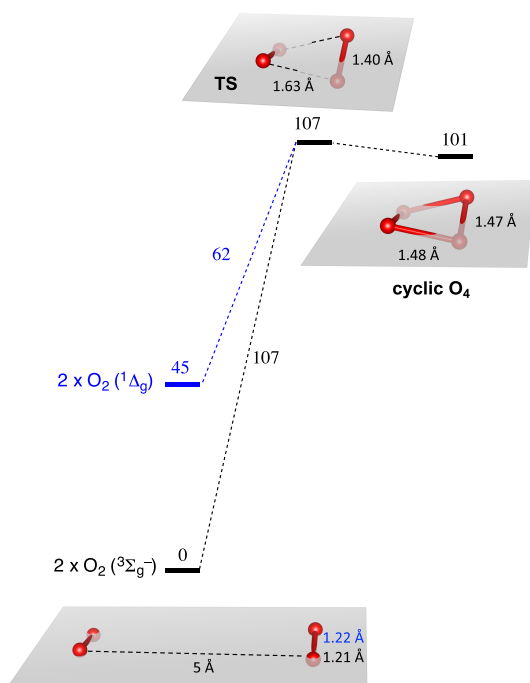


Figure 46. Potential energy surfaces (energies in kcal/mol) for the dimerizations of two molecules of $^3\Sigma_g^-$ O₂ and two molecules of $^1\Delta_g$ O₂, forming singlet, cyclic O₄. All structures were optimized in *D*₂ symmetry. The transition state was calculated to have only one imaginary frequency of $i1337\text{ cm}^{-1}$, which corresponds to the in-phase stretching of the pair of long O–O bonds. Calculations were done at multistate (MS)CASPT2/cc-pVTZ level of theory, with state-averaged CASSCF/cc-pVTZ reference wave functions. A (16/12) active space was used. The active orbitals are given in Supporting Information.

further to form the silylperoxide H₃SiOOH. This reaction is expected to be very fast; we did not consider it in detail here.

As in the previous examples of reactions of the singlet and triplet states of diradicals, the energy difference between the singlet and triplet surfaces decreases as the reaction proceeds from reactant to TS, and finally, to product. The singlet state of the product is calculated to be even slightly lower than the corresponding triplet. In section 3, we discussed that ΔE_{ST} is roughly $2K_{xy}$, where K_{xy} is the exchange integral for the two singly occupied orbitals. As the H atom of SiH₄ is abstracted by O₂, the two unpaired electrons are spatially separated, from both on O₂ to one on $\bullet\text{SiH}_3$ and the other on HOO \bullet . Consequently, the spatial overlap between the orbitals of the two unpaired electrons decreases, leading to a reduced K_{xy} and therefore reduced ΔE_{ST} . The two SOMOs for the TS are shown in Figure 47. They are of different symmetries in the *C*_s geometry.

Figure 48 shows the calculated PES of O₂ addition to ethylene via a stepwise (or diradical) mechanism, in which only one C–O bond is formed in the first step. The addition of $^1\Delta_g$ O₂ is calculated to have a lower barrier and an earlier TS than the addition of $^3\Sigma_g^-$ O₂. The latter is evident from the longer C–O bond and shorter C–C and O–O bonds in the singlet TS. Of the 23 kcal/mol difference in energy between the two reactants, more than 2/3 disappears in the TS and only about 5% remains in the products. This reduction of ΔE_{ST} has the same origin as in the previous H abstraction reactions, that is, the separation of unpaired electrons and the decrease in the orbital overlap between the two SOMOs leads to a reduced exchange integral K_{xy} . In the product, the two unpaired electrons can be viewed as

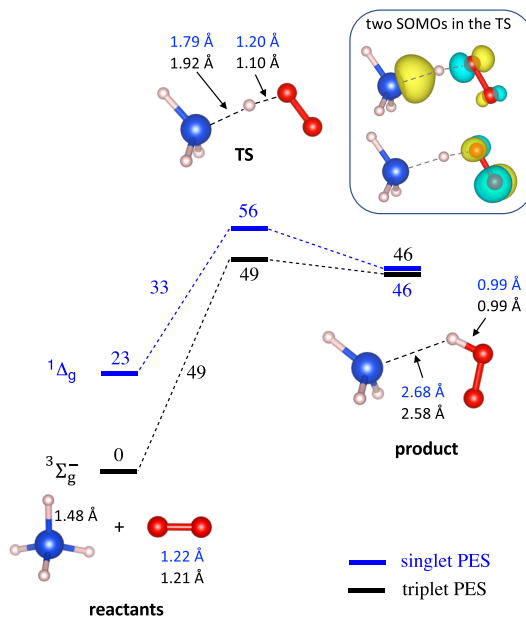


Figure 47. Potential energy surfaces (energies in kcal/mol) for H atom abstraction from SiH₄ by $^3\Sigma_g^-$ and $^1\Delta_g$ O₂. Key bond distances are shown. The two active orbitals with occupation number of about 1 for the TS are shown. Numbers in black and blue correspond to triplet and singlet PES, respectively. Reactants were optimized as separate molecules. The structures of TS and product were optimized in *C*_s symmetry. Calculations were done at the CASPT2/cc-pVTZ level of theory. (6/4), (2/2), and (8/6) active spaces were used for O₂, SiH₄, and TS and product, respectively. See Supporting Information for active orbitals.

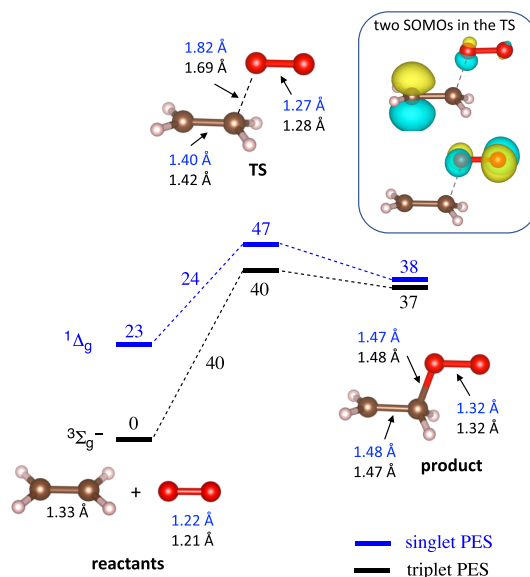


Figure 48. Potential energy surfaces (energies in kcal/mol) of additions to ethylene by $^3\Sigma_g^-$ and $^1\Delta_g$ O₂. Key bond distances are shown. The two active orbitals with occupation number of about 1 for the TS are shown. Numbers in black and blue correspond to triplet and singlet PES, respectively. Reactants were optimized as separate molecules. The structures of TS and product were optimized in *C*_s symmetry. Calculations were done at CASPT2/cc-pVTZ level of theory. (8/6), (2/2), and (10/8) active spaces were used respectively for O₂, ethylene, and TS and product. See Supporting Information for active orbitals.

localized on the terminal carbon and oxygen atoms, and their orbitals are of different symmetry; therefore, ΔE_{ST} is almost zero in the product. Interestingly, in this reaction a class 2 diradical reactant O_2 has converted to a class 1 diradical product.

The least-motion, concerted mechanism for the reaction between singlet O_2 and ethylene to give a dioxetane is symmetry-forbidden (Figure 49). Dioxetane is a fascinating, unstable

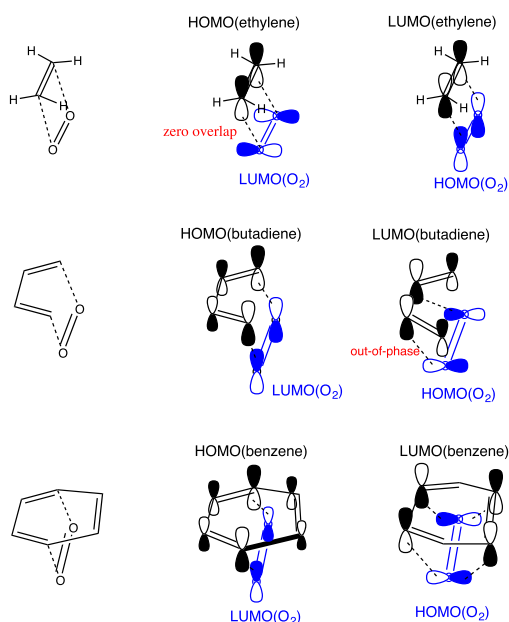


Figure 49. Frontier orbital interactions in reactions of singlet $\text{O}=\text{O}$ with ethylene, butadiene, and benzene. Previous calculations suggest that, among the three reactions, only the $[4 + 2]$ cycloaddition of benzene with $\text{O}=\text{O}$ occurs concertedly.

molecule responsible for bioluminescence in fireflies;^{219,220} its dioxo derivative, dioxetanedione, is an intermediate involved in the chemiluminescence of glowsticks.^{221,222} No transition structure was found for such a pathway.

Next, we discuss the closed-shell reactivity of the $^1\Delta_g$ state of O_2 . With its ambiguous resonance structure, one would expect $\text{O}=\text{O}$ to participate in concerted pericyclic reactions as ethylene (with a $\text{C}=\text{C}$ double bond) does. However, unlike ethylene, where the HOMO and LUMO are π and π^* MOs, respectively, the HOMO and LUMO in $\text{O}=\text{O}$ are both π^* MOs, and they are in two orthogonal π systems. The two π^* MOs are initially degenerate in $^1\Delta_g \text{O}_2$, but as the O_2 molecule interacts with another reagent during a pericyclic reaction, the two MO levels will split so that the closed-shell representation $\text{O}=\text{O}$ becomes valid.

Indeed, $^1\Delta_g \text{O}_2$ participates in Lewis acid–base reactions, concerted Diels–Alder cycloaddition reactions, and formally concerted ene reactions, exactly what would be expected for a typical closed-shell molecule.^{223–228} We should note that computational studies have pointed to (aside from the concerted reaction mechanisms) potentially competing stepwise (diradical) reactions,^{229–231} in the same way as these mechanisms have been identified for traditional Diels–Alder reactions (ethylene and butadiene).^{232,233} Whereas for traditional Diels–Alder reactions, these proposed stepwise diradical mechanisms require in general greater activation energy than the concerted mechanism (and thus are assumed not to play an important role), for singlet oxygen, the diradical, nonconcerted

mechanisms, can come awfully close. Some calculations even point toward real competition between the two mechanisms.^{230,231}

Still, even for the few instances where the activation energy of the stepwise diradical mechanism has been calculated to be slightly lower than that of the concerted mechanism, the potential energy surface (PES) was found to be very flat, and the concerted path was lower than the stepwise path in some parts. That makes the avoidance of the intermediate diradical during dynamical sampling of the PES quite probable. Additionally, some studies have indicated that the activation energies for such diradical mechanisms could easily be underestimated, if correlation is treated inadequately.^{12,13} As a result, even these reactions can be considered effectively concerted.

Most experimental data supports this view, pointing to retention of stereoselectivity, an indication of concertedness, in the vast majority of the reactions with singlet oxygen, thus making the existence of long-living diradical intermediates unlikely.^{224,226,228} As such, one can expect singlet oxygen to react, in most cases, in a similar fashion to ordinary closed-shell molecules.

Finally, we would like to examine the reactivity of $^1\Delta_g \text{O}_2$ in cycloadditions from the point of view of frontier orbitals. Computational studies suggested that the reaction of ethylene with $^1\Delta_g \text{O}_2$ proceeds via a stepwise diradical pathway,²³⁴ which is expected for a symmetry-forbidden $[2 + 2]$ cycloaddition. Interestingly, the stepwise diradical pathways for symmetry-allowed $[4 + 2]$ cycloadditions of butadiene²³⁵ and 1,3-cyclohexadiene²³⁶ with $^1\Delta_g \text{O}_2$ were also calculated to be more favorable than the concerted pathways. However, calculations do suggest that the $[4 + 2]$ cycloaddition of benzene with $^1\Delta_g \text{O}_2$ occurs concertedly.

In Figure 49, we examine the frontier orbital interactions for cycloadditions of ethylene, butadiene, and benzene with $\text{O}=\text{O}$. For cycloaddition of $\text{O}=\text{O}$ with ethylene or butadiene, there is only one HOMO–LUMO pair that has compatible symmetry for a favorable interaction. The other HOMO–LUMO pair either has zero overlap (the ethylene case) or incompatible symmetry (the butadiene case). This might be the reason that the concerted pathways for the two cycloadditions were calculated to have higher barriers than the corresponding stepwise diradical pathways. On the other hand, Figure 49 shows that for the $4 + 2$ cycloaddition of benzene and $\text{O}=\text{O}$, both of the two HOMO–LUMO pairs have compatible symmetry, favoring unequivocally a concerted mechanism.

11. WAYS TO THINK ABOUT DIRADICALOID REACTIVITY

That was a long haul, through a multitude of real and potential diagnostic reactions of diradicals. It was needed; the literature does not contain as systematic an account of reactivity, using a single, consistent, methodology, as that presented above. We now need to extract from the multitude of theoretical and experimental details a general, qualitative approach to diradical reactivity. This will be done in steps.

11.1. Radical Reactions and Preparation

Let us first examine typical monoradical reactions, focusing on how the wave function of the reactant transforms into that of the product. In this section, we switch several times between delocalized and localized perspectives. Note that the principal ideas presented below, originating from a pure MO perspective,

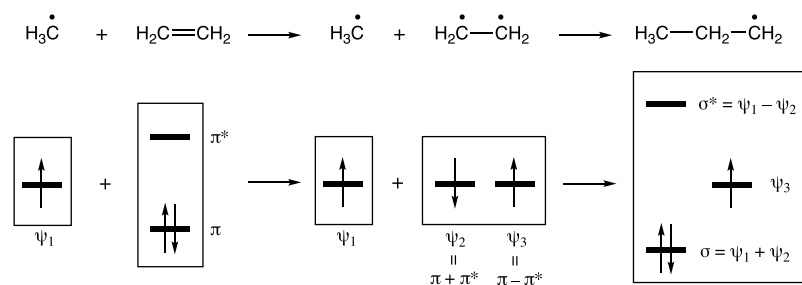


Figure 50. MO analysis of a typical reaction of a radical with a closed-shell molecule. The combinations of orbitals are not normalized.

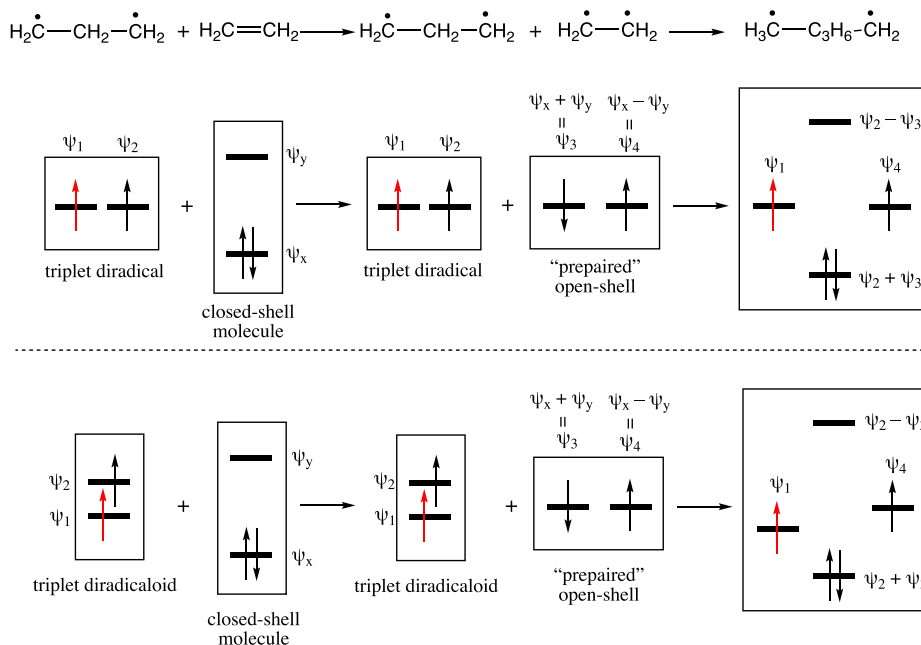


Figure 51. MO view of a typical radical-type reaction of a triplet diradical (top) and a triplet diradicaloid (bottom) with a closed-shell molecule. The coefficients are not normalized. The diagram also applies to open-shell singlet states of diradical(oid)s by flipping the highlighted spins.

are closely related to some aspects of the VB viewpoint on reactivity of Shaik, Hiberty, and co-workers.^{237–239}

Consider first a radical reaction, methyl radical reacting with ethylene, affording a propyl radical (Figure 50). The reaction breaks the π bond of ethylene, forms a CC σ bond and generates a new radical center, all concurrently. Conceptually, one way to analyze the course of the reaction is to imagine a first, discrete step of breaking the π bond of ethylene into two radicals. In a second step, one of the two radicals recombines with the methyl radical, forming a σ bond, while the other remains as the new radical center in propyl.

In MO language, in the first step, linear combinations of the π and π^* orbitals of ethylene generate two nonbonding orbitals ψ_2 and ψ_3 ; equal mixing of the $(\pi)^2$ and $(\pi^*)^2$ closed-shell singlet configurations (with a minus sign) results in an open-shell singlet configuration $(\psi_2)^1(\psi_3)^1$ that corresponds to a singlet “dimethylene” diradical. The two electrons originally occupying the π bonding orbital have now been decoupled.

In the second step, ψ_2 combines with ψ_1 , giving σ and σ^* orbitals (the new C–C bond); the σ orbital is doubly occupied. ψ_3 remains singly occupied. The first step clearly has a substantial cost, the energy of a π bond. In the second step, the system is just as clearly stabilized upon σ bond formation. Taken together, they lead to a small activation energy.

Let us express this in another way: From the point of view of the “triradical” waypoint in this dissected process, a virtual $\psi_1^1\psi_2^1\psi_3^1$, combining ψ_2 and ψ_3 leads to the formation of the π bond in the reactant while combining ψ_1 and ψ_2 leads to the formation of the σ bond in the product.

$$\begin{aligned} (\psi_1)^1(\psi_2)^1(\psi_3)^1 &\rightarrow (\psi_2 + \psi_3)^2(\psi_1)^1 = (\pi)^2(\psi_1)^1 \\ (\psi_1)^1(\psi_2)^1(\psi_3)^1 &\rightarrow (\psi_1 + \psi_2)^2(\psi_3)^1 = (\sigma)^2(\psi_3)^1 \end{aligned} \quad (38)$$

However, in reality, this reaction will certainly not proceed through a real triradical state for the breaking of the π bond and the formation of the σ occur concurrently. The TS of the actual pathway is hence considerably lower in energy than any state of a triradical $\psi_1^1\psi_2^1\psi_3^1$, and the barrier of the reaction is only about 10 kcal/mol.

Note importantly that the orbital transformation in the “preparation” step is of the same kind as discussed in section 5 for diradicals. The localization of unpaired electrons “prepares” the molecule (ethylene) for reaction with a radical (methyl), using one of the unpaired electrons of the ethylene in a radical recombination fashion. As we will see later, the “preparation” idea is also applicable to understanding radical reactivity of closed-shell singlet states of diradical(oid)s.

We also want to mention here that the viewpoint presented above, in which a preparation step with an associated energy cost

is conceptualized, is closely related to the concept of a promotion energy G associated to the reactants, determining the barrier height for a chemical reaction in a typical VB diagram. An in-depth discussion of the VB perspective on reactivity in which the factors determining the promotion gap for different types of reactions are discussed can be found in ref 240.

11.2. Preparation as a Way to Think about Diradical(oid) Reactivity

The “preparation” way of thinking can be extended easily to diradicaloids. We start with the triplet state of a diradical(oid), which, as far as the reactivity is concerned, can be conveniently viewed as a radical twice over, whether there is any interaction between the two unpaired electrons or not. These triplets will show typical radical reactivity which can be understood based on the analysis above for radicals. Let us use trimethylene + ethylene \rightarrow pentamethylene as an example (Figure 51, top)

The reaction starts with a diradical and ends up with a diradical, going through a formal or virtual tetraradical intermediate stage following the “preparation” of ethylene. In this case, it is more convenient to start with the **localized** orbitals of trimethylene ψ_1 and ψ_2 , each corresponding to a radical on the terminus. Only one of the radical centers (ψ_2) participates in the reaction, forming a new σ bond ($\psi_2 + \psi_3$) and generating a new radical (ψ_4), and the other radical center (ψ_1) remains intact. The same analysis applies when the two initial orbitals are no longer degenerate (Figure 51, bottom).

Note the use of localized orbitals for the diradical reactant to maximize the resemblance of the singly occupied ψ_1 in the product to the one in the reactant. It is almost always possible in a triplet state to form linear combinations of the delocalized SOMOs to yield a more localized set that has one of the unpaired electrons primarily localized on the reacting site (ψ_2). Note that O_2 , as a class 2 diradical, is an exception (cf. section 10.7). This orbital transformation for the triplet diradical(oid) does not change the energy of the system because there will always be two unpaired electrons for a triplet diradical whether one chooses delocalized or localized orbitals.

However, for a singlet diradical or diradicaloid, such an orbital localization does change the closed-shell/open-shell character of the singlet as a consequence of the available transformation discussed several times above. For a singlet diradical(oid) to participate in a radical reaction, it is preferable to have an unpaired electron in a largely localized orbital at the reaction site. In general, the open-shell singlet of a diradical(oid) based on localized orbitals satisfies the above condition. This is the two-configuration closed-shell singlet based on delocalized canonical orbitals, which is usually the lowest energy singlet.

To understand the radical reactivity of a singlet diradical(oid), we can use the same analysis as in Figure 51, except one needs to flip one of the spins in the initial diradical, e.g., the red spin in ψ_1 , keeping in mind ψ_1 and ψ_2 are localized orbitals. If one starts with delocalized orbitals, an orbital localization step similar to the “preparation” step of ethylene is needed, and it is shown in Figure 52. For diradicals with degenerate orbital levels, the “preparation” costs no extra energy. For diradicaloids with a nonzero orbital gap, the “preparation” polarizes the doubly occupied ψ_x orbital in opposite directions for the two electrons by mixing in the empty orbital ψ_y , differently [$\sqrt{(1 - \lambda^2)}\psi_x \pm \lambda\psi_y$]. The extent of polarization grows with the mixing coefficient. The larger λ , the more polarized and hence more localized the transformed orbitals are, and the more prepared the

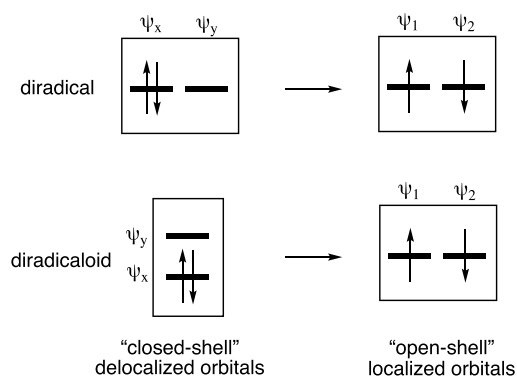


Figure 52. Orbital transformation for singlet diradical (top) and singlet diradicaloid (bottom). Only one of the two equivalent closed-shell configurations of the singlet diradical is shown.

molecule is for subsequent radical reaction. But also, the larger the HOMO–LUMO gap, the more difficult it is to have a large λ .

Let us illustrate this process with the reaction of PQDM addition to ethylene in radical fashion (Figure 53). The mixing of PQDM HOMO and LUMO (ψ_x and ψ_y) transforms the quinoid structure to the benzylic structure with two unpaired electrons largely localized on the two methylene groups. Please note that the localized orbitals are distributed solely on the starred or the unstarred C atoms of this alternant hydrocarbon, which has the same numbers of the two sets of atoms. The similar “preparation” of ethylene breaks the π bond and generates two unpaired electrons. The two “prepared” molecules then react. A σ bond forms from the in-phase interaction between ψ_2 and ψ_3 . The localized radical orbitals ψ_1 of PQDM and ψ_4 of ethylene remain largely unchanged, becoming a benzylic orbital and a carbon 2p orbital that correspond to the two radicals in the final product.

In section S5 of the Supporting Information, we discuss the last remaining reaction type, the closed-shell reactivity of singlet diradical(oid)s.

The “preparation” perspective is a way to bring together disparate reactivity patterns for triplets and singlets for open-shell and closed-shell species. To summarize, we find it more convenient to analyze diradical(oid) reactivity by making use of localized orbitals with unpaired electrons for reactions that involve decoupling and recoupling of electron pairs (even if the initial MOs are delocalized), but for closed-shell reactions, the reactivity is analyzed more easily with delocalized diradical(oid) MOs with formally paired electrons. The view presented applies to not only diradical(oid)s, irrespective of their spin states, but also monoradicals and closed-shell molecules.

12. PRELIMINARY SUMMARY OF DIRADICAL REACTIVITY

Let us go back to the two questions raised at the beginning of the section of radical and diradical reactivity:

1. Is a diradical more or less reactive than a closely related monoradical? and
2. What is the difference, if any, in reactivity between the triplet and singlet states of a diradical?

We think a three-step approach to these questions is appropriate. First, we consider the triplet state of the diradical and we take the magnitude of the activation energy calculated for its reactions as a measure of the reactivity. From our analysis above, we can conclude that the main factor determining the

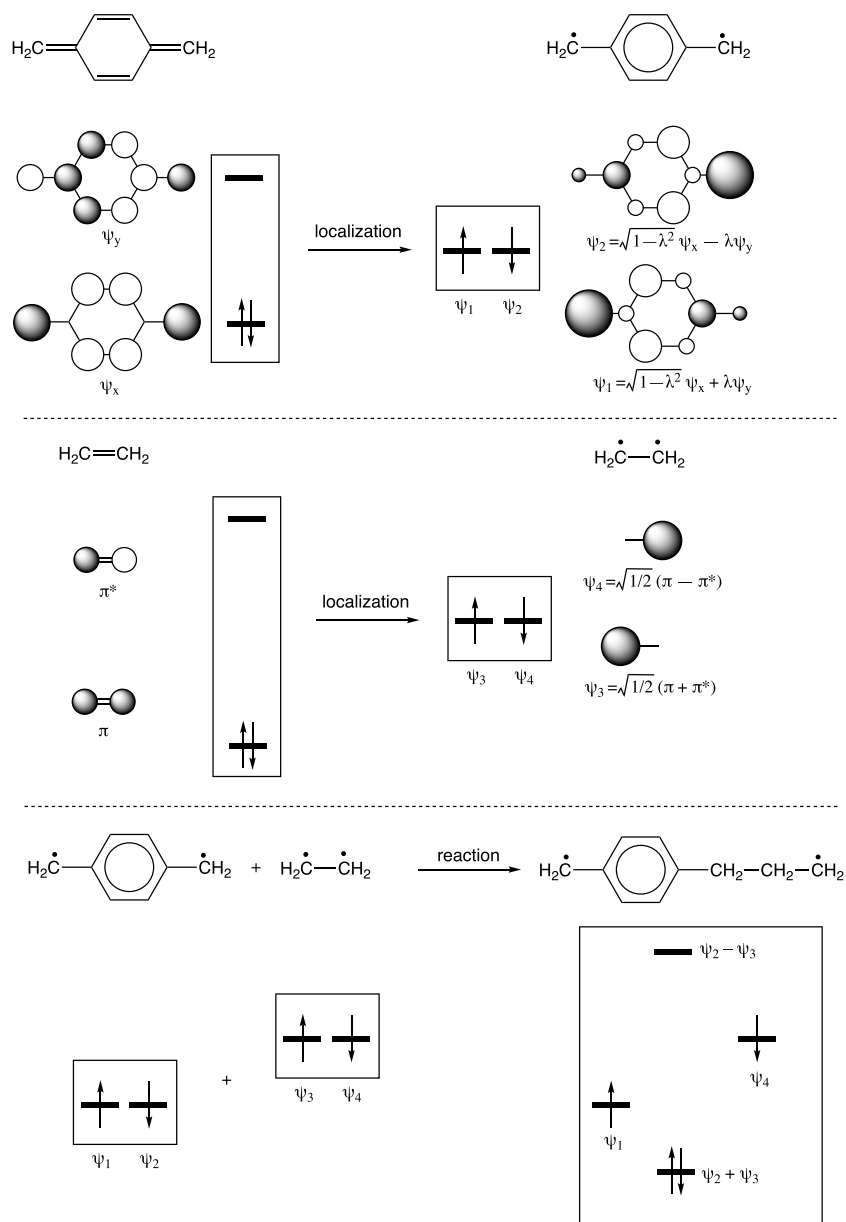


Figure 53. Illustration of radical addition of PQDM to ethylene, showing the localization of PQDM orbitals (top), localization of ethylene orbitals (mid), and subsequent reaction (bottom).

reactivity of these states is the spin density at the radical site, in exactly the same way as it is the case for monoradicals. As we have demonstrated, increases/decreases in the reactivity of the triplet state of a diradical compared to its closely related monoradical can generally be connected to an increase/decrease in the spin density. Comparisons of the reactivity of triplet TMM/triplet CBD/allyl, and PQDM/MQDM/benzyl provide good examples for this reasoning.

However, *spin density is hardly the only factor governing the reactivity of mono/diradicals*, and these other factors may obscure a clear quantitative correlation between spin densities and radical reactivity.

The most eye-catching exception to the general reactivity-spin density correlation is found in the relatively low reactivity of triplet O_2 ; even though the spin density on both sites of this molecule is unity, its reactivity is considerably lower than for related localized monoradicals. In the previous section, we

showed that this unusual behavior can be attributed to resonance stabilization, a thermodynamic effect, which turns out to have a much bigger impact on the reactivity of this molecule than the relatively high spin density.

Other, less pronounced, factors have also been discussed in the previous sections. For example, triplet CBD contains significant ring strain, which is partially released upon reaction. This release of strain causes the reactivity of this compound to exceed the value which could be expected based solely on the spin density. A host of other factors moderating or intensifying the reactivity of the triplet states of diradical(oid)s, many of which we did not touch throughout our analysis, can be envisioned as well (cf. steric hindrance), further demonstrating that even though the spin density can be considered as the main driver of the reactivity of most diradical(oid)s, one should be cautious not to focus solely on a single factor.

The second step of this three-step approach to diradical reactivity is to focus on the singlet–triplet gap ΔE_{ST} of the system as the reaction proceeds. In the reactant state, the singlet–triplet gap is just that of the diradical itself, which can be understood on the basis of the discussions we laid out in section 3 for diradicals and section 4 for diradicaloids. Two important factors affecting ΔE_{ST} are the HOMO–LUMO gap (or SOMO–SOMO gap) and the exchange integral K_{xy} . As reactions proceed to TSs and finally on to products, those are also factors to look at, defining the change of ΔE_{ST} along the reaction course.

To put it another way, once we understand how ΔE_{ST} changes along the reaction course, we can compare the reactivity of singlet vs triplet. For example, if a diradical has a triplet ground state, and the magnitude of ΔE_{ST} decreases along the reaction course, then the reaction will have a lower barrier on the singlet PES and the singlet will be more reactive than the triplet. Although this conclusion seems evident, that an excited state is more reactive than the ground state, we believe the spin state evolution argument gives us a deeper understanding of how that is so in the context of diradical reactions. We can relate the higher reactivity of an excited state to the reduction of the relevant singlet–triplet gap along the reaction course, a variable which can be analyzed and understood qualitatively, often without any calculations (or with some quick calculations).

How then is this done, i.e., how does one analyze the ΔE_{ST} change along the reaction course, focusing on the HOMO–LUMO gap (or SOMO–SOMO gap) and the exchange integral K_{xy} ? If a reaction starts with a diradical and ends up with a diradical (or two radicals) as product, as for most of the H-atom abstractions from SiH_4 and additions to ethylene that we examined, the SOMO–SOMO gap is small throughout the reaction course, and ΔE_{ST} is mainly determined by the exchange integral K_{xy} , i.e., the difference in interelectron interaction between the two spin states (cf. section 3.2). The magnitude of K_{xy} is determined by the spatial overlap (extent in space, not overlap integral) of the two most localized MOs involved. Analyzing how the spatial overlap of the participating orbitals changes will thus provide a qualitative answer as to how ΔE_{ST} would change. Many of the diagnostic reactions we examined end up separating the two radical centers in the products; clearly, the spatial overlap of the two MOs decreases, with it the magnitude of the exchange integral, which leads to a reduction of the magnitude of ΔE_{ST} .

If the reactant and product of a reaction are different, in the sense that one is a diradical and the other a diradicaloid (or closed-shell molecule), there ought to be a substantial change in the HOMO–LUMO gap over the course of the reaction. A reduced HOMO–LUMO gap would be expected if a reaction goes from diradicaloid to diradical and vice versa. One example is the H-atom abstraction from SiH_4 by PQDM. PQDM is a diradicaloid with a singlet ground state and an appreciable HOMO–LUMO gap, whereas the products of the above reaction are two radicals with reduced SOMO–SOMO gap. A reduced HOMO–LUMO gap generally leads to reduced singlet–triplet gap and thus more diradical character. Triplet PQDM, being higher in energy than the singlet state, is thus more reactive than singlet PQDM.

In general, a radical type reaction (H-atom abstraction, radical addition to ethylene) ends up with spatially separating the two radical centers in the diradical reactant or creates two spatially separated radical centers from the diradicaloid reactant. In either case, a reduced singlet–triplet gap is expected, regardless of the ground state spin of the reactant diradical(oid). Figure 54 shows

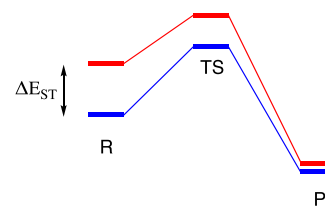


Figure 54. Generic reaction profile for the two spin states (singlet and triplet) of a diradical(oid) in a radical-type reaction, showing the decreased ΔE_{ST} along the reaction course. R, TS, and P label reactant, transition state, and product, respectively.

a generic reaction profile for reaction of the singlet and triplet spin states of a diradical(oid), with this characteristic feature of a reduced ΔE_{ST} along the reaction course. The figure is drawn for an exothermic reaction, but one sees it also for endothermic ones.

In step two, we essentially compared the reactivity of triplet vs singlet in reactions (e.g., H-atom abstraction) that are similar and accessible for both spin states. These reactions are also typical monoradical ones (which is why we chose them in the comparison). A localized view with unpaired electrons in the two orbitals is best suited for analyzing this type of reaction, as we have done in section 11. Given the open-shell/closed-shell duality, to which we have repeatedly alluded in this paper, it is the open-shell wave function based on localized orbitals that best exhibits the underlying familiar radical reactivity.

The third step in the analysis of the reactivity of any diradical or diradicaloid states is to examine additional reaction modes for a singlet diradical(oid), pathways that are in principle unavailable for the triplet states. There is nothing mysterious about these; these are, for example, the concerted reactions involving both radical centers (e.g., formation of two bonds) that resemble cycloadditions of closed-shell molecules. This kind of reactivity originates from the “closed-shell” two-configuration wave function based on delocalized orbitals for the singlet state of a diradical. During the reaction, one configuration becomes dominant so that the diradical evolves into a closed-shell precursor for the subsequent concerted reaction.

Examples of this type that we examined are cycloadditions between ethylene and the singlet states of CBD, TMM, and O_2 . The degenerate MOs of these diradicals split in energy, substantially so, over the course of the cycloadditions in the requisite specific geometry with reduced symmetry. This splitting is a result of the different interactions of the degenerate MOs with the frontier MOs of its reaction partner. The Woodward–Hoffmann rules may be applied to determine the allowedness/forbiddenness of the reaction, as we showed for the aforementioned three cycloadditions. Lower barriers are usually expected for symmetry-allowed cycloadditions, compared with the stepwise reaction modes that are available, and often competitive, for both the triplet and singlet states.

A diradical in the “closed-shell” singlet state that can be described by a two-configuration wave function can be viewed as having simultaneously a high-lying HOMO and a low-lying LUMO. Therefore, the “closed-shell” singlet state of a diradical may also engage in reactions as either a nucleophile or an electrophile. Examples of diradicals reacting as electrophiles have been reported.^{240–244}

Finally, we note that the lowest singlet of a radical(oid) gives rise to both radical and closed-shell reactivities. We see here the advantage of viewing the mathematical open-shell/closed-shell ambiguity as a chemical duality. It allows us to view singlet

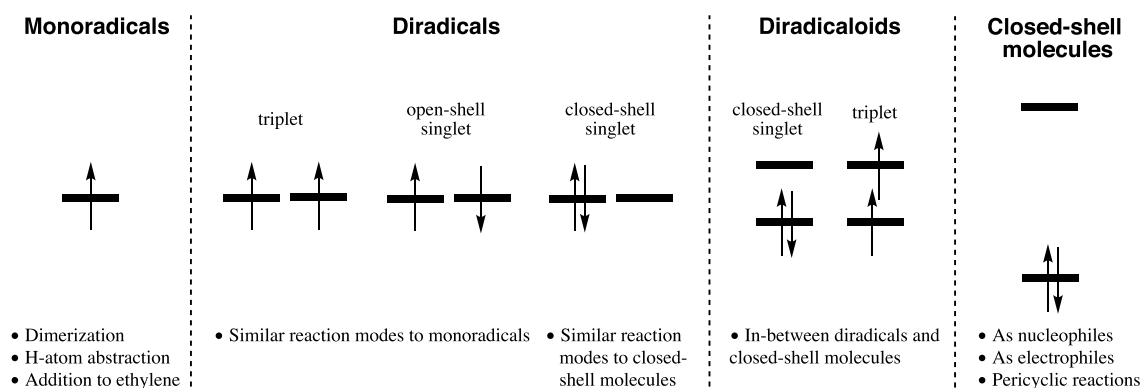


Figure 55. A molecular orbital point of view of the continuous spectrum of reactivity for monoradicals—diradicals—diradicaloids—closed-shell molecules. Only one of the two equivalent closed-shell configurations of the closed-shell singlet diradical is shown.

diradical(oid)s as reacting in both open-shell and closed-shell modes. The analysis is not ambiguous because we know very clearly in which situation we should choose which point of view, localized or delocalized. It all depends on the incoming species and its orientation as it approaches the singlet diradical(oid).

With the three-step approach outlined above, one can understand the reactivity of:

- Monoradicals vs triplet diradicals;
- The triplet vs singlet states of a diradical, in reactions involving one radical center;
- A singlet diradical, in concerted reactions involving both radical centers.

The knowledge obtained from this approach bridges different fields, and it provides a unified view of the continuous spectrum of reactivity for monoradicals—diradicals—diradicaloids—closed-shell molecules (Figure 55). From a MO point of view, a monoradical is a one-electron-one-orbital system, with its representative reactivity: dimerization, H-atom abstraction, and addition to ethylene. On the right-hand side of this schematic characterization, closed-shell molecules participate in reactions as nucleophiles/electrophiles, or engage in (concerted) pericyclic reactions. A diradical is a two-electron—two-orbital system. The triplet state can be viewed as $2\times$ a monoradical and thus has similar reaction modes to monoradicals. The singlet states of diradicals either behave as typical closed-shell molecule, being able to engage in pericyclic reactions, or react as nucleophiles/electrophiles, or they can behave in a similar to the triplet states and monoradicals.

Diradicaloids are species in-between the two previously discussed extremes. Thus, depending on their location along the continuum, they will either be more inclined to favor typical closed-shell reactivity, or there will be a clear competition between concerted and stepwise mechanisms, the latter stemming either from the singlet ground state or from the excited, yet sufficiently close in energy—triplet state.

13. MEASURES OF DIRADICAL CHARACTER

In the previous sections, we have given a broad and detailed overview of the reactivity of diradicals, and we constructed a general framework according to which the reactivity patterns of diradicaloids can be judged. However, we have not yet addressed one utterly important question, namely, can one judge how “diradical-like” one system is compared to another? To enable such a judgment, many chemists have turned to the concept of diradical character. Like atomic charge and bond index, diradical

character (or, more generally, polyradical character in a molecule) is not an observable; it does not correspond to a hermitian operator in quantum mechanics. Yet the need for measuring radical character is palpable, so it is no wonder that a variety of indexes have been proposed. Let us review these measures and their merits and shortcomings.

13.1. For Molecular Orbital Wave Functions

13.1.1. Diradical Character Indices Based on Configuration Interaction (CI) Coefficients. In the simplest symmetric two-orbital—two-electron ($2o2e$) picture, i.e., considering only the bonding between two symmetry-related sites, the singlet ground state wave function has the general form (see also Figure 10 and Figure 11),

$$\begin{aligned}
 |\Psi_g\rangle &= C_0|\psi_H^2\rangle - C_d|\psi_L^2\rangle \\
 &= \frac{C_0 - C_d}{\sqrt{2}} \frac{1}{\sqrt{2}} (|\chi_a^2\rangle + |\chi_b^2\rangle) \\
 &\quad + \frac{C_0 + C_d}{\sqrt{2}} \frac{1}{\sqrt{2}} (|\chi_a^\alpha\chi_b^\beta\rangle + |\chi_b^\alpha\chi_a^\beta\rangle) \\
 &= C_I|\Phi_{\text{Ion}}\rangle + C_C|\Phi_{\text{Cov}}\rangle; \\
 C_0^2 + C_d^2 &= 1; \quad C_0 \geq 0; \quad C_d \geq 0
 \end{aligned} \tag{39}$$

We use the subscript 0 to denote the coefficient for the $|\psi_H^2\rangle$ determinant, which is the “ground state” in the Hartree–Fock approximation, and the subscript d to denote the coefficient for the $|\psi_L^2\rangle$ determinant that features a double-electron excitation. The transformation between the delocalized ψ_H and ψ_L bonding and antibonding orbitals and the localized χ_a and χ_b nonbonding orbitals follows eqs 19 and 20, with ψ_x and ψ_y being replaced by ψ_H and ψ_L (see also Figure 8).

In the language of valence bond theory, the first parentheses in eq 39 give the ionic term (subscript “Ion”) and the second the covalent (subscript “Cov”) term to $|\Psi_g\rangle$. The first identification we make is of the covalent term with the open-shell diradical wave function of the two localized orbitals. Certainly, when $C_0 = C_d = \frac{1}{\sqrt{2}}$, $|\Psi_g\rangle$ is 100% covalent/diradical, and it is more appropriate to call it a diradical ground state in this limit. When $C_0 = 1$, $C_d = 0$, $|\Psi_g\rangle = |\psi_H^2\rangle$, the covalent/diradical function and ionic function contribute equally to the total wave function. Despite the 50% contribution of the covalent/diradical function, this noncorrelated, bonding limit, which is achieved only in a perfect closed-shell molecule with an infinite HOMO–LUMO gap, is generally considered to have null diradical character, and

it is more appropriate to call $\frac{1}{\sqrt{2}}(|\chi_a^\alpha \chi_b^\beta\rangle + |\chi_b^\alpha \chi_a^\beta\rangle)$ a covalent function, despite the fact that the singlet diradical corresponding to the two sites being infinitely far apart is described by the same wave function.

Considering that $C_d = 0$ corresponds to a bonding limit, and $C_d = \frac{1}{\sqrt{2}}$ to a dissociated diradical limit, Bachler et al. proposed a straightforward diradical measure,²⁴⁵

$$y = \sqrt{2} C_d = C_C - C_I \quad (40)$$

This indicator (y has become the traditional label for diradical character) measures the excess of the covalent amplitude relative to the ionic. Can $C_d > \frac{1}{\sqrt{2}}$ and thus give $y > 1$? This should not happen if ψ_H is a bonding orbital of lower energy than ψ_L . The same group also proposed an improved version²⁴⁶

$$y = 2C_0 C_d = C_C^2 - C_I^2 \quad (41)$$

This index represents the difference in probability of the $|\Phi_{\text{Cov}}\rangle$ and $|\Phi_{\text{Ion}}\rangle$ contributions, which is more meaningful statistically.

A similar index is

$$y = 2C_d^2 = (C_C - C_I)^2 \quad (42)$$

which is just the square of $y = \sqrt{2} C_d$, but was proposed decades earlier by Hayes and Siu.²⁴⁷ It directly connects the diradical character of $|\Psi_g\rangle$ to the percentage of $|\psi_L^2\rangle$.

This index in eq 42 can be extracted from experimental measurements. Kamada et al., using the valence full configuration interaction formalism, derived that for a 2o2e model,²⁴⁸

$$y = 2C_d^2 = 1 - \sqrt{1 - \left(\frac{E_{S_{1u}, S_{1g}} - E_{T_{1u}, S_{1g}}}{E_{S_{2g}, S_{1g}}} \right)^2} \quad (43)$$

$E_{S_{1u}, S_{1g}}$ and $E_{T_{1u}, S_{1g}}$ are the excitation energies of the first singlet and triplet excited states corresponding to HOMO-to-LUMO single excitation that gives an *ungerade* symmetry. $E_{S_{2g}, S_{1g}}$ is the excitation energy of the second singlet excited state dominated by HOMO-to-LUMO double excitation that gives a *gerade* symmetry. The energy levels of the four states are shown in Figure 56. Note that the energy levels in the equation and the figure are the adiabatic energies, not the energies of the well-characterized configurations introduced in section 3, and, although excitation energies are involved in obtaining the y in

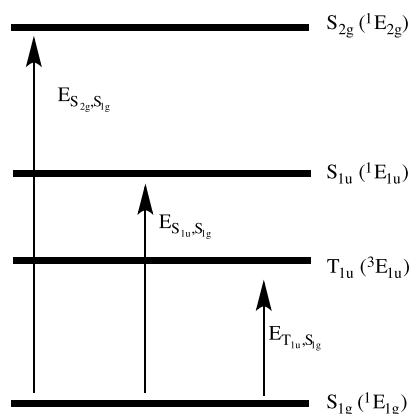


Figure 56. Different states and their ordering in the 2o2e model with the excitation energies considered in eq 43 denoted by arrows.

eqs 42 and 43, this indicator is fundamentally a characteristic of the ground state wave function.

While the T_{1u} and S_{1u} states correspond to the T and $S_{\text{TC-}}$ configurations with the localized χ_a and χ_b , the S_{1g} and S_{2g} states arise from mixing the S_{OS} and $S_{\text{TC+}}$ configurations through their interaction, and all energies in eq 43 depend on the energy splitting in this mixing. Note that in the limit of a pure diradical with the two electrons located far apart, the adiabatic states are identical to the configurations, with S_{1g} and T_{1u} being degenerate and S_{1u} and S_{2g} being degenerate. Equation 43 associates the diradical character to experimentally observable energies, thus making it a measurable quantity. Please note the difference in meaning between “observable” and “measurable”. Diradical character is not observable because it does not correspond to a hermitian operator. However, it can be indirectly measured, e.g., in this 2o2e scheme and taking the $y = 2C_d^2$ index through observing the relevant excitation energies.

From the three y indices above, we can see the origin of the diversity of diradical character indicators. The physically well-defined bonding and dissociation limits only impose the following boundary conditions on the function $y(C_d)$:

$$y(0) = 0; \quad y\left(\frac{1}{\sqrt{2}}\right) = 1 \quad (44)$$

Additionally, y should be a monotonically increasing function with respect to C_d , up to $C_d = \frac{1}{\sqrt{2}}$. These requirements are certainly insufficient to unambiguously define the y function. The different y functions shown above represent different ways to interpolate the diradical character between the zero and full diradical limits. There is an infinity of ways to do so, e.g. (but not limited to), $y = (\sqrt{2} C_d)^p$ or $y = (2C_0 C_d)^p$ with any $p > 0$; all these y functions satisfy the requirements. In this pool, people select the y functions that seem most appropriate to the physical meaning they are trying to glean.

13.1.2. An Indicator for Polar Bonds. More recently, Nakano et al. proposed a new diradical indicator that is applicable for two *asymmetric* bonding sites, e.g., polar molecules.²⁴⁹ Within the 2o2e picture but with nonsymmetry-related nonbonding orbitals, the ground state wave function has the general expression

$$|\Psi_g\rangle = C_{a\bar{a}}|\chi_a^2\rangle + C_{b\bar{b}}|\chi_b^2\rangle + C_{\text{Cov}}\frac{1}{\sqrt{2}}(|\chi_a^\alpha \chi_b^\beta\rangle + |\chi_b^\alpha \chi_a^\beta\rangle) \quad (45)$$

Because of the asymmetry, the ionic amplitudes $C_{a\bar{a}} \neq C_{b\bar{b}}$. When $|\Psi_g\rangle$ contains more covalent than ionic character (i.e., $C_{\text{Cov}}^2 > C_{a\bar{a}}^2 + C_{b\bar{b}}^2$), Nakano et al. consider the system to be in the diradical zone, and the diradical index is defined as the excess of the covalent contribution in $|\Psi_g\rangle$ over the ionic contributions:

$$y^N = C_{\text{Cov}}^2 - (C_{a\bar{a}}^2 + C_{b\bar{b}}^2) = 2C_{\text{Cov}}^2 - 1 \quad (46)$$

where the superscript “ N ” indicates the “neutral diradical” component in the wave function. When $|\Psi_g\rangle$ contains less covalent than ionic components (note that this is impossible for symmetric bonding, as indicated by eqs 40 and 41), it is in the ionic zone and then an ionic index, defined as the excess of the ionic contributions over the covalent:

$$y^I = (C_{a\bar{a}}^2 + C_{b\bar{b}}^2) - C_{\text{Cov}}^2 = 1 - 2(C_{a\bar{a}}^2 + C_{b\bar{b}}^2) \quad (47)$$

better characterizes the state. Clearly, y^N changes from 1 to 0 as the system changes from purely diradical to a closed-shell wave

function with half covalent and half ionic contributions, and y^I changes from 0 to -1 as the system continues to change to pure ionic character. Connecting the y^N and y^I curves at $C_{\text{Cov}}^2 = \frac{1}{2}$ leads to a continuous curve that smoothly connects the pure ionic and pure diradical limits.

13.1.3. The Essential Link Between Diradical Measures and Correlation. All diradical indices introduced above are functions of the configuration interaction coefficients C_0 and C_d , or equivalently, C_C and C_I . This is a reflection of the intimate connection between diradical character and electron correlation. It is the strong correlation (i.e., nondynamical correlation) between two electrons that leads to their unpaired nature in a diradical: when one electron is distributed in a certain region in space, the other is forced to be distributed on average elsewhere. *Diradical character may be understood as a chemical concept that demonstrates electron correlation in wave function. Or, in other words, electron correlation bridges the chemical concept of diradical and the physical concept of wave function.*

13.1.4. Polyradical Character Indices Based on Natural Occupancies. The $y = 2C_d^2$ quantity also emerges as a natural occupation number. The 1-electron density operator of $|\Psi_g\rangle$ in eq 39 is

$$\hat{\rho} = 2C_0^2|\psi_H\rangle\langle\psi_H| + 2C_d^2|\psi_L\rangle\langle\psi_L| \quad (48)$$

and therefore, the occupation number of the lowest unoccupied natural orbital (LUNO, with the symbol φ_L , which is equivalent to ψ_L in this 2o2e picture), is equal to $2C_d^2$. In any wave function (not restricted to the present 2o2e one), LUNO is the natural orbital with the occupation number closest to but less than 1. Those with smaller and smaller occupation numbers are labeled as LUNO+1, LUNO+2, etc. The highest occupied natural orbital (HONO) has its occupation number closest to but larger than 1. HONO-1, HONO-2, etc. are those with larger and larger occupation numbers. One can then use the occupation number of LUNO (n_{LUNO}) to indicate the diradical character,^{250–254} and this indicator can be generalized to more flexible wave functions with a larger active space than 2o2e.

In general, polyradical indicators based on natural orbitals are more applicable than those based on CI coefficients. Almost all computational methods can give natural orbitals but not necessarily CI coefficients (e.g., density functional theory methods). Also, in complete-active-space-type calculations, electronic wave functions are invariant with respect to orthogonal rotation among active orbitals, with the CI coefficients correspondingly rotated. One example is the $\{\psi_H, \psi_L\}$ -to- $\{\chi_a, \chi_b\}$ transformation in eq 39. Therefore, the active orbitals and the CI coefficients are not uniquely determined. On the contrary, the natural orbitals and their occupancies are fixed for one wave function.

n_{LUNO} is a very natural indicator for diradical character: when two electrons are paired in a bonding orbital, $n_{\text{LUNO}} = 0$; when the two electrons are completely unpaired, $n_{\text{LUNO}} (= n_{\text{HONO}}) = 1$; when they are partially unpaired, $n_{\text{HONO}} = 2 - x$ and $n_{\text{LUNO}} = x$, with $x < 1$. However, please note that this method is only applicable to the ground state of a molecule. When such a calculation is performed for excited states, $n_{\text{LUNO}} = 1$ may indicate fully ionic character, e.g., in the $\frac{1}{\sqrt{2}}(|\sigma_g^\alpha \sigma_u^\beta\rangle + |\sigma_u^\alpha \sigma_g^\beta\rangle)$ HOMO-to-LUMO single-electron excited state of H_2 .

Occupation numbers can also be used to indicate polyradical character. For a system with an even number of electrons and described by spin-unrestricted Hartree–Fock (UHF) and

density functional theory (UDFT) methods, the equality $n_{\text{HONO}-i} + n_{\text{LUNO}+i} = 2$ holds strictly;²⁵⁵ for general multi-determinantal wave functions, the equality is approximately satisfied.²⁵⁶ Therefore, we can consider each pair of HONO- i and LUNO+ i as the delocalized bonding and antibonding orbitals for a pair of electrons. Correspondingly, $y_i = n_{\text{LUNO}+i}$ indicates how much the pair of electrons are correlated, avoiding each other and occupying the localized nonbonding orbitals that make up HONO- i and LUNO+ i . Therefore, $n_{\text{LUNO}+i}$ indicates how much the $(i + 1)$ -th pair of electrons are uncoupled, i.e., the $2(i + 1)$ -ple radical character. When $n_{\text{LUNO}} = 1$ and $n_{\text{LUNO}+1} = 0$, we have a pure diradical; when $n_{\text{LUNO}} = n_{\text{LUNO}+1} = 1$, we have two diradicals that give a tetraradical; when $n_{\text{LUNO}} = 0.8$ and $n_{\text{LUNO}+1} = 0.4$, we can think of the molecule having 80% and 40% diradical characters in the two most decoupled pairs of electrons, or, if only focusing on $n_{\text{LUNO}+1}$, 40% tetraradical character.

In a pure diradical whose $n_{\text{HONO}} = n_{\text{LUNO}} = 1$, one can transform HONO and LUNO, if they are delocalized, into localized orbitals that describe the local distributions of the two unpaired electrons. The localized orbitals are called magnetic orbitals. Similar transformations can be applied to each pair of HONO- i and LUNO+ i , whose occupancies are in general different, and the electrons in the pairwise magnetic orbitals are coupled to different degrees, indicated by the difference between $n_{\text{HONO}-i}$ and $n_{\text{LUNO}+i}$. Because of symmetry, there may be degenerate $n_{\text{HONO}-i}$ and $n_{\text{HONO}-(i+1)}$, as well as $n_{\text{LUNO}+i}$ and $n_{\text{LUNO}+(i+1)}$. One can freely transform among the degenerate natural orbitals. However, a transformation limited exclusively to occupied natural orbitals (and/or to unoccupied ones) does not give the localized *precoupled* SOMOs. A transformation of a combination of occupied and unoccupied natural orbitals is required to give the magnetic orbitals.

13.1.5. Caution. Our discussion below of polyradical indicators is heavily oriented toward UHF and UDFT calculations, despite their well-known problems, e.g., spin-contamination and results that depend on the choice of functional.²⁹ The reason is pragmatic: they are the most efficient methods and provide results with decent accuracy for large open-shell systems. As we will demonstrate in detail below, there are real dangers under the surface of these useful calculations.

13.1.6. Distribution of Unpaired Electrons. Naturally, if we consider all natural orbitals, we can obtain the total number of unpaired electrons. Furthermore, we can obtain the distribution of the unpaired electrons. Such a density of effectively unpaired electrons was first proposed by Takatsuka et al.²⁵⁷ and later independently by Staroverov and Davidson:²⁵⁸

$$u(\mathbf{r}) = 2\rho(\mathbf{r}) - \int \rho(\mathbf{r}\mathbf{r}')\rho(\mathbf{r}'\mathbf{r}) \, d\mathbf{r}' \quad (49)$$

where $\rho(\mathbf{r})$ is the spinless electron density and $\rho(\mathbf{r}\mathbf{r}')$ the spinless density matrix. For a single determinant closed-shell wave function with every occupied orbital containing two electrons, the eigenvalues of $\rho(\mathbf{r}\mathbf{r}')$ are either 0 or 2; the self-contraction $\int \rho(\mathbf{r}\mathbf{r}')\rho(\mathbf{r}'\mathbf{r}) \, d\mathbf{r}'$ results in $2\rho(\mathbf{r})$ and thus $u(\mathbf{r}) = 0$. Therefore, $u(\mathbf{r})$ indicates the deviation from the closed-shell single determinantal wave function, and hence the distribution density of the unpaired electrons. Note that with the spin coordinates having been integrated, $\rho(\mathbf{r}\mathbf{r}')$ is nonidempotent.

Expressed in terms of the natural orbitals $\{\varphi_k\}$, which are eigenstates of $\rho(\mathbf{r}\mathbf{r}')$, i.e.,

$$\int \rho(\mathbf{r}|\mathbf{r}')\varphi_k(\mathbf{r}') \, d\mathbf{r}' = n_k\varphi_k(\mathbf{r}),$$

$$u(\mathbf{r}) = \sum_k n_k(2 - n_k)\varphi_k^*(\mathbf{r})\varphi_k(\mathbf{r}) \quad (50)$$

$n_k(2 - n_k)$, the intensity of each φ_k 's contribution to the unpaired density, has a maximum of 1 when $n_k = 1$ and minimum of 0 when $n_k = 0$ or 2. It assigns a number of effectively unpaired electrons in each natural orbital. Integrating over the whole space,

$$N_D = \int u(\mathbf{r}) \, d\mathbf{r} = \sum_k n_k(2 - n_k) \quad (51)$$

gives the total number of effectively unpaired electrons, which quantitatively indicates the polyradical character of a molecule: $N_D = 1$ for a radical, $N_D = 2$ for a diradical, etc. Given two active electrons, $N_D/2$ serves as a natural indicator for diradical character. Like electron density, $u(\mathbf{r})$ (and N_D as well) can be decomposed into contributions from constituent atoms using the Mulliken^{259,260} or Bader partitioning schemes.^{261,262} Such decomposition directly reveals the radical centers in a polyradicaloid system and may predict its active sites for radical-like reactions.

Staroverov and Davidson²⁶⁴ also proved that $N_D = \sum_k n_k(2 - n_k)$ is connected to the average spin of an UHF wave function as

$$N_D = 2[\langle \hat{S}^2 \rangle - M_S] \quad (52)$$

where M_S is the spin projection and equals 0 if the wave function approximates a singlet state. Evidently, $\langle \hat{S}^2 \rangle$ and N_D give identical information for the polyradical character of a UHF wave function.

One drawback of $u(\mathbf{r})$ is that it may overestimate the number of actually unpaired electrons: Staroverov and Davidson derived that the upper bound of $N_D = \sum_k n_k(2 - n_k)$ is twice the number of electrons.²⁶³ Although this is an extreme case and for regular wave functions, and it is rare to have N_D greater than the number of electrons, we cannot exclude the possibility of an overestimation of the polyradical character when compared to other methods. This problem is most serious when the occupation number n_k is slightly different from 2 or 0, i.e., when a pair of electrons are weakly correlated and when there are many such pairs (i.e., dynamic correlation). To alleviate this problem, Head-Gordon suggested one use (labeled as HG-I below),

$$\min(n_k, 2 - n_k) \quad (53)$$

as the intensity of each natural orbital in constructing $u(\mathbf{r})$.^{264,265} $N_D = \sum_k \min(n_k, 2 - n_k)$ is bound by the number of electrons. Recalling that $n_{\text{LUNO}+i} + n_{\text{HONO}-i} \approx 2$,

$$\sum_k \min(n_k, 2 - n_k) \approx 2 \sum_i n_{\text{LUNO}+i} \quad (54)$$

The HG-I N_D is hence related to the aforementioned polyradical character considering $n_{\text{LUNO}+i}$. Another option (HG-II) for the intensity is

$$n_k^2(2 - n_k)^2 \quad (55)$$

This expression also diminishes the overestimation (e.g., see Figure S7 below), and compared to HG-I, it is a smooth function of n_k .

13.1.7. Overestimation of Polyradical Character Due to Dynamic Correlation. An important thing to keep in mind

when considering diradical measures is the following. A real diradical (polyradical) features one (a few) pair(s) of strongly correlated electrons that avoid each other and are located in different regions of space. However, diradical measures such as N_D , as summed-over quantities, do not differentiate the situation of a small number of strongly correlated pairs (with a few n_k s close to 1), and the situation of a large number of weakly correlated pairs (with many n_k s close to 0 or 2). The latter circumstance is also identified with (we would say mistaken for) diradical and polyradical character. Therefore, these measures generally overestimate diradical and polyradical character. This is what Orms et al. mean by " N_D does not suppress dynamic correlation contributions to the total number of unpaired electrons."²⁶⁶ Obviously, the overestimation increases with the size of the system, as more and more weak correlations are included.⁶

Another way to understand the overestimation is through the overlap integrals between spatial functions of spin orbitals that accommodate the correlated electron pair with opposite spins. Head-Gordon derived for a UHF wave function that²⁶⁵

$$N_D = N_e - 2 \sum_{i=1}^{N_\beta} T_i^2 \quad (56)$$

where N_e is the number of electrons, N_β the number of β electrons, and T_i the overlap between the corresponding i th pair of spatial orbitals associated with α and β spins. For a true diradical that has $N_e/2 - 1$ pairs of identical spatial orbitals ($T_i = 1$), and one pair of nonoverlapping orbitals ($T_i = 0$), certainly $N_D = 2$ and $\langle \hat{S}^2 \rangle = 1$. However, $N_D = 2$ or even larger may arise from accumulating lots of T_i s that are slightly different from 1.

These nonperfect overlaps of the i th pair of spatial orbitals manifest the correlation between the two electrons with opposite spins: their distributions are different so that they can avoid each other; as a result, fractional occupation numbers $1 + T_i$ and $1 - T_i$ are obtained for the corresponding i th pair of natural orbitals. The closer T_i is to 1, the smaller the correlation effect. Therefore, large N_D and $\langle \hat{S}^2 \rangle$ may just reflect the accumulated weak correlation effects of many pairs of electrons instead of strong correlation among a few pairs of electrons. As the size of the system increases, more miscellaneous correlations are accumulated and mistaken for polyradical character. This is basically a reiteration of the size-scaling problem of N_D .

Consider the following example: Let us reasonably assume that a 2o2e full CI calculation of an H_2 molecule at its equilibrium internuclear distance gives occupation numbers 1.98 and 0.02 in its HONO and LUNO, and hence $N_D = 0.04$ using the HG-I intensity. The same calculation for 50 H_2 molecules far away from each other will increase N_D to 2, misleadingly suggesting that the 50 closed-shell molecules make a diradical. Therefore, we need to exercise caution when using N_D as a measure of polyradical character, especially for large systems. In the words of Hachmann et al., the number of effective unpaired electrons "must not be taken literally."⁶ One way to convert N_D to an intensive index is to normalize it through dividing it by the number of electrons.²⁶⁷ The normalized index phenomenologically indicates how unpaired each electron is.

A more relevant example is C_{60} , whose natural occupancies are never smaller than 1.4 or greater than 0.6 at the spin-purified generalized Hartree–Fock level.¹⁵ The close to 10 effective unpaired electrons of Buckminsterfullerene arise from accumulation of the HG-I intensities (eq 53) over a large number of

natural orbitals.²⁶⁸ The large number of effective unpaired electrons is hence reconciled with the nonradical-like reactivity of C_{60} (vide infra).

13.1.8. Measures Based on Collectivity Number and Hole–Particle Density. Luzanov and Zhikol (LZ) proposed another N_D formula based on the collectivity number κ , which is a measure of multiconfigurational character of wave function.^{269,270} The detailed derivation for the κ and LZ N_D formulas is given in ref 270; it involves more than the density matrix. The LZ formula gives N_D value between the Yamaguchi and HG-I. Luzanov and Prezhdo (LP) proposed another N_D formula based on the hole–particle density.²⁷¹ Expressed using the natural orbitals, the density operator can be written as

$$\begin{aligned} \hat{\rho} &= \sum_k n_k |\varphi_k\rangle\langle\varphi_k| \\ &= \sum_{k=1}^{N/2} 2|\varphi_k\rangle\langle\varphi_k| + \sum_{k=1}^{N/2} (n_k - 2)|\varphi_k\rangle\langle\varphi_k| \\ &+ \sum_{k>N/2} n_k |\varphi_k\rangle\langle\varphi_k| = \hat{\rho}_0 + \hat{\rho}_{h-p} \end{aligned} \quad (57)$$

The natural orbitals are ordered according to their occupation numbers: n_k is smaller for a larger k . $\hat{\rho}_0 = \sum_{k=1}^{N/2} 2|\varphi_k\rangle\langle\varphi_k|$ is a reference density operator corresponding to a single-determinant wave function with the $N/2$ most substantially occupied natural orbitals being doubly occupied. $\hat{\rho}_{h-p}$ describes the hole–particle density that differentiates the reference and actual states. The $(2 - n_k)$ s give us the hole number in the first $N/2$ reference orbitals, while the n_k s of the other orbitals give the particle number. The LP hole–pair index is defined as the summation of the hole and particle numbers

$$N_{h-p} = \sum_{k=1}^{N/2} (2 - n_k) + \sum_{k>N/2} n_k = 2 \sum_{k>N/2} n_k \quad (58)$$

N_{h-p} can be used to estimate the number of unpaired electrons. Please note that if $n_{N/2} > 1$ and $n_{N/2+1} < 1$, N_{h-p} gives the same value as the HG-I N_D , and this condition is usually satisfied for the singlet ground state. Therefore, the hole–particle picture enriches the physical meaning of the HG-I N_D .

13.1.9. Overestimation from Spin Contamination. The spin-contamination in UHF and UDFT calculations can affect estimation of the polyradical character through the use of occupation numbers.²⁷² For example, when ignoring the electrons in pairs, a UHF wave function for a diradicaloid system reads

$$|\Psi^{\text{UHF}}\rangle = |\psi_{\text{HOMO}}^\alpha \psi_{\text{HOMO}}^\beta\rangle \quad (59)$$

with the symmetry-broken orbitals $\psi_{\text{HOMO}}^\alpha$ and ψ_{HOMO}^β that gives spatial overlap $\langle\psi_{\text{HOMO}}^\alpha|\psi_{\text{HOMO}}^\beta\rangle = T$, and $n_{\text{HONO}} = 1 + T$; $n_{\text{LUNO}} = 1 - T$. As mentioned above, the smaller overlap between the two orbitals (larger n_{LUNO}) reflects that the two electrons are located in different regions, i.e., a larger diradical character. When the spin-contaminants are projected out (the projection, however, impairs the size-consistency of the wave function), the LUNO occupation number ($n_{\text{LUNO}}^{\text{PUHF}}$) of the leftover wave function ($|\Psi^{\text{PUHF}}\rangle$) gives the following diradical indicator:²⁷³

$$y_0^{\text{PUHF}} = n_{\text{LUNO}}^{\text{PUHF}} = \frac{n_{\text{LUNO}}^2}{1 + T^2} = \frac{2n_{\text{LUNO}}^2}{n_{\text{HONO}}^2 + n_{\text{LUNO}}^2} \quad (60)$$

y_0^{PUHF} scales as n_{LUNO}^2 when n_{LUNO} is small and hence has a slower increase. This reflects that the spin-contamination overestimates the diradical character. Numerical evidence of such an overestimation is shown in Figure 7 in ref 274, where the HONO–LUNO occupation gaps for a series of polycyclic aromatic hydrocarbons obtained from the UHF and spin-projected UHF wave functions are compared. This index can again be generalized to indicate polyradical character:

$$y_i^{\text{PUHF}} = \frac{2n_{\text{LUNO}+i}^2}{n_{\text{HONO}-i}^2 + n_{\text{LUNO}+i}^2} \quad (61)$$

N_D of UHF suffers another source of overestimation from spin-contamination. Let us use the two electrons UHF determinant ($|\Psi^{\text{UHF}}\rangle$) as an example again. From eq 60, we have

$$n_{\text{LUNO}} = \frac{y_0^{\text{PUHF}} - \sqrt{y_0^{\text{PUHF}}(2 - y_0^{\text{PUHF}})}}{y_0^{\text{PUHF}} - 1} \quad (62)$$

Using the original Yamaguchi definition of number of effective unpaired electrons,

$$\begin{aligned} N_D^Y &= 2n_{\text{LUNO}}(2 - n_{\text{LUNO}}) \\ &= \frac{4\sqrt{y_0^{\text{PUHF}}(2 - y_0^{\text{PUHF}})} \left(1 - \sqrt{y_0^{\text{PUHF}}(2 - y_0^{\text{PUHF}})}\right)}{(y_0^{\text{PUHF}} - 1)^2} \end{aligned} \quad (63)$$

Shown in Figure 57 is a plot of N_D^Y against y_0^{PUHF} . Obviously, N_D^Y increases way faster than y_0^{PUHF} in the small y_0^{PUHF} region, and this

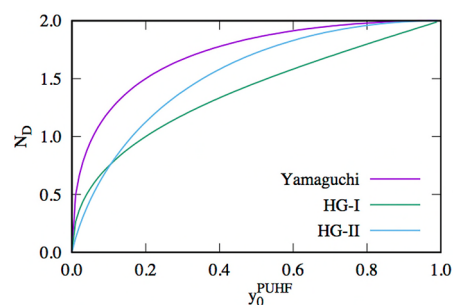


Figure 57. N_D vs y_0^{PUHF} for a two electrons UHF wave function.

arises from the spin-contamination. Using the HG-I and HG-II intensities, we have

$$\begin{aligned} N_D^{\text{HG-I}} &= 2n_{\text{LUNO}} = 2 \frac{y_0^{\text{PUHF}} - \sqrt{y_0^{\text{PUHF}}(2 - y_0^{\text{PUHF}})}}{y_0^{\text{PUHF}} - 1}; \\ N_D^{\text{HG-II}} &= \frac{(N_D^Y)^2}{2} \end{aligned} \quad (64)$$

which are also plotted in Figure 57. As expected, they increase more slowly than N_D^Y . However, the overshoot is still obvious, and again mostly occurs at small y_0^{PUHF} . When the “spin-clean” $y_0^{\text{PUHF}} = 0.1$, which reflects weak to intermediate correlation between the two electrons and by no means makes us think of a diradical, the Yamaguchi, HG-I and HG-II N_D s have reached 1.2, 0.75, and 0.72, indicating strong and fairly strong diradical character, respectively. Again, this problem is more pronounced for large systems. These arguments for UHF also apply to UDFT calculations.

13.1.10. Comparison of the Occupancy-Based Diradical Indicators Using H₂ and PQDM as Test Examples. A comparison between some of the indicators discussed so far is shown in Figure 58. The indices are obtained from complete

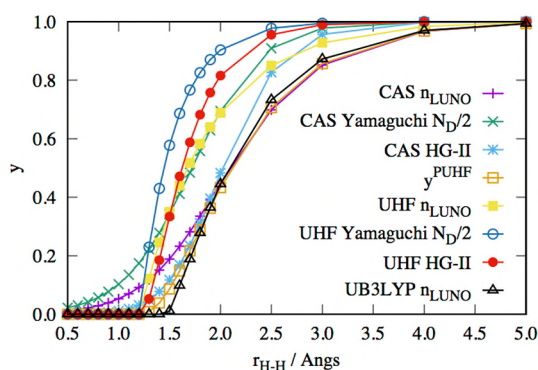


Figure 58. Comparison of the diradical measures that are based on occupation numbers in the H₂ dissociation.

active space self-consistent field calculations with a 2o2e active space (labeled by “CAS”), the UHF, and the UDFT calculations with the B3LYP functional.^{275,276} The cc-pVDZ basis set²⁷⁷ is used in the calculations. For this two electrons system, n_{LUNO} equals half of the HG-I N_{D} (see the definition of HG-I in eq 53). All indices grow from (close to) zero at the bonding limit to 1 at the dissociation limit, as they must. The CAS wave function captures the weak correlation between the two electrons at the bonding limit and hence gives nonzero yet minute diradical character, using all three indices: n_{LUNO} , the Yamaguchi $N_{\text{D}}/2$, and the HG-II $N_{\text{D}}/2$. The CAS-calculated indices smoothly rise as the H–H bond is stretched, reflecting the seamless conversion from the weak correlation in H₂ to the strong correlation in 2H•. The Yamaguchi $N_{\text{D}}/2$ always indicates greater diradical character than the other two indices, as discussed above.

The UHF calculation actually results in a RHF wave function in the bonding limit and thus zero diradical character. As the bond is stretched, the triplet instability of the RHF wave function results in the symmetry-broken spin-contaminated UHF wave function. Such an instability comes into effect abruptly at around $r_{\text{H-H}} = 1.3 \text{ \AA}$, so that all three UHF diradical indices feature unphysical sharp rises. Both the singlet open-shell and the triplet-contaminant contribute to the increase. With the contaminant being removed, the y^{PUHF} rises way more smoothly (see Figure 57 above too) and merges into the CAS n_{LUNO} curve at $r_{\text{H-H}} > 2 \text{ \AA}$; the CAS and PUHF wave functions are similar in the large $r_{\text{H-H}}$ region.

Incorporating the electron correlation into an effective potential, B3LYP is able to describe H₂ using a restricted Kohn–Sham determinant to a longer $r_{\text{H-H}}$. The B3LYP n_{LUNO} becomes nonzero at $r_{\text{H-H}} = 1.5 \text{ \AA}$, later than the UHF counterpart.²⁷⁸ The slower rise of the UB3LYP n_{LUNO} also reflects its milder spin-contamination. For example, at $r_{\text{H-H}} = 2.0 \text{ \AA}$, $\langle \hat{S}^2 \rangle = 0.903$ and 0.692 for UHF and UB3LYP, respectively.

Through the n_{LUNO} curves in Figure 58, we see that the same index obtained using different electronic structure methods can give quantitatively very different diradical characters despite their qualitatively consistent trends. Therefore, in comparing diradical characters of different molecules or one molecule in different structures, consistency in both diradical index and electronic structure method must be maintained.

We also compare the same set of diradical indicators for one molecule, *para*-quinodimethane, PQDM; the results are shown in Table 12. This comparison shows the different diradical

Table 12. Diradical Characters of PQDM Calculated with t Different Methods^a

method	diradical character	method	diradical character
CAS ^b n_{LUNO}	0.182	y^{PUHF}	0.256
CAS Yamaguchi $N_{\text{D}}/2$	0.323	UHF $n_{\text{LUNO}}/\text{HG-I}$	0.554
CAS HG-I ^d	0.177	UHF Yamaguchi $N_{\text{D}}/2$	0.801
CAS HG-II	0.105	UHF HG-II	0.642
		UB3LYP n_{LUNO}	0

^aThe CAS, UHF, and UB3LYP results are obtained at the structures optimized using the respective methods. ^bThe full 8o8e valence π active space is used in the CASSCF calculations. ^cOnly the HONO and LUNO's contributions to N_{D} are considered. ^dFor systems with more than two electrons, the CAS HG-I index is not equivalent to the CAS n_{LUNO} .

indicators obtained at the respective calculated equilibrium geometry. A similar trend as shown in Figure 58 is seen. Even at the equilibrium geometry of PQDM, there is a significant spin contamination in the UHF wave function. The associated overshoot UHF diradical indices are mitigated in y^{PUHF} . UB3LYP gives zero diradical character as the electron correlation is incorporated in the effective potential of the functional, not polarization of orbitals associated with different spins. The CAS calculation is free from spin contamination and gives reasonably lower diradical characters. The overestimation of the diradical character using the Yamaguchi index is still obvious in the CAS calculation.

13.1.11. A Polyradical Index Based on “Thermal” Occupation. It is clear that polyradical character is closely related to strong nondynamical electron correlation in a system. Such nondynamical correlation is signified by small energy gaps between occupied and unoccupied orbitals, which lead to difficulty in SCF convergence in DFT calculations. Finite-temperature (FT-) DFT is an approach to solve this problem, as it allows fractional occupations of the frontier orbitals close in energy through formally thermal excitation.^{279,280} The fractional occupation of each spin orbital follows the Fermi–Dirac distribution

$$f_i = \frac{1}{e^{(\epsilon_i - E_{\text{F}})/kT_{\text{el}}} + 1} \quad (65)$$

with ϵ_i being the energy of Kohn–Sham orbital ϕ_i , E_{F} the Fermi energy, k the Boltzmann constant, and T_{el} a functional-dependent electronic temperature (recalling the functional-dependence of HOMO–LUMO gap). The fractional occupations naturally indicate the unpaired nature of the electrons. The fractional orbital density,²⁸¹

$$\rho^{\text{FOD}}(\mathbf{r}) = \sum_i^N (\delta_i - \delta_j f_i) |\phi_i(\mathbf{r})|^2 \quad (66)$$

was proposed by Grimme and Hansen to represent the distribution of the unpaired electrons, whose summation is over all occupied orbitals. $\delta_1 = \delta_2 = 1$ for $\epsilon_i < E_{\text{F}}$, so that for the spin orbitals below the Fermi level, the deviation from 1 (i.e., the hole) contributes. $\delta_1 = 0$ and $\delta_2 = 0$ for $\epsilon_i > E_{\text{F}}$, so that for the spin

orbitals above the Fermi level, the fractional occupation (i.e., the particle) contributes. It follows the same logic as the HG-I intensity but for different types of orbitals. Despite their different definitions, $\rho^{\text{FOD}}(r)$ and $u(r)$ in eq 49 bear the same physical meaning. The spatial integration $N^{\text{FOD}} = \int \rho^{\text{FOD}}(r) dr$ hence quantifies the number of unpaired electrons, and thus the polyradical character of a system. N^{FOD} exhibits a good linear correlation with the γ in eq 43.²⁸²

13.2. Diradical Measures from Valence Bond Theory

13.2.1. Wave Functions in Valence Bond Theory. In valence bond (VB) type calculations, the wave function is expressed as a linear combination of different valence bond functions (structures).²⁸³ For instance, the most concise unnormalized VB wave function of H_2 reads

$$|\Psi_{\text{H}_2}^{\text{VB}}\rangle = (|1s_{\text{A}}1\bar{s}_{\text{B}}\rangle + |1s_{\text{B}}1\bar{s}_{\text{A}}\rangle) + \lambda(|1s_{\text{A}}1\bar{s}_{\text{A}}\rangle + |1s_{\text{B}}1\bar{s}_{\text{B}}\rangle) \quad (67)$$

This function is identical to the 2o2e CI wave function in eq 39, with the first parenthesized term representing the covalent and the second the ionic VB structures. λ is the variational parameter that adjusts the two contributions. Despite their identical form of wave function, VB calculations take the coefficients of VB structures and the localized (typically atomic) orbitals that make up the structures as variational parameters, while MO-based calculations vary completely delocalized molecular orbitals and CI coefficients.

Because the VB structures clearly have the character of Lewis structures, it is very natural to extract the di(poly)radical contributions in a VB wave function and determine its di(poly)radical character. Please note the nonorthogonality between the orbitals used in expressing the VB wave function and the consequent nonorthogonality between the VB structures. This is the case in general. A partitioning scheme is hence needed to partition their overlaps to the respective VB structures, e.g., the Chirgwin–Coulson equal division scheme²⁸⁴ and the Gallup–Norbeck inverse weights scheme.²⁸⁵ Here we present several recent studies on diradical character by directly decomposing ground state wave functions to contributions of VB structures. Please note that all measures based on natural occupancies introduced above are applicable to VB wave functions.

13.2.2. Ozone and Its Sulfur Analogues. Braïda et al. examined the weights of the three major VB structures (shown in Figure 59) in O_3 and its five S-substituted isomers.^{286,287} The

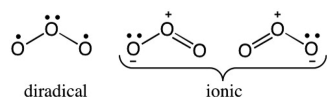


Figure 59. Three major VB structures of O_3 .

diradical structure contributes about 45% to the ground state wave function of O_3 . Considering there are two ionic vs one diradical structures, this weight indicates significant diradical character in O_3 , which is consistent with the molecule's high reactivity, especially at its termini. For the six molecules examined, the weights of the diradical structures correlate well with their energies and the molecules' reactivities and stabilities.

The authors also compared the diradical VB weight and the conventional indicators based on the coefficient of the HOMO-to-LUMO double excitation in the MO wave functions. The latter were found to systematically underestimate the diradical

characters of the series of molecules (e.g., 18% for O_3). This is not unanticipated because the double-excitation-based indicators are derived for a 2o2e wave function, while the electronic structures of the O_3 series involve a 3o4e active space. The 3o4e active space is intrinsically relevant for 3-center 4-electron bonding interaction. The diradical VB weights are similar to the diradical character index defined by Glezakou et al., namely the occupation of the central π orbital minus 1.²⁸⁸ The success of Glezakou et al.'s index tells us that if we can unambiguously associate di(poly)radical character to some properties, the properties are natural indicators of the di(poly)radical character. Spin properties proposed as diradical indicators that are introduced in section 13.3 are based on the same idea.

Braïda et al. employed the same VB-based method to probe the diradical character of the E_2N_2 and E_4^{2+} systems with $\text{E} = \text{S}, \text{Se}, \text{Te}$, and 6 electrons distributed in 4 π orbitals.²⁸⁹ All the 4-membered rings have $\sim 50\%$ diradical weight. The vertical resonance energies of diradical, covalent, and ionic VB structures of S_2N_2 and S_4^{2+} were estimated to be 80% of that of benzene. The large resonance energies and the high weights of diradical VB structure demonstrate the compatibility of aromaticity and diradical character in these systems.

13.2.3. Polyenes. Gu et al. performed VB calculations for polyenes C_nH_{2n} with $n = 2-9$ and analyzed their polyradical characters.⁷⁹ The ground state wave functions for these compounds were found to be mainly made up of VB structures of alternating π bonds (fully bonded) and those of a 1,4-diradical nature. The VB structures are shown in Figure 60. The 1,4-

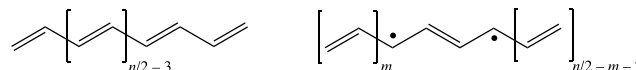


Figure 60. Two types of VB structures that contribute. n is the number of C atoms, and m ranges from 0 to $n/2 - 2$.

diradical structures break two short π bonds and form one long π bond and are hence higher in energy than the fully bonded one, with an approximately constant energy gap regardless of the length n . 1,6-, 1,8-, and other 1,2 k -diradical structures break k short π bonds and form $k-1$ long π bonds and are hence of higher energy. Their energies are higher than that of the 1,4-analogue because of the breaking of more shorter π bonds and the formation of more longer π bonds, although effectively, only one π bond is broken in all the diradical structures.

All the other VB structures break more than one π bond and are of even higher energy. Only the 1,4-diradical structures are sufficiently low in energy to contribute considerably to the ground state. Note that the VB structures implicitly contain ionic character because the basis orbitals were allowed to have small delocalization “tails”, contributions on neighboring atoms. The number of the 1,4-diradical VB structures increases linearly with n . As a result, they collectively contribute more and more to the ground state, and the fully bonded structure contributes less than half above around $n = 5$ but maintains the largest (Coulson–Chirgwin) weight.²⁸⁵ This suggests significant diradical character for long polyenes.

However, the authors caution against viewing long polyenes as true diradicals, no matter how large the contributions of the diradical VB structures. Despite the increased chemical reactivity of the long polyenes, their nonnegligible 1.5 eV band gap at the $n = \infty$ limit is evidence of the nondiradical nature of their ground states. Also, chemically long polyenes do not abstract H atoms nor dimerize (cross-link) easily. Actually,

the increasing diradical weight is to be understood in the context of size extensivity. The VB method used in the calculations is a size-extensive method. Each 1,3-butadienic unit of the polyenes features an about $\frac{\sqrt{3}}{2}$ weight of the alternating bonded (classical) wave function, and the rest is largely the 1,4-diradical VB structure. Viewing a polyene as being comprised of overlapping butadienic units (overlapping, because positions 3 and 4 of one butadienic unit can be positions 1 and 2 of another), a size-extensive computational method will give a ground state wave function as an antisymmetrized product of the butadienic wave functions. Correspondingly, the weight of the fully bonded structure decreases as the power of $\frac{\sqrt{3}}{2}$, taking the length as the power (see eq 9 in ref 79) and eventually reaches zero.

The apparently significant diradical character in long polyenes hence arises partially as a cumulative result, similar to the examples of 50 H₂ molecules and C₆₀ above. This is the fundamental reason for why “one should be cautious to attribute too many physical manifestations to the diradical character of polyenes.”⁷⁹ Long polyenes do exhibit diradical character, as evidenced by their reactivity but not as much as the accumulated weight of the diradical VB structures would suggest (see also below).

13.3. Measures Based on Spin Properties

13.3.1. A Peep at the Wave Function Through Spin.

Other than being directly extracted from wave functions, diradical character can also be reflected by properties, especially spin properties. A diradical indicator based on $\langle \hat{S}^2 \rangle$ of a UHF wave function was proposed by Yamaguchi et al.^{246,290,291} In general, a UHF wave function of two spin orbitals (i.e., ignoring all the other electrons in pairs) $|\Psi^{\text{UHF}}\rangle = |\chi_a^\alpha \chi_b^\beta\rangle$ can be written as

$$|\Psi^{\text{UHF}}\rangle = \cos^2\theta |\psi_{\text{H}}^\alpha \psi_{\text{H}}^\beta\rangle - \sin^2\theta |\psi_{\text{L}}^\alpha \psi_{\text{L}}^\beta\rangle + \sin\theta \cos\theta (|\psi_{\text{L}}^\alpha \psi_{\text{H}}^\beta\rangle - |\psi_{\text{H}}^\alpha \psi_{\text{L}}^\beta\rangle) \quad (68)$$

given the following orbital transformation

$$\begin{aligned} \chi_a &= \cos\theta \psi_{\text{H}} + \sin\theta \psi_{\text{L}} \\ \chi_b &= \cos\theta \psi_{\text{H}} - \sin\theta \psi_{\text{L}} \end{aligned} \quad (69)$$

ψ_{H} and ψ_{L} are again the bonding HOMO and antibonding LUMO. Note that χ_a and χ_b are just the GVB orbitals in eqs 27 and 28, but ψ_{H} and ψ_{L} are orthogonal to each other. As θ increases from 0 to $\pi/4$, χ_a and χ_b change from the identical ψ_{H} to two orthogonal localized nonbonding orbitals. Correspondingly, $|\Psi^{\text{UHF}}\rangle$ changes from the closed-shell $|\psi_{\text{H}}^\alpha \psi_{\text{H}}^\beta\rangle$ to an equal mixture of singlet $\frac{1}{2}(|\psi_{\text{H}}^\alpha \psi_{\text{H}}^\beta\rangle - |\psi_{\text{L}}^\alpha \psi_{\text{L}}^\beta\rangle)$ and triplet $\frac{1}{2}(|\psi_{\text{L}}^\alpha \psi_{\text{H}}^\beta\rangle - |\psi_{\text{H}}^\alpha \psi_{\text{L}}^\beta\rangle)$, and the singlet is just a pure diradical function. Only the triplet function with the $\sin\theta \cos\theta$ coefficient contributes to $\langle \hat{S}^2 \rangle$,

$$\langle \hat{S}^2 \rangle = 4\sin^2\theta \cos^2\theta \quad (70)$$

with the \hbar spin unit being dropped. This expression for $\langle \hat{S}^2 \rangle$ gives

$$\cos^2\theta = \frac{1 + \sqrt{1 - \langle \hat{S}^2 \rangle}}{2} \quad (71)$$

Recalling that $\cos^2\theta = 1$ ($\theta = 0$) corresponds to a closed-shell and $\cos^2\theta = 1/2$ ($\theta = \pi/4$) corresponds to an equal mixture of singlet and triplet diradical functions, one can use

$$y = 2(1 - \cos^2\theta) = 2\sin^2\theta = 1 - \sqrt{1 - \langle \hat{S}^2 \rangle} \quad (72)$$

to indicate the diradical character of the UHF wave function. It is straightforward to show that ψ_{H} and ψ_{L} are the natural orbitals of $|\Psi^{\text{UHF}}\rangle$ with occupation numbers $2\cos^2\theta$ and $2\sin^2\theta$, respectively. Therefore, the y in eq 72 is equal to half of the HG-IND_D for the two-electron system and is strongly related to the correlation treatment as discussed before for H₂ (cf. the comparison of UHF and UB3LYP results in section 13.1.10).

13.3.2. Measures Based on Local Spin Properties.

Polyradical character can also be indexed by local spin. This is deeply rooted in the connection between the polyradical character and unpaired electrons, which bear nonzero spin individually. A spin correlator is one such indicator. Luzanov and Prezhdo^{292,293} defined a local spin operator as $\hat{S}_A = \sum_{i=1}^N \hat{s}_i \hat{I}_A(i)$, where $\hat{I}_A = \sum_{\mu \in A} |\chi_\mu\rangle \langle \chi_\mu|$ is the local projection operator onto the orthonormal basis functions that belong to fragment A. One can then calculate the average fragment spin $\langle \hat{S}_A^2 \rangle$ and the interfragment spin correlation $\langle \hat{S}_A \cdot \hat{S}_B \rangle$. The total spin can be decomposed as

$$\langle \hat{S}^2 \rangle = \sum_A \langle \hat{S}_A^2 \rangle + \sum_{A, B \neq A} \langle \hat{S}_A \cdot \hat{S}_B \rangle \quad (73)$$

For a singlet diradical composed of radical fragments A and B, we expect to have $\langle \hat{S}_A^2 \rangle = \langle \hat{S}_B^2 \rangle = \frac{3}{4}$ and $\langle \hat{S}_A \cdot \hat{S}_B \rangle = \langle \hat{S}_B \cdot \hat{S}_A \rangle = -\frac{3}{4}$.

Luzanov and Prezhdo decomposed the total spin into fragment basis functions spaces. This is similar to partitioning total molecular charge into Mulliken charges of fragments. On the other hand, Ramos-Cordoba et al. decomposed the total spin into real volume spaces of fragments.^{294–297} Analogously, this is similar to partitioning molecular charge into Bader charges. Similar to eq 73, Ramos-Cordoba et al. decomposed the total spin into diagonal and off-diagonal contributions from fragments:

$$\langle \hat{S}^2 \rangle = \sum_A \langle \hat{S}^2 \rangle_A + \sum_{A, B \neq A} \langle \hat{S}^2 \rangle_{AB} \quad (74)$$

These authors showed that $\langle \hat{S}^2 \rangle$ can be expressed as

$$\begin{aligned} \langle \hat{S}^2 \rangle &= a \int u(\mathbf{r}_1) d\mathbf{r}_1 \\ &- (1 - a) \iint \left[\Gamma(\mathbf{r}_1, \mathbf{r}_2) - \frac{1}{2} \rho^s(\mathbf{r}_1; \mathbf{r}_2) \rho^s(\mathbf{r}_2; \mathbf{r}_1) \right] d\mathbf{r}_1 d\mathbf{r}_2 \\ &- \frac{1}{2} \iint \left[\Gamma(\mathbf{r}_1, \mathbf{r}_2; \mathbf{r}_2, \mathbf{r}_1) - \frac{1}{2} \rho^s(\mathbf{r}_1; \mathbf{r}_1) \rho^s(\mathbf{r}_2; \mathbf{r}_2) \right] d\mathbf{r}_1 d\mathbf{r}_2 \end{aligned} \quad (75)$$

(see ref 297 and the references therein). Here, $u(\mathbf{r})$ is the unpaired electron density introduced above, $\rho^s(\mathbf{r}; \mathbf{r}') = \rho^\alpha(\mathbf{r}; \mathbf{r}') - \rho^\beta(\mathbf{r}; \mathbf{r}')$ is the spin density matrix, and $\Gamma(\mathbf{r}_1, \mathbf{r}_2; \mathbf{r}_1', \mathbf{r}_2')$ is the cumulant of the second-order density matrix. $\Gamma(\mathbf{r}_1, \mathbf{r}_2; \mathbf{r}_1', \mathbf{r}_2')$ describes the deviation of the second-order density matrix from that of a single determinant wave function; its diagonal form $\Gamma(\mathbf{r}_1, \mathbf{r}_2)$ is the two-electron analogue of $u(\mathbf{r})$. The parameter a is set to be 3/4 so that for a one electron system, the proper $\langle \hat{S}^2 \rangle$ density, $\frac{3}{4} \rho(\mathbf{r})$, is obtained. The 3D space is then partitioned into different atomic (or fragment) domains, e.g., using the Bader scheme. Restricting both $\int d\mathbf{r}_1$ and $\int d\mathbf{r}_2$ over one domain (say A) gives the one-center $\langle \hat{S}^2 \rangle_A$, and if the integrations are over

two different domains (say A and B), the two-center $\langle \hat{S}^2 \rangle_{AB}$ is obtained.

The decomposition results in nonzero one- and two-center contributions to overall spin even for a pure singlet ground state, for which the spin-density is zero. The one-center $\langle \hat{S}^2 \rangle_A$ indicates the partial spin on atom A , and the two-center $\langle \hat{S}^2 \rangle_{AB}$ reflects the coupling between the partial spins on atoms A and B , positive for ferromagnetic and negative for antiferromagnetic interaction. Atoms with formal unpaired electrons in dominant resonance structures are found to possess the large partial spins. For typical closed-shell systems, all one- and two-center spin contributions are close to zero, as expected. The decomposition nicely reproduces the transition from $\langle \hat{S}^2 \rangle_A \approx 0$ to $\langle \hat{S}^2 \rangle_A = 3/4$, 2 for $A = \text{H}, \text{O}$ in the dissociation of A_2 .²⁹⁶

The polyradical character of a molecule can be judged based on comparing the $\langle \hat{S}^2 \rangle_A$ and $\langle \hat{S}^2 \rangle_{AB}$ values with some well-defined references. In practice, it is more convenient to consider only the one-atom contributions, and a RMSD measure of k -radical character is defined as

$$\Delta^{(k)} = \sqrt{\frac{\sum_{A=1}^n (\langle \hat{S}^2 \rangle_A - \langle \hat{S}^2 \rangle_A^{\text{id},k})^2}{n}} \quad (76)$$

$\langle \hat{S}^2 \rangle_A^{\text{id},k}$ is the ideal atomic expectation value of \hat{S}^2 of atom A in the k -radical reference state. For instance, for an H_2 in its dissociation limit, the $\langle \hat{S}^2 \rangle_A^{\text{id},2}$ of each H atom is $3/4$. The smaller $\Delta^{(k)}$, the closer the state to the k -radical reference state. Unlike the occupation number indicator, this RMSD measure is applicable to both ground and excited states. We do not see any problem of using $\langle \hat{S}^2 \rangle_A$ of Luzanov and Prezhdo to calculate $\Delta^{(k)}$, and it is easier to calculate $\langle \hat{S}^2 \rangle_A$ than $\langle \hat{S}^2 \rangle_{AB}$.

13.4. Closing Comments on Di(poly)radical Indices

In closing this section, we would like to emphasize the approximate nature of all polyradical indices. As we mentioned at the outset, polyradical character is not an observable. Different indices may have quantitatively different values for a system, but the qualitative trends as the system changes should be consistent. We should be cautious, very cautious, in interpreting polyradical characters using the number of effectively unpaired electrons (and $\langle \hat{S}^2 \rangle$ for UHF wave function), as an accumulation of weak correlations between many pairs of electrons can be misinterpreted as strong correlations between a few pairs, leading to overestimated polyradical character. Also, for larger systems, this issue is aggravated (e.g., the examples of 50 H_2 molecules and polyenes) because there are more electron pairs featuring the weak correlations.

To return to the context of this paper, a diradical measure is an index derived from wave function analysis or property evaluation, intended to measure the extent a molecule deviates from a pure closed-shell or pure diradical limit. With the caveats (many) mentioned above, and the obvious differences displayed for one and the same system by different diradical measures, a genuine diradical measure, based on whether there are a few large fractional natural occupancies or not, does provide a simple and quick way to get a feeling for the electronic structure of a molecule. However, a genuine polyradical measure, whichever index one uses, still may not directly relate to reactivity and may not necessarily serve as a gauge of classical radical reactivity.

Instead, we believe that the most effective way of assessing the reactivity of compounds with (significant) diradical character is to take the conclusions drawn in section 12 into account. This means focusing on the spin density at radical sites, the singlet–

triplet gap, ΔE_{ST} , and paying attention to potential competing reaction modes due to the open-shell/closed-shell duality.

Let us apply this approach to the acene, fullerene and polyene systems and try to explain their reactivity trends. Figure 61 presents the spin densities for the lowest triplet states of some example molecules.

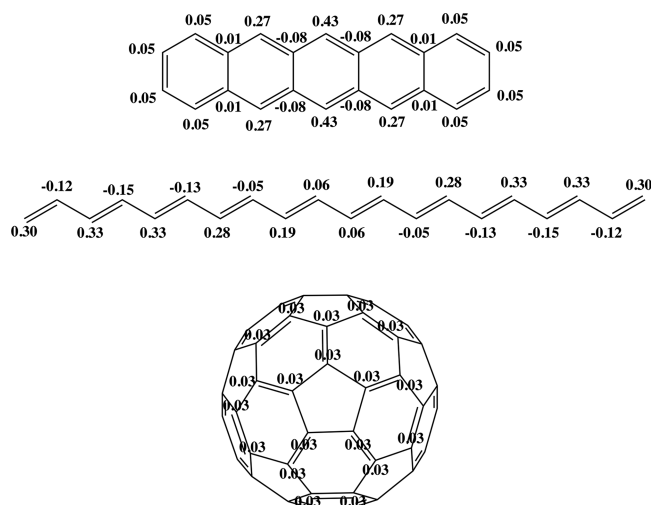


Figure 61. (Mulliken) spin densities calculated for the lowest triplet states of pentacene (top), $\text{C}_{20}\text{H}_{22}$ (middle, planar), and C_{60} in its I_h geometry (bottom). For pentacene and $\text{C}_{20}\text{H}_{22}$, calculations were performed at UB3LYP/cc-pVTZ level of theory. For C_{60} , spin densities were determined analytically for the non-Jahn–Teller distorted I_h geometry (the geometry changes due to Jahn–Teller distortions have been demonstrated to be small).²⁹⁸

On the basis of symmetry arguments, we can conclude that for C_{60} , the spin density is evenly spread out over the system. For the long polyene, $\text{C}_{20}\text{H}_{22}$, there is a moderate buildup of spin density on specific sites, whereas for pentacene, the spin density is unequivocally centered on the central zigzag edges. Because other factors such as strain, steric hindrance, etc., can be expected to play only minor roles in each of these systems, the localization of the spin density determines the radical reactivity of the triplet states. As a consequence, we can expect the lowest triplet state of acenes to be more reactive than those of the polyenes and fullerenes. Furthermore, for acenes, ΔE_{ST} decreases with length (in the limit, it approaches 0–10 kcal/mol); for pentacene, it amounts to 20–24 kcal/mol.^{13,299} For polyenes, ΔE_{ST} goes down with length as well, although a finite gap (vertical ΔE_{ST} estimated to be 21 kcal/mol^{300,301}) remains even in the limit of infinity. For the longer acenes and polyenes, the reaction barriers and energies for radical reactivity of the singlet state can be expected to approach those of the triplet state (because the singlet ground state is lower in energy than the triplet state, the singlet is yet less reactive).

C_{60} , on the other hand, still has a significant ΔE_{ST} of 36–41 kcal/mol.^{302,303} Thus, we do not expect to see radical reactivity for the buckminsterfullerene singlet state; the triplet state already shows little reactivity due to the extensive delocalization, which leads to a low and almost uniform spin density. For the singlet ground state, this is even more pronounced because the reaction barriers in this state go up significantly due to the energy gap to the triplet state, a gap which has to be partially conquered if radical reactions are to proceed. Because of the inertness of fullerene toward radical reactions, we can expect that the concerted/

nonradical reactivity of C_{60} dominates, even if the barriers toward these reactions are relatively elevated. Experimentally, this is what happens: cycloadditions to the molecule take place; carbenes add to it.

For longer polyenes and acenes, one cannot easily predict which type of reactivity will dominate (detailed calculations are required here). But it should be clear that irrespective of whether the competing concerted reactions of the singlet state end up leading to slightly higher or lower reaction barriers and energies than the radical reaction modes, these intermediate molecules, with significant diradical character, will be inherently reactive. Specifically, long polyacenes are more reactive than long polyenes, as their respective instabilities and multiradical character demonstrate.

To summarize, the analysis above is in accord with the profoundly different reactivity and stability ascribed to these three types of molecules in the literature; fullerene is characterized as a kinetically very stable molecule, exhibiting essentially no radical reactivity whatsoever, long polyenes are reactive and prone to cross-linking, and acenes become increasingly reactive, in a number of ways, and are hard to obtain as their length increases.

Polyacenes deserve more detailed attention, so that a subsection of the next section will be devoted to these molecules.

14. SOME TYPICAL DIRADICALS AND DIRADICALOIDS

In this section, some diradicals and diradicaloids that have been intensely investigated over the past few decades are introduced and discussed. We focus on their interesting properties instead of using them as models to demonstrate the wave function characters of diradical(oid)s.

14.1. Polyacenes

Polyacenes (cf. Figure 2) and their derivatives have been subjects of intense research in the past three decades, primarily due to their remarkable optoelectronic properties.^{13,304–309} The following conclusions about this family of molecules have been drawn:^{11,310–314}

- (1) As their length increases, the ground states of polyacenes gain more and more diradical and polyradical character. Their wave functions become multireference in nature.
- (2) Along with the increase of diradical character, ΔE_{ST} decreases to vanishingly small, yet still positive, values. A singlet open-shell ground state is attained in the infinite limit. The estimated limiting ΔE_{ST} varies based on different calculations, ranging from 2 to 12 kcal/mol. Despite the uncertainty in the limiting ΔE_{ST} , it is certainly lower than the ~ 21 kcal/mol analogue of polyene, indicating stronger diradical character in long polyacenes.
- (3) A ~ 28 kcal/mol optical gap, which is larger than the limiting ΔE_{ST} , is estimated for the infinite length limit.^{315,316} This is the energy gap between the ground and the first singlet excited state that can be reached by photoexcitation. This large optical gap should not be taken for evidence of low diradical character of infinitely long polyacene;
- (4) The higher diradical character of polyacenes is attributed to the weaker bonding/antibonding character in their HOMOs and LUMOs and the consequent milder Peierls distortion^{300,311,317} compared to polyenes.

The diradical character of long polyacenes can be understood using the localized orbitals shown in Figure 62a,b for the 10-ring

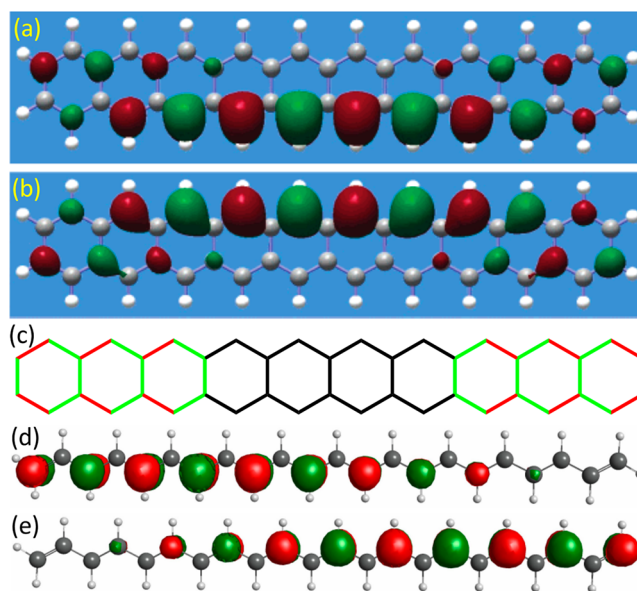


Figure 62. Localized orbitals transformed from HOMO and LUMO of decacene are shown in (a) and (b). The addition (subtraction) of the two orbitals strengthens (weakens) the green bonds as shown in (c) and weakens (strengthens) the red bonds. The similar localized orbitals of the $C_{22}H_{24}$ polyene are shown in (d) and (e). (a,b) Reproduced with permission from ref 311. Copyright 2004 American Chemical Society.

molecule, decaene. These orbitals are obtained from a symmetry-broken unrestricted DFT calculation and correspond to the transformation of the HOMO and LUMO according to eqs 19 and 20, with ψ_x and ψ_y being replaced by ψ_H and ψ_L . They can be viewed as singly occupied molecular orbitals (SOMOs) of two intercalated radicals.³¹⁸ As expected for alternant hydrocarbons with equal numbers of starred and unstarred C atoms, one SOMO has amplitudes solely on the starred C atoms, while the other one has them on the unstarred C atoms. Together, the two SOMOs make a disjoint diradical, which favors a singlet ground state. Given the orbital phases in Figure 62, their addition leads to bonding (antibonding) interaction in the green (red) bonds in Figure 62c, while their subtraction swaps the bonding and antibonding interactions.

Other than the energy splitting in the orbital addition and subtraction, the Peierls distortion driven by the different bonding/antibonding patterns of the resultant HOMO and LUMO further opens their gap and favors a singlet ground state. It is the subtraction of the two localized orbitals that gives the HOMO of decacene, i.e., the bonding interactions in the red bonds dominate over the antibonding interactions in the green bonds. However, the largest amplitudes of the localized orbitals at the center of the long edges remain nonbonding in the orbital addition and subtraction and do not contribute to the Peierls distortion. This has as a consequence that the HOMO–LUMO gap opening is not very significant, especially when compared to polyenes.

The corresponding localized orbitals arising from HOMO and LUMO of polyenes, as exemplified by Figure 62d,e, are more evenly distributed over the chain and almost every lobe participates in the bonding/antibonding interaction in HOMO and LUMO. The stronger bonding/antibonding interactions also lead to a more significant Peierls distortion, which further opens up the HOMO–LUMO gap. This is why long polyacenes have more substantial diradical character than polyenes, and

their peripheral C atoms do not feature alternating single and double bonds as much as polyenes.

As their lengths increase, polyacenes also have more substantial occupations of $n_{\text{LUNO}+1}$, $n_{\text{LUNO}+2}$, etc. This is clearly shown in Figure 63. The increase of tetraradical and other higher-order polyradical character is evident.

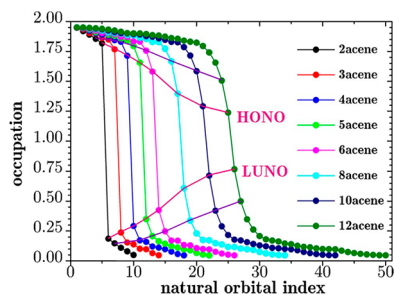


Figure 63. Natural orbital occupation numbers for the polyacene series calculated at the DMRG level with the STO-3G basis set. Reproduced with permission from ref 6. Copyright 2007 American Institute of Physics.

Finally, we note that using Hückel–Hubbard Hamiltonians, Malrieu and Trinquier performed a topological analysis for long polyacenes.²⁷⁹ They concluded that long polyacenes can be viewed as consisting of shorter oligoacene fragments, and the polyradical characters of long polyacenes arise from the diradical characters of these shorter fragments.

14.2. Extended π -Diradicaloids

In recent years, we have seen a rich extension of the chemistry of quinoids (cf. Figure 2) to larger π systems. A consistent theme in the chemistry of these compounds is the pitting of a diradical structure with a certain degree of aromaticity (called by Wu’s group “proaromatic”) vs a closed-shell valence structure with reduced aromaticity.^{319–321}

The situation is exemplified by *para*-quinodimethane itself, whose reactivity and singlet–triplet splitting were discussed in section 10.6.

The degree of diradical character and the stability of these molecules is eminently tunable. For instance, tetracyano derivatives (at the terminal methylenes) of these molecules become kinetically persistent.^{322,323} Quinoid compounds and their analogues have attracted significant interest within the field of single-molecule electronics. As previously mentioned, the diradical character of a compound has recently been connected to the magnitude of conductance through it when that compound is linked up within a circuit.^{53,56} This relationship has been exploited to tune the conductivity of compounds through chemical modification.^{54,54,55} Furthermore, PQDM has been proposed as a monomer for a molecular nanowire with an increasing conductance with length (Figure 64).^{324–326}

Chichibabin’s, Dimroth’s, and Müller’s hydrocarbons, novelties in their time, have become exemplars of another extension, now linear, of quinoid hydrocarbons (Figure 65).^{327–332} In some of the compounds made, the radical character may reside on heteroatoms.³²⁰

The units linked up to form a diradicaloid may derive from any monoradicals known to be persistent. Thus, a rich chemistry has developed from the phenalenyl radical, shown in Figure 66.³²⁰ Two such radicals are in a way fused in zethrene, a poster child of the extended π -system diradicaloid family (Figure 67).

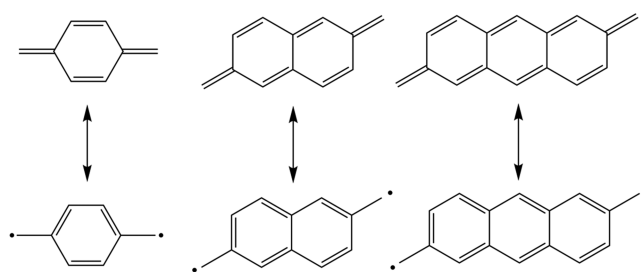


Figure 64. PQDM (left), 2,6-naphthoquinodimethane (middle), 2,6-antraquinodimethane (right).

There are many other ways to link up phenalenyls; several are shown below in Figure 68.^{333,334}

With appropriate protecting groups these molecules achieve some kinetic persistence,^{335,336} turning them into interesting candidates for a variety of applications as optical and electronic materials.^{337,338} We refer the reader to several excellent reviews of the field of zethrene chemistry.^{177,339,340}

The diradicaloid nature of these molecules is not in doubt; in all of these molecules, a singlet and a triplet are relatively close to each other in energy. For example, in a nonazethrene derivative, the singlet–triplet splitting is measured as 5.2 kcal/mol.³⁴¹

Consequently, all these compounds are characterized as having open-shell singlet ground states. This is the most natural way to think about the molecules because the prefix “di-” suggests two radicals, i.e., an open-shell with two unpaired electrons. However, we do want to stress that the open-shell nature does not prevent the singlet molecules from reacting in a closed-shell manner. This aspect of singlet diradical(oid)s has been thoroughly discussed in section 10.

14.3. Arynes

A final class of carbon-based diradicals and diradicaloids we would like to mention briefly are the arynes,^{342–344} dihydrogenated benzenoids. These compounds play an important role in a variety of biological processes, in combustion reactions, heterogeneous catalysis, and in both organic and organometallic synthesis. Focusing on the smallest representatives (benzynes, cf. Figure 2), three isomers can be distinguished as *ortho*-, *meta*-, and *para*-benzyne, respectively (cf. Figure 69).

These three isomers exhibit stark differences in their aromaticity,³⁴⁵ structural detail, and reactivity. The main driver of the divergent reactivity of the benzynes is the difference in the S–T splitting: from 38 kcal/mol for *o*-benzyne, over 21 kcal/mol for *m*-benzyne to 4 kcal/mol for *p*-benzyne.³⁴⁶ This remarkable variation in S–T gaps is the outcome of quite specific pathways for radical site interaction in these molecules, and results in a varying degree of diradical character. Whereas *p*-benzyne can arguably be considered as a true diradical according to the criteria outlined in the previous paragraphs, *m*-benzyne, and especially *o*-benzyne, is better described as a diradicaloid because the two “radical” sites are far from perfectly uncoupled.

Not that it matters much what one calls them; it is their structure and reactivity that matter. As expected from its large singlet–triplet gap, *o*-benzyne shows mainly typical closed-shell reactivity cycloadditions, certainly facile, are a typical reaction pattern. The remarkable revelation of *p*-benzyne in a reaction by Jones and Bergman³⁴⁷ was followed by its observation in a matrix.³⁴⁸ It is the radical reactivity of *p*-benzynes that has made the system so useful,³⁴⁹ and the involvement of certain C–C σ bonds in coupling the radical sites has been important in teaching us about through-bond coupling.

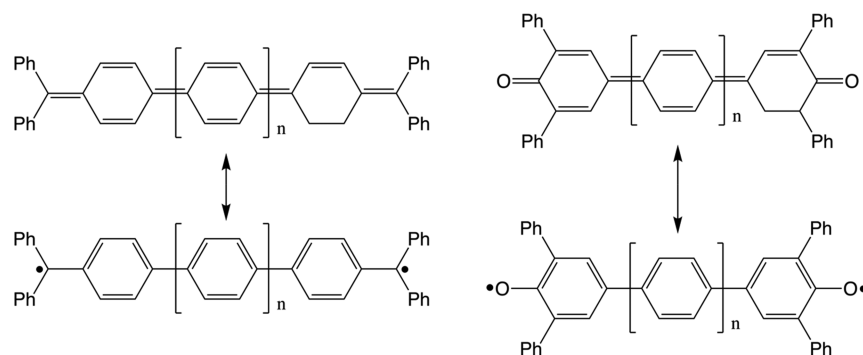


Figure 65. Chichibabin's hydrocarbon ($n = 0$), Müller's hydrocarbon ($n = 1$) (left), Dimroth's hydrocarbons ($n = 1, 2$) (right).

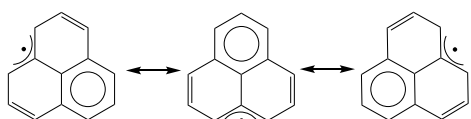


Figure 66. Some phenalenyl resonance structures.

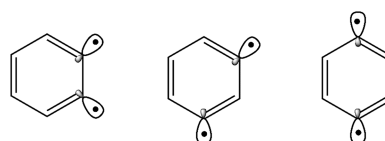


Figure 69. From left to right: *o*-benzyne, *m*-benzyne, and *p*-benzyne.

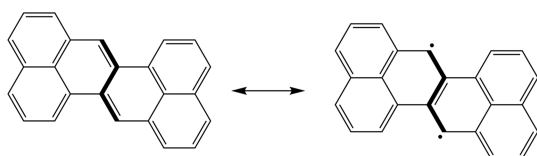


Figure 67. Zethrene resonance structures

meta-Benzyne is structurally the most interesting of the benzyne. There is in this diradicaloid the potential for the two

radical sites to interact directly through space (depending on their separation, of course) or through intervening C–C or C–H bonds. The net result is a soft and eminently tunable (by substitution) surface between extremes of benzene-like diradical structures, and a “bicyclic structure” with a 1–3 σ bond.³⁵⁰ If the diradical (easily generated by chemical ionization of an iodo-substituted precursor) is charged, its reactions can be studied in great detail mass spectrometrically. Studies of Kenttämaa and co-workers have in this fashion provided us with much carefully

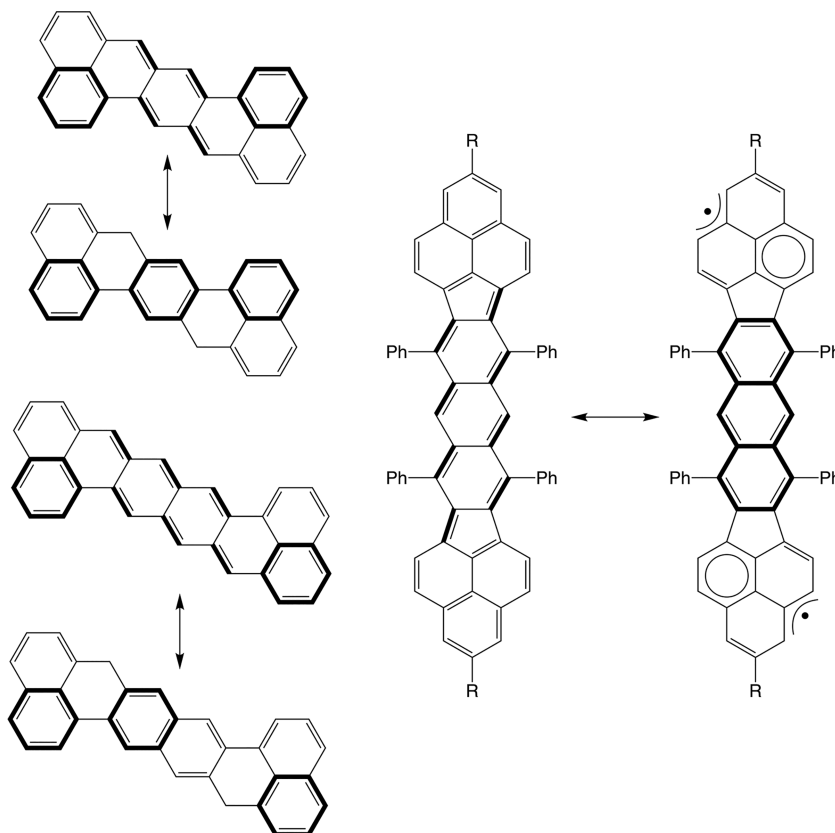


Figure 68. Analogues of zethrene: heptazethrene (top left), octazethrene (bottom left), and a PQDM bridged biphenyl compound (right).

reasoned experimental detail on *m*-benzyne reactivity.^{351–353} These molecules behave primarily as radicals but can be induced to react as electrophiles upon heteroatomic substitution.²⁴² These reactivity patterns are in line with the expectations resulting from our general analysis outlined in section 12.

We apologize for not being able to do justice to the great sweep of excellent chemistry, from theory to matrix isolation to biochemistry, that marks the great field of aryne chemistry and the diradicaloids that it contains.

14.4. Main Group Diradical(oid)s

Throughout this work, we have reluctantly limited ourselves almost exclusively to organic (di)radical(oid)s and put our main focus on simple hydrocarbons. As we mentioned, a rich literature on other types of radical(oid) systems exists as well. The goal of this section is to give a short overview of these systems, discuss some of the anticipated reactivity trends, and provide some leading references for further reading.

Let us first consider main group diradical(oid)s. As mentioned in section 9, the introduction of heteroatoms, down Mendeleev's table, is an important strategy for the stabilization of monoradicals. Equivalently, substitution strategies have been successfully deployed to synthesize stable diradicals as well. Several groups have focused on the synthesis and/or computational study of heteroatomic four- and five-membered diyl ring systems (cf. Figure 2 and Figure 70).^{354–367}

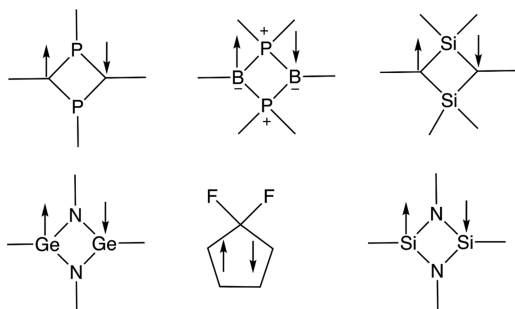


Figure 70. Some common patterns of main group singlet diyls based on four- and five-membered rings.

The relative stability of these diyls, most of which have a singlet ground state, arises from a combination of electronic, steric, and strain effects preventing a barrier-less ring closure.³⁶³

Another important class of stable, localized main group diradicals are the (bis)aminoxyls, hydrazyls, thiazyls, and verdazyls,^{368,369} etc. (cf. compound 4 in Figure 71). The stability of these compounds can be attributed to destabilization of the reaction products of their dimerization. The process has been studied in detail, for instance, for H₂NO.¹¹¹

Heteroatomic analogues of TMM, MQDM, and PQDM have also been reported (Figure 71).^{370–372} The substitutions in

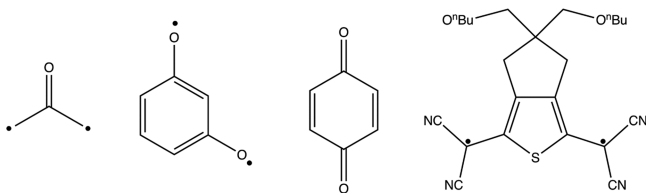


Figure 71. Some heteroatomic analogues to previously discussed diradicals.

these compounds are often accompanied by significant changes in the singlet–triplet gap or even a reversal of the ground state multiplicity, although a uniform trend cannot be identified. For oxocarbons, (CO)_{*n*},^{373,374} for example, the ground state multiplicity is largely dependent, in well-understood ways, on the value of *n*, with a triplet ground state for (CO)₂ and (CO)₄ and a singlet ground state for CO, (CO)₃, (CO)₅, and (CO)₆.²⁴ For a complete overview of the different main group diradicals synthesized up to 2013, we refer to the review by M. Abe.²⁴

14.5. Transition Metal Diradicaloids

Even though they are often not perceived as such, many transition metal complexes can also be considered as di/multiradical systems; multiple states compete for the ground state and spin crossover events are common. This is not only the case for bridged dimetal complexes, such as the copper(II) acetate dimer shown in Figure 2, but also for regular weak field complexes containing a single metal center. High-spin transition metal complexes are relatively stable compared to main group di/multiradicals (and especially carbon-based compounds) due to their lower electronegativity and the availability of low-energy orbitals to accept electrons.¹¹² Because of the accessibility of several spin states, a myriad of reaction pathways are generally available to these compounds. It has been proposed that spin-crossing events even play an active and important role in the reaction mechanisms involving these compounds, directly affecting rate constants, branching ratios, and temperature behaviors of organometallic transformations.³⁷⁵ Especially in biological systems, such as the cytochrome P450 enzymes, this phenomenon, generally called multistate reactivity (MSR), plays a significant role in the catalytic activity (Figure 72).³⁷⁶

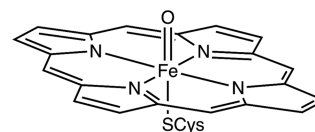


Figure 72. Catalytic center of cytochrome P450 involved in MSR.

For an excellent introduction into MSR, we refer to the overview article by Schröder, Shaik, and Schwarz.³⁷⁷

It is actually for inorganic metal-based diradicals that we think the most incisive analysis of diradical states has been performed. The most informative work here is that of Malrieu, Caballol, Calzado, de Graaf, Guihéry, and their co-workers;²⁹ in the remainder of this section, we will take the time to describe it in intermediate detail. The reader is also referred to the excellent text by Launay and Verdager for further discussion.³⁷⁸

The archetypical situation is that of two Cu(II) centers as, for instance, in the one illustrated in Figure 73 for [Cu₂(OH)₂L₂]²⁺ (L = tetramethylethylenediamine).³⁷⁹ For Cu(II) in a

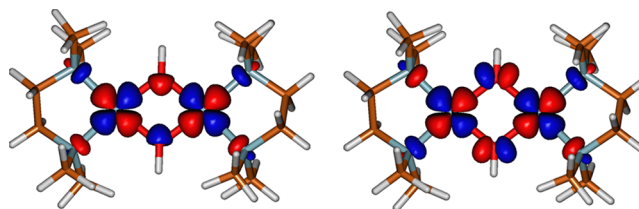


Figure 73. Symmetry-adapted magnetic orbitals for the Cu(II)dimer, [Cu₂(OH)₂L₂]²⁺ (L = tetramethylethylenediamine). Reproduced with permission from ref 29. Copyright 2014 American Chemical Society.

square-planar coordination environment, the ligand-field destabilized $d_{x^2-y^2}$ orbital is the “magnetic orbital”, the one bearing an unpaired electron.

With two such centers in proximity, the classical diradical situation emerges. In the inorganic realm this set of problems has been phenomenologically analyzed by a Heisenberg–Dirac–van Vleck Hamiltonian. The singlet–triplet energy difference is labeled as J . It will be noticed that the magnetic orbitals in this 2-electron, 2-orbital scheme are orthogonal, symmetry-adapted (g or u), but not localized to the metal ions. They possess small tails on the ligand atoms.

Calculations in the 4-determinant, 2-orbital space give values of J whose sign (whether singlet or triplet is lower) is correct, but whose absolute values are way off, “rarely more than 25% of the values derived from experiment”.

The Malrieu group then embarked on a deliberate journey of improving on this. This could be done in a variety of ways, all of which technically involved the turning on of configuration interaction with certain classes of configurations, excitations, and orders of perturbation theory. Or, to put it another way, correlation of electronic motions had to be included, and with it a variety of physical effects not part of the simple canonical model. The quest was rewarded; today one can estimate the singlet–triplet gaps in these diradicals quantitatively. But, more importantly, one can understand them.

Let us describe approximately what had to be done. Clearly, one had to leave the minimal valence space. The configurations enlisted in getting a better description are economically described by excitations labeled h for hole, and p (for particle = electron). Inorganic chemists would be at home with the idea of involving these from ligand-to-metal and metal-to-ligand charge transfer electronic transitions. h and p naturally refer to orbitals outside the valence set, what might be called respectively, ligand or core, and virtual orbitals.

Adding $1h$, $1p$, and $1h-1p$ excitations, which introduce dynamic charge and spin polarization, “help”. But insufficiently so. It takes $2h-1p$ and $1h-2p$ excitations to get J (the singlet–triplet splitting) on the mark. The journey there may be traced in the original papers; the main effect is a state-dependent modification, a reshaping (not great, but important) of the magnetic orbitals.^{380–382}

Similar effects are at work in organic diradicals and in cases (which we have pointed to) of “Hund’s rule violations”. In our opinion, the sometimes transformative role of correlation and polarization has been better *understood* for the complex transition metal cases than for the simpler all-organic ones.

Again revealing an omission in our coverage, the field of spin-crossover compounds has been an important part of inorganic and solid state chemistry for nearly 90 years.³⁸³ The early role it played in the development of ligand and crystal field theory was significant. We point here to some references on the chemistry and physics of spin-crossover compounds.³⁸⁴

15. CONCLUSIONS

In this review, we have tried to address the question: “How do diradical(oid)s react?” Starting from the typical diradical situation of two (nearly) degenerate orbitals in which two electrons reside, we discussed the characteristic electronic structure of diradical molecules and how diradicaloids form the natural bridge connecting these species to the more conventional closed-shell molecules.

The (pseudo)degenerate orbitals in diradicals and diradicaloids can be considered from two distinct perspectives, a

localized one and a delocalized one, giving rise to what could be called a “closed-shell/open-shell ambiguity”. That ambiguity pervades the discussions of diradicaloids in the literature. The underlying wave function transformations may seem to add a complexity to the diradical problem, but (a) we have worked hard to make its development as transparent as possible, and (b) it adds conceptual advantages, consistent with the rich chemistry of diradicaloids. We argue for a flexible approach, in which one switches back and forth between localized and delocalized perspectives, and tries to use, judiciously, an underlying duality of the wave functions.

Subsequently, we identified a diverse set of prototypical diradical(oid) systems (mostly organic: alkyl chain diradicals, cyclobutadiene, trimethylenemethane, *para*- and *meta*-quinodimethane, and O_2) and studied the reactivity of their lowest singlet and triplet states. In these reactivity studies, we distinguished between typical radical reactivity on one hand and typical “closed-shell”/concerted reactivity on the other. Radical reactivity in these systems was probed by considering the activation and reaction energies of three archetypical radical reactions: addition to ethylene, hydrogen abstraction from SiH_4 , and dimerization. “Closed-shell” reactivity was studied by considering alternative concerted pathways for the radical reactions. To bridge these two distinct types of reactivity, we introduced a conceptual “preparation” step for diradical(oid)s reacting, enabling the versatile switch from a closed-shell to an open-shell representation of the wave function and vice versa. The ambiguity alluded to in the previous paragraph exhibits itself as a duality in reaction, that the singlet diradical(oid)s can react either as open-shell or as closed-shell species.

The detailed analysis of dioxygen reveals just how special this diradical is: a clear, resonance-stabilized ground state triplet, yet showing no radical reactivity at ambient temperature with a very reactive excited singlet state. If it were not for those special features of dear oxygen, we would all go up in a puff of smoke!

Next, we reviewed the multitude of measures of diradical character described in the literature so far, clarifying the relationship between diradical character and electron correlation. We emphasized the approximate nature of all polyradical indices. There are dangers of misinterpreting an accumulation of weak correlations between many pairs of electrons as strong correlations between a few pairs, leading to an overestimation of the diradical character. The UHF method, because it is cheap and particularly seductive in this context, and so its use should be accompanied by a due warning.

H_2 dissociating, ozone, *para*-quinodimethane, buckminsterfullerene, oligoenes, and acenes serve us as test cases, showing how one might approach measures of diradical character. The zeroth-order answer is “Carefully”. Whichever index one uses, it may not necessarily serve as a reliable gauge of classical radical reactivity. One has to examine specific reactions.

With exceptions, often due to delocalization, there is a natural correlation between spin density at a site in a molecule and radical-like reactivity of a triplet diradical(oid), with oxygen again as an exception. The singlet–triplet gap in the diradical is, in general, a good indicator of reactivity. As typical reactions proceed, the sites where the spin is localized generally become more distant from each other, the corresponding exchange integral decreases, leading to a smaller singlet–triplet gap. The higher component of the multiplet, be it singlet or triplet, is then more reactive.

There is nothing better than a picture to illustrate this, so we repeat one earlier in the paper, in [Figure 74](#). Singlet states do

have additional reaction channels open to them, often allowed concerted reactions. These need to be considered.

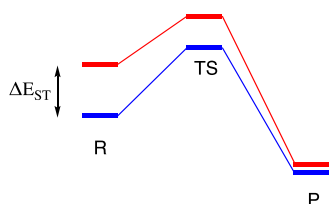


Figure 74. A generic reaction profile for the two spin states (singlet and triplet) of a diradical(oid) in a radical-type reaction, showing the decreased ΔE_{ST} along the reaction course. R, TS, and P label reactant, transition state, and product, respectively.

Finally, we sketched very briefly the rich literatures on some types of diradicals and diradicaloids, such as polyacenes and extended π -system diradicaloids (of much interests in the recent optoelectronic and synthetic literatures, respectively), arynes, and those with their radical centers on main group atoms (such as Si or P) and on transition metals.

In summary, we have tried to paint a picture as complete as possible for the vibrant and ever expanding field of (di)radical(oid) chemistry, with a special focus on the reactivity of these compounds. The conceptual framework presented has a thorough theoretical underpinning; we calculate activation energies and justify why they are what they are. We believe that our understanding of diradical reactivity bridges different fields of organic, physical, and theoretical chemistry and offers a unified view of the continuous spectrum of reactivity for monoradicals, diradicals, diradicaloids, and closed-shell molecules.

ASSOCIATED CONTENT

Supporting Information

The Supporting Information is available free of charge on the ACS Publications website at DOI: [10.1021/acs.chemrev.9b00260](https://doi.org/10.1021/acs.chemrev.9b00260).

Derivation of eqs 6, 9, and 10, active spaces for the CASPT2 calculations, GVB transformations for $C_5H_5^+$ and $C_3H_3^-$, singlet wave functions for O_2 , orbital correlation diagram analysis for the dimerization reaction of O_2 , preparation perspective on closed-shell reactivity, geometries and electronic energies of the molecules studied (PDF)

AUTHOR INFORMATION

Corresponding Authors

*Phone: 607-255-3419. E-mail: rh34@cornell.edu.

*E-mail: Thijs.Stuyver@vub.be.

*E-mail: cberic@hotmail.com.

*E-mail: tzeng@yorku.ca.

ORCID

Thijs Stuyver: 0000-0002-8322-0572

Bo Chen: 0000-0002-5084-1321

Tao Zeng: 0000-0002-1553-7850

Roald Hoffmann: 0000-0001-5369-6046

Present Address

[†]B.C.: Department of Chemistry, The Pennsylvania State University, University Park, Pennsylvania 16801, United States.

Notes

The authors declare no competing financial interest.

Biographies

Thijs Stuyver (1992) received his Ph.D. degree under the supervision of Prof. Paul Geerlings, Prof. Frank De Proft, and Dr. Stijn Fias at the Vrije Universiteit Brussel in 2018. He visited Roald Hoffmann's group at Cornell University in 2016. As an FWO postdoctoral fellow, he is currently working with Prof. Sason Shaik at the Hebrew University of Jerusalem. His research interests involve single-molecule electronics, diradical chemistry, and valence bond theory.

Bo Chen obtained his B.S. at the University of Science and Technology Beijing in 2006, and his Ph.D. at the Shanghai Institute of Organic Chemistry in 2011, under the direction of Profs. Yun-Dong Wu and Yu-Xue Li. After postdoctoral appointments at the University of North Texas (2012–2014), working with Prof. Weston Thatcher Borden, and at Cornell University (2014–2018), working with Prof. Roald Hoffmann, he joined the Pennsylvania State University as an assistant research professor in Chemistry. His recent research focus includes nanowire formation mechanism, effect of pressure on organic reactions in fluid and solid-state phases, reactivity of diradicals, and computational negative ion photoelectron spectroscopy.

Tao Zeng received his MSc degree under the supervision of Prof. Haijun Jiao at the Institute of Coal Chemistry, Chinese Academy of Sciences in 2005, and his PhD degree under the supervision of Prof. Mariusz Klobukowski at the University of Alberta in 2011. He then did his NSERC and MRI-Ontario postdoctoral research with Prof. Pierre-Nicholas Roy at the University of Waterloo (2011–2013), and held a Banting Postdoctoral Fellowship with Prof. Nandini Ananth and Prof. Roald Hoffmann at Cornell University (2013–2015). He joined Carleton University as an assistant professor in 2015 and moved to York University in 2019. His research interest is in theoretical studies of organic optoelectronic processes, vibronic coupling, Jahn–Teller and pseudo-Jahn–Teller effects, relativistic effects in chemistry, and microscopic superfluidity.

Paul Geerlings (1949) is Emeritus Professor at the Vrije Universiteit Brussel where he also obtained his PhD and Habilitation. His past and present research has concentrated on conceptual and computational density functional theory with applications in organic, inorganic, bio- and materials chemistry, with a particular focus on reactivity, also of radicals. He is the author or coauthor of more than 480 publications in international journals or book chapters. Besides research, he has always had a deep interest in chemical education, having taught the Freshman General Chemistry course for 25 consecutive years.

Frank De Proft (1969) obtained his PhD in Sciences from the Vrije Universiteit Brussel (VUB) in 1995. From 1995 to 1999, he was a postdoctoral researcher at the Research Foundation Flanders (FWO), during which he was a postdoctoral fellow in the group of Professor R. G. Parr at the University of North Carolina in Chapel Hill, USA. He is the author or coauthor of more than 350 research publications, mainly involving the use chemical concepts from quantum mechanics, with special attention to the concepts introduced within the framework of the so-called “Conceptual Density Functional Theory”. His present work involves the development and/or interpretative use of these concepts to study the properties and reactivity of organic, inorganic, biochemical and solid state compounds, catalysis and the in silico design of new compounds with optimal chemical properties and reactivity.

Roald Hoffmann's attention was captured by spectroscopic studies on methylene in the period just before the 1964–1965 collaboration with Woodward; Roald's notebooks of the period have much on methylene

and cyclopropane. It was natural then to think about breaking a CC bond in the latter molecule to give trimethylene, or how to tune the spin states of carbenes. His work on the interaction of lone pairs in pyrazine led him naturally to the interaction of orbitals through bonds in *p*-benzynes. Thus, diradicals became a leitmotif for Roald over 50 years ago.

ACKNOWLEDGMENTS

We are grateful to Weston Borden, Marc Garner, Martin Head-Gordon, Hilka Kenttämä, and especially Jean-Paul Malrieu for their comments on this work. T.S. acknowledges the Research Foundation-Flanders (FWO) for a position as postdoctoral research fellow (grant 1203419N). F.D.P. and P.G. acknowledge the Vrije Universiteit Brussel (VUB) and the Research Foundation Flanders (FWO) for continuous support to the ALGC research group. Among others, the Strategic Research Program funding of the VUB is thanked for financial support. F.D.P. also acknowledges the Francqui foundation for a position as “Francqui research professor”. T.Z. acknowledges funding from Carleton University (186853), York University (481333), and the Natural Sciences and Engineering Research Council (NSERC) of Canada (RGPIN-2016-06276).

DEDICATION

This paper is dedicated to Lionel Salem. In his work, Lionel consistently combined three attributes: formalistic brilliance; an interest in real chemistry, keeping the experimentalist always in mind; and, *very, very important*, great pedagogical skills. His work remains alive and important because of its rare combination of these qualities.

ABBREVIATIONS USED

A	asymmetric
AF	tetramethylenediamine
AO	atomic orbitals
CAS	complete active space
CASSCF	complete active space self-consistent field
CASPT2	complete active space perturbation theory to the second order
CBD	cyclobutadiene
CCSD	coupled cluster with inclusion of singles and doubles
cc-pVTZ	Dunning’s correlation consistent basis set with triple- ζ
CI	configuration interaction
Cov	covalent
DMRG	density matrix renormalization group
EPR	electron paramagnetic resonance
ESR	electron spin resonance
FT	finite temperature
GVB	generalized valence bond
HG	Head–Gordon
HOMO	highest occupied molecular orbital
HONO	highest occupied natural orbital
H_x	one-electron energy
Ion	ionic
J_{xy}	Coulomb integral
K_{xy}	exchange integral
LP	Luzanov and Prezbdó
LUMO	lowest occupied molecular orbital
LUNO	lowest unoccupied natural orbital
LZ	Luzanov and Zhikol

MO	molecular orbital
MQDM	<i>meta</i> -quinodimethane
MSR	multistate reactivity
N_D	number of effectively unpaired electrons
OS	open-shell
PES	potential energy surface
PQDM	<i>para</i> -quinodimethane
RDM-CASSCF	reduced-density-matrix-driven complete active space self-consistent field
RHF	restricted Hartree–Fock
RMSD	root-mean-square deviation
ROHF	restricted, open-shell, Hartree–Fock
S	symmetric
SCF	self-consistent field
SOMO	singly occupied molecular orbital
TC	two-configuration
TCSCF	two-configuration self-consistent field
TMM	trimethylenemethane
TS	transition state
(U)B3LYP	(unrestricted) Becke, three-parameter, Lee–Yang–Parr
UDFT	unrestricted density functional theory
UHF	unrestricted Hartree–Fock
VB	valence bond
ZPE	zero-point energy
ΔE_{ST}	energy difference between the lowest singlet and triplet state

REFERENCES

- (1) Nonhebel, D. C.; Walton, J. C. *Free-Radical Chemistry: Structure and Mechanism*; CUP Archive: Cambridge, UK, 1974.
- (2) Longuet-Higgins, H. C. Some studies in molecular orbital theory I. Resonance structures and molecular orbitals in unsaturated hydrocarbons. *J. Chem. Phys.* **1950**, *18*, 265–274.
- (3) Borden, W. T.; Davidson, E. R. Effects of electron repulsion in conjugated hydrocarbon diradicals. *J. Am. Chem. Soc.* **1977**, *99*, 4587–4594.
- (4) Salem, L.; Rowland, C. The electronic properties of diradicals. *Angew. Chem., Int. Ed. Engl.* **1972**, *11*, 92–111.
- (5) Fukui, K.; Kazuyoshi, T. A theoretical study on biradicals I. Theoretical characteristics of biradicals. In: *Frontier Orbitals and Reaction Paths: Selected Papers of Kenichi Fukui*; World Scientific, 1997, 333–340.
- (6) Hachmann, J.; Dorando, J. J.; Avilés, M.; Chan, G. K.-L. The radical character of the acenes: a density matrix renormalization group study. *J. Chem. Phys.* **2007**, *127*, 134309.
- (7) Sun, Z.; Wu, J. Open-shell polycyclic aromatic hydrocarbons. *J. Mater. Chem.* **2012**, *22*, 4151–4160.
- (8) Nagai, H.; Nakano, M.; Yoneda, K.; Kishi, R.; Takahashi, H.; Shimizu, A.; Kubo, T.; Kamada, K.; Ohta, K.; Botek, E.; Champagne, B. Signature of multiradical character in second hyperpolarizabilities of rectangular graphene nanoflakes. *Chem. Phys. Lett.* **2010**, *489*, 212–218.
- (9) Shimizu, A.; Hirao, Y.; Kubo, T.; Nakano, M.; Botek, E.; Champagne, B. Theoretical consideration of singlet open-shell character of polyperiacenes using Clar’s aromatic sextet valence bond model and quantum chemical calculations. *AIP Conf. Proc.* **2009**, *1504*, 399–405.
- (10) Pelzer, K.; Greenman, L.; Gidofalvi, G.; Mazziotti, D. A. Strong correlation in acene sheets from the active-space variational two-electron reduced density matrix method: effects of symmetry and size. *J. Phys. Chem. A* **2011**, *115*, S632–S640.
- (11) Yang, Y.; Davidson, E. R.; Yang, W. Nature of ground and electronic excited states of higher acenes. *Proc. Natl. Acad. Sci. U. S. A.* **2016**, *113*, E5098–E5107.

- (12) Hajgato, B.; Huzak, M.; Deleuze, M. S. Focal point analysis of the singlet–triplet energy gap of octacene and larger acenes. *J. Phys. Chem. A* **2011**, *115*, 9282–9293.
- (13) Hajgato, B.; Szieberth, D.; Geerlings, P.; De Proft, F.; Deleuze, M. S. A benchmark theoretical study of the electronic ground state and of the singlet–triplet split of benzene and linear acenes. *J. Chem. Phys.* **2009**, *131*, 224321.
- (14) Biermann, D.; Schmidt, W. Diels–Alder reactivity of polycyclic aromatic hydrocarbons. 1. Acenes and benzologs. *J. Am. Chem. Soc.* **1980**, *102*, 3163–3173.
- (15) Jiménez-Hoyos, C. A.; Rodriguez-Guzman, R.; Scuseria, G. E. Polyradical character and spin frustration in fullerene molecules: an ab initio non-collinear Hartree–Fock study. *J. Phys. Chem. A* **2014**, *118*, 9925–9940.
- (16) Sheka, E. F. Odd electrons and covalent bonding in fullerenes. *Int. J. Quantum Chem.* **2004**, *100*, 375–387.
- (17) Sheka, E. F.; Chernozatonskii, L. A. Broken spin symmetry approach to chemical reactivity and magnetism of graphenium species. *J. Exp. Theor. Phys.* **2010**, *110*, 121–132.
- (18) Hirsch, A. *Fullerenes and Related Structures*; Springer: Berlin, 1999.
- (19) Muhammad, S.; Fukuda, K.; Minami, T.; Kishi, R.; Shigeta, Y.; Nakano, M. Interplay between the diradical character and third-order nonlinear optical properties in fullerene systems. *Chem. - Eur. J.* **2013**, *19*, 1677–1685.
- (20) Borden, W. T. In *Diradicals*; Ed., Borden, W. T., Wiley: New York, 1982, pp. 1–72.
- (21) Lineberger, W. C.; Thatcher Borden, W. The synergy between qualitative theory, quantitative calculations, and direct experiments in understanding, calculating, and measuring the energy differences between the lowest singlet and triplet states of organic diradicals. *Phys. Chem. Chem. Phys.* **2011**, *13*, 11792–11813.
- (22) Bally, T.; Borden, W. T. *Reviews in Computational Chemistry*; Wiley: New York, 2007; Vol. 13, pp 1–97.
- (23) Michl, J.; Bonacic-Koutecky, V. *Electronic Aspects of Organic Photochemistry*; Wiley: New York, 1990.
- (24) Abe, M. Diradicals. *Chem. Rev.* **2013**, *113*, 7011–7088.
- (25) Gryn'ova, G.; Coote, M. L.; Corminboeuf, C. Theory and practice of uncommon molecular electronic configurations. *WIREs: Comput. Mol. Sci.* **2015**, *5*, 440–459.
- (26) Roothaan, C. C. J. New developments in molecular orbital theory. *Rev. Mod. Phys.* **1951**, *23*, 69–89.
- (27) Kollmar, H.; Staemmler, V. Violation of Hund's rule by spin polarization in molecules. *Theor. Chim. Acta* **1978**, *48*, 223–239.
- (28) Karafiloglou, P.; Malrieu, J. P. Origin of the conical intersection between the singlet ionic excited surfaces of twisted ethylene. *Theor. Chim. Acta* **1985**, *67*, 275–286.
- (29) Malrieu, J. P.; Caballol, R.; Calzado, C. J.; de Graaf, C.; Guihéry, N. Magnetic interactions in molecules and highly correlated materials: physical content, analytical derivation, and rigorous extraction of magnetic Hamiltonians. *Chem. Rev.* **2014**, *114*, 429–492.
- (30) Borden, W. T.; Davidson, E. R.; Hart, P. The potential surfaces for the lowest singlet and triplet states of cyclobutadiene. *J. Am. Chem. Soc.* **1978**, *100*, 388–392.
- (31) Salem, L. *The Molecular Orbital Theory of Conjugated Systems*; Benjamin: New York, 1966; pp 72–74.
- (32) Salem, L. *Electrons in Chemical Reactions*; Wiley: New York, 1982; pp 13, 21, 192–195.
- (33) Salem, L. The sudden polarization effect and its possible role in vision. *Acc. Chem. Res.* **1979**, *12*, 87–92.
- (34) Karafiloglou, P. The double (or dynamic) spin polarization in π diradicals. *J. Chem. Educ.* **1989**, *66*, 816–818.
- (35) Note that, in order to avoid confusion, we opt to refer consequently to degenerate frontier orbitals (often nonbonding) as ψ_x and ψ_y , whereas ψ_H and ψ_L are used for the frontier orbitals whenever such a degeneracy is not present.
- (36) Here, t stands for the transfer integral between the localized orbitals (or magnetic orbitals) that overlap to form HOMO and LUMO, and U is the difference of Coulombic interactions of two electrons occupying the same magnetic orbitals vs occupying different orbitals.
- (37) Smith, M. B.; Michl, J. Singlet fission. *Chem. Rev.* **2010**, *110*, 6891–6936.
- (38) Smith, M. B.; Michl, J. Recent advances in singlet fission. *Annu. Rev. Phys. Chem.* **2013**, *64*, 361–386.
- (39) Paci, I.; Johnson, J. C.; Chen, X. D.; Rana, G.; Popovic, D.; David, D. E.; Nozik, A. J.; Ratner, M. A.; Michl, J. Singlet fission for dye-sensitized solar cells: can a suitable sensitizer be found? *J. Am. Chem. Soc.* **2006**, *128*, 16546–16553.
- (40) Minami, T.; Nakano, M. Diradical character view of singlet fission. *J. Phys. Chem. Lett.* **2012**, *3*, 145–150.
- (41) Ito, S.; Nagami, T.; Nakano, M. Molecular design for efficient singlet fission. *J. Photochem. Photobiol., C* **2018**, *34*, 85–120.
- (42) Zeng, T.; Hoffmann, R.; Ananth, N. The low-lying electronic states of pentacene and their roles in singlet fission. *J. Am. Chem. Soc.* **2014**, *136*, 5755–5764.
- (43) Zeng, T.; Ananth, N.; Hoffmann, R. Seeking small molecules for singlet fission: a heteroatom substitution strategy. *J. Am. Chem. Soc.* **2014**, *136*, 12638–12647.
- (44) Zeng, T.; Goel, P. Design of small intramolecular singlet fission chromophores: an azaborine candidate and general small size effects. *J. Phys. Chem. Lett.* **2016**, *7*, 1351–1358.
- (45) Zeng, T. Through-linker intramolecular singlet fission: general mechanism and designing small chromophores. *J. Phys. Chem. Lett.* **2016**, *7*, 4405–4412.
- (46) Zeng, T.; Mellerup, S. K.; Yang, D.; Wang, X.; Wang, S.; Stampelcoskie, K. Identifying (BN)₂-pyrenes as a new class of singlet fission chromophores: significance of azaborine substitution. *J. Phys. Chem. Lett.* **2018**, *9*, 2919–2927.
- (47) Japahuge, A.; Zeng, T. Theoretical studies of singlet fission: searching for materials and exploring mechanisms. *ChemPlusChem* **2018**, *83*, 146–182.
- (48) Casanova, D. Theoretical modeling of singlet fission. *Chem. Rev.* **2018**, *118*, 7164–7207.
- (49) Messelberger, J.; Grünwald, A.; Pinter, P.; Hansmann, M. M.; Munz, D. Carbene derived diradicaloids—building blocks for singlet fission? *Chem. Sci.* **2018**, *9*, 6107–6117.
- (50) Japahuge, A.; Lee, S.; Choi, C. H.; Zeng, T. Design of singlet fission chromophores with cyclic (alkyl)(amino) carbene building blocks. *J. Chem. Phys.* **2019**, *150*, 234306.
- (51) Herrmann, C.; Elmisz, J. Electronic communication through molecular bridges. *Chem. Commun.* **2013**, *49*, 10456–10458.
- (52) Proppe, J.; Herrmann, C. Communication through molecular bridges: different bridge orbital trends result in common property trends. *J. Comput. Chem.* **2015**, *36*, 201–209.
- (53) Stuyver, T.; Fias, S.; De Proft, F.; Geerlings, P.; Tsuji, Y.; Hoffmann, R. Enhancing the conductivity of molecular electronic devices. *J. Chem. Phys.* **2017**, *146*, 092310.
- (54) Stuyver, T.; Zeng, T.; Tsuji, Y.; Fias, S.; Geerlings, P.; De Proft, F. Captodative substitution: a strategy for enhancing the conductivity of molecular electronic devices. *J. Phys. Chem. C* **2018**, *122*, 3194–3200.
- (55) Stuyver, T.; Zeng, T.; Tsuji, Y.; Geerlings, P.; De Proft, F. Diradical character as a guiding principle for the insightful design of molecular nanowires with an increasing conductance with length. *Nano Lett.* **2018**, *18*, 7298–7304.
- (56) Tsuji, Y.; Hoffmann, R.; Strange, M.; Solomon, G. C. Close relation between quantum interference in molecular conductance and diradical existence. *Proc. Natl. Acad. Sci. U. S. A.* **2016**, *113*, E413–E419.
- (57) Stuyver, T.; Danovich, D.; Shaik, S. Captodative substitution enhances the diradical character of compounds, reduces aromaticity and controls single molecule conductivity patterns: a valence bond study. *J. Phys. Chem. A* **2019**, *123*, 7133.
- (58) Garner, M. H.; Bro-Jørgensen, W.; Pedersen, P. D.; Solomon, G. C. Reverse bond-length alternation in cumulenes: candidates for increasing electronic transmission with length. *J. Phys. Chem. C* **2018**, *122*, 26777–26789.

- (59) Kröncke, S.; Herrmann, C. Designing long-range charge delocalization from first-principles. *J. Chem. Theory Comput.* **2019**, *15*, 165–177.
- (60) Nakano, M.; Champagne, B. Theoretical design of open-shell singlet molecular systems for nonlinear optics. *J. Phys. Chem. Lett.* **2015**, *6*, 3236–3256.
- (61) Nakano, M.; Champagne, B. Nonlinear optical properties in open-shell molecular systems. *WIREs Comput. Mol. Sci.* **2016**, *6*, 198–210.
- (62) Voigt, B. A.; Steenbock, T.; Herrmann, C. Structural diradical character. *J. Comput. Chem.* **2019**, *40*, 854–865.
- (63) Zhivonitko, V. V.; Bresien, J.; Schulz, A.; Koptuyg, I. V. Parahydrogen-induced polarization with a metal-free P–P biradicaloid. *Phys. Chem. Chem. Phys.* **2019**, *21*, 5890–5893.
- (64) Nakano, M.; Kishi, R.; Nitta, T.; Kubo, T.; Nakasuji, K.; Kamada, K.; Ohta, K.; Champagne, B.; Botek, E.; Yamaguchi, K. Second hyperpolarizability (γ) of singlet diradical system: dependence of γ on the diradical character. *J. Phys. Chem. A* **2005**, *109*, 885–891.
- (65) Nakano, M.; Kishi, R.; Ohta, S.; Takebe, A.; Takahashi, H.; Furukawa, S.-i.; Kubo, T.; Morita, Y.; Nakasuji, K.; Yamaguchi, K.; Kamada, K.; Ohta, K.; Champagne, B.; Botek, E. Origin of the enhancement of the second hyperpolarizability of singlet diradical systems with intermediate diradical character. *J. Chem. Phys.* **2006**, *125*, 074113.
- (66) Ito, S. Topics of 1,3-diphosphacyclobutane-2,4-diyl derivatives: Structural aspects and functionality of isolable heavier congeners of cyclobutane-1,3-diyl and the related molecules. *Tetrahedron Lett.* **2018**, *59*, 1–13.
- (67) Schoeller, W. W. The Niecke biradicals and their congeners – the journey from stable biradicaloids to their utilization for the design of nonlinear optical properties. *Eur. J. Inorg. Chem.* **2019**, *2019*, 1495–1506.
- (68) Gleiter, R.; Hoffmann, R. Stabilizing a singlet methylene. *J. Am. Chem. Soc.* **1968**, *90*, 5457–5460.
- (69) Hoffmann, R.; Zeiss, G. D.; Van Dine, G. W. The electronic structure of methylenes. *J. Am. Chem. Soc.* **1968**, *90*, 1485–1499.
- (70) Note that there is some disagreement in the literature and in discussion among experts on what “disjoint” actually means.
- (71) Trinquier, G.; Malrieu, J. P. Kekulé versus Lewis: when aromaticity prevents electron pairing and imposes polyradical character. *Chem. - Eur. J.* **2015**, *21*, 814–828.
- (72) Murrell, J. N.; Teixeira-Dias, J. J. C. The dependence of exchange energy on orbital overlap. *Mol. Phys.* **1970**, *19*, 521–531.
- (73) Söderhjelm, P.; Karlström, G.; Ryde, U. Comparison of overlap-based models for approximating the exchange-repulsion energy. *J. Chem. Phys.* **2006**, *124*, 244101.
- (74) Ovchinnikov, A. A. Multiplicity of the ground state of large alternant hydrocarbons with conjugated bonds. *Theor. Chim. Acta* **1978**, *47*, 297–304.
- (75) Bohr, N. The quantum postulate and the recent development of atomic theory. *Nature* **1928**, *121*, 580–590.
- (76) Bohr, N. *Atomic Theory and the Description of Nature*; Cambridge University Press: Cambridge, UK, 1934.
- (77) Bohr, N. *Essays 1958–1962 on Atomic Physics and Human Knowledge*; Wiley: New York, 1963.
- (78) Shaik, S. Is my chemical universe localized or delocalized? Is there a future for chemical concepts? *New J. Chem.* **2007**, *31*, 2015–2028.
- (79) Gu, J.; Wu, W.; Danovich, D.; Hoffmann, R.; Tsuji, Y.; Shaik, S. Valence bond theory reveals hidden delocalized diradical character of polyenes. *J. Am. Chem. Soc.* **2017**, *139*, 9302–9316.
- (80) Foster, J. M.; Boys, S. F. Canonical configurational interaction procedure. *Rev. Mod. Phys.* **1960**, *32*, 300.
- (81) Edmiston, C.; Ruedenberg, K. Localized atomic and molecular orbitals. *Rev. Mod. Phys.* **1963**, *35*, 457–464.
- (82) Figeys, H. P.; Geerlings, P.; Raeymaekers, P.; Van Lommen, G.; Defay, N. An INDO-LMO and ^{13}C NMR spectroscopic study of the CH bonds in tetracyclo [3.2.0.0^{2,7}.0^{4,6}] heptane (quadracyclane) and tricyclo [3.1.0.0^{2,4}] hexane. *Tetrahedron* **1975**, *31*, 1731.
- (83) Davies, D. I.; Parrott, M. J. *Free Radicals in Organic Synthesis*; Springer: Berlin, Heidelberg, 2012.
- (84) Tedder, J. M. Which factors determine the reactivity and regioselectivity of free radical substitution and addition reactions? *Angew. Chem., Int. Ed. Engl.* **1982**, *21*, 401–410.
- (85) Sosa, C.; Schlegel, H. B. Ab initio calculations on the barrier height for the hydrogen addition to ethylene and formaldehyde. The importance of spin projection. *Int. J. Quantum Chem.* **1986**, *29*, 1001–1015.
- (86) Lee, J. H.; Michael, J. V.; Payne, W. A.; Stief, L. J. Absolute rate of the reaction of atomic hydrogen with ethylene from 198 to 320 K at high pressure. *J. Chem. Phys.* **1978**, *68*, 1817–1820.
- (87) Kistiakowsky, G. B.; Roberts, E. K. Rate of association of methyl radicals. *J. Chem. Phys.* **1953**, *21*, 1637–1643.
- (88) Kerr, J. A.; Parsonage, M. J. *Evaluated Kinetic Data on Gas Addition Reactions: Reaction of Atoms and Radicals with Alkenes, Alkynes and Aromatic Compounds*; Butterworths: London, 1972.
- (89) Kerr, J. A. *Free Radicals*; Wiley: New York, 1972.
- (90) Landers, L. C.; Volman, D. H. The free radical initiated polymerization of gaseous unsaturated hydrocarbons. *J. Am. Chem. Soc.* **1957**, *79*, 2996–2999.
- (91) Brinton, R. K. Reaction of methyl radicals with ethylene. *J. Chem. Phys.* **1958**, *29*, 781–786.
- (92) Gonzalez, C.; Sosa, C.; Schlegel, H. B. Ab initio study of the addition reaction of the methyl radical to ethylene and formaldehyde. *J. Phys. Chem.* **1989**, *93*, 2435–2440.
- (93) Hoyland, J. R. MINDO/2 calculations on the reaction of methyl radicals with ethylene and butadiene. *Theor. Chim. Acta* **1971**, *22*, 229–233.
- (94) Blanksby, S. J.; Ellison, G. B. Bond dissociation energies of organic molecules. *Acc. Chem. Res.* **2003**, *36*, 255–263.
- (95) Arthur, N. L.; Bell, T. N. An evaluation of the kinetic data for hydrogen abstraction from silanes in the gas phase. *Rev. Chem. Intermed.* **1978**, *2*, 37–74.
- (96) Morris, E. R.; Thynne, J. C. Hydrogen atom abstraction from silane, trimethylsilane, and tetramethylsilane by methyl radicals. *J. Phys. Chem.* **1969**, *73*, 3294–3298.
- (97) Strausz, O. P.; Jakubowski, E.; Sandhu, H. S.; Gunning, H. E. Arrhenius parameters for the abstraction reactions of methyl radicals with silanes. *J. Chem. Phys.* **1969**, *51*, 552–560.
- (98) Rüchardt, C. Steric effects in free radical chemistry. *Top. Curr. Chem.* **1980**, *88*, 1–32.
- (99) Tedder, J. M.; Walton, J. C. The importance of polarity and steric effects in determining the rate and orientation of free radical addition to olefins: rules for determining the rate and preferred orientation. *Tetrahedron* **1980**, *36*, 701–707.
- (100) Griller, D.; Ingold, K. U. Persistent carbon-centered radicals. *Acc. Chem. Res.* **1976**, *9*, 13–19.
- (101) Tsang, W. The stability of alkyl radicals. *J. Am. Chem. Soc.* **1985**, *107*, 2872–2880.
- (102) Sabacky, M. J.; Johnson, C. S., Jr.; Smith, R. G.; Gutowsky, H. S.; Martin, J. C. Triarylmethyl radicals. Synthesis and electron spin resonance studies of sesquioxanthryl dimer and related compounds. *J. Am. Chem. Soc.* **1967**, *89*, 2054–2058.
- (103) Baldock, R. W.; Hudson, P.; Katritzky, A. R.; Soti, F. Stable free radicals. Part I. A new principle governing the stability of organic free radicals. *J. Chem. Soc., Perkin Trans. 1* **1974**, *0*, 1422–1427.
- (104) Viehe, H. G.; Janousek, Z.; Merenyi, R.; Stella, L. The captodative effect. *Acc. Chem. Res.* **1985**, *18*, 148–154.
- (105) Alfassi, Z. B. *S-Centered Radicals*; Wiley: New York, 1999.
- (106) Preston, K. F.; Sutcliffe, L. H. Electron spin resonance spectroscopy of free radicals containing sulphur linked to nitrogen. *Magn. Reson. Chem.* **1990**, *28*, 189–204.
- (107) Glass, R. S. Sulfur radiated cations. *Top. Curr. Chem.* **1999**, *205*, 1–87.
- (108) Cordes, A. W.; Haddon, R. C.; Oakley, R. T. In *Chemistry of Inorganic Ring Systems*; Elsevier: Amsterdam, 1992.
- (109) Forrester, A. R.; Hay, J. M.; Thomson, R. H. *Organic Chemistry of Stable Free Radicals*; Academic Press: London, 1968.

- (110) Hicks, R. G. *Stable Radicals*; Wiley: Chichester, UK, 2010.
- (111) Xu, P.; Hoffmann, R. The dimerization of H₂NO. *J. Phys. Chem. A* **2016**, *120*, 1283–1296.
- (112) Power, P. P. Persistent and stable radicals of the heavier main group elements and related species. *Chem. Rev.* **2003**, *103*, 789–810.
- (113) Conner, K. M.; Arostegui, A. C.; Swanson, D. D.; Brown, S. N. When do strongly coupled diradicals show strongly coupled reactivity? Thermodynamic and kinetics of hydrogen atom transfer reactions of palladium and platinum bis (iminosemiquinone) complexes. *Inorg. Chem.* **2018**, *57*, 9696–9707.
- (114) Singlet butane-1,4-diyl ($\bullet\text{CH}_2\text{CH}_2\text{CH}_2\text{CH}_2\bullet$), refs 81–83 (Dewar 1974, Huisgen 1977, Sirjean 2006).
- (115) Hoffmann, R.; Imamura, A.; Hehre, W. J. Benzynes, dehydroconjugated molecules, and the interaction of orbitals separated by a number of intervening sigma bonds. *J. Am. Chem. Soc.* **1968**, *90*, 1499–1509.
- (116) Hoffmann, R. Interaction of orbitals through space and through bonds. *Acc. Chem. Res.* **1971**, *4*, 1–9.
- (117) Hoffmann, R.; Swaminathan, S.; Odell, B. G.; Gleiter, R. Potential surface for a nonconcerted reaction. Tetramethylene. *J. Am. Chem. Soc.* **1970**, *92*, 7091–7097.
- (118) Dewar, M. J. S.; Kirschner, S. Dimerization of ethylene to cyclobutane. *J. Am. Chem. Soc.* **1974**, *96*, 5246–5247.
- (119) Huisgen, R. Can tetramethylene intermediates be intercepted? *Acc. Chem. Res.* **1977**, *10*, 199–206.
- (120) Sirjean, B.; Glaude, P. A.; Ruiz-Lopez, M. F.; Fournet, R. Detailed kinetic study of the ring opening of cycloalkanes by CBS-QB3 calculations. *J. Phys. Chem. A* **2006**, *110*, 12693–12704.
- (121) Hoffmann, R. Trimethylene and the addition of methylene to ethylene. *J. Am. Chem. Soc.* **1968**, *90*, 1475–1485.
- (122) Carpenter, B. K. Dynamic behavior of organic reactive intermediates. *Angew. Chem., Int. Ed.* **1998**, *37*, 3340–3350.
- (123) Furlani, T. R.; King, H. F. Theory of spin-orbit coupling. Application to singlet–triplet interaction in the trimethylene biradical. *J. Chem. Phys.* **1985**, *82*, 5577–5583.
- (124) Horsley, J. A.; Jean, Y.; Moser, C.; Salem, L.; Stevens, R. M.; Wright, J. S. Organic transition state. *J. Am. Chem. Soc.* **1972**, *94*, 279–282.
- (125) Goldberg, A. H.; Dougherty, D. A. Effects of through-bond and through-space interactions on singlet–triplet energy gaps in localized biradicals. *J. Am. Chem. Soc.* **1983**, *105*, 284–290.
- (126) Skancke, A.; Hrovat, D. A.; Borden, W. T. Ab initio calculations of the effects of geminal silyl substituents on the stereomutation of cyclopropane and on the singlet–triplet splitting in trimethylene. *J. Am. Chem. Soc.* **1998**, *120*, 7079–7084.
- (127) Wu, J. I.-C.; von Ragué Schleyer, P. Hyperconjugation in hydrocarbons: not just a “mild sort of conjugation”. *Pure Appl. Chem.* **2013**, *85* (5), 921–940.
- (128) Kaldor, U.; Shavitt, I. LCAO-SCF computations for ethylene. *J. Chem. Phys.* **1968**, *48*, 191–203.
- (129) Pittner, J.; Nachtigall, P.; Carsky, P.; Masik, J.; Hubac, I. Assessment of the single-root multireference Brillouin–Wigner coupled-cluster method: test calculations on CH₂, SiH₂, and twisted ethylene. *J. Chem. Phys.* **1999**, *110*, 10275–10282.
- (130) Balkova, A.; Bartlett, R. J. A multireference coupled-cluster study of the ground state and lowest excited states of cyclobutadiene. *J. Chem. Phys.* **1994**, *101*, 8972–8987.
- (131) Eckert-Maksić, M.; Vazdar, M.; Barbatti, M.; Lischka, H.; Maksić, Z. B. Automerization reaction of cyclobutadiene and its barrier height: an ab initio benchmark multireference average-quadratic coupled cluster study. *J. Chem. Phys.* **2006**, *125*, 064310.
- (132) Calculation performed at CASPT2(4,4)/cc-pVTZ.
- (133) Kostenko, A.; Tumanski, B.; Kobayashi, Y.; Nakamoto, M.; Sekiguchi, A.; Apeloig, Y. Spectroscopic observation of the triplet diradical state of a cyclobutadiene. *Angew. Chem., Int. Ed.* **2017**, *56*, 10183–10187.
- (134) Lee, E. P.; Wright, T. G. A study of the lowest-lying triplet and singlet states of the cyclopentadienyl cation (c-C₅H₅⁺). *Phys. Chem. Chem. Phys.* **1999**, *1*, 219–225.
- (135) Shiota, Y.; Kondo, M.; Yoshizawa, K. Role of molecular distortions in the spin–orbit coupling between the singlet and triplet states of the 4π electron systems C₄H₄, C₅H₅⁺, and C₃H₃[–]. *J. Chem. Phys.* **2001**, *115*, 9243–9254.
- (136) Kayi, H.; Garcia-Fernandez, P.; Bersuker, I. B.; Boggs, J. E. Deviations from Born–Oppenheimer theory in structural chemistry: Jahn–Teller, pseudo Jahn–Teller, and hidden pseudo Jahn–Teller effects in C₃H₃ and C₃H₃[–]. *J. Phys. Chem. A* **2013**, *117*, 8671–8679.
- (137) Slipchenko, L. V.; Krylov, A. I. Electronic structure of the trimethylenemethane diradical in its ground and electronically excited states: bonding, equilibrium geometries, and vibrational frequencies. *J. Chem. Phys.* **2003**, *118*, 6874–6883.
- (138) Lewis, S. B.; Hrovat, D. A.; Getty, S. J.; Thatcher Borden, W. Ab initio calculations of the potential surfaces for rearrangement of methylenecyclopropane and 2,2-difluoromethylenecyclopropane. Why do the geminal fluorines have little effect on lowering the activation energy? *J. Chem. Soc., Perkin Trans. 2* **1999**, *11*, 2339–2347.
- (139) Davidson, E. R.; Borden, W. T. Some aspects of the potential surface for singlet trimethylenemethane. *J. Am. Chem. Soc.* **1977**, *99*, 2053–2060.
- (140) Dowd, P. Trimethylenemethane. *J. Am. Chem. Soc.* **1966**, *88*, 2587–2589.
- (141) Dowd, P.; Sachdev, K. Trimethylenemethane from photolysis of 3-methylenecyclobutanone. *J. Am. Chem. Soc.* **1967**, *89*, 715–716.
- (142) Dowd, P.; Gold, A.; Sachdev, K. Trimethylenemethane. Proton hyperfine splitting. *J. Am. Chem. Soc.* **1968**, *90*, 2715.
- (143) Baseman, R. J.; Pratt, D. W.; Chow, M.; Dowd, P. Trimethylenemethane. Experimental demonstration that the triplet state is the ground state. *J. Am. Chem. Soc.* **1976**, *98*, 5726–5727.
- (144) Maier, G.; Reisenauer, H. P.; Lanz, K.; Tross, R.; Jürgen, D.; Hess, B. A., Jr; Schaad, L. J. Detection of trimethylenemethane by IR spectroscopy: the result of an unexpected photoisomerization of methylenecyclopropane in a halogen-doped Xe matrix. *Angew. Chem., Int. Ed. Engl.* **1993**, *32*, 74–76.
- (145) Wenthold, P. G.; Hu, J.; Squires, R. R.; Lineberger, W. C. Photoelectron spectroscopy of the trimethylene–methane negative ion. The singlet–triplet splitting of trimethylenemethane. *J. Am. Chem. Soc.* **1996**, *118*, 475–476.
- (146) Hood, D. M.; Schaefer, H. F., III; Pitzer, R. M. Planar ³A₂[–]–orthogonal ¹B₁ energy separation for trimethylenemethane. *J. Am. Chem. Soc.* **1978**, *100*, 8009–8010.
- (147) Auster, S. B.; Pitzer, R. M.; Platz, M. S. Excitation energies in trimethylenemethane derivatives. *J. Am. Chem. Soc.* **1982**, *104*, 3812–3815.
- (148) Yarkony, D. R.; Schaefer, H. F., III Triplet electronic ground state of trimethylenemethane. *J. Am. Chem. Soc.* **1974**, *96*, 3754–3758.
- (149) Davis, J. H.; Goddard, W. A., III Electronic states of trimethylenemethane. *J. Am. Chem. Soc.* **1977**, *99*, 4242–4247.
- (150) Ma, B.; Schaefer, H. F., III Singlet–triplet energy separation and barrier for ring closure for trimethylenemethane and its complexes. *Chem. Phys.* **1996**, *207*, 31–41.
- (151) Bersuker, I. *The Jahn–Teller Effect*; Cambridge University Press: Cambridge, UK, 2006.
- (152) McConnell, H. M. Spin density matrices for paramagnetic molecules. *J. Chem. Phys.* **1958**, *28*, 1188–1192.
- (153) Pople, J. A.; Gill, P. M. W.; Handy, N. C. Spin-unrestricted character of Kohn–Sham orbitals for open-shell systems. *Int. J. Quantum Chem.* **1995**, *56*, 303–305.
- (154) Geerlings, P.; Langenaeker, W.; De Proft, F. Conceptual density functional theory. *Chem. Rev.* **2003**, *103*, 1793–1873.
- (155) De Proft, F.; Chamorro, E.; Perez, P.; Duque, M.; De Vleeschouwer, F.; Geerlings, P. Spin polarized reactivity indices from density functional theory: theory and applications. In *Chemical Modelling: Applications and Theory*; Springborg, M., Ed.; Specialist Periodical Report RSC; Royal Society of Chemistry, 2009; Vol. 6, pp 63–111.
- (156) Jaque, P.; Toro-Labbé, A.; Geerlings, P.; De Proft, F. Theoretical study of the regioselectivity of [2 + 2] photocycloaddition reactions of acrolein with olefins. *J. Phys. Chem. A* **2009**, *113*, 332–344.

- (157) Perez, P.; Chamorro, E.; Ayers, P. W. Universal mathematical identities in Density Functional Theory: results from three different spin-resolved representations. *J. Chem. Phys.* **2008**, *128*, 204108.
- (158) Limanto, J.; Tallarico, J. A.; Porter, J. R.; Khuong, K. S.; Houk, K. N.; Snapper, M. L. Intramolecular cycloadditions of cyclobutadiene with olefins. *J. Am. Chem. Soc.* **2002**, *124*, 14748–14758.
- (159) Limanto, J.; Khuong, K. S.; Houk, K. N.; Snapper, M. L. Intramolecular cycloadditions of cyclobutadiene with dienes: experimental and computational studies of the competing (2+2) and (4+2) modes of reaction. *J. Am. Chem. Soc.* **2003**, *125*, 16310–16321.
- (160) Li, Y.; Houk, K. N. The dimerization of cyclobutadiene. An ab initio CASSCF theoretical study. *J. Am. Chem. Soc.* **1996**, *118*, 880–885.
- (161) Di Valentin, C.; Freccero, M.; Gandolfi, R.; Rastelli, A. Concerted vs stepwise mechanism in 1, 3-dipolar cycloaddition of nitron to ethene, cyclobutadiene, and benzocyclobutadiene. A computational study. *J. Org. Chem.* **2000**, *65*, 6112–6120.
- (162) Nouri, D. H.; Tantillo, D. J. They came from the deep: syntheses, applications, and biology of ladderanes. *Curr. Org. Chem.* **2006**, *10*, 2055–2074.
- (163) Mehta, G.; Viswanath, M. B.; Sastry, G. N.; Jemmis, E. D.; Reddy, D. S. K.; Kunwar, A. C. Quest for higher ladderanes: oligomerization of a cyclobutadiene derivative. *Angew. Chem., Int. Ed. Engl.* **1992**, *31*, 1488–1490.
- (164) Little, R. D. Diyl trapping and electroreductive cyclization reactions. *Chem. Rev.* **1996**, *96*, 93–114.
- (165) Dowd, P. Trimethylenemethane. *Acc. Chem. Res.* **1972**, *5*, 242–248.
- (166) Nakamura, E.; Yamago, S. Thermal reactions of dipolar trimethylenemethane species. *Acc. Chem. Res.* **2002**, *35*, 867–877.
- (167) Berson, J. A. The chemistry of trimethylenemethanes, a new class of biradical reactive intermediates. *Acc. Chem. Res.* **1978**, *11*, 446–453.
- (168) Lautens, M.; Klute, W.; Tam, W. Transition metal-mediated cycloaddition reactions. *Chem. Rev.* **1996**, *96*, 49–92.
- (169) Trost, B. M. Cycloaddition approaches to five-membered rings via trimethylenemethane and its equivalents [new synthetic methods (55)]. *Angew. Chem., Int. Ed. Engl.* **1986**, *25*, 1–20.
- (170) Corwin, L. R.; McDaniel, D. M.; Bushby, R. J.; Berson, J. A. Dimerization and cycloaddition reactions of a trimethylenemethane derivative, 2-isopropylidene-cyclopenta-1, 3-diyl. Mechanistic separation of triplet and singlet reactions. *J. Am. Chem. Soc.* **1980**, *102*, 276–287.
- (171) Mazur, M. A.; Berson, J. A. Formal kinetic proof of reversible unimolecular transformation to a biradical as an obligatory first step in the mechanism of cycloaddition of 5-isopropylidenebicyclo [2.1. 0] pentane to olefins. *J. Am. Chem. Soc.* **1982**, *104*, 2217–2222.
- (172) Berson, J. A.; Corwin, L. R.; Davis, J. H. Mechanistic separation of singlet and triplet reactions of a trimethylenemethane. Stereospecificity and regioselectivity in the cycloadditions of 2-isopropylidene-cyclopentane-1, 3-diyl to olefins. *J. Am. Chem. Soc.* **1974**, *96*, 6177–6179.
- (173) Siemionko, R. K.; Berson, J. A. Regioselectivity in cycloadditions of singlet 2-methylenecyclopenta-1, 3-diyl species. *J. Am. Chem. Soc.* **1980**, *102*, 3870–3882.
- (174) Little, R. D. The intramolecular diyl trapping reaction. A useful tool for organic synthesis. *Chem. Rev.* **1986**, *86*, 875–884.
- (175) Abe, M.; Ye, J.; Mishima, M. The chemistry of localized singlet 1,3-diradicals (biradicals): from putative intermediates to persistent species and unusual molecules with a pi-single bonded character. *Chem. Soc. Rev.* **2012**, *41*, 3808–3820.
- (176) Iwatsuki, S. Polymerization of quinodimethane compounds. In *Polymerization Reactions*; Springer: Berlin, Heidelberg, 1984; pp 93–120.
- (177) Zeng, Z.; Shi, X.; Chi, C.; Lopez Navarrete, J. T.; Casado, J.; Wu, J. Pro-aromatic and anti-aromatic π -conjugated molecules: an irresistible wish to be diradicals. *Chem. Soc. Rev.* **2015**, *44*, 6578–6596.
- (178) Coulson, C. A.; Craig, D. P.; Maccoll, A.; Pullman, A. P-quinodimethane and its diradical. *Discuss. Faraday Soc.* **1947**, *2*, 36–38.
- (179) Poidevin, C.; Malrieu, J. P.; Trinquier, G.; Lepetit, C.; Allouti, F.; Alikhani, M. E.; Chauvin, R. Towards magnetic carbo-meric molecular materials. *Chem. - Eur. J.* **2016**, *22*, 5295–5308.
- (180) Vaeth, K. M.; Jensen, K. F. Selective growth of poly (p-phenylene vinylene) prepared by chemical vapor deposition. *Adv. Mater.* **1999**, *11*, 814–820.
- (181) Hrovat, D. A.; Murcko, M. A.; Lahti, P. M.; Thatcher Borden, W. The effects of heteroatom substitution on the singlet–triplet energy differences in diradicals—ab initio calculations of ΔE_{ST} in meta-benzoquinomethane and in 1, 3-naphthoquinomethane. *J. Chem. Soc., Perkin Trans. 2* **1998**, *5*, 1037.
- (182) Wang, T.; Krylov, A. I. The effect of substituents on electronic states' ordering in meta-xylylene diradicals: Qualitative insights from quantitative studies. *J. Chem. Phys.* **2005**, *123*, 104304.
- (183) Maneru, D. R.; Pal, A. K.; Moreira, P. R.; Datta, S. N.; Illas, F. The triplet-singlet gap in metaxylylene: A not so simple one. *J. Chem. Theory Comput.* **2014**, *10*, 335–345.
- (184) Wenthold, P. G.; Kim, J. B.; Lineberger, W. C. Photoelectron spectroscopy of m-xylylene anion. *J. Am. Chem. Soc.* **1997**, *119*, 1354–1359.
- (185) Shimizu, A.; Tobe, Y. Indeno[2,1-a]fluorene: An air-stable ortho-quinodimethane derivative. *Angew. Chem.* **2011**, *123*, 7038–7042.
- (186) Malrieu, J. P.; Guihéry, N.; Ferré, N. Magnetic properties of conjugated hydrocarbons from topological Hamiltonians. In *Applications of Topological Methods in Molecular Chemistry*; Springer: New York, 2016; pp 361–395.
- (187) Ruamps, R.; Suaud, N.; Guihéry, N.; Malrieu, J. P. A Strategy to determine appropriate active orbitals and accurate magnetic couplings in organic magnetic systems. *J. Chem. Theory Comput.* **2012**, *8*, 4127–4137.
- (188) Suaud, N.; Ruamps, R.; Malrieu, J. P.; Guihéry, N. Singly occupied MOs in mono- and diradical conjugated hydrocarbons: comparison between variational single-reference, π -fully correlated and Hückel descriptions. *J. Phys. Chem. A* **2014**, *118*, 5876–5884.
- (189) Zhu, X.; Tsuji, H.; Nakabayashi, K.; Ohkoshi, S.; Nakamura, E. Air- and heat-stable planar tri-p-quinodimethane with distinct biradical characteristics. *J. Am. Chem. Soc.* **2011**, *133*, 16342–16345.
- (190) Zeng, Z.; Ishida, M.; Zafra, J. L.; Zhu, X.; Sung, M. Y.; Bao, N.; Webster, R.; Lee, B. S.; Li, R.; Zeng, W.; Li, Y.; Chi, C.; Lopez Navarrete, J. T.; Ding, J.; Casado, J.; Kim, D.; Wu, J. Pushing extended p-quinodimethanes to the limit: stable tetracyano-oligo (N-annulated perylene) quinodimethanes with tunable ground states. *J. Am. Chem. Soc.* **2013**, *135*, 6363–6371.
- (191) Nomura, S.; Itoh, T.; Nakasho, H.; Uno, T.; Kubo, M.; Sada, K.; Inoue, K.; Miyata, M. Crystal structures and topochemical polymerizations of 7, 7, 8, 8-tetrakis (alkoxycarbonyl) quinodimethanes. *J. Am. Chem. Soc.* **2004**, *126*, 2035–2041.
- (192) Nakano, M.; Minami, T.; Fukui, H.; Yoneda, K.; Shigeta, Y.; Kishi, R.; Champagne, B.; Botek, E. Approximate spin-projected spin-unrestricted density functional theory method: application to the diradical character dependences of the (hyper) polarizabilities in p-quinodimethane models. *Chem. Phys. Lett.* **2010**, *501*, 140–145.
- (193) Müller, E. Neuere ergebnisse der theoretischen organischen chemie: das verhalten der organischen stoffe im elektrischen und magnetischen feld. *Naturwissenschaften* **1937**, *25*, 545–556.
- (194) Szwarc, M. The C–H Bond Energy in Toluene and Xylenes. *Nature* **1947**, *160*, 403.
- (195) Szwarc, M. The C–H bond energy in toluene and xylenes. *J. Chem. Phys.* **1948**, *16*, 128–136.
- (196) Szwarc, M. Some remarks on the CH₂=CH₂ molecule. *Discuss. Faraday Soc.* **1947**, *2*, 46–49.
- (197) Errede, L. A.; Szwarc, M. Chemistry of p-xylylene, its analogues, and polymers. *Q. Rev., Chem. Soc.* **1958**, *12*, 301–320.
- (198) Issaris, A.; Vanderzande, D.; Gelan, J. Polymerization of a p-quinodimethane derivative to a precursor of poly (p-phenylene vinylene)—Indications for a free radical mechanism. *Polymer* **1997**, *38*, 2571–2574.

- (199) Greiner, A.; Mang, S.; Schäfer, O.; Simon, P. Poly (p-xylylene)s: Synthesis, polymer analogous reactions, and perspectives on structure–property relationships. *Acta Polym.* **1997**, *48*, 1–15.
- (200) Vaeth, K. M.; Jensen, K. F. Transition metals for selective chemical vapor deposition of parylene-based polymers. *Chem. Mater.* **2000**, *12*, 1305–1313.
- (201) Senkevich, J. J.; Wiegand, C.; Yang, G.-R.; Lu, T.-M. Selective deposition of ultrathin poly(p-xylylene) films on dielectrics versus copper surfaces. *Chem. Vap. Deposition* **2004**, *10*, 247–249.
- (202) Trahanovsky, W. S.; Lorimor, S. P. Room temperature observation of p-xylylenes by ¹H NMR and evidence for diradical intermediates in their oligomerization. *J. Org. Chem.* **2006**, *71*, 1784–1794.
- (203) Trahanovsky, W. S.; Miller, D. L.; Wang, Y. Oligomerization of the thiophene-based p-quinodimethanes 2, 5-dimethylene-2, 5-dihydrothiophene and 2-ethylidene-5-methylene-2, 5-dihydrothiophene. *J. Org. Chem.* **1997**, *62*, 8980–8986.
- (204) Goodman, J. L.; Berson, J. A. Formation and intermolecular capture of m-quinodimethane. *J. Am. Chem. Soc.* **1984**, *106*, 1867–1868.
- (205) Goodman, J. L.; Berson, J. A. m-Quinodimethane, parent hydrocarbon of the m-quinonoid non-Kekule series. Low-temperature isolation and solution-phase chemical reactivity. *J. Am. Chem. Soc.* **1985**, *107*, 5409–5424.
- (206) Goodman, J. L.; Berson, J. A. Stereochemistry and mechanism of m-cyclophane formation in the 1, 4-additions of dienes to the m-quinodimethane biradical. On the question of formal 1, 2-addition via sequential 1, 4-addition and rearrangement. *J. Am. Chem. Soc.* **1985**, *107*, 5424–5428.
- (207) Borden, W. T.; Hoffmann, R.; Stuyver, T.; Chen, B. Dioxygen: what makes this triplet diradical kinetically persistent? *J. Am. Chem. Soc.* **2017**, *139*, 9010–9018.
- (208) McWeeny, R. On the nature of the oxygen double bond. *J. Mol. Struct.: THEOCHEM* **1991**, *229*, 29–38.
- (209) Su, P.; Song, L.; Wu, W.; Hiberty, P. C.; Shaik, S. A valence bond study of the dioxygen molecule. *J. Comput. Chem.* **2007**, *28*, 185–197.
- (210) Harcourt, R. D. Valence bond studies of oxygen and superoxide: a note on one-electron and two-electron transfer resonances. *J. Phys. Chem.* **1992**, *96*, 7616–7619.
- (211) Heitler, W.; Pöschl, G. Ground state of C₂ and O₂ and the theory of valency. *Nature* **1934**, *133*, 833.
- (212) Nordheim-Pöschl, G. Bahnvalenz und richtungseigenschaften in der theorie der chemischen bindung. *Ann. Phys.* **1936**, *418*, 258–280.
- (213) Wheland, G. W.; Lennard-Jones, J. E. The valence-bond treatment of the oxygen molecule. *Trans. Faraday Soc.* **1937**, *33*, 1499–1502.
- (214) We provide here some leading references: (a) Biennier, L.; Romanini, D.; Kachanov, A.; Campargue, A.; Bussery-Honvault, B.; Bacis, R. Structure and rovibrational analysis of the [O₂ (¹Δ_g)_{v=0}]₂ ← [O₂ (³Σ_g)_{v=0}]₂ dimer. *J. Chem. Phys.* **2000**, *112*, 6309–6321. Aquilanti, V.; Ascenzi, D.; Bartolomei, M.; Cappelletti, D.; Cavalli, S.; de Castro Vitores, M.; Pirani, F. Quantum interference scattering of aligned molecules: bonding in O₄ and role of spin coupling. *Phys. Rev. Lett.* **1999**, *82*, 69–72. (b) trimer: Hernández-Lamonedá, R.; Pérez-Ríos, J.; Carmona-Novillo, E.; Bartolomei, M.; Campos-Martínez, J.; Hernández, M. Properties of the molecular oxygen trimer from pairwise additive interactions. *Chem. Phys.* **2012**, *399*, 80–85. (c) tetramer: Bartolomei, M.; Carmona-Novillo, E.; Hernández, M. I.; Pérez-Ríos, J.; Campos-Martínez, J.; Hernández-Lamonedá, J. Molecular oxygen tetramer (O₂)₄: intermolecular interactions and implications for the ε solid phase. *Phys. Rev. B: Condens. Matter Mater. Phys.* **2011**, *84*, 092105.
- (215) Chemically bonded rings of composition O₃, O₄, O₆, and O₈, very much unstable with respect to nO₂, are also local minima; we will return to these below.
- (216) Filatov, M.; Reckien, W.; Peyerimhoff, S. D.; Shaik, S. What are the reasons for the kinetic stability of a mixture of H₂ and O₂? *J. Phys. Chem. A* **2000**, *104*, 12014–12020.
- (217) Bozzelli, J. W.; Dean, A. M. Hydrocarbon radical reactions with oxygen: comparison of allyl, formyl, and vinyl to ethyl. *J. Phys. Chem.* **1993**, *97*, 4427–4441.
- (218) Durif, M. T.; Averbuch-Pouchot, A. *Topics in Phosphate Chemistry*; World Scientific: Singapore, 1996.
- (219) Kopecky, K. R.; Mumford, C. Luminescence in the thermal decomposition of 3,3,4-trimethyl-1,2-dioxetane. *Can. J. Chem.* **1969**, *47*, 709–711.
- (220) Vacher, M.; Fdez. Galvan, I.; Ding, B.-W.; Schramm, S.; Berraud-Pache, R.; Naumov, P.; Ferré, N.; Liu, Y.-J.; Navizet, I.; Roca-Sanjuan; Baader, W. J.; Lindh, R. Chemi- and bioluminescence of cyclic peroxides. *Chem. Rev.* **2018**, *118*, 6927–6974.
- (221) Bos, R.; Barnett, N. W.; Dyson, G. A.; Lim, K. F.; Russell, R. A.; Watson, S. P. Studies on the mechanism of the peroxyoxalate chemiluminescence reaction: part 1. Confirmation of 1,2-dioxetane-dione as an intermediate using ¹³C nuclear magnetic resonance spectroscopy. *Anal. Chim. Acta* **2004**, *502*, 141–147.
- (222) Bos, R.; Tonkin, S. A.; Hanson, G. R.; Hindson, C. M.; Lim, K. F.; Barnett, N. W. In search of a chemiluminescence 1,4-dioxy biradical. *J. Am. Chem. Soc.* **2009**, *131*, 2770–2771.
- (223) Bartlett, P. D.; Schaap, A. P. Stereospecific formation of 1, 2-dioxetanes from cis- and trans-dithoxyethylenes by singlet oxygen. *J. Am. Chem. Soc.* **1970**, *92*, 3223–3225.
- (224) Wasserman, H. H.; De Simone, R. W.; Chia, K. R.; Banwell, M. G. *Encyclopedia of Reagents for Organic Synthesis*; Wiley: New York, 2001.
- (225) Houk, K. N.; Williams, J. C., Jr.; Mitchell, P. A.; Yamaguchi, K. Conformational control of reactivity and regioselectivity in singlet oxygen ene reactions: relationship to the rotational barriers of acyclic alkylethylenes. *J. Am. Chem. Soc.* **1981**, *103*, 949–951.
- (226) Hasty, N. M.; Kearns, D. R. Mechanisms of singlet oxygen reactions. Intermediates in the reaction of singlet oxygen with dienes. *J. Am. Chem. Soc.* **1973**, *95*, 3380–3381.
- (227) Frimer, A. A. The reaction of singlet oxygen with olefins: the question of mechanism. *Chem. Rev.* **1979**, *79*, 359–387.
- (228) Al-Nu'airat, J.; Altarawneh, M.; Gao, X.; Westmoreland, P. R.; Dlugogorski, B. Z. Reaction of aniline with singlet oxygen (O₂ ¹Δ_g). *J. Phys. Chem. A* **2017**, *121*, 3199–3206.
- (229) Leach, A. G.; Houk, K. N. Diels–Alder and ene reactions of singlet oxygen, nitroso compounds and triazolinediones: transition states and mechanisms from contemporary theory. *Chem. Commun.* **2002**, *12*, 1243–1255.
- (230) Reddy, A. R.; Bendikov, M. Diels–Alder reaction of acenes with singlet and triplet oxygen—theoretical study of two-state reactivity. *Chem. Commun.* **2006**, *11*, 1179–1181.
- (231) McCarrick, M. A.; Wu, Y. D.; Houk, K. N. Hetero-Diels–Alder reaction transition structures: reactivity, stereoselectivity, catalysis, solvent effects, and the exo-lone-pair effect. *J. Org. Chem.* **1993**, *58*, 3330–3343.
- (232) Goldstein, E.; Beno, B.; Houk, K. N. Density functional theory prediction of the relative energies and isotope effects for the concerted and stepwise mechanisms of the Diels–Alder reaction of butadiene and ethylene. *J. Am. Chem. Soc.* **1996**, *118*, 6036–6043.
- (233) Firestone, R. A. The low energy of concert in many symmetry-allowed cycloadditions supports a stepwise-diradical mechanism. *Int. J. Chem. Kinet.* **2013**, *45*, 415–428.
- (234) Tonachini, G.; Schlegel, H. B.; Bernardi, F.; Robb, M. A. MC-SCF study of the addition reaction of the ¹Δ_g oxygen molecule to ethene. *J. Am. Chem. Soc.* **1990**, *112*, 483–491.
- (235) Bobrowski, M.; Liwo, A.; Oldziej, S.; Jeziorek, D.; Ossowski, T. CAS MCSCF/CAS MCQDPT2 study of the mechanism of singlet oxygen addition to 1,3-butadiene and benzene. *J. Am. Chem. Soc.* **2000**, *122*, 8112–8119.
- (236) Sevin, F.; McKee, M. L. Reactions of 1,3-cyclohexadiene with singlet oxygen. A theoretical study. *J. Am. Chem. Soc.* **2001**, *123*, 4591–4600.
- (237) Shaik, S. S. What happens to molecules as they react? A valence bond approach to reactivity. *J. Am. Chem. Soc.* **1981**, *103*, 3692–3701.

- (238) Pross, A. A General approach to organic reactivity: the configuration mixing model. In *Advances in Physical Organic Chemistry*; Elsevier: Amsterdam, 1985; Vol. 21, pp 99–196.
- (239) Shaik, S.; Shurki, A. Valence bond diagrams and chemical reactivity. *Angew. Chem., Int. Ed.* **1999**, *38*, 586–625.
- (240) Nelson, E. D.; Artau, A.; Price, J. M.; Kenttämaa, H. I. m-Benzynes reacts as an electrophile. *J. Am. Chem. Soc.* **2000**, *122*, 8781–8782.
- (241) Nelson, E. D.; Artau, A.; Price, J. M.; Tichy, S. E.; Jing, L.; Kenttämaa, H. I. meta-Benzynes reacts as an electrophile. *J. Phys. Chem. A* **2001**, *105*, 10155–10168.
- (242) Perrin, C. L.; Rodgers, B. L.; O'Connor, J. M. Nucleophilic addition to a p-benzyne derived from an enediyne: a new mechanism for halide incorporation into biomolecules. *J. Am. Chem. Soc.* **2007**, *129*, 4795–4799.
- (243) Du, L.; Qiu, Y.; Lan, X.; Zhu, R.; Phillips, D. L.; Li, M.-D.; Dutton, A. S.; Winter, A. H. Direct detection of the open-shell singlet phenyloxonium ion: An atom-centered diradical reacts as an electrophile. *J. Am. Chem. Soc.* **2017**, *139*, 15054–15059.
- (244) Frazier, B. A.; Williams, V. A.; Wolczanski, P. T.; Bart, S. C.; Meyer, K.; Cundari, T. R.; Lobkovsky, E. B. C–C Bond formation and related reactions at the CNC backbone in (smif) FeX (smif = 1, 3-Di-(2-pyridyl)-2-azaallyl): dimerizations, 3+ 2 cyclization, and nucleophilic attack; transfer hydrogenations and alkyne trimerization (X = N (TMS) 2, dpma = (Di-(2-pyridyl-methyl)-amide)). *Inorg. Chem.* **2013**, *52*, 3295–3312.
- (245) Bachler, V.; Olbrich, G.; Neese, F.; Wieghardt, K. Theoretical evidence for the singlet diradical character of square planar nickel complexes containing two o-semiquinonato type ligands. *Inorg. Chem.* **2002**, *41*, 4179–4193.
- (246) Herebian, D.; Wieghardt, K. E.; Neese, F. Analysis and interpretation of metal-radical coupling in a series of square planar nickel complexes: correlated ab initio and density functional investigation of [Ni(L^{ISQ})₂](L^{ISQ} = 3,5-di-tert-butyl-o-diiminobenzo-semiquinonato (1-)). *J. Am. Chem. Soc.* **2003**, *125*, 10997–11005.
- (247) Hayes, E. F.; Siu, A. K. Electronic structure of the open forms of three-membered rings. *J. Am. Chem. Soc.* **1971**, *93*, 2090–2091.
- (248) Kamada, K.; Ohta, K.; Shimizu, A.; Kubo, T.; Kishi, R.; Takahashi, H.; Botek, E.; Champagne, B.; Nakano, M. Singlet diradical character from experiment. *J. Phys. Chem. Lett.* **2010**, *1*, 937–940.
- (249) Nakano, M.; Fukuda, K.; Ito, S.; Matsui, H.; Nagami, T.; Takamuku, S.; Kitagawa, Y.; Champagne, B. Diradical and ionic characters of open-shell singlet molecular systems. *J. Phys. Chem. A* **2017**, *121*, 861–873.
- (250) Flynn, C. R.; Michl, J. pi.. pi-Biradicaloid hydrocarbons. o-Xylylene. Photochemical preparation from 1, 4-dihydrophthalazine in rigid glass, electric spectroscopy, and calculations. *J. Am. Chem. Soc.* **1974**, *96*, 3280–3288.
- (251) Döhnert, D.; Koutecký, J. Occupation numbers of natural orbitals as a criterion for biradical character. Different kinds of biradicals. *J. Am. Chem. Soc.* **1980**, *102*, 1789–1796.
- (252) Bonacic-Koutecký, V.; Koutecký, J.; Michl, J. Neutral and charged biradicals, zwitterions, funnels in S1, and proton translocation: their role in photochemistry, photophysics, and vision. *Angew. Chem., Int. Ed. Engl.* **1987**, *26*, 170–189.
- (253) Jung, Y.; Head-Gordon, M. How diradicaloid is a stable diradical? *ChemPhysChem* **2003**, *4*, 522–525.
- (254) Seierstad, M.; Kinsinger, C. R.; Cramer, C. J. Design optimization of 1, 3-diphospha-2, 4-diboretane diradicals. *Angew. Chem., Int. Ed.* **2002**, *41*, 3894–3896.
- (255) Amos, A. T.; Hall, G. G. Single determinant wave functions. *Soc. London A* **1961**, *263*, 483–493.
- (256) Nakano, M.; Fukui, H.; Minami, T.; Yoneda, K.; Shigeta, Y.; Kishi, R.; Champagne, B.; Botek, E.; Kubo, T.; Ohta, K.; Kamada, K. (Hyper) polarizability density analysis for open-shell molecular systems based on natural orbitals and occupation numbers. *Theor. Chem. Acc.* **2011**, *130*, 711–724.
- (257) Takatsuka, K.; Fueno, T.; Yamaguchi, K. Distribution of odd electrons in ground-state molecules. *Theor. Chem. Acc.* **1978**, *48*, 175–183.
- (258) Staroverov, V. N.; Davidson, E. R. Diradical character of the Cope rearrangement transition state. *J. Am. Chem. Soc.* **2000**, *122*, 186–187.
- (259) Mulliken, R. S. Electronic population analysis on LCAO–MO molecular wave functions. II. Overlap populations, bond orders, and covalent bond energies. *J. Chem. Phys.* **1955**, *23*, 1833–1846.
- (260) Staroverov, V. N.; Davidson, E. R. Transition regions in the Cope rearrangement of 1, 5-hexadiene and its cyano derivatives. *J. Am. Chem. Soc.* **2000**, *122*, 7377–7385.
- (261) Bader, R. F. W. *Atoms in Molecules, A Quantum Theory*; Clarendon Press: Oxford, 1994.
- (262) Lain, L.; Torre, A.; Bochicchio, R. C.; Ponc, R. On the density matrix of effectively unpaired electrons. *Chem. Phys. Lett.* **2001**, *346*, 283–287.
- (263) Staroverov, V. N.; Davidson, E. R. Distribution of effectively unpaired electrons. *Chem. Phys. Lett.* **2000**, *330*, 161–168.
- (264) Head-Gordon, M. Characterizing unpaired electrons from the one-particle density matrix. *Chem. Phys. Lett.* **2003**, *372*, 508–511.
- (265) Head-Gordon, M. Reply to comment on ‘characterizing unpaired electrons from the one-particle density matrix’. *Chem. Phys. Lett.* **2003**, *380*, 488–489.
- (266) Orms, N.; Rehn, D. R.; Dreuw, A.; Krylov, A. I. Characterizing bonding patterns in diradicals and triradicals by density-based wave function analysis: a uniform approach. *J. Chem. Theory Comput.* **2018**, *14*, 638–648.
- (267) Lee, J.; Small, D. W.; Epifanovsky, E.; Head-Gordon, M. Coupled-cluster valence-bond singles and doubles for strongly correlated systems: block-tensor based implementation and application to oligoacenes. *J. Chem. Theory Comput.* **2017**, *13*, 602–615.
- (268) Stück, D.; Baker, T. A.; Zimmerman, P.; Kurlancheek, W.; Head-Gordon, M. On the nature of electron correlation in C₆₀. *J. Chem. Phys.* **2011**, *135*, 194306.
- (269) Luzanov, A. V.; Zhikol, O. A. Collectivity, shell openness indices, and complexity measures of multiconfigurational states: Computations within full CI scheme. *Int. J. Quantum Chem.* **2005**, *104*, 167.
- (270) Luzanov, A. V., Effectively unpaired electrons for singlet states: from diatomics to graphene nanoclusters. In *Practical Aspects of Computational Chemistry*; Leszczynski, J.; Shukla, M. K., Eds.; Springer: New York, 2016; Chapter 6.
- (271) Luzanov, A. V.; Prezhdo, O. V. Analysis of multiconfigurational wave functions in terms of hole-particle distributions. *J. Chem. Phys.* **2006**, *124*, 224109.
- (272) Nakano, M. Open-shell-character-based molecular design principles: applications to nonlinear optics and singlet fission. *Chem. Rec.* **2017**, *17*, 27–62.
- (273) Yamaguchi, K. The electronic structures of biradicals in the unrestricted Hartree-Fock approximation. *Chem. Phys. Lett.* **1975**, *33*, 330–335.
- (274) Rivero, P.; Jiménez-Hoyos, C. A.; Scuseria, G. E. Entanglement and polyradical character of polycyclic aromatic hydrocarbons predicted by projected Hartree-Fock theory. *J. Phys. Chem. B* **2013**, *117*, 12750–12758.
- (275) Becke, A. D. Density-functional thermochemistry. I. The effect of the exchange-only gradient correction. *J. Chem. Phys.* **1992**, *96*, 2155–2160.
- (276) Lee, C.; Yang, W.; Parr, R. G. Development of the Colle-Salvetti correlation-energy formula into a functional of the electron density. *Phys. Rev. B: Condens. Matter Mater. Phys.* **1988**, *37*, 785.
- (277) Dunning, T. H., Jr Gaussian basis sets for use in correlated molecular calculations. I. The atoms boron through neon and hydrogen. *J. Chem. Phys.* **1989**, *90*, 1007–1023.
- (278) Malrieu, J. P.; Trinquier, G. Can a topological approach predict spin-symmetry breaking in conjugated hydrocarbons? *J. Phys. Chem. A* **2016**, *120*, 9564–9578.

- (279) Mermin, N. D. Thermal properties of the inhomogeneous electron gas. *Phys. Rev.* **1965**, *137*, A1441–A1443.
- (280) Grimme, S. Towards first principles calculation of electron impact mass spectra of molecules. *Angew. Chem., Int. Ed.* **2013**, *52*, 6306–6312.
- (281) Grimme, S.; Hansen, A. A practicable real-space measure and visualization of static electron-correlation effects. *Angew. Chem., Int. Ed.* **2015**, *54*, 12308–12313.
- (282) Bauer, C. A.; Hansen, A.; Grimme, S. The fractional occupation number weighted density as a versatile analysis tool for molecules with a complicated electronic structure. *Chem. - Eur. J.* **2017**, *23*, 6150–6164.
- (283) Shaik, S.; Hiberty, P. C. *A Chemist's Guide to Valence Bond Theory*; Wiley-Interscience, 2008.
- (284) Chirgwin, B. H.; Coulson, C. A. The electronic structure of conjugated systems. VI. *Proc. R. Soc. London, Ser. A* **1950**, *201*, 196–209.
- (285) Gallup, G. A.; Norbeck, J. M. Population analyses of valence-bond wavefunctions and BeH₂. *Chem. Phys. Lett.* **1973**, *21*, 495–500.
- (286) Braïda, B.; Walter, C.; Engels, B.; Hiberty, P. C. A clear correlation between the diradical character of 1, 3-dipoles and their reactivity toward ethylene or acetylene. *J. Am. Chem. Soc.* **2010**, *132*, 7631–7637.
- (287) Braïda, B.; Galembeck, S. E.; Hiberty, P. C. Ozone and other 1, 3-dipoles: toward a quantitative measure of diradical character. *J. Chem. Theory Comput.* **2017**, *13*, 3228–3235.
- (288) Glezakou, V. A.; Elbert, S. T.; Xantheas, S. S.; Ruedenberg, K. Analysis of bonding patterns in the valence isoelectronic series O₃, S₃, SO₂, and OS₂ in terms of oriented quasi-atomic molecular orbitals. *J. Phys. Chem. A* **2010**, *114*, 8923–8931.
- (289) Braïda, B.; Lo, A.; Hiberty, P. C. Can aromaticity coexist with diradical character? An ab initio valence bond study of S₂N₂ and related 6 π -electron four-membered rings E₂N₂ and E₄2+ (E = S, Se, Te). *ChemPhysChem* **2012**, *13*, 811–819.
- (290) Yamaguchi, K.; Fukui, H.; Fueno, T. Molecular orbital (MO) theory for magnetically interacting organic compounds. Ab-initio MO calculations of the effective exchange integrals for cyclophane-type carbene dimers. *Chem. Lett.* **1986**, *15*, 625–628.
- (291) Caballol, R.; Castell, O.; Illas, F.; de P. R. Moreira, I.; Malrieu, J. P. Remarks on the proper use of the broken symmetry approach to magnetic coupling. *J. Phys. Chem. A* **1997**, *101*, 7860–7866.
- (292) Luzanov, A. V.; Prezhdo, O. V. High-order entropy measures and spin-free quantum entanglement for molecular problems. *Mol. Phys.* **2007**, *105*, 2879–2891.
- (293) Luzanov, A. V. Some spin and spin-free aspects of coulomb correlation in molecules. *Int. J. Quantum Chem.* **2012**, *112*, 2915–2923.
- (294) Ramos-Cordoba, E.; Salvador, P.; Reiher, M. Local spin analysis and chemical bonding. *Chem. - Eur. J.* **2013**, *19*, 15267–15275.
- (295) Ramos-Cordoba, E.; Matito, E.; Mayer, I.; Salvador, P. Toward a unique definition of the local spin. *J. Chem. Theory Comput.* **2012**, *8*, 1270–1279.
- (296) Ramos-Cordoba, E.; Salvador, P. Characterization and quantification of polyradical character. *J. Chem. Theory Comput.* **2014**, *10*, 634–641.
- (297) Ramos-Cordoba, E.; Salvador, P. Diradical character from the local spin analysis. *Phys. Chem. Chem. Phys.* **2014**, *16*, 9565–9571.
- (298) Surjan, P. R.; Udvardi, L.; Nemeth, K. Electronic excitations in fullerenes: Jahn-Teller distorted structures of C₆₀. *J. Mol. Struct.* **1994**, *311*, 55–68.
- (299) Houk, K. N.; Lee, P. S.; Nendel, M. Polyacene and cyclacene geometries and Electronic structures: bond equalization, vanishing band gaps, and triplet ground states contrast with polyacetylene. *J. Org. Chem.* **2001**, *66*, 5517–5521.
- (300) Rohlfing, M.; Louie, S. G. Optical excitations in conjugated polymers. *Phys. Rev. Lett.* **1999**, *82*, 1959–1962.
- (301) Becke, A. D. Communication: optical gap in polyacetylene from a simple quantum chemistry exciton model. *J. Chem. Phys.* **2018**, *149*, 081102.
- (302) Hung, R. R.; Grabowski, J. J. A precise determination of the triplet energy of carbon (C₆₀) by photoacoustic calorimetry. *J. Phys. Chem.* **1991**, *95*, 6073–6075.
- (303) Guldi, D. M.; Prato, M. Excited-state properties of C₆₀ fullerene derivatives. *Acc. Chem. Res.* **2000**, *33*, 695–703.
- (304) Kivelson, S.; Chapman, O. L. Polyacene and a new class of quasi-one-dimensional conductors. *Phys. Rev. B: Condens. Matter Mater. Phys.* **1983**, *28*, 7236–7243.
- (305) Schon, J. H.; Berg, S.; Kloc, C.; Batlogg, B. Ambipolar pentacene field-effect transistors and inverters. *Science* **2000**, *287*, 1022–1023.
- (306) Anthony, J. E. The larger acenes: versatile organic semiconductors. *Angew. Chem., Int. Ed.* **2008**, *47*, 452–483.
- (307) Rutenberg, I. M.; Scherman, O. A.; Grubbs, R. H.; Jiang, W.; Garfunkel, E.; Bao, Z. Synthesis of polymer dielectric layers for organic thin film transistors via surface-initiated ring-opening metathesis polymerization. *J. Am. Chem. Soc.* **2004**, *126*, 4062–4063.
- (308) Mattheus, C. C.; de Wijs, G. A.; de Groot, R. A.; Palstra, T. T. M. Modeling the polymorphism of pentacene. *J. Am. Chem. Soc.* **2003**, *125*, 6323–6330.
- (309) Coropceanu, V.; Cornil, J.; da Silva Filho, D. A.; Olivier, Y.; Silbey, R.; Brédas, J.-L. Charge transport in organic semiconductors. *Chem. Rev.* **2007**, *107*, 926–952.
- (310) Bendikov, M.; Duong, H. M.; Starkey, K.; Houk, K. N.; Carter, E. A.; Wudl, F. Oligoacenes: theoretical prediction of open-shell singlet diradical ground states. *J. Am. Chem. Soc.* **2004**, *126*, 7416–7417.
- (311) Gao, Y.; Liu, C.-G.; Jiang, Y.-S. The valence bond study for benzenoid hydrocarbons of medium to infinite sizes. *J. Phys. Chem. A* **2002**, *106*, 2592–2597.
- (312) Bettinger, H. F.; Tönshoff, C.; Doerr, M.; Sanchez-Garcia, E. Electronically excited states of higher acenes up to nonacene: a density functional theory/multireference configuration interaction study. *J. Chem. Theory Comput.* **2016**, *12*, 305–312.
- (313) Raghu, C.; Pati, Y. A.; Ramasesha, S. Structural and electronic instabilities in polyacenes: density-matrix renormalization group study of a long-range interacting model. *Phys. Rev. B: Condens. Matter Mater. Phys.* **2002**, *65*, 155204.
- (314) Qu, Z.; Zhang, D.; Liu, C.; Jiang, Y. Open-shell ground state of polyacenes: a valence bond study. *J. Phys. Chem. A* **2009**, *113*, 7909–7914.
- (315) Tönshoff, C.; Bettinger, H. Photogeneration of octacene and nonacene. *Angew. Chem., Int. Ed.* **2010**, *49*, 4125–4128.
- (316) Shen, B.; Tatchen, J.; Sanchez-Garcia, E.; Bettinger, H. F. Evolution of the optical gap in the acene series: undecacene. *Angew. Chem., Int. Ed.* **2018**, *57*, 10506–10509.
- (317) Fukui, K.; Tanaka, K. A theoretical study on biradicals. I. Theoretical characteristics of biradicals. *Bull. Chem. Soc. Jpn.* **1977**, *50*, 1391–1398.
- (318) Trinquier, G.; David, G.; Malrieu, J. P. Qualitative views on the polyradical character of long acenes. *J. Phys. Chem. A* **2018**, *122*, 6926–6933.
- (319) Gopalakrishna, T. Y.; Zeng, W.; Lu, X.; Wu, J. From open-shell singlet diradicaloids to polyradicaloids. *Chem. Commun.* **2018**, *54*, 2186–2199.
- (320) Trinquier, G.; Malrieu, J. P. Kekulé versus Lewis: when aromaticity prevents electron pairing and imposes polyradical character. *Chem. - Eur. J.* **2015**, *21*, 814–828.
- (321) Trinquier, G.; Malrieu, J. P. Predicting the open-shell character of polycyclic hydrocarbons in terms of Clar sextets. *J. Phys. Chem. A* **2018**, *122*, 1088–1201.
- (322) Bond, A. M.; Fletcher, S.; Marken, F.; Shaw, S. J.; Symons, P. G. Electrochemical and X-ray diffraction study of the redox cycling of nanocrystals of 7, 7, 8, 8-tetracyanoquinodimethane. Observation of a solid–solid phase transformation controlled by nucleation and growth. *J. Chem. Soc., Faraday Trans.* **1996**, *92*, 3925–3933.
- (323) Kistenmacher, T. J.; Phillips, T. E.; Cowan, D. O. The crystal structure of the 1:1 radical cation–radical anion salt of 2,2'-bis-1,3-dithiole (TTF) and 7, 7, 8, 8-tetracyanoquinodimethane (TCNQ). *Acta Crystallogr., Sect. B: Struct. Crystallogr. Cryst. Chem.* **1974**, *30*, 763–768.

- (324) Ramos-Berdullas, N.; Mandado, M. Electronic properties of p-xylylene and p-phenylene chains subjected to finite bias voltages: a new highly conducting oligophenyl structure. *Chem. - Eur. J.* **2013**, *19*, 3646–3654.
- (325) Ramos-Berdullas, N.; Ferro-Costas, D.; Mandado, M. Resonance assisted electron transport in oligophenyl conductors. *Comput. Theor. Chem.* **2015**, *1053*, 263–269.
- (326) Stuyver, T.; Fias, S.; De Proft, F.; Geerlings, P. The relation between delocalization, long bond order structure count and transmission: an application to molecular wires. *Chem. Phys. Lett.* **2015**, *630*, 51–56.
- (327) Müller, E.; Pfanz, H. Über biradikaloide terphenyl-derivate. *Ber. Dtsch. Chem. Ges. B* **1941**, *74*, 1051–1074.
- (328) Tan, G.; Wang, X. Isolable bis (triarylamine) dications: analogues of Thiele's, Chichibabin's, and Müller's hydrocarbons. *Acc. Chem. Res.* **2017**, *50*, 1997–2006.
- (329) Montgomery, L. K.; Huffman, J. C.; Jurczak, E. A.; Grendze, M. P. The molecular structures of Thiele's and Chichibabin's hydrocarbons. *J. Am. Chem. Soc.* **1986**, *108*, 6004–6011.
- (330) Hansmann, M. M.; Melaimi, M.; Munz, D.; Bertrand, G. Modular approach to Kekulé diradicaloids derived from cyclic (alkyl)(amino) carbenes. *J. Am. Chem. Soc.* **2018**, *140*, 2546–2554.
- (331) Rottschäfer, D.; Ho, N. K. T.; Neumann, B.; Stämmler, H. G.; van Gastel, M.; Andrada, D. M.; Ghadwal, R. S. N-Heterocyclic carbene analogues of Thiele and Chichibabin hydrocarbons. *Angew. Chem.* **2018**, *130*, 5940–5944.
- (332) Wang, J.; Xu, X.; Phan, H.; Herg, T. S.; Gopalakrishna, T. Y.; Li, G.; Ding, J.; Wu, J. Stable oxindolyl-based analogues of Chichibabin's and Müller's hydrocarbons. *Angew. Chem., Int. Ed.* **2017**, *56*, 14154–14158.
- (333) Ohashi, K.; Kubo, T.; Masui, T.; Yamamoto, K.; Nakasuji, K.; Takui, T.; Kai, Y.; Murata, I. 4, 8, 12, 16-Tetra-tert-butyl-s-indaceno [1, 2, 3-cd: 5, 6, 7-c'd'] diphenalene: A four-stage amphoteric redox system. *J. Am. Chem. Soc.* **1998**, *120*, 2018–2027.
- (334) Sun, Z.; Huang, K. W.; Wu, J. Soluble and stable heptazethrenebis (dicarboximide) with a singlet open-shell ground state. *J. Am. Chem. Soc.* **2011**, *133*, 11896–11899.
- (335) Yadav, P.; Das, S.; Phan, H.; Herg, T. S.; Ding, J.; Wu, J. Kinetically blocked stable 5, 6:12, 13-dibenzozethrene: a laterally π -extended zethrene with enhanced diradical character. *Org. Lett.* **2016**, *18*, 2886–2889.
- (336) Sun, Z.; Wu, J. 7, 14-Diaryl-substituted zethrene diimides as stable far-red dyes with tunable photophysical properties. *J. Org. Chem.* **2013**, *78*, 9032–9040.
- (337) Shan, L.; Liang, Z.; Xu, X.; Tang, Q.; Miao, Q. Revisiting zethrene: synthesis, reactivity and semiconductor properties. *Chem. Sci.* **2013**, *4*, 3294–3297.
- (338) Nakano, M.; Kishi, R.; Takebe, A.; Nate, M.; Takahashi, H.; Kubo, T.; Kamada, K.; Ohta, K.; Champagne, B.; Botek, E. Second hyperpolarizability of zethrenes. *Comput. Lett.* **2007**, *3*, 333–338.
- (339) Sun, Z.; Zeng, Z.; Wu, J. Zethrenes, extended p-quinodimethanes, and periacenes with a singlet biradical ground state. *Acc. Chem. Res.* **2014**, *47*, 2582–2591.
- (340) Hu, P.; Wu, J. Modern zethrene chemistry. *Can. J. Chem.* **2017**, *95*, 223–233.
- (341) Huang, R.; Phan, H.; Herg, T. S.; Hu, P.; Zeng, W.; Dong, S.-q.; Das, S.; Shen, Y.; Ding, J.; Casanova, D.; Wu, J. *J. Am. Chem. Soc.* **2016**, *138*, 10323–10330.
- (342) Sander, W. m-Benzyne and p-benzyne. *Acc. Chem. Res.* **1999**, *32*, 669–676.
- (343) Hoffmann, R. W.; *Dehydrobenzene and Cycloalkynes*; Academic Press: New York, 1967.
- (344) Gilchrist, L.; Arynes. In *The Chemistry of Triple-Bonded Functional Groups, Supplement C*; Patai, S., Rappoport, Z., Eds.; John Wiley and Sons: New York, 1983; Vol. 1, pp 383–419.
- (345) De Proft, F.; von Ragué Schleyer, P.; van Lenthe, J. H.; Stahl, F.; Geerlings, P. Magnetic properties and aromaticity of o-, m-, and p-benzyne. *Chem. - Eur. J.* **2002**, *8*, 3402–3410.
- (346) Wenthold, P. G.; Squires, R. R.; Lineberger, W. C. Ultraviolet photoelectron spectroscopy of the o-, m-, and p-benzyne negative ions. electron affinities and singlet–triplet splittings for o-, m-, and p-benzyne. *J. Am. Chem. Soc.* **1998**, *120*, 5279–5290.
- (347) Jones, R. R.; Bergman, R. G. p-Benzyne. Generation as an intermediate in a thermal isomerization reaction and trapping evidence for the 1,4-benzenediyl structure. *J. Am. Chem. Soc.* **1972**, *94*, 660–661.
- (348) Marquardt, R.; Balster, A.; Sander, W.; Kraka, E.; Cremer, D.; Radziszewski, J. G. p-Benzyne. *Angew. Chem., Int. Ed.* **1998**, *37*, 955–958.
- (349) Hoffmann, R. Of what use enediynes? *American Scientist* **1993**, *81*, 324–326.
- (350) Bachrach, S. M. *Computational Organic Chemistry*, 2nd ed.; Wiley, 2014; pp 333–366.
- (351) Gao, J.; Jankiewicz, B. J.; Reece, J.; Sheng, H.; Cramer, C. J.; Nash, J. J.; Kenttämä, H. I. On the factors that control the reactivity of meta-benzynes. *Chem. Sci.* **2014**, *5*, 2205–2215.
- (352) Williams, P. E.; Jankiewicz, B. J.; Yang, L.; Kenttämä, H. Properties and reactivity of gaseous distonic radical ions with aryl radical sites. *Chem. Rev.* **2013**, *113*, 6949–6985.
- (353) Kotha, R. R.; Yerabolu, R.; Ding, D.; Szalwinski, L.; Ma, X.; Wittig, A.; Kong, J.; Nash, J. J.; Kenttämä, H. I. Spin–spin coupling between two meta-benzyne moieties in a quinolinium tetraradical cation increases their reactivities. *Chem. - Eur. J.* **2019**, *25*, 4472–4477.
- (354) Niecke, E.; Fuchs, A.; Baumeister, F.; Nieger, M.; Schoeller, W. W. A P2C2 four-membered ring with unusual bonding—Synthesis, structure, and ring opening of a 1, 3-diphosphacyclobutane-2, 4-diyl. *Angew. Chem., Int. Ed. Engl.* **1995**, *34*, 555–557.
- (355) Sugiyama, H.; Ito, S.; Yoshifuji, M. Synthesis of a 1, 3-Diphosphacyclobutane-2, 4-diyl from mes* C. P. *Angew. Chem.* **2003**, *115*, 3932–3934.
- (356) Sebastian, M.; Nieger, M.; Szieberth, D.; Nyulászi, L.; Niecke, E. Synthesis and structure of a 1, 3-diphosphacyclobutadienediide: an anionomolytic fragmentation of a 1, 3-diphosphetane-2, 4-diyl in solution. *Angew. Chem., Int. Ed.* **2004**, *43*, 637–641.
- (357) Scheschke, D.; Amii, H.; Gornitzka, H.; Schoeller, W. W.; Bourissou, D.; Bertrand, G. Singlet diradicals: from transition states to crystalline compounds. *Science* **2002**, *295*, 1880–1881.
- (358) Seierstad, M.; Kinsinger, C. R.; Cramer, C. J. Design optimization of 1,3-diphospho-2,4-diboretane diradicals. *Angew. Chem.* **2002**, *114*, 4050–4052.
- (359) Cui, C.; Brynda, M.; Olmstead, M. M.; Power, P. P. Synthesis and characterization of the non-Kekulé, singlet biradicaloid Ar'Ge (μ -NSiMe₃)₂GeAr' (Ar' = 2,6-dipp₂C₆H₃, dipp = 2,6-i-Pr₂C₆H₃). *J. Am. Chem. Soc.* **2004**, *126*, 6510–6511.
- (360) Ma, J.; Ding, Y.; Hattori, K.; Inagaki, S. Theoretical designs of singlet localized 1,3-diradicals. *J. Org. Chem.* **2004**, *69*, 4245–4255.
- (361) Xu, J. D.; Hrovat, D. A.; Borden, W. T. Ab initio calculations of the potential surfaces for the lowest singlet and triplet states of 2,2-difluorocyclopentane-1,3-diyl. The singlet diradical lies below the triplet. *J. Am. Chem. Soc.* **1994**, *116*, 5425–5427.
- (362) Adam, W.; Borden, W. T.; Burda, C.; Foster, H.; Heidenfelder, T.; Heubes, M.; Hrovat, D. A.; Kita, F.; Lewis, S. B.; Scheutzow, D.; Wirz, J. Transient spectroscopy of a derivative of 2,2-difluoro-1,3-diphenylcyclopentane-1,3-diyl a persistent localized singlet 1,3-diradical. *J. Am. Chem. Soc.* **1998**, *120*, 593–594.
- (363) Takeuchi, K.; Ichinohe, M.; Sekiguchi, A. Access to a stable Si₂N₂ four-membered ring with non-Kekule singlet biradical character from a disilyne. *J. Am. Chem. Soc.* **2011**, *133*, 12478–12481.
- (364) Mondal, K. C.; Roy, S.; Roesky, H. W. Silicon based radicals, radical ions, diradicals and diradicaloids. *Chem. Soc. Rev.* **2016**, *45*, 1080–1111.
- (365) Schulz, A. Group 15 biradicals: synthesis and reactivity of cyclobutane-1,3-diyl analogues. *Dalton Trans* **2018**, *47*, 12827–12837.
- (366) Abe, M.; Akisaka, R. Is π -single bonding (C- π -C) possible? A challenge in organic chemistry. *Chem. Lett.* **2017**, *46*, 1586–1592.
- (367) Yoshidomi, S.; Abe, M. 1,2-Diazacyclopentane-3,5-diyl diradicals: electronic structure and reactivity. *J. Am. Chem. Soc.* **2019**, *141*, 3920–3933.

(368) Hicks, R. G. Verdazyls and related radicals containing the hydrazyl [R_2N-NR] group. In *Stable Radicals: Fundamentals and Applied Aspects of Odd-Electron Compounds*; John Wiley & Sons: Chichester, UK, 2010; pp 245–279.

(369) Hicks, R. G. The synthesis and characterization of stable radicals containing the thiazyl (SN) fragment and their use as building blocks for advanced functional materials. In *Stable Radicals: Fundamentals and Applied Aspects of Odd-Electron Compounds*; John Wiley & Sons: Chichester, UK, 2010; pp 317–380.

(370) Takahashi, T.; Matsuoka, K. I.; Takimiya, K.; Otsubo, T.; Aso, Y. Extensive quinoidal oligothiophenes with dicyanomethylene groups at terminal positions as highly amphoteric redox molecules. *J. Am. Chem. Soc.* **2005**, *127*, 8928–8929.

(371) Fu, Q.; Yang, J.; Wang, X. B. On the electronic structures and electron affinities of the m-benzoquinone (BQ) diradical and the o-, p-BQ molecules: a synergetic photoelectron spectroscopic and theoretical study. *J. Phys. Chem. A* **2011**, *115*, 3201–3207.

(372) Ichino, T.; Villano, S. M.; Gianola, A. J.; Goebbert, D. J.; Velarde, L.; Sanov, A.; Blanksby, S. J.; Zhou, X.; Hrovat, D. A.; Borden, W. T.; Lineberger, W. C. The lowest singlet and triplet states of the oxyallyl diradical. *Angew. Chem., Int. Ed.* **2009**, *48*, 8509–8511.

(373) Hopf, H. Phospharadialenes—A new kid in town. *Angew. Chem., Int. Ed.* **2012**, *51*, 11945–11947.

(374) Bao, X.; Zhou, X.; Flener Lovitt, C.; Venkatraman, A.; Hrovat, D. A.; Gleiter, R.; Hoffmann, R.; Borden, W. T. Molecular orbitals of the oxocarbons $(CO)_n$, $n=2-6$. Why does $(CO)_4$ have a triplet ground state? *J. Am. Chem. Soc.* **2012**, *134*, 10259–10270.

(375) de Visser, S. P.; Ogliaro, F.; Harris, N.; Shaik, S. Multi-state epoxidation of ethene by cytochrome P450: a quantum chemical study. *J. Am. Chem. Soc.* **2001**, *123*, 3037–3047.

(376) Kumar, D.; de Visser, S. P.; Shaik, S. Multistate reactivity in styrene epoxidation by compound I of cytochrome P450: mechanisms of products and side products formation. *Chem. - Eur. J.* **2005**, *11*, 2825–2835.

(377) Schröder, D.; Shaik, S.; Schwarz, H. Two-state reactivity as a new concept in organometallic chemistry. *Acc. Chem. Res.* **2000**, *33*, 139–145.

(378) Launay, J.-P.; Verdaguer, M. *Electrons in Molecules*; Oxford University Press: Oxford, UK, 2014.

(379) Mitchell, T. P.; Bernard, W. H.; Wasson, J. R. The crystal structure of di- μ -hydroxo-bis(N,N,N',N' -tetramethylethylenediamine) dicopper (II) bromide. *Acta Crystallogr., Sect. B: Struct. Crystallogr. Cryst. Chem.* **1970**, *26*, 2096.

(380) Calzado, C. J.; Cabrero, J.; Malrieu, J.-P.; Caballol, R. J. Analysis of the magnetic coupling in binuclear complexes. II. Derivation of valence effective Hamiltonians from ab initio CI and DFT calculations. *J. Chem. Phys.* **2002**, *116*, 3985.

(381) Calzado, C. J.; Cabrero, J.; Malrieu, J.-P.; Caballol, R. Analysis of the magnetic coupling in binuclear complexes. I. Physics of the coupling. *J. Chem. Phys.* **2002**, *116*, 2728.

(382) Calzado, C. J.; Angeli, C.; Taratiel, D.; Caballol, R.; Malrieu, J.-P. Analysis of the magnetic coupling in binuclear systems. III. The role of the ligand to metal charge transfer excitations revisited. *J. Chem. Phys.* **2009**, *131*, 044327.

(383) Cambi, L.; Szegö, L. Über die magnetische susceptibilität der komplexen verbindungen. *Ber. Dtsch. Chem. Ges. B* **1931**, *64*, 2591–2598.

(384) *Spin Crossover in Transition Metal Compounds I–III*; Gülich, P., Goodwin, H. A., Eds.; Springer: Berlin, Heidelberg, 2004; pp 233–235.